AD-A267 963



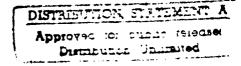


Woods Hole Oceanographic Institution



Abstracts of Manuscripts Submitted in 1992 for Publication

Technical Report WHOI-93-11





93-18865

WHOI-93-11

Research In Progress

Abstracts of Manuscripts Submitted in 1992 for Publication

Woods Hole Oceanographic Institution Woods Hole, Massachusetts

Editor: Alora K. Paul

Approved for Distribution:

Robert B. Gagosian Senior Associate Director and Director of Research

DTIC QUALITY INSPECTED 3

When citing this report, it should be referenced as:

Woods Hole Oceanographic Institution Technical Report No. WHOI-93-11

1177		
Accesio	on F or	
NTIS	CRA&I	Ø
DHC	TAB	
Unanni	ounc ed	⊡
Justific	ation	
By to Distrib	ution /	m 50
A	vailability	Codes
Dist	Avail ari Spec	•
4-1		

PREFACE

This volume contains the abstracts of manuscripts submitted for publication during calendar year 1992 by the staff and students of the Woods Hole Oceanographic Institution. We identify the journal of those manuscripts which are in press, have been submitted for publication or have been published. The volume is intended to be informative, but not a bibliography.

The abstracts are listed by title in the Table of Contents and are grouped into one of our five departments, Marine Policy Center, Coastal Research Center, or the student category. An author index is presented in the back to facilitate locating specific papers.

Acknowledgements

Special thanks to Suzanne B. Volkmann, Research Associate; Staff Assistants Shirley Bowman, Applied Ocean Physics and Engineering; Ethel LeFave, Biology; Pamela Foster, Geology and Geophysics; Molly Lumping, Marine Chemistry and Geochemistry; Debbie Taylor, Physical Oceanography; Mary Schumacher, Marine Policy Center; Olimpia McCall, Coastal Research Center; Pamela Goulart, Education; and Maureen O'Donnell, Library Assistant.

TABLE OF CONTENTS

DEPARTMENT OF APPLIED OCEAN PHYSICS AND ENGINEERING

Colonization of Freshly Deposited Barite and Silica Sediments by Marine Microorganisms in a Laboratory Flume Flow Robert L. Findlay, Stacy L. Kim and Cheryl Ann Butman	PE-1
Spatial Correlation of Acoustic Waves Scattered from a Random Ocean Bottom Dajun Tang and George V. Frisk	PE-1
Listening for Climatic Temperature Change in the Ocean John L. Spiesberger	PE-1
Micro-CTD Instrument Development for the Ocean Sciences Alan Fougere, Neil L. Brown, Daniel Frye and John Toole	PE-2
Prototype Expendable Surface Mooring with Inductive Telemetry Daniel Frye, Alan Fougere, and Sean Kery	PE-2
A Simple Low Cost Acoustic Current Meter Neil L. Brown	PE-2
Acoustic Measurements of Surface Gravity Wave Spectra in Monterey Bay using Mode Travel Time	
Fluctuations James H. Miller, James F. Lynch, Ching-Sang Chiu, Eric L. Westreich, James S. Gerber, Ralph Hippenstiel and Edwin Chaulk	PE-3
On the Linear Dependence of Temperature Structure and Acoustic Backscatter at the Western Edge of the Gulf Stream Using Optimal Least Squares Filtering J. Michael Jech, Clarence S. Clay, and Timothy K. Stanton	PE-3
Active Habitat Selection by Capitella sp. I Larvae. I. Two-Choice Experiments in Still Water and Flume Flows Cheryl Ann Butman and Judith P. Grassle	PE-3
Modeling Pulse Transmission in the Monterey Bay Using Parabolic Equation Methods Eric L. Westreich, Ching-Sang Chiu, James H. Miller, James F. Lynch and Michael D. Collins AOF	PE-4
Three-Dimensional Tidal Flow Around Headlands W. Rockwell Geyer	PE-4
Evaluation of High-Resolution Frequency Estimation Methods for Determining Frequencies of Eigenmodes in Shallow Water Acoustic Field Subramaniam D. Rajan and Saurav D. Bhatta	PE-4
Active Habitat Selection by Capitella sp. I Larvae. II. Multiple-Choice Experiments in Still Water and Flume Flows Judith P. Grassle, Cheryl Ann Butman, and Susan W. Mills	PE-5
Effects of Barite on Aspects of the Ecology of the Polychaete Mediomastus ambiseta Victoria R. Starczak, Charlotte M. Fuller and Cheryl Ann Butman	PE-5
Static and Dynamic Response of Natural Multicomponent Oceanic Surface Films to Compression and Dilation: Laboratory and Field Observations Erik J. Bock and Nelson M. Frew	PE-6
Converting Jason Junior, a Small ROV, to Fiber Optics Robert L. Elder	

Low Power Navigation and Control for Long Range Autonomous Underwater Vehicles Albert M. Bradley
Telemetry Concepts for Deep Sea Moorings Daniel E. Frye and Henri O. Berteaux
Inversion of Towed Cable Dynamics: Theory and Experiments Franz S. H. ver and Dana R. Yoerger
Listening for Climatic Temperature Change in the Northeast Pacific: 1983-1989 John L. Spiesberger, Kurt Metzger and John A. Furgerson
Precise Navigation and Control of an ROV at 2200 Meters Depth Dana R. Yoerger and David A. Mindell
Ocean Acoustic Tomography in the Greenland Sea P. Worcester, J. Lynch, W. Morawitz, R. Pawlowicz, P. Sutton, B. Cornuelle, O. Johannessen, W. Munk, B. Owens, R. Shuchman, and R. Spindel
Minimizing the Dynamic Response of Oceanographic Surface Moorings Mark A. Grosenbaugh
Robust Multiuser Communications for Underwater Acoustic Channels David Brady and Josko A. Catipovic
Ray Representation of Sound Scattering by Weakly Scattering Deformed Fluid Cylinders: Applications to Zooplankton Timothy K. Stunton, Clarence S. Clay, and Dezhang Chu
Hydrodynamic Modulation of Short Wind-Wave Spectra Due to Long Waves Measured by Microwave Radar Tetsu Hara and William J. Plant
Settlement of a Marine Tube Worm as a Function of Current Velocity: Interacting Effects of Hydrodynamics and Behavior Joseph R. Pawlik and Cheryl Ann Butman
Enhanced Dissipation of Kinetic Energy Beneath Surface Waves Y. C. Agrawal, E. A. Terray, M. A. Donelan, P. A. Hwang, A. J. Williams III, W. M. Drennan, K. K. Kahma and S. A. Kitaigorodskii
Near-Real-Time GIS in Deep-Ocean Exploration Jonathan C. Howland, Martin Marra, Daniel F. Potter, W. Kenneth Stewart
Case Study: Configuration of a Super Computer for Alternating Secure and Networked Operations Marguerite K. McElroy and Janet J. Fredericks
Is Del Grosso's Algorithm for Sound Speed in Seawater Correct? John L. Spiesberger
Measured Wavefront Fluctuations in 1000-km Pulse Propagation in the Pacific Ocean T. F. Duda, S. M. Flatté, J. A. Colosi, B. D. Cornuelle, J. A. Hildebrand, W. S. Hodgkiss Jr., P. F. Worcester, B. M. Howe, J. A. Mercer, R. C. Spindel
A Quantitative Measure of Similarity for Tursiops truncatus Signature Whistles John R. Buck, Peter L. Tyack
Traps For Measuring Horizontal Larval Flux Keith D. Stolzenbach and Cherul Ann Butman

Analysis of Finite-Duration Wide-Band Frequency Sweep Signals for Ocean Tomography Timothy F. Duda
Optical Measurements of Ripples Using a Scanning Laser Slope Gauge Part I: Instrumentation and Preliminary Results *Robert J. Martinsen and Erik J. Bock
Optical measurements of ripples using a scanning laser slope gauge part II: Data analysis and interpretation from a laboratory wave tank and Field Experiments Erik J. Bock and Tetsu Hara
Solar-Powered, Temperature/Conductivity/Doppler Profiler Moorings for Coastal Waters with ARGOS Positioning and GOES Telemetry J. D. Irish, K. E. Morey and N. R. Pettigrew
In-Situ Processing of ADCM Data For Real Time Telemetry Robin C. Singer, Albert J. Plueddemann, Andrea L. Oien and Stephen P. Smith AOPE-14
Status of Acoustic Scattering Models of Zooplankton Timothy K. Stanton, Dezhang Chu and Kenneth G. Foote
Determination of compressional wave and shear wave speed profiles in sea ice by crosshole tomography- Theory and experiment Subramaniam D. Rajan, George V. Frisk, James A. Doutt and Cynthia J. Sellers AOPE-14
Power Transformer Design for Tethered Underwater Vehicles Ned C. Forrester
A Hierarchical Approach to Seafloor Classification Using Neural Networks W. K. Stewart, M. Marra and M. Jiang
Technology for the Measurement of Oceanic Low Frequency Electric Fields Robert A. Petitt, Jr., Jean H. Filloux and Alan D. Chave
Data Direct from the Ocean Bottom to the Laboratory Richard L. Koehler and Albert J. Williams 3rd
A Software Based Operation Interface for an Unmanned Underwater Vehicle Roger P. Stokey
A Submersible, All Electric, Remotely Operated Vehicle Tether Management System M. Purcell, T. Austin and R. Stokey
Ocean Technology: Beneficiary of and Benefactor to Energy and Data Storage, Communications, and Material Developments in Sister Fields Albert J. Williams 3rd
LEO-15 An Unmanned Long Term Environmental Observatory Christopher J. von Alt and J. Frederick Grassle
A Minmax Approach to Adaptive Matched Field Processing in an Uncertain Propagation Environment James C. Preisig
Further Analysis of Target Strength Measurements of Antarctic Krill at 38 kHz and 120 kHz: Comparison with Deformed Cylinder Model and Inference of Orientation Distribution Dezhang Chu, Kenneth G. Foote and Timothy K. Stanton
Effects of Sea Ice Cover on Acoustic Ray Travel Times, with Applications to the Greenland Sea Tomography Experiment Guoliang Jin, James F. Lynch, Richard Pawlowicz and Peter Wadhams

Near Ocean Bottom Explosive Launcher — NOBEL Donald E. Koelsch, G. M. Purdy and James E. Broda
Sound Scattering by rough elongated elastic objects. III. Experiment John V. Gurley and Timothy K. Stanton
The Dynamoor Experiment Henri Berteaux, Alessandro Bocconcelli, Cal Eck, Sean Kery and Pierre Wansek AOPE-19
Sound Field Computations in a stratified, Moving Medium D. Keith Wilson
Acoustic Tomographic Monitoring of the Atmospheric Surface Layer D. Keith Wilson and Dennis W. Thomson
Development and Evaluation of Electromechanical Terminations for Deep Sea Buoy Applications Sean Kery and Alessandro Bocconcelli
On the Feasibility of Purely Tomographic Imaging of Flow Fields D. Keith Wilson
Predictions and Observations of Seafloor Infrasonic Noise Generated by Sea Surface Orbital Motion Timothy E. Lindstrom and George V. Frisk
Acoustical and Optical Backscatter Measurements of Sediment Transport in the 1988-89 STRESS
Experiment James F. Lynch, Thomas F. Gross, Christopher R. Sherwood, James D. Irish and Blair H. Brumley
Quantitative Seafloor Characterization Using a Bathymetric Sidescan Sonar W. Kenneth Stewart, Dezhang Chu, Sandipa Malik, Steve Lerner and Hannuman Singh AOPE-21
Relaxation-Matched Modelling of Sound Propagation in Porous Media, Including Fractal Pore Surfaces D. Keith Wilson
Average Echoes From Randomly-Oriented Random-Length Finite Cylinders: Zooplankton Models Timothy K. Stanton, Dezhang Chu, Peter H. Wiebe and Clarence S. Clay
The Importance of Stratification on the Formation of the Estuarine Turbidity Maximum W. Rockwell Geyer
Ambient Noise Measurements in the 200-300 Hz Band from the Greenland Sea Tomography
Experiment J. Lynch, H. X. Wu, R. Pawlowicz, P. Worcester, R. Keenan, H. Graber, P. Wadhams, O. Johannessen and R. Shuchman
Passive Acoustic Localization of the Atlantic Bottlenose Dolphin Using Whistles and Echolocation Clicks
Lee E. Freitag and Peter L. Tyack
A Neural-Network Approach to Classification of Sidescan-Sonar Imagery from a Mid-Ocean-Ridge Area
W. Kenneth Stewart, Min Jiang and Martin Marra
Is it Cheaper to Map Rossby Waves in the Global Ocean than the Global Atmosphere? John L. Spiesberger
Temporal Variation in Bed Configuration and One-Dimensional Bottom Roughness at the Mid-Shelf STRESS Site Robert A. Wheatcroft

Bivalve Feeding and the Benthic Boundary Layer Marcel Fréchette, Denis Lefaivre and Cheryl Ann Butman	24
Flume Experiments on Food Supply to the Blue Mussel Mytilus edulis L. as a Function of Boundary- Layer Flow Cheryl Ann Butman, Marcel Fréchette, W. Rockwell Geyer and Victoria R. Starczak AOPE	-25
Undersea Visualization: A Tool for Scientific and Engineering Progress Lawrence J. Rosenblum, W. Kenneth Stewart and Behzad Kamgar-Parsi	-25

DEPARTMENT OF BIOLOGY

An Immunofluorescent Survey of the Brown Tide Chrysophyte Aureococcus anophagefferens Along the Northeast Coast of the United States Donald M. Anderson, Bruce A. Keafer, David M. Kulis, Robert M. Waters and R. Nuzzi B.
Discrimination Between Domoic-Acid-Producing and Non-Toxic Forms of the Diatom Nitzschia pungens Using Immunofluorescence S. S. Bates, C. Leger, Bruce A. Keafer and Donald M. Anderson B-1
Mixotrophic Algae in Three Ice-Covered Lakes of the Pocono Mountains, USA Ulrike-G. Berninger, David A. Caron and Robert W. Sanders
Pod-Specific Demography of Killer Whales (Orcinus orca) Solange Brault and Hal Caswell
Enrichment, Isolation and Culture of Free-Living Heterotrophic Flagellates David A. Caron
Light-Dependent Phagotrophy in the Freshwater Mixotrophic Chrysophyte Dinobryon cylindricum David A. Caron, Robert W. Sanders, Ee Lin Lim, Celia Marrasé, Linda A. Amaral, Sheri Whitney, Rika B. Aoki and Karen G. Porter
From Patch-Occupancy Models to Cellular Automaton Models for Ecological Interactions Hal Caswell and Ron J. Etter
Evidence for Methylotrophic Symbionts in a Hydrothermal Vent Mussel (Bivalvia: Mytilidae) From the Mid-Atlantic Ridge Colleen M. Cavanaugh, Carl O. Wirsen and H. W. Jannasch
Prochlorococcus marinus Nov. Gen. Nov. Sp.: An Oxyphototrophic Marine Prokaryote Containing Divinyl Chlorophyll a and b S. W. Chisholm, S. L. Frankel, R. Goericke, R. J. Olson, P. Palenik, J. B. Waterbury, L. West-Johnsrud and E. R. Zettler
Single Cell Identification Using Fluorescently Labeled, Ribosomal RNA-Specific Probes Edward F. DeLong
Effects of Nitrate and Nitrite on Dissimilatory Iron Reduction by Shewanella putrefaciens 200 Thomas J. DiChristina
Intracellular Distribution of Saxitoxin in Alexandrium fundyense Gregory J. Doucette and Donald M. Anderson
Mechanism for Iron Control of the Vibrio fischeri Luminescence System: Involvement of Cyclic AMP and Cyclic AMP Receptor Protein and Modulation of DNA Level P. V. Dunlap
Recent Developments in the Study of Symbiosis of Luminous Bacteria Paul V. Dunlap
Cell Density-Dependent Modulation of the Vibrio fischeri Luminescence System in the Absence of Autoinducer and LuxR Protein Paul V. Dunlap and Alan Kuo
The Advantages of Dispersal in a Patch Environment: Effects of Disturbance in a Cellular Automaton Model Ron J. Etter and Hal Caswell

Hydrothermal Vent Site: Preference for Aromatic Carboxylic Acids Frederick E. Goetz and Holger W. Jannasch	. В-7
Nutrient and Energy Flow Through Marine Plankton Food Chains: Impact on New and Regenerated Primary Production Joel C. Goldman	. B-8
Chemical Characterization of Three Large Oceanic Diatoms: Potential Impact on Water Column Chemistry Joel C. Goldman, Dennis A. Hansell and Mark R. Dennett	R-8
Size-Structured Demography of the Compound Ascidian Podoclavella moluccenis in a Seasonal Environment Nicholas J. Gotelli, Andrew R. Davis and Hal Caswell	
Mats of Giant Sulfur Bacteria on Deep-Sea Sediments Due to Fluctuating Hydrothermal Flow Jens K. Gundersen, Bo Barker Jorgensen, Einer Larsen, Holger W. Jannasch	. B -9
Cytochrome P4501A Induction and Inhibition by 3,3',4,4'-Tetrachlorobiphenyl in an Ah Receptor-Containing Fish Hepatoma Cell Line (PLHC-1) Mark E. Hahn, Teresa M. Lamb, Mary E. Schultz, Roxanna M. Smolowitz, Alan Poland and John J. Stegeman	.' B-10
The Ecology of Buzzards Bay: An Estuarine Profile Brian L. Howes and Dale D. Goehringer	B-10
Equivalence and the Adaptationist Program Edward M. Hulburt	B-11
Microbial Growth Kinetics: A Historical Account Holger W. Jannasch and Thomas Egli	B-12
Comparative Physiological Studies on Hyperthermophilic Archaea Isolated From Deep-Sea Hot Vents With Emphasis on Pyrococcus Strain GB-D Holger W. Jannasch, Carl O. Wirsen, Stephen J. Molyneaux and Thomas A. Langworthy	B-12
Bacterial Sulfate Reduction Above 100°C in Deep-Sea Hydrothermal Vent Sediments Bo Barker Jorgensen, Mai F. Isaksen and Holger W. Jannasch	B-12
Amphipods on a Deep-Sea Hydrothermal Treadmill S. Kaartvedt, C. L. Van Dover, L. S. Mullineaux, P. H. Wiebe, and S. M. Bollens	B-13
Use of Remotely-Sensed Sea Surface Temperatures in Studies of Alexandrium tamarense Bloom Dynamics Bruce A. Keafer and Donald M. Anderson	
Isotopic Fractionation Of Oxygen By Respiring Marine Organisms John Kiddon, Michael Bender, Joe Orchardo, Joel Goldman, David A. Caron and Mark Dennett	B-13
Effects of Temperature Acclimation on the Expression of Hepatic Cytochrome P4501A and mRNA and Protein in the Fish Fundulus heteroclitus Pamela J. Kloepper-Sams and John J. Stegeman	B-14
Elevated Ornithine Decarboxylase Activity, Polyamines and Cell Proliferation in Neoplastic and Vacuolated Liver Cells of Winter Flounder (Pleuronectes americanus)	R-14

Initiation and Promotion of Hematopoietic Neoplasia in Soft Shell Clams Exposed to Natural Sediment D. F. Leavitt, D. Miosky Dragos, B. A. Lancaster, A. C. Craig, C. L. Reinisch and J. McDowell Capuzzo	B-15
Temporal Variation in Populations of the Marine Isopod Excirolana: How Stable are Gene Frequencies and Morphology? H. A. Lessios, James R. Weinberg and Victoria R. Starczak	B-15
The Law of the Fishes Phillip S. Lobel	
Seasonal and Daily Changes in Bacterivory in a Coastal Plankton Community Celia Marrasé, Ee Lin Lim and David A. Caron	B-16
Matrix Methods for Avian Demography David B. McDonald and Hal Caswed	B-16
The Bioaccumulation and Biological Effects of Lipophilic Organic Contaminants in Oysters Judith McDowell Capuzzo	B-17
Responses of Molluscs to Chemical Contaminants in Coastal Environments Judith McDowell Capuzzo	B-17
Induced Cytochrome P450IA in Winter Flounder from Georges Bank and Coastal Sites of the Northeastern United States and Canada Emily Monosson and John J. Stegeman	B-17
Bromodeoxyuridine Uptake in Hydropic Vacuolation and Neoplasms in Winter Flounder Liver Michael J. Moore and John J. Stegeman	B-18
Implications of Mesoscale Flows for Dispersal of Deep-Sea Larvae Lauren S. Mullineaux	B-18
Larval Recruitment in Response to Manipulated Field Flows Lauren S. Mullineaux and Elizabeth D. Garland	B-19
Interlaboratory Comparison and Optimization of Hepatic Microsomal Ethoxyresorufin O-deethylase Activity in White Sucker (Catostomus commersoni) Exposed to Bleached Kraft Pulp Mill Effluent K. R. Munkittrick, M. R. van den Heuvel, D. A. Metner, W. L. Lockhart and J. J. Stegeman.	B-19
Salt Marsh Development Studies at Waquoit Bay, Massachusetts: Influence of Geomorphology on Long-Term Plant Community Structure Richard R. Orson and Brian L. Howes	B-19
Diffusion-Induced Chaos in a Spatial Predator-Prey System Mercedes Pascual	B-20
Novel Intervening Sequences in an Archaea DNA Polymerase Gene F. B. Perler, D. G. Comb, W. E. Jack, L. S. Moran, B. Qiang, R. B. Kucera, J. Benner, B. E. Slatko, D. O. Nwankwo, S. K. Hempstead, C. K. Carlow and H. W. Jannasch	B-20
Harbour Porpoises and Gill Nets in the Gulf of Maine A. J. Read, S. D. Kraus, K. D. Bisack and D. Palka	B-20
Patterns of Growth in Wild Bottlenose Dolphins, Tursiops truncatus A. J. Read, R. S. Wells, A. A. Hohn and M. D. Scott	B-21
Relationships Between Bacteria and Heterotrophic Nanoplankton in Marine and Fresh Waters: An Inter-Ecosystem Comparison	
Robert W. Sanders, David A. Caron and Ulrike-(i. Berninger	B-21

Recording Underwater Sounds of Free-Ranging Dolphins While Underway in a Small Boat Lacla S. Sayigh, Peter L. Tyack and Randall S. Wells	B-22
Aplacophora as Progenetic Aculiferans and the Coelomate Origin of Mollusks as Sister Taxon to Sipuncula Amélie II. Scheltema	B-22
Adaptations for Reproduction Among Deep-Sea Benthic Molluscs: An Appraisal of the Existing Evidence Rudolf S. Scheltema	B-22
Population Analysis of Toxic and Nontoxic Alexandrium Species Using Ribosomal RNA Signature Sequences Christopher A. Scholin and Donald M. Anderson	B-23
The Existence of Two Distinct Small-Subunit rRNA Genes in the North American Toxic Dinoflagellate Alexandrium fundyense (Dinophyceae) Christopher A. Scholin, Donald M. Anderson and Mitchell L. Sogin	
Cytochrome P4501A Induction in Tissues, Including Olfactory Epithelium, of Topminnows (Poeculiopsis spp.) by Waterborne Benzo(a)Pyrene Roxanna M. Smolowitz, Mary E. Schultz and John J. Stegeman	
Animal-Sediment Relationships Revisited: What Do We Really Know About Cause and Effect? Paul V. R. Snelgrove and Cheryl Ann Butman	
Hydrodynamic Enhancement of Larval Settlement of the Bivalve Mulinia Lateralis (Say) and the Polychaete Capitella sp. 1 in Microdepositional Environments Paul V. R. Snelgrove, Cheryl Ann Butman and Judith P. Grassle	B-25
The Cytochromes P450 in Fish John J. Stegeman	B-25
Effect of Sampling Frequency on Measurements of Se sonal Primary Production and Oxygen Status in Near-Shore Coastal Ecosystems Craig D. Taylor and B. L. Howes	B-26
Nutrient Processing in an Artificial Wetland Engineered for High Loading: A Septage Treatment Example	n oc
J. M. Teal, B. L. Howes, S. B. Peterson, J. E. Petersen, and A. Armstrong Signature Whistle Development of Three Captive Bottlenose Dolphins, Tursiops Truncatus Peter L. Tyack, Kurt Fristrup and Janet S. McIntosh	B-26 B-26
Marine Mammals, Ocean Acoustics and the Current Regulatory Environment Peter Tyack, William A. Watkins and Kurt M. Fristrup	
Resistance To Co-Occurring Phages Enables Marine Synechococcus To Co-Exist With Cyanophages Abundant In Seawater John B. Waterbury and Frederica W. Valois	B-27
Abundant In Seawater	B-27
Abundant In Seawater John B. Waterbury and Frederica W. Valois Underwater Sound Recording of Animals	

Microbial Degradation of a Starch-Based Biopolymer in the Marine Environment Carl O. Wirsen and Holger W. Jannasch	B-28
Chemosynthetic Microbial Activity at Mid-Atlantic Ridge Hydrothermal Vent Sites Carl O. Wirsen, Holger W. Jannasch and Stephen J. Molyneaux	B-2 9
Induction of P4501A in Intertidal Fish in Prince William Sound as a Result of the Exxon Valdez Oil Spill	
Bruce R. Woodin and John J. Stegeman	B-29

DEPARTMENT OF GEOLOGY AND GEOPHYSICS

ACCELED ATION MACC CRECTROMETRY

ACCELERATOR MASS SI ECTROMETRI
AMS-Graphite Target Production Methods at the Woods Hole Oceanographic Institution During 1986-1991 Alan R. Gagnon and Glenn A. Jones
A Shell-Derived Time History of Bomb-14C on Georges Bank and Its Labrador Sea Implications Christopher R. Weidman and Glenn A. Jones
Radiocarbon Chronology of Black Sea Sediments Glenn A. Jones and Alan R. Gagnon
GEOCHEMISTRY
Fluid Circulation in the Oceanic Crust: Contrast Between Volcanic and Plutonic Regimes Stanley R. Hart, Jerzy Blusztajn, Henry J. B. Dick and James R. Lawrence
Experimental Cpx/Melt Partitioning of 24 Trace Elements Stanley R. Hart and Todd Dunn
Mantle Plumes and Entrainment: Isotopic Evidence S. R. Hart, E. H. Hauri, L. A. Oschmann and J. A. Whitehead
Response: "Mantle Plumes and Mantle Sources. K.A. Farley and H. Craig" S. R. Hart, E. H. Hauri, L. A. Oschmann and J. A. Whitehead
GEOLOGY
Coastal Bench Formation at Hanauma Bay, Oahu, Hawaii Wilfred B. Bryan and Robert A. Stephens
Uncontrolled Growth of Human Populations, Geological Background, and Future Prospects K. O. Emery
Morphotectonics of the Mid-Atlantic Ridge (24°- 30°N) L. Escartin Guiral and J. Lin GG-4

Practical Geological Comparison of Seafloor Survey Instruments

Seismic Structure of the Southern East Pacific Rise R. S. Detrick, A. J. Harding, G. M. Kent, J. A. Orcutt, J. C. Mutter and P. Buhl
A Utilitarian Approach to Modeling Non-Gaussian Characteristics of a Topographic Field John A. Goff
Quantitative Characterization of Abyssal Hill Morphology Along Flow Lines in the Atlantic Ocean John A. Goff
The Wilkes Transform System and "Nannoplate" John A. Goff, Daniel J. Fornari, James R. Cochran, Christopher Keeley, and Alberto Malinverno GG-7
Abyssal Hill Segmentation: Quantitative Analysis of the East Pacific Rise Flanks 7°S-9°S John A. Goff, Alberto Malinverno, Daniel J. Fornari and James R. Cochran
The Role of Density in the Accumulation and Eruptability of Basaltic Melts at Mid-Ocean Ridges E. E. Hooft and R. S. Detrick
Geoelectromagnetism L. J. Lanzerotti, R. A. Langel and A. D. Chave
Two-Dimensional Velocity Inversion/Imaging of Large Offset Seismic Data via the Tau-p Domain Edmund C. Reiter, G. M. Purdy and M. N. Toksoz
A Semblance Guided Median Filter Edmund C. Reiter, M. N. Toksoz and G. M. Purdy
Paleomagnetism of Some Ocean Drilling Program Leg 138 Sediments: Detailing Miocene Magnetostratigraphy David A. Schneider
Age Variations of Oceanic Crust Poisson's Ratio: Inversion and a Porosity Evolution Model Peter R. Shaw
Ridge Segmentation, Faulting, and Crustal Thickness in the Atlantic Peter R. Shaw
Quantitative Comparison of Seismic Data Sets with Waveform Inversion: Testing the Age-Dependent Evolution of Crustal Structure Peter R. Shaw
Change in Failure Stress on the Southern an Andreas Fault System Caused by the 1992 Magnitude=7.4 Landers Earthquake Ross S. Stein, Geoffrey C. P. King and Jian Lin
A Numerical Scattering Chamber for Studying Reverberation in the Seafloor R. A. Stephen
How Much Gabbro is in Ocean Seismic Layer 3? Stephen A. Swift and Ralph A. Stephen
Comment on "The Electrical Conductivity of the Oceanic Upper Mantle" by G. Heinson and S. Constable Pascal Tarits, Alan D. Chave and Adam Schultz
Physical Properties and Logging of the Lower Oceanic Crust: Hole 735B R. P. Von Herzen, D. Goldberg and M. Manghnani

The New National Ocean Sciences Accelerator Mass Spectrometer Facility at Woods Hole Oceanographic Institution - Progress and First Results K. F. Von Reden, G. A. Jones, R. J. Schneider, A. P. McNichol, G. J. Cohen, and
K. H. Purser
Seismic Propagation Across the the East Pacific Rise: Finite Difference Experiments and Implications for Seismic Tomography William S. D. Wilcock, Martin E. Dougherty, Sean C. Solomon, G. M. Purdy, and
Douglas R. Toomey
Microearthquakes On and Near the East Pacific Rise, 9-10°N William S. D. Wilcock, G. M. Purdy, Sean C. Solomon, David L. DuBois, and Douglas R. Toomey
The Seismic Attenuation Structure of a Fast-Spreading Mid-Ocean Ridge William S. D. Wilcock, Sean C. Solomon, G. M. Purdy and Douglas R. Toomey
HYDROTHERMAL
Process of Brine Generation and Circulation in the Oceanic Crust: Fluid Inclusion Evidence from the Troodos Ophiolite, Cyprus Deborah S. Kelley, Paul T. Robinson and John G. Malpas
OCEAN ACOUSTICS
Mean and Rms Scattering Strength Formulation Under an Intrinsic Separation of Scales Hypothesis John A. Goff
Monostatic Shadowing of Homogeneous Fractal Profiles John A. Goff
PALEOCEANOGRAPHY
Foraminiferal Production and Monsoonal Upwelling in the Arabian Sea: Evidence from Sediment
Traps W. B. Curry, D. R. Ostermann, M. V. S. Guptha and V. Ittekkot
Assessing the Completeness of the Deglacial-Marine Stratigraphic Record on West Spitsbergen by Accelerator Mass Spectrometry Radiocarbon Dating: Implications for correlation to Deep-Sea Records
Steven L. Forman, Scott J. Lehman and William Briggs
Mid-Depth Circulation of the Subpolar North Atlantic During the Last Glacial Maximum D. W. Oppo and S. J. Lehman
Enhanced Ventilation of the North Atlantic Subtropical Gyre Thermocline During the Last Glaciation Niall C. Slowey, and William B. Curry
PALEONTOLOGY
Cretaceous Radiolaria from the Ontong-Java Plateau, Western Pacific: Holes 803D and 807C of ODP Leg 130
Kozo Takahashi and Hsin Yi Ling GG-17
PETROLOGY
The Plutonic Foundation of a Slow-Spreading Ridge Henry J. B. Dick, Paul Robinson and Peter S. Meyer
Re-Os Isotope Systematics of HIMU and EMII Oceanic Island Basalts from the South Pacific Ocean Figh H. Hauri and Stanley R. Hart

SEDIMENTOLOGY

Annual Biogenic Particle Fluxes to the Interior of the North Atlantic Ocean; Studied at 34°N 21°W	7
and 48°N 21°W	
Susumu Honjo and Stephen J. Manganini	GG-19

DEPARTMENT OF MARINE CHEMISTRY AND GEOCHEMISTRY

BIOGEOCHEMISTRY
Sedimentary Nitrogen Isotopic Ratio Records Surface Ocean Nitrate Utilization Mark A. Altabet and Roger Francois
Indicators of Sewage Contamination in Sediments Beneath a Deep-Ocean Dump Site off New York M. H. Bothner, H. Takada, I. T. Knight, R. T. Hill, S. Butman, J. W. Farrington, R. R. Colwell, and J. F. Grassle
Thorium Isotopes as Indicators of Particle Dynamics in the Upper Ocean: Results from the JGOFS North Atlantic Bloom Experiment J. Kirk Cochran, Ken O. Buesseler, Michael P. Bacon, and Hugh D. Livingston MCG-1
Cycling of Dissolved and Particulate Organic Matter in the Open Ocean Ellen R. M. Druffel, Peter M. Williams, James E. Bauer, and John R. Ertel MCG-2
Changes in the δ^{13} C of Surface Water Particulate Organic Matter Across the Subtropical Convergence in the S.W. Indian Ocean Roger Francois, Mark A. Altabet, Ralf Goericke, Daniel C. McCorkle, Christian Brunet, and Alain Poisson
Dynamics of the Transition Zone in CZCS-sensed Ocean Color in the North Pacific during Oceanographic Spring David M. Glover, J. S. Wroblewski, and Charles R. McClain
Biochemical Properties of the Oceanic Carbon Cycle Catherine Goyet and Peter G. Brewer
Dissolved Organic Carbon Concentrations in Marine Pore Waters Determined by High-temperature Oxidation William R. Martin and Daniel C. McCorkle
The Relationship between Cerium and Manganese Oxidation in the Marine Environment James W. Moffett
Kinetics of the Removal of Dissolved Aluminum by Diatoms in Seawater: A Comparison with Thorium
S. B. Moran and h. 1. Moore
The Relationship Between δ^{13} C of Organic Matter and [CO ₂ (aq)] in Ocean Surface Water: Data from a JGOFS Site in the Northeast Atlantic Ocean and a Model G. H. Rau, T. Takahashi, D. J. Des Marais, D. J. Repeta, and J. H. Martin MCG-4
Improved HPLC Method for the Analysis of Chlorophylls and Carotenoids from Marine Phytoplankton S. W. Wright, S. W. Jeffrey, R. F. C. Mantoura, C. A. Llewellyn, T. Bjørnland, D. Repeta, and N. Welschmeyer
ORGANIC GEOCHEMISTRY
Aspartic Acid Racemization and Protein Diagenesis in Corals Over the Last 350 Years Glenn A. Goodfriend, P. E. Hare, and Ellen R. M. Druffel

Pressure Seals—Interactions with Organic Matter, Experimental Observations. Relation to a "Hydrocarbon Plugging" Hypothesis for Pressure Seal Formation Jean K. Whelan, Lorraine Buxton Eglinton, and Larry Cathles
GEOCHEMISTRY—INORGANIC, ISOTOPIC
Large Variations of Surface Ocean Radiocarbon: Evidence of Circulation Changes in the SW Pacific Ellen R. M. Druffel and Sheila Griffin
A Large Drop in Atmospheric ¹⁴ C/ ¹² C and Greatly Reduced Glacial Melting During the Younger Dryas, Documented with ²³⁰ Th Ages of Corals R. Lawrence Edwards, J. Warren Beck, G. Burr, D. Donahue, J. M. A. Chappell, A. L. Bloom, E. R. M. Druffel, and F. W. Taylor
Glacial/Interglacial Changes in Sediment Rain Rate in the S.W. Indian Sector of Subantarctic Water as Recorded by ²³⁰ Th, ²³¹ Pa, U and δ ¹⁵ N Roger François, Michael P. Bacon, Mark A. Altabet, and Laurent D. Labeyrie
Metabasalts from the Mid-Atlantic Ridge: New Insights into Hydrothermal Systems in Slow Spreading
Crust Kathryn M. Gillis and Geoffrey Thompson
Comparison of the 1991 pCO ₂ Distribution in the Equatorial Pacific Ocean along 150°W with that measured in 1979: An Indication of Global Change? Catherine Goyet and Edward T. Peltzer
Helium Isotope Geochemistry of Some Volcanic Rocks from Saint Helena David W. Graham, Susan E. Humphris, William J. Jenkins and Mark D. Kurz MCG-9
Helium Isotope Geochemistry of Mid-Ocean Ridge Basalts from the South Atlantic David W. Graham, William J. Jenkins, Jean-Guy Schilling, Geoffrey Thompson, Mark D. Kurz and Susan E. Humphris
Annual Cycles of Mass Flux and Isotopic Composition of Pteropod Shells Settling into the Deep Sargasso Sea John P. Jasper and Werner G. Deuser
Mantle Heterogeneity beneath Oceanic Islands: Some Inferences from Isotopes Mark D. Kurz
A Radiotracer Study of Cerium and Manganese Uptake on to Suspended Particles in Chesapeake Bay
James W. Moffett
Comments on "Redox Cycling of Rare Earth Elements in the Suboxic Zone of the Black Sea" by C. R. German, B. P. Holliday and H. Elderfield, Geochimica et Cosmochimica Acta, 55:3553-3558, 1991
Edward R. Sholkovitz
Chemical Evolution of Rare Earth Elements: Fractionation between Colloidal and Solution Phases of Filtered River Water Edward R. Sholkovitz
The Geochemistry of Rare Earth Elements in the Amazon River Estuary Edward R. Sholkovitz
Experimental Measurements of ³ He and ⁴ He Mobility in Olivine and Clinopyroxene at Magmatic Temperatures MCC 12

Ventilation and Transport of Thermocline and Intermediate Waters in the Northeast Pacific Durin Recent El Niños	ng
Kim A. Van Scoy and Ellen R. M. Druffel	MCG-13
A Comparison of Dissolved and Particulate Mn and Al distributions in the Western North Atlanti Philip A. Yeats, John A. Dalziel and S. Bradley Moran	
MARINE CHEMISTRY	
Temperature Dependence of CO ₂ Partial Pressure in Seawater Catherine Goyet, Frank J. Millero, Alain Poisson, and Deborah K. Shafer	MCG-13
Lanthanide Luminescence in Seawater: Application to a Study of Cerium Redox Chemistry James W. Moffett	MCG-14
Authigenic Apatite Formation and Burial in Sediments from Non-Upwelling, Continental Marg Environments Kathleen C. Ruttenberg and Robert A. Berner	•
INSTRUMENTS AND METHODS	
Measurement of Seawater pCO ₂ using a Renewable-Reagent Fiber Optic Sensor with Colorimetro	ic
Michael D. DeGrandpre	MCG-15
The Chlorophyll-Labeling Method: The Radiochemical Purity of Chlorophyll a—A Response to Jepersen et al., 1992, J. Plankton Res. Ralf Goericke	
High Accuracy Measurements of Total Dissolved Inorganic Carbon in the Ocean: Comparison Alternate Detection Methods	
C. Goyet and A. K. Snover	MCG-10
Inherent Optical Properties of the Ocean: Retrieval of the Absorption Coefficient of Chromophor Dissolved Organic Matter from Fluorescence Measurements	
Frank E. Hoge, Anthony Vodacek and Neil V. Blough	MCG-16
Development of a Sequential Extraction Method for Different Forms of Phosphorus in Marine Secuents	li-
Kathleen C. Ruttenberg	MCG-16

DEPARTMENT OF PHYSICAL OCEANOGRAPHY

OCEAN CIRCULATION & LOW FREQUENCY VA	RIABII	$\sf JITY$
--------------------------------------	--------	------------

Evidence for Barotropic Wave Radiation from the Gulf Stream Amy S. Bower and Nelson G. Hogg	O-1
Ocean Heat Transport Across 24°N Latitude Harry L. Bryden	O-1
Sill Exchange To and From Enclosed Seas Harry L. Bryden	O-1
Generation of Internal Lee Waves Trapped Over a Tall Isolated Seamount David C. Chapman and Dale B. Haidvogel	O-2
Energetics of Gravitational Adjustment for Mesoscale Chimneys Albert J. Hermann and W. Brechner Owens	O-2
Toward Parameterization of the Eddy Field Near the Gulf Stream Nelson G. Hogg	O-2
Real Fresh Water Flux as the Upper Boundary Condition for the Salinity Balance and Thermohaline Circulation Forced by Evaporation and Precipitation Rui Xin Huang	O-3
Parameter Sensitivity Study of the Haline Circulation Rui Xin Huang and Ru Ling Chou	
The Goldsbrough-Stommel Circulation of the World Oceans Rui Xin Huang and Raymond W. Schmitt	O-3
Convective Flow Patterns in an Eight-Box Cube Driven by Combined Wind Stress, Thermal, and Saline Forcing Rui Xin Huang and Henry M. Stommel	'O-4
Wind-Forced Variations in Sea Surface Height in the Northeast Pacific Ocean Kathryn A. Kelly, Michael J. Caruso and Jay A. Austin	O-4
Note on the Sources of North Atlantic Deep Water James Luyten, Michael McCartney, Henry Stommel, Robert Dickson and Ed Gmitrowicz Po	O-4
The Crossing of the Equator by the Deep Western Boundary Current in the Western Atlantic Ocean Michael S. McCartney	O-5
The Transport of Antarctic Bottom Water at 4°N in the Western Basin of the North Atlantic Ocean Michael S. McCartney	O-5
Trans-Equatorial Flow of Antarctic Bottom Water in the Western Atlantic Ocean: Abyssal Geostrophy at the Equator Michael S. McCartney and Ruth A. Curry	O-5
On the Baroclinic Structure of the Abyssal Circulation and the Role of Topography Joseph Pedlosky and David C. Chapman	'O-6
Self-Sustained Inertial Oscillations Joseph Pedlosky and Henry Stommel	O-6
How Does the Deep Western Boundary Current Cross the Gulf Stream? Robert S. Pickart and William M. Smethie, Jr	O-6

Bo Qiu	. PO-7
A Census of Eddies Observed in North Atlantic SOFAR Float Data Philip L. Richardson	. PO-7
Deep Cross Equatorial Flow in the Atlantic Measured with SOFAR Floats Philip L. Richardson and William J. Schmitz, Jr.	. PO-8
Man-Induced Salinity and Temperature Increases in Western Mediterranean Deep Water Eelco J. Rohling and Harry L. Bryden	. PO-8
Variations in Sea Level, Freshwater Budget, and Hydrography in the Mediterranean Eelco J. Rohling and Harry L. Bryden	. PO-9
Surface-Intensified Rossby Waves Over Rough Topography R. M. Samelson	. PO-9
Triangular and Asymmetric Planforms for Salt Fingers Raymond W. Schmitt	. PO-9
The Role of the Oceans in the Global Water Cycle Raymond W. Schmitt and Susan E. Wijffels	PO-10
On the Florida Current T/S Envelope William J. Schmitz, Jr., James R. Luyten and Raymond W. Schmitt	PO-10
A Mechanism for Low Frequency Variability and Salt Flux in the Mediterranean Salt Tongue Michael A. Spall	PO-10
Variability of Sea Surface Salinity in Stochastically Forced Systems Michael A. Spall	PO-11
Dianeutral Motion, Water-Mass Conversion and Non-Linear Effects on the Density Ratio in the Pacific Thermocline Yuzhu You, Trevor J. McDougall and Raymond W. Schmitt	
THEORETICAL AND LABORATORY MODELS	
A General Theory for Equivalent Barotropic Thin Jets Benoit Cushman-Roisin, Larry Pratt and Elise Ralph	PO-12
Time-Dependent Isolated Anomalies in Zonal Flows Karl R. Helfrich and Joseph Pedlosky	PO-12
Laboratory Simulation of Exchange Through Fram Strait Kenneth Hunkins and J. A. Whitehead	PO-12
The Reflection of Unstable Baroclinic Waves and the Production of Mean Coastal Currents Joseph Pedlosky	PO-13
Linear and Finite-Amplitude Localized Baroclinic Instability Joseph Pedlosky, Roger Samelson and Stang Peng Oh	PO-13
Linear Instability of a Mixed-Layer Front R. M. Samelson	PO-13
A Laboratory Model of Cooling over the Continental Shelf	PO-13

Flows Due to Surface Cooling in a Rotating Fluid J. A. Whitehead, R. E. Frazel and Brian Racine	PO-14
Stirring a Stratified Fluid-Energetics and Microstructure Generation J. A. Whitehead, Young Gyu Park and Anand Gnanadesikan	PO-14
COASTAL CIRCULATION & DYNAMICS	
A Numerical Study of Stratified Tidal Rectification Over A Finite-Amplitude Symmetric Bank Changsheng Chen and Robert C. Beardsley	PO-14
A Numerical Study of Stratified Tidal Rectification Over Georges Bank Changsheng Chen, Robert C. Beardsley and Richard Limeburner	PO-15
On the Establishment of the Seasonal Pycnocline in the Middle Atlantic Bight David C. Chapman and Glen Gawarkiewicz	PO-15
Trapping of a Coastal Density Front by the Bottom Boundary Layer David C. Chapman and Steven J. Lentz	PO-15
Sediment Resuspension over the Continental Shelf East of the Delmarva Peninsula James H. Churchill, Creighton D. Wirick, Charles N. Flagg and Leonard J. Pietrafesa	PO-16
Steady Wind Forcing and Relaxation of a Density Front Over a Circular Bank Glen Gawarkiewicz	PO-16
The Response of the Shallow Polar Shelf Water to Negative Bouyancy Forcing: A Negative Study Hsiao-ming Hsu	PO-17
INSTRUMENTATION & EXPERIMENTAL NUMERICAL METHODOLOGY	
A Vertical Coordinate Mapping Technique for Semi-Spectral Primitive Equation Models of Oceanic	:
Circulation Albert J. Hermann and Hsiao-ming Hsu	PO-17
A Note on the Accuracy of Tide Gauge Measurements at Subtidal Frequencies Steven J. Lentz	PO-17
A Comparison of Techniques for Referencing Geostrophic Velocities Robert S. Pickart and Scott S. Lindstrom	PO-18
OTHER	
Bathymetry at the Vema Sill Walter Zenk, Kevin G. Speer and Nelson G. Hogg	PO-18

MARINE POLICY CENTER

North Sea Herring Fluctuations Roger S. Bailey and John H. Steele
Biodiversity, Riodiversity James M. Broadus
Creature Feature Too: Principium precautionarium James M. Broadus
Joint Development of Nonfuel Marine Minerals In Asian Seas James M. Broadus and Porter Hoagland
Protecting Biodiversity James M. Broadus
Regard d'outre-Atlantique (On European Ocean Policy and Security) James M. Broadus
Regulatory/Economic Instruments for Agricultural Pollution: Accounting for Input Substitution Mark E. Eiswerth
Universities, Research Institutions, and Patent Assignments R. Scott Farrow and Porter Hoagland
The Woods Hole Oceanographic Institution, Massachusetts Arthur G. Gaines
Measuring Voting Power on the Council of the International Seabed Authority *Porter Hoagland**
Technology Transfer in Oceanography Porter Hoagland and Hauke Kite-Powell
China Sea Coastal and Marine Nonfuel Minerals: Investigation and Development Porter Hoagland, J. Yang, James M. Broadus, and David K. Y. Chu
Supply and Demand of New Oil Tankers Di Jin
Environmental Compliance and Energy Exploration and Production: Application to Offshore Oil and
Gas Di Jin and Thomas A. Grigalunas
Environmental Compliance and Offshore Oil and Gas Exploration and Production Di Jin and Thomas A. Grigalunas
Antarctica and the Law of the Sea Christopher C. Joyner
The 1991 Madrid Environmental Protocol: Rethinking the World Park Status for Antarctica Christopher C. Joyner
Chile's "Presential Sea" Proposal: Implications for Straddling Stocks and the International Law of Fisheries Christopher C. Joyner and Peter N. DeCola
Commerical Activities and the Movement Toward Standards In Electronic Chart Display and Information Systems Hauke Kite-Powell

Patch Dynamics Simon A. Levin, Thomas A. Powell, and John H. Steele, eds MPC-6
Government Support of Marine Science and Technology in Japan: The Case of Marine Electronic Instrumentation
Matthew J. LaMourie and Porter Hoagland MPC-
Searching for Uncertain Benefits and the Conservation of Biological Diversity Stephen Polasky, Andrew R. Solow, and James M. Broadus
Fisheries Exploitation as a Threat to Environmental Security: The North Pacific Ocean Natalia S. Mirovitskaya and Christopher J. Haney
Development of the United States Electronic Chart Display and Information (ECDIS) Test Bed Project
David J. Scott and Arthur G. Gaines MPC-8
Emerging Marine Environmental Protection Strategies for the Arctic Alexei Yu. Roginko and Matthew J. LaMourie
Detecting Extinction In a Declining Population Andrew R. Solow
Estimating Record Inclusion Probabilities Andrew R. Solow
Inferring Extinction from Sighting Data Andrew R. Solow
On the Efficiency of the Indicator Approach in Geostatistics Andrew R. Solow
The Response of Sea Level to Global Warming Andrew R. Solow
A Simple Test For Change In Community Structure Andrew R. Solow
Statistical Methods in Atmospheric Science Andrew R. Solow
An Empirical Bayes Approach to Monitoring Water Quality Andrew R. Solow and Arthur G. Gaines
Mapping Water Quality by Local Scoring Andrew R. Solow and Arthur G. Gaines
On the Consistency of the Historic Temperature Record with Greenhouse Warming Andrew R. Solow and Anand Patwardhan
Statistical Analysis with an Ordered Categorical Regressor: The Effect of Rainfall on Attendance Andrew R. Solow and Victoria E. Starczak
A Simple Model for Plankton Patchiness John H. Steele and Eric W. Henderson MPC-10

COASTAL RESEARCH CENTER

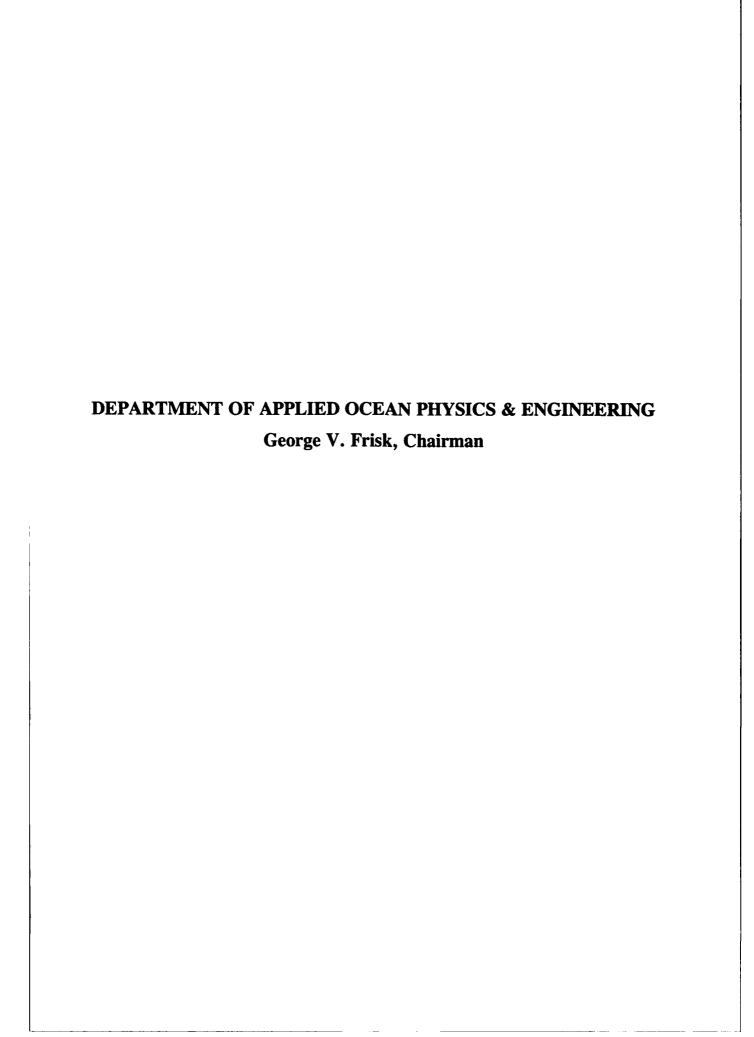
TECHNICAL REPORTS	
Hydroblack 91, Report of the CTD Intercalibration Workshop D. G. Aubrey, T. Oguz, E. Demirev, V. Ivanov, T. McSherry, V. Diaconu, and E. Nikolaenko	CRC-1
The Black Sea General Circulation and Climatic Temperature and Salinity Fields Dimitur Ivanov Trukhchev and Yurii Leonidovich Demin	CRC-1



GRADUATE STUDENTS

Electronic Automation of a Remotely Deployable Seawater Sampling Device Jonathan N. Betts	GS-1
Variability of Currents in Great South Channel and Over Georges Bank: Observation and Modeling Changsheng Chen	GS-1
Kinematic Evaluation of End Effector Design Gary Wayne Edwards	GS-2
Applications of Fluorescence Spectroscopy to Environmental Chemistry Sarah Anita Green	GS-2
Experimental Investigation of Scattering from Randomly Rough Elastic Cylinders John Van Gurley	GS-3
Eddy Generation at a Convex Corner by a Coastal Current in a Rotating System Barry A. Klinger	GS-3
Time-Dependent Ventilated Thermocline Zhengyu Liu	GS-4
Laboratory Measurements of the Sound Generated by Breaking Waves Mark Richard Loewen	GS-5
Global Positioning System Measurement of Crustal Deformation in Central California Mark Hunter Murray	GS-6
Study of Basin Scale Acoustic Transmissions John Richard Nystrom	GS-7
Adaptive Matched Field Processing in an Uncertain Propagation Environment James Calvin Preisig	GS-7
An Analytical Two-Layer Coupled Hydrodynamic and Ice Floe Movement Model Mindy Lynn Roberts	GS-7
A Model of a Mediterranean Salt Lens in External Shear David Walsh	GS-8
The Seismic Attenuation Structure of the East Pacific Rise William Sam Douglas Wilcock	GS-8
Ambient Noise Measurement in the 200-300 Hz Band During the Greenland Sea Tomography Experiment Huixia Wu	GS-9
Investigation of the Dynamics of Low-Tension Cables Christopher Todd Howell	GS-10
Development and Functions of Signature Whistles of Free-Ranging Bottlenose Dolphins, Tursiops Truncatus Laela Suad Sayigh	CS 10
Geochemical and Fluid Dynamic Investigations Into the Nature of Chemical Heterogeneity in the Earth's Mantle	
Erik Harold Hauri	GS-11
Interaction of an Eddy with a Continental Slope Xiaoming Wang	GS-13

Observations of Turbulence, Internal Waves and Background Flows: An Inquiry into the Relationships	
Between Scales and Motion	
Kurt Louis Polzin	GS-14
Meridional Circulation in the Tropical North Atlantic	
Marjorie A.M. Friedrichs	GS-15
Analysis and Application of an Underwater Optical-Ranging System	
John Gerald Kusters, Jr	GS-15
Modeling a 300 kHz Bathymetric Sonar System	
Kenneth Alan Malmquist	GS-16



COLONIZATION OF FRESHLY DEPOSITED BARITE AND SILICA SEDIMENTS BY MARINE MICROORGANISMS IN A LABORATORY FLUME FLOW

Robert L. Findlay, Stacy L. Kim and Cheryl Ann Butman

The biomass and structure of microbial communities colonizing barite freshly deposited onto natural marine mud was investigated in a laboratory flume. Modern biochemical methods based on the lipid content of microbial cells were used to quantify microbial colonization. The experiment involved 3 treatments: 1) fresh barite deposited onto the surface of a natural muddy sediment, 2) fresh silica (utilized as a colonization control) also deposited onto natural mud; and 3) the muddy sediment itself. The treatments were placed in an open-channel flow with 10 um filtered sea water and sampled every other day for 16 d. The flow was set at a shear velocity (u_*) of about 0.30 cm s^{-1} , which is less than the critical u_{\bullet} to initiate sediment motion of these particles. After 48 h, the barite and silica treatments contained approximately 60 times less microbial biomass than the natural mud. Little change in microbial biomass was observed in the barite and silica treatments until 13 d of incubation when microbial biomass began to increase. The carbon content of the fresh barite and silica treatments was 60 to 570 times less than in the natural mud and this lower carbon content is the likely proximal cause of the lower microbial biomass. The structure of microbial communities was analyzed after 13 d of incubation. Despite the large difference in total biomass, microbial communities in the natural mud and barite treatments were similar in structure. In the silica treatment, however, community structure was highly variable and dissimilar to the natural mud community. The community in flowing sea water was more similar to communities in natural mud and barite than in silica. These results suggest that natural marine sediments receiving inputs of barite can be expected, given sufficient time, to develop microbial communities similar in structure and possibly biomass to those found in ambient sediments.

Published in: Marine Ecology Progress Series, 90:73-88, 1992.

Supported by: MMS (U.S. Dept. of the Interior) contract 14-12-0001-30262, and Coastal Research Center.

WHOI Contribution No. 7856.

SPATIAL CORRELATION OF ACOUSTIC WAVES SCATTERED FROM A RANDOM OCEAN BOTTOM

Dajun Tang and George V. Frisk

Acoustic wave scattering from a random bottom is studied. The bottom is modeled as a fluid medium with a layer where the sound speed is composed of a small random component superimposed upon a constant background sound speed. Emphasize is placed on the spatial correlation of the scattered field. It is found that the spatial correlation length of the scattered acoustic field is related to the correlation length of the random sound speed in the bottom, and by sweeping acoustic frequencies, it is possible to invert the bottom correlation length through measuring the spatial correlation of the scattered field by using a receiving array. Also studied is the influence of anisotropy of the bottom scatterer. A comparison is made to the Born approximation.

Submitted to: Journal of the Acoustical Society of America.

Supported by: ONR contract N00014-86-C-0338. WHO! Contribution No. 7948.

LISTENING FOR CLIMATIC TEMPERATURE CHANGE IN THE OCEAN

John L. Spiesberger

I often wondered how the American oceanographers Ewing, Iselin, Worzel, and Vine started thinking about how sound travels through the ocean (Menard, 1986). According to Worzel, who I met in October 1991, Ewing was a faculty member in the physics department at Lehigh University in Pennsylvania who had previous experience searching for terrestrial pockets of oil using seismic techniques. In the middle of the 1930's, Ewing was approached by two eminent individuals, William Bowie of the Coast and Geodetic Survey, and Richard Field of the American Geological Society. They offered Ewing a \$2,000 grant to measure the thicknesses of ocean sediments using terrestrial seismic techniques adapted to the marine environment. This was a significant grant and represented a uncommon opportunity since there was no equivalent of the National Science Foundation at that time. Nothing was known of seafloor spreading and the oceans were thought of as a big bowl where sediments accumulated by what Worzel calls the "reign of death". Ewing, and his students Worzel and Vine. set up bombs and seismic recording gear on the

sea-floor. By timing the arrival of energy at colinearily located receivers, they used ray theory to infer sediment thicknesses. After overcoming numerous technical obstacles, they succeeded in measuring a sediment thickness of greater than one-quarter mile in the Atlantic in 1940 (Ewing et al., 1946). When the war started, Ewing and his students came to Woods Hole Oceanographic Institution, then under the direction of Columbus Iselin. They were shown anomalous transmission loss data for sound in shallow water measured by the Semmes, a Coastal and Geodetic Survey vessel. Working with vertical profiles of the speed of sound, derived from temperature, salinity, and pressure data supplied by Iselin, Worzel remembers working overnight to apply ray theory to the propagation of sound in seawater. He successfully explained the anomalous transmission losses in terms of shadow zones (Woods Hole Oceanographic Institution report, 1941). Ewing and his students also thought about the hypothetical possibility that sound could propagate long distances in the sound channel without contacting the surface or the bottom (Woods Hole Oceanographic Institution report, 1941). Their experimental verification of this hypothesis (Ewing and Worzel, 1948) led to great advances in the acoustical detection of submarines and motivated the military to provide much of the funding in underwater acoustics for the next two generations of scientists.

In Press: Oceanology International '92 Conference, Brighton, England, March 1992.

Supported by: ONR contract N00014-86-C-0358 and ONT contract N00014-90-C-0098.

WHOI Contribution No. 7949.

MICRO-CTD INSTRUMENT DEVELOPMENT FOR THE OCEAN SCIENCES

Alan Fougere, Neil L. Brown, Daniel Frye and John Toole

Scientists involved in climate related research problems are increasingly in need of long-duration measurements of ocean characteristics such as temperature and salinity. Available instrumentation for these tasks is severely limited by accuracy, power, long-term stability, and high cost. We have developed a very small, low cost, deployable CTD (the Micro-CTD) to meet these increasingly important needs. In addition to small size and high sampling speed, the Micro-CTD incorporates a new inductive conductivity sensor which is highly accurate and can be treated with an anti-foul coating to minimize the effects of bio-fouling. This is a major advantage for long duration observations over existing high accuracy

conductivity sensors. Size and measurement performance of the instrument allow use with a wide variety of new sensing system platforms such as drifters and pop-up buoys. Micro-CTD architecture allows for either data storage or data telemetry by acoustic, inductive, or hardwired telemetry. Paper covers system architecture, preliminary specifications and calibration data.

AGU Poster Session, New Orleans, Louisiana, January 1992.

Supported by: ONR contract N00014-86-K-0751. WHOI Contribution No. 7950.

PROTOTYPE EXPENDABLE SURFACE MOORING WITH INDUCTIVE TELEMETRY

Daniel Frye, Alan Fougere, and Sean Kery

A lightweight, inexpensive surface mooring designed for general purpose telemetry has been deployed at Site D (39°N, 70°W) to test its reliability in the ocean environment. The mooring incorporates telemetry from instruments in the water column using inductive modems to transfer information via standard, plastic-jacketed wire rope. An inverse catenary design eliminates the need to accurately measure water depth prior to deployment and allows deployment to be carried out from a ship of opportunity. Mooring component size has been minimized to reduce costs and handling requirements. Inductive modems are installed at three depths to telemeter data from digital temperature and pressure sensors clamped to the wire. Data rates are 1200 b/s for data sent up the wire and 300 b/s for commands sent down the wire. Power required for the inductive link is modest; 350 mW when transmitting, 5 mW when quiescent. The paper describes the mooring and telemetry systems in detail and summarizes the results obtained to date.

AGU Poster Session, New Orleans, Louisiana, January 1992.

Supported by: ONR contract N00014-86-K-0751. WHOI Contribution No. 7951.

A SIMPLE LOW COST ACOUSTIC CURRENT METER

Neil L. Brown

This paper describes an experimental acoustic current meter presently under development. The objective of the development program is to develop a current meter that was inherently low cost, low power consumption, small and yet be capable of good performance, both static and dynamic. The rationale for this development is as follows.

Published in: Proceedings of Oceanology International, 1992. Advanced Technical Approaches II. March 10-13, 1992, Brighton, UK. IEEE, Washington, DC, 2:626-631, 1992.

Supported by: ONR contract N00014-86-K-0751. WHO! Contribution No. 7962.

ACOUSTIC MEASUREMENTS OF SURFACE GRAVITY WAVE SPECTRA IN MONTEREY BAY USING MODE TRAVEL TIME FLUCTUATIONS

James H. Miller, James F. Lynch, Ching-Sang Chiu, Eric L. Westreich, James S. Gerber, Ralph Hippenstiel and Edwin Chaulk

Earlier work by Miller et al.[1] suggested that the surface gravity wave frequency-direction spectrum could be measured using acoustic tomography signals. An experiment was performed in Monterey Bay, California, from the 12th to the 16th of December, 1988 to validate this earlier work. During that period, a 224 Hz, 16 Hz bandwidth source was deployed, continuously repeating its pulsed transmissions every 1.9375 seconds to a number of inexpensive, modified sonobuoy receivers. Although the acoustic propagation was complicated by the presence of the Monterey Submarine Canyon, a hybrid ray-mode interpretation explains the observations. The main effect of the surface waves on the acoustic signals is determined to occur in shallow continental shelf portion of the path. On the shelf, it is shown that the resolved acoustic normal modes exhibit the fluctuations in travel time described in the earlier work. The acoustic measurement of the surface wave spectrum compared well with measurements made by a pitch-roll wave buoy maintained in the area by the National Data Buoy Center (NDBC). The acoustic and buoy spectra agreed well on the location of the peak swell frequency; the rms wave amplitudes from the two measures agreed to within 7%.

Submitted to: Journal of the Acoustical Society of America.

Supported by: ONR contract N00014-89-K-0041. WHOI Contribution No. 7969.

ON THE LINEAR DEPENDENCE OF TEMPERATURE STRUCTURE AND ACOUSTIC BACKSCATTER AT THE WESTERN EDGE OF THE GULF STREAM USING OPTIMAL LEAST SQUARES FILTERING

J. Michael Jech, Clarence S. Clay, and Timothy K. Stanton

A quantitative approach, Wiener's optimal least squares filtering, was used to determine the linear relationship between physical and biological structure at the western edge of the Gulf Stream. Coordinated temperature and 70 and 120 kHz acoustic backscatter data were obtained 105 km northeast of Cape Hatteras along a transect perpendicular to the Gulf Stream front. The authors determined temperature, vertical temperature gradient and diurnal effects on the vertical distribution of biological sound scatterers in the top 200 m of a Gulf Stream frontal region. Data show that temperature is a better predictor of 70 and 120 kHz scattering than is temperature gradient at the meso to finescale. Diurnal differences in the predictability of scattering suggest other abiotic and biotic factors influence nekton and zooplankton distribution. A pair of generalized filters are derived for each frequency to predict nekton distribution. This technique is new in its application to marine ecology and the authors feel that optimal filtering may be a powerful tool in applying sonar to aquatic ecology.

Submitted to: Journal of the Acoustical Society of America.

Supported by: ONR grant N00014-89-J-1729. WHOI Contribution No. 7970.

ACTIVE HABITAT SELECTION BY CAPITELLA SP. I LARVAE. I. TWO-CHOICE EXPERIMENTS IN STILL WATER AND FLUME FLOWS

Cheryl Ann Butman and Judith P. Grassle

Sediment selection by settling larvae of the opportunistic polychaete Capitella sp. I was determined in laboratory still-water and flume experiments, where larvae were given a choice between two highly contrasting sediment treatments. In most cases, 2-h experiments were conducted with a natural, organic-rich mud and an abiotic, glass-bead mixture with a grain-size distribution similar to the mud, as the sediment treatments. Spatial settlement patterns were also determined in sediment arrays containing mud only. Two types of flume flows were tested, both

with a near-surface velocity of ~5 cm s⁻¹, but one flow was cyclical, varying between about 2 and 7 cm s⁻¹ with a period of 6.3 min, and one was steady with a boundary shear velocity of 0.26 cm s⁻¹. Plastic spheres were added to the experiments as passive larval mimics. Capitella sp. I larvae selected the muddy sediment as opposed to the glass beads in all experiments conducted, consistent with food requirements of the deposit-feeding adults and with field distributions. Selectivity was insensitive to a range of experimental conditions, including flow, water temperature, light regime, experimental duration, distance sediment treatments were separated, time of year and larval batch. Experiments furthermore suggested that contact with the sediment is required to elicit a settlement response. Flows tested were weak compared to the range likely encountered by larvae of this species, even in depositional areas in the field; however, horizontal flow speeds within larval search distances of the bottom exceeded horizontal swim speeds of the larvae (determined in still water). A model for sediment selection in the field is proposed where larvae move up and down close to the bottom, while being transported by the flow, and test sediments on contact. Selection is thus accomplished by active acceptance or rejection of touchdown sites. This model was qualitatively supported by observations of larvae in still water and manipulative flume experiments. These results suggest that active sediment selection may be responsible, at least in part, for field distributions of this species.

Published in: Journal of Marine Research, 50:669-715, 1992.

Supported by: NSF grants OCE-85000875, OCE-8812651, OCE-8813584, MMS (U.S. Dept. of the Interior) contract 14-12-0001-30262, and Coastal Research Center.

WHOI Contribution No. 7971.

MODELING PULSE TRANSMISSION IN THE MONTEREY BAY USING PARABOLIC EQUATION METHODS

Eric L. Westreich, Ching-Sang Chiu, James H. Miller, James F. Lynch and Michael D. Collins

Acoustic tomography signal transmissions made in Monterey Bay are modelled using the time-domain parabolic equation method of Collins (1991). Comparison with the measured arrival structures shows that Fourier synthesis can produce good agreement with data. Furthermore, identification of the measured modal arrivals is possible by decomposing the PE model output into

individual normal modes. This identification problem is critical to the success of tomography.

Submitted to: Journal of the Acoustical Society of America.

Supported by: ONR contract N00014-89-K-0041. WHOI Contribution No. 7972.

THREE-DIMENSIONAL TIDAL FLOW AROUND HEADLANDS

W. Rockwell Geyer

Field measurements of tidal flow around a headland indicate secondary circulation induced by flow curvature. The secondary flow, defined to be the flow in the plane normal to the direction of the vertically averaged current, is directed toward the headland near the bottom and seaward near the surface, consistent with theoretical predictions. The strength of the secondary flow varies from 5-15% of the streamwise flow. It is strongest when the water column is stratified, due both to the enhanced shear of the streamwise flow and the reduced frictional damping of the secondary flow. The transverse exchange accomplished by the secondary flow significantly influences the structure of the streamwise flow, causing a broadening of the transverse shear and changing the horizontal and vertical distributions of momentum. Although the secondary circulation enhances transverse mixing, it is likely to reduce the large-scale dispersion accomplished by the tidal flow. Upwelling by the secondary flow is likely to have an important influence on water properties near headlands; however vertical momentum transport (i.e., Ekman pumping) tends to be small relative to the influence of bottom stress.

Published in: Journal of Geophysical Research, 98(C1):955-966, 1993.

Supported by: NSF grant OCE-8917002.

WHOI Contribution No. 7976.

EVALUATION OF HIGH-RESOLUTION FREQUENCY ESTIMATION METHODS FOR DETERMINING FREQUENCIES OF EIGENMODES IN SHALLOW WATER ACOUSTIC FIELD

Subramaniam D. Rajan and Saurav D. Bhatta

In shallow water, the acoustic field in the far field, due to a point source, can be modelled as a sum of contributions from trapped modes propagating in the wave guide. In many applications, it is necessary to estimate the eigenvalues of these modes from a measurement of

the acoustic field made on a horizontal array using a monochromatic source. In this paper we evaluate the performance of two high resolution methods (MUSIC and ESPRIT) in estimating the eigenvalues of the modes from the measured acoustic field. In particular, we investigate the ability of these methods to estimate the frequencies accurately for various signal to noise ratios and their ability to resolve closely spaced frequencies using synthetic noisy data. Of the two methods ESPRIT had the better performance in terms the variance of the estimates. Simulation performed to study the effect of modelling errors on the performance of the algorithms showed that, for a medium that is weakly range dependent, the performance of the algorithms is not adversely affected. But errors in ranging and presence of colored noise in data have considerable impact on their performance. The MUSIC algorithm show marked degradation in performance when there are ranging errors. Taken overall, ESPRIT has the most acceptable performance levels, both in terms of its accuracy of the estimates and its robustness in the presence of modelling errors.

Published in: Journal of the Acoustical Society of America, 93(1):378-389, 1993.

Supported by: ONR contract N00014-89-K-0055.

WHOI Contribution No. 7983.

ACTIVE HABITAT SELECTION BY CAPITELLA SP. I LARVAE. II. MULTIPLE-CHOICE EXPERIMENTS IN STILL WATER AND FLUME FLOWS

Judith P. Grassle, Cheryl Ann Butman, and Susan W. Mills

Experiments on larval settlement of the opportunistic polychaete, Capitella sp. I, using three natural sediment treatments from the Buzzards Bay area (organic-rich mud from Sippewissett Marsh, organic-rich mud from New Bedford Harbor and low-organic sand from off the Weepecket Island), and a glass bead mixture similar in grain size distribution to the New Bedford Harbor mud, were carried out in still water and two flume flows (near-surface velocities of 5 cm s⁻¹ and 15 cm s⁻¹; boundary-shear velocities of 0.26 cm s⁻¹ and 0.64 cm s⁻¹). For all three flow conditions the larvae settled in significantly greater numbers in the two mud treatments than in the glass beads. In some experiments there was significant discrimination between one or both mud treatments and sand. There was significantly higher settlement in sand than in glass beads in two of three experiments in both slow and fast flow. There was no difference in the ability of larvae to discriminate between the

sediment treatments in the slow and fast flow. Strong row and column effects in the settlement of larvae in flow experiments (row 1 at the leading edge and column 4 toward the inner wall of the flume having the highest settlement) lend support to a model of interaction between larval swimming behavior and noar-bottom flow. Larvae that were not offered a settlement cue for 3-6 d showed no diminution in their subsequent settlement rate of capacity for habitat selection in fast flow. Capitella sp. I larvae are adapted to contribute to the large, local population increases that characterize the species by virtue of being competent to settle immediately after hatching. Once they are mixed up into the water column, however, their capacity for postponing metamorphosis and their habitat selectivity will promote dispersal and discriminate settlement in organic-rich patches.

Published in: Journal of Marine Research, 50:717-743, 1992.

Supported by: NSF grants OCE-85000875, OCE-8812651, OCE-8813584 and Coastal Research Center.

WHOI Contribution No. 7986.

EFFECTS OF BARITE ON ASPECTS OF THE ECOLOGY OF THE POLYCHAETE MEDIOMASTUS AMBISETA

Victoria R. Starczak, Charlotte M. Fuller and Cheryl Ann Butman

Barite (BaSO₄), a major component of drilling muds, can change the texture and erosion properties of surface sediments near offshore drilling sites. The effects of barite on the ecology of the marine polychaete Mediomastus ambiseta (Hartman) were examined in laboratory experiments: a migration experiment, 2 feeding experiments and a growth experiment. In the migration experiment, 18 of 19 worms left 100% barite within 2 d. This was significantly more worm movement than from natural mud to 100% barite; only 3 of 15 worms moved into 100% barite. Worms did not move into 10% barite sediments, but neither did they show high movement out of 10% barite. There was no difference in worm movement into and out of 1.0% barite sediment or natural mud with a 1 mm barite cover. In 2 separate feeding experiments, lasting 6 d and 18 d, the mean number of fecal pellets produced per worm per day did not differ between treatments with barite concentrations ranging from 0% barite (natural mud) to 50% barite, by weight, and a treatment with 1 mm barite layer over mud. In the second feeding experiment, growth (number of setigers added) differed between males and females. Females grew more than males, but

growth did not differ between treatments. In the fourth experiment, growth of worms in natural mud did not differ from worms in 10% barite sediments after 8 wk. Worm tube production (number of tube openings per worm) did not differ between natural mud and barite treatments in the 2 feeding experiments and the growth experiment. These experiments show essentially no deleterious effect on fecal pellet production, growth and tube production of adult M. ambiseta living in realistic concentrations of barite found in marine sediments subjected to drilling activity, although worms may migrate out of 100% barite patches.

Published in: Marine Ecology Progress Series, 85:269-282, 1992.

Supported by: MMS (U.S. Department of the Interior) contract 14-12-0001-300262.

WHOI Contribution No. 7988.

STATIC AND DYNAMIC RESPONSE OF NATURAL MULTICOMPONENT OCEANIC SURFACE FILMS TO COMPRESSION AND DILATION: LABORATORY AND FIELD OBSERVATIONS

Erik J. Bock and Nelson M. Frew

The quasi-static elasticity (Gibbs' elasticity) of sea surface films collected in North American coastal waters has been examined using a large number of surface pressure-area isotherms. The films examined show considerable variability in elastic properties. Differences among films appear to be the result of chemical variability due to differences in source; they are also affected by dynamic physical processes (e.g., film compression). Elasticity of adsorbed films from subsurface and microlayer water are observed to exhibit a bimodal distribution at 0.5 mN m⁻¹ reference spreading pressure; films from organized banded slicks are shown to have generally higher elastic moduli. Mechanisms of surface-selectivity and competitive adsorption are suggested to explain this effect; results of studies of film aging and work-hardening are presented in support. Significant hysteresis effects are observed for cyclical compression-dilation of the films suggesting the prevalence of relaxation processes that lead to compositional changes and higher elastic moduli. Field measurements of capillary and ripple spectra are presented to infer information on wave damping and dynamic viscoelasticity. Results obtained in regions where surface convergence is absent imply damping enhancement over a broad frequency range consistent with theory for films of low elastic moduli. Films found in surface convergence zones,

the result of surface upwelling, exhibit damping enhancements consistent with higher elastic moduli. Damping maxima are observed in multiple frequency bands; this banding is not readily explained with current theories. Results similar to these have been observed in laboratory studies with other chemical systems. In both the laboratory and field experiments, the tendency of the films to group into a few subsets with similar surface characteristics implies that natural films might be modeled by a small number of representative end members. This would facilitate remote sensing applications by providing a basis for determining the effects of films on surface waves under various conditions (e.g., diurnal variation, history of variability of wind stress).

In Press: Journal of Geophysical Research.
Supported by: ONR contract N00014-87-K-007 and ONR grants N00014-89-J-1080 and N00014-90-J-1717.

WHOI Contribution No. 8000.

CONVERTING JASON JUNIOR, A SMALL ROV, TO FIBER OPTICS

Robert L. Elder

Jason, Junior, a small deep water ROV, was originally designed to be used with a coaxial/twisted pair cable, and was used successfully from the minisub, Alvin. Even though the vehicle has performed quite well, there was a desire to improve the video quality as well as simplify the control electronics.

Drawing from our experience gained from building and operating the fiber optical controlled ROV JASON, it seemed reasonable to retrofit Jason Junior with fiber optics. Not only would fiber optics improve the video quality, it would also provide for increased bandwidth for the telemetry link.

This paper discusses what we hoped to gain from a refit, the process of redesign, and the results of how well we did.

Published in: Intervention/ROV '92 Conference and Exposition, San Diego, CA, June 10-12, 1992.

Supported by: ONR contract N00014-86-C-0038.

WHOI Contribution No. 8003.

LOW POWER NAVIGATION AND CONTROL FOR LONG RANGE AUTONOMOUS UNDERWATER VEHICLES

Albert M. Bradley

This paper discusses the ultimate limits to the range of conventionally powered deep ocean

Autonomous Underwater Vehicles (AUV's). It is intended as an introduction to the unique problems of vehicles designed for the 0.2 to 2 knot speed range. We first present the relationship between range, size, non-propulsion energy requirements and flotation efficiency for vehicles using various common battery technologies. We then demonstrate that, in this speed range, the non-propulsion energy requirements severely limit the ultimate range. We next discuss strategies for implementing navigation and control systems at power levels of 0.1 to 1 Watt. We present systems which are based on existing technologies in use in various areas of oceanographic research but not generally utilized in the AUV community. Last, we present a design example of a vehicle suitable for economical monitoring of a hypothetical deep ocean dumpsite.

In Press: Offshore and Polar Engineering Conference Proceedings, June 14-19, 1992.

Supported by: NSF grants OCE-8612101 and OCE-8820227.

WHOI Contribution No. 8007.

TELEMETRY CONCEPTS FOR DEEP SEA MOORINGS

Daniel E. Frye and Henri O. Berteaux

To expand the state of the art in moored array technology, Woods Hole Oceanographic Institution (WHOI) is pursuing a series of engineering tests conducted from buoys moored offshore Bermuda. Assessment of new sensors and data transmission techniques are included in the evaluation of new buoy and mooring components of markedly improved performance, measurement of buoy system dynamics, and long term exposure of new materials.

Published in: Sea Technology, 33(5):29-34, 1992.

Supported by: ONR grant N00014-90-J-1719 and ONR contract N00014-86-K-0751.

WHOI Contribution No. 8010.

INVERSION OF TOWED CABLE DYNAMICS: THEORY AND EXPERIMENTS

Franz S. Hover and Dana R. Yoerger

Position control of a towed underwater vehicle in large depths in complicated by the distributed nature of the cable and the non-linear fluid drag which acts upon it. In this paper, we develop an approach for inverting the non-linear plant dynamics, in the spirit of recent work on flexible manipulators. This approach is specifically for the trajectory-following problem, in which preshaping of the ship motions is necessary to achieve predefined trajectories of the towed body. The theoretical results are verified in laboratory tests and full-scale experiments at sea.

Submitted to: International Society of Offshore and Polar Engineering.

Supported by: ONR contract N00014-89-D-0255 and ONR grant N00014-90-J-1912.

WHOI Contribution No. 8013.

LISTENING FOR CLIMATIC TEMPERATURE CHANGE IN THE NORTHEAST PACIFIC: 1983-1989

John L. Spiesberger, Kurt Metzger and John A. Furgerson

We present data from an acoustic experiment designed to detect climatic trends of temperature in the ocean with basin-scale resolution. These data are presented as an intriguing new way to recognize changes in spatially averaged temperature. In 1983, we began measuring travel times of acoustic signals (133 Hz, 60 ms resolution) over 4000 km between a source and receiver mounted near Oahu and northern California respectively. In 1987, we also began measuring travel times along six additional sections in the northeast Pacific, each at a distance of 3000 to 4000 km. Travel times changed by about ± 0.2 s at each receiver at inter-annual periods. Changes in acoustic travel time exceeding about ± 0.03 s are due to changes in the spatially averaged temperature along each section. A change of ± 0.03 s is equivalent to a change in spatially averaged temperature of only about ± 0.02 °C in the upper kilometer of the ocean. The dynamical processes responsible for the temperature variability along the acoustic sections are not yet identified. No evidence for a long term change in climate is seen from intermittent data between 1983 and 1989 along a 4000 km section.

Published in: Journal of the Acoustical Society of America, 92(1):384-396, 1992.

Supported by: ONR contracts N00014-82-C-0019 and N00014-86-C-0358.

WHOI Contribution No. 8014.

PRECISE NAVIGATION AND CONTROL OF AN ROV AT 2200 METERS DEPTH

Dana R. Yoerger and David A. Mindell

This paper describes the navigation and control techniques used to perform a survey with

centimeter precision at an ocean depth of 2200 meters. The scientific objective of the survey was to map the conductivity and temperature above an active "hot smoker" hydrothermal vent. Using two broadband, 300 kHz transponders and a precision depth sensor, the position of the Jason ROV could be fixed nearly three times a second. Jason's control system used this information to hover and fly precise tracklines over a twelve hour period. The paper describes the operation, shows trackline and hover data, and concludes with a summary of future planned work.

Submitted to: Proceedings of the Intervention/ROV '92, MTS, San Diego, CA, June 1992.

Supported by: ONR contracts N00014-85-C-0410, N00014-86-C-0038 and N00014-90-J-1912.

WHOI Contribution No. 8018.

OCEAN ACOUSTIC TOMOGRAPHY IN THE GREENLAND SEA

P. Worcester, J. Lynch, W. Morawitz,

R. Pawlowicz, P. Sutton, B. Cornuelle,

O. Johannessen, W. Munk, B. Owens, R. Shuchman, and R. Spindel

The Greenland Sea plays a role in the circulation of the world's oceans far out of proportion to its tiny size, as it is one of only a few ocean sites where surface waters become sufficiently dense to contribute to the formation of the deepest water masses in the world's oceans. The Greenland Sea Ocean Acoustic Tomography Experiment was conducted during 1988-89 as one component of the international Greenland Sea Project to study the formation of Greenland Sea Deep Water. The response of the Greenland Sea Gyre to variations in wind stress and ice cover is also being studied as part of this experiment.

Submitted to: Nature.

Supported by: ONR contract N00014-87-K-0017.

WHOI Contribution No. 8022.

MINIMIZING THE DYNAMIC RESPONSE OF OCEANOGRAPHIC SURFACE MOORINGS

Mark A. Grosenbaugh

Oceanographic surface moorings, made from a combination of nylon rope and wire rope, are susceptible to high dynamic tensions. This is due to the fact that, when the length of the nylon rope is greater than 1000 m, the elastic natural frequency of the mooring coincides with the frequency range of ocean waves. Attaching large

oceanographic instruments of masses to the upper portion of the mooring has little effect on the elastic natural frequency and the shape of the mooring's transfer function. The only effect is a magnification of the dynamic tension by a factor that is equal to the combined mass of the wire rope and the attached instruments. The sensitivity of the dynamic response to the size and placement of attached instruments or masses can be enhanced greatly by using, throughout the mooring, line of the same material.

Submitted to: International Offshore Engineering Conference.

Supported by: ONR contract N00014-92-J-1269. WHOI Contribution No. 8023.

ROBUST MULTIUSER COMMUNICATIONS FOR UNDERWATER ACOUSTIC CHANNELS

David Brady and Josko A. Catipovic

This paper presents a method for easing acoustic channel congestion present whenever multiple acoustic systems or multiple UUV-s are operating concurrently. We consider the acoustic environment as a multi-user network, where multiple systems (users) need to operate asynchronously, with minimal regard for other channel users. In many multipoint random access networks, the collision of data packets from two cochannel and asynchronous transmitters is viewed as unresolvable. Network protocols are usually designed to avoid and discard packet collisions, and to utilize a side channel for retransmission requests to both transmitters. This paper presents a random-access communication network capable of resolving collisions between several asynchronous and cochannel packets without side channel communication.

The algorithm differs from standard capture schemes by demodulating the data from both strong and weak transmitters. The resulting acoustic network protocol requires roughly the same transmission bandwidth as other networks at the expense of an increased computational complexity at the receiver processor. Examples are given and illustrate that this technique is extremely desirable for underwater acoustic local area networks and underwater autonomous vehicles with both side-scan sonar as well as acoustic telemetry links.

Submitted to: Symposium on Autonomous Underwater Vehicle Technology.

Supported by: DARPA grant MDA 972-91-J-1004. WHOI Contribution No. 8024.

RAY REPRESENTATION OF SOUND SCATTERING BY WEAKLY SCATTERING DEFORMED FLUID CYLINDERS: APPLICATIONS TO ZOOPLANKTON

Timothy K. Stanton, Clarence S. Clay, and Dezhang Chu

Data indicate that certain important types of marine organisms behave acoustically like weakly scattering fluid bodies (i.e. their material properties appear fluid-like and similar to those of the surrounding fluid medium). Use of this boundary condition, along with certain assumptions, allows reduction of what is a very complex scattering problem to a relatively simple, approximate ray-based solution. Because of the diversity of this problem, the formulation is presented in two articles: this first one in which the basic physics of the scattering process is described where the incident sound wave is nearly normally incident upon a single target (i.e. the region in which the scattering amplitude is typically at or near a maximum value for the individual) and the second one (T.K. Stanton et al., submitted to J. Acoust. Soc. Am.) where the formulation is heuristically extended to all angles of incidence and then statistically averaged over a range of angles and target sizes to produce a collective echo involving an aggregation of randomly oriented different sized scatterers. In this article, a simple ray model is employed in the deformed cylinder formulation [T.K. Stanton, J. Acoust. Soc. Am. 86:691-705 (1989)] to describe the scattering by finite length deformed fluid bodies in the general shape of elongated organisms. The work involves single realizations of the length and angle of orientation. Straight and bent finite cylinders and prolate spheroids are treated in separate examples. There is reasonable qualitative comparison between the structure of the data collected by Chu et al. [ICES J. mar. Sci., 49:97-106 (1992)] involving two decapod shrimp and this single-target normal-incidence theory. This analysis forms the basis for successful comparison (presented in the companion article) between the extended formulation that is averaged over an ensemble of realizations of length and angle of orientation and scattering data involving aggregations of up to 100's of animals.

Submitted to: Journal of the Acoustical Society of America.

Supported by: ONR grant N00014-89-J-1729.

WHOI Contribution No. 8029.

HYDRODYNAMIC MODULATION OF SHORT WIND-WAVE SPECTRA DUE TO LONG WAVES MEASURED BY MICROWAVE RADAR

Tetsu Hara and William J. Plant

Radar remote sensing has proved to be a powerful technique to observe various features at the air-sea interface. In particular surface gravity waves can be detected through the modulation transfer function (MTF), which is defined as the amplitude modulation of the microwave radar return relative to the long wave orbital velocity. The MTF consists of hydrodynamic modulation and geometric effects, where the former (hydrodynamic MTF) corresponds to the modulation of the two-dimensional wavenumber spectrum at the Bragg resonant wavenumber.

We employ the published analytical form for the geometric effects in order to calculate the hydrodynamic MTF at X-band from the field data of SAXON-FPN (1990) as well as other past experiments. One of the striking features of the results is that the hydrodynamic MTF estimated from the horizontally polarized (H-pol) return is roughly 1.5 to 2 times larger than that from vertically polarized (V-pol) return. This discrepancy cannot be explained by the conventional composite surface scattering theory. Since past measurements of normalized cross section suggest that scattering mechanisms other than Bragg resonance take place in H-pol return, the hydrodynamic MTF from the V-pol signal is more likely to correspond to the real modulation of the wavenumber spectrum.

A simplified relaxation model is proposed for the modulation of the gravity-capillary wavenumber spectrum based on the relaxation rate and the equilibrium wavenumber spectrum. The model is then employed to estimate the wind shear stress modulation along the long wave profile from the observed hydrodynamic MTF. We also examine the possible effects of surface films on the hydrodynamic MTF, which is likely cause of the significant increase of the observed hydrodynamic MTF in the Gulf of Mexico compared with those in other locations.

Submitted to: Journal of Geophysical Research.

Supported by: ONR grant N00014-89-J-1897.

WHOI Contribution No. 8034.

SETTLEMENT OF A MARINE TUBE WORM AS A FUNCTION OF CURRENT VELOCITY: INTERACTING EFFECTS OF HYDRODYNAMICS AND BEHAVIOR

Joseph R. Pawlik and Cheryl Ann Butman

Settlement experiments were conducted with larvae of Phragmatopoma lapidosa californica, a reef-building sabellariid polychaete, in turbulent flume flows over a hydrodynamically smooth bed. The flows tested had boundary shear velocities (u_*) of 0.26, 0.47, 0.64, 0.86, 1.03, 1.22, and 1.42 cm s^{-1} (near-surface velocities of 5, 10, 15, 20, 25, 30, and 35 cm s⁻¹, respectively), a range that spans the critical shear velocity for initiation of particle motion (u_{*crit}) and for suspended-load transport $(u_{*,u*p})$ of passive larval mimics. Larvae were given a choice of two substrata (tube sand, a natural inducer of metamorphosis, and a non-inductive control) in a 2 × 2 sediment array and were allowed only a single pass over the array. Maximum numbers of metamorphosed juveniles and total animals (larvae + juveniles) were present in arrays subjected to 15, 20, and 25 cm s⁻¹ flows, whereas very few were present in arrays exposed to slower or faster flows. For all replicates, >96% of metamorphosed juveniles were present in the tube sand treatment, whereas the majority of unmetamorphosed larvae were present in the non-inductive sand treatment. Delivery of larvae to the array was the result of interactions between the flow regime and larval behavior. At intermediate flows where larval delivery to the array was highest, larvae were observed tumbling along the flume bottom, as were the passive larval mimics. At slower flows, larvae actively left the bottom and swam into the water column, passing over the array. At the fastest flows tested, hydrodynamics alone may have reduced settlement because larvae, like the mimics, were eroded from the bed and carried as suspended load over the array, or because enhanced turbulent mixing distributed larvae more evenly in the water column, reducing their concentration close to the bottom. Behavioral responses to chemical cues were ultimately responsible for metamorphosis of larvae that were delivered by the flow to an inductive substream.

Submitted to: Limnology and Oceanography.

Supported by: NSF grant OCE-8812651, ONR grant N00014-89-J-1112, Woods Hole Oceanographic Institution Fellowship and NSF Presidential Young Investigator Award OCE-9158065.

WIIOI Contribution No. 8035.

ENHANCED DISSIPATION OF KINETIC ENERGY BENEATH SURFACE WAVES

Y. C. Agrawal, E. A. Terray, M. A. Donelan, P. A. Hwang, A. J. Williams III, W. M. Drennan, K. K. Kahma and S. A. Kitaigorodskii

Transfer of momentum from wind to the surface layer of lakes and oceans plays a central part in driving horizontal and vertical circulation of water masses. Much work has been devoted to understanding the role of waves in momentum transfer across the air-sea interface, but less is known about the energetics of the near-surface turbulence responsible for the mixing of momentum and mass into the underlying water column. In particular, it has remained unclear whether the structure of the turbulence in the surface layer can be described by analogy to wall-bounded shear flows or whether waves, either through breaking or wave-current interaction, introduce new length- and timescales which must be modelled explicitly. Here we report observations of turbulence in Lake Ontario, taken under conditions of strong wave breaking, which reveal a greatly enhanced dissipation rate of kinetic energy close to the air-water interface, relative to the predictions of wall-layer theory. Because wave breaking is intermittent, short-term measurements of the kinetic energy dissipation in the near-surface layer may therefore result in considerable underestimates, and any general treatment of upper mixed layer dynamics will have to take wave breaking explicitly into account.)

Published in: Nature, 359(6392):219-220, 1992.

Supported by: NSF grant OCE-94187711 and ONR contract N00014-87-K-007 NR 083-004.

WHOI Contribution No. 8041.

NEAR-REAL-TIME GIS IN DEEP-OCEAN EXPLORATION

Jonathan C. Howland, Martin Marra, Daniel F. Potter, W. Kenneth Stewart

During a 1991 oceanographic research expedition to the Juan de Fuca Ridge, the Deep Submergence Laboratory (DSL) of the Woods Hole Oceanographic Institution (WHOI) applied interactive mapping with a geographic information system (GIS) in conjunctions with real-time navigation inputs. As DSL's remotely operated vehicle (ROV), Jason, surveyed a hydrothermal vent field, acoustic navigation inputs were combined with maps generated to the specifications of participating scientists. The maps, which were generated in near-real time, were used

to plan vehicle operations in the hazardous vent environment and to monitor survey progress and data quality.

Geological observations made in real-time by scientists monitoring ROV sensors were logged into data files, combined with processed navigation, and used to produce preliminary updates to maps of the vent field. This experimental combination of GIS technology with navigation and visualization software was highly successful. Future scientific efforts will include further processing of sensor data, integration of image products into the GIS database, and the production of high-quality mapping products.

Published in: Proceedings of '92
ASPRS/ACSM/RT92 Convention, The
American Society of Photogrammetry and
Remote Sensing and the American Congress on
Surveying and Mapping, Washington, DC,
August 1992, :428-435, 1992.

Supported by: ONR grants N00014-90-K-0070, N00014-90-J-1848, N00014-90-J-1912, OP-23 contract N00014-89-D-0255 and a Mellon grant.

WHOI Contribution No. 8046.

CASE STUDY: CONFIGURATION OF A SUPER COMPUTER FOR ALTERNATING SECURE AND NETWORKED OPERATIONS

Marguerite K. McElroy and Janet J. Fredericks

A need for a flexible multi-user classified super computing facility resulted when several projects required access to classified data. Coupled with a need for high speed processing of larger data sets by computationally intensive algorithms, a Convex C-220 parallel processor was selected. Such a powerful system could not be justified if limited only to the relatively few classified processing tasks. This necessitated designing a configuration that could easily be switched into a completely unclassified operating mode with network access. This goal of alternating modes made the target configuration relatively unique.

Currently there are no parallel processors of this class the DOD "Evaluated Products list" of trusted systems. Severe budget restrictions and a facility with no closed or access controlled areas contributed to the challenge of designing a security plan that could be approved by the oversight agency. Additionally, unique aspects of the hardware design required modification to meet the goal of C-2 "system high" level operations.

This paper will provide a guide for system managers in preparing a System Practices and Procedures (SPP) document for a system that initially appears unsuitable for the targeted level of

secure operation. The study will define the DOD requirements for C-2 system high mode operation and specify how each was met by implementation of system options, customized configuration and modification of system hardware and software. A step-by-step approach and specific examples will be used to bridge the gap between system manager and security officer points of view. The problem approach will be analyzed and alternatives suggested. The subject system is a Convex C-220.

Submitted to: Eight Annual Computer Security Applications Conference, IEEE Computer Society, November 1992, San Antonio, Texas.

WHOI Contribution No. 8050.

IS DEL GROSSO'S ALGORITHM FOR SOUND SPEED IN SEAWATER CORRECT?

John L. Spiesberger

Given reasonable assumptions concerning acoustic propagation and thermal variability in the ocean, acoustic tomography data from a 3000 km section in the northeast Pacific are consistent with Del Grosso's algorithm for the speed of sound in seawater [J. Acoust. Soc. Am. 56:1084-1091 (1974)]. Because tomographic derivations for the algorithm are sensitive to modelling assumptions, the accuracy of Del Grosso's algorithm is difficult to test without more data.

In Press: Journal of the Acoustical Society of America.

Supported by: ONR contract N00014-86-C-0358. WHOI Contribution No. 8051.

MEASURED WAVEFRONT FLUCTUATIONS IN 1000-KM PULSE PROPAGATION IN THE PACIFIC OCEAN

T. F. Duda, S. M. Flatté, J. A. Colosi, B. D. Cornuelle, J. A. Hildebrand, W. S. Hodgkiss Jr., P. F. Worcester, B. M. Howe, J. A. Mercer, R. C. Spindel

A 1000-km acoustical transmission experiment has been carried out in the North Pacific, with pulses broadcast between a moored broadband source (250-Hz center frequency) and a moored sparse vertical line of receivers. We report on two data records: a period of nine days at a pulse rate of one per hour, and a 21-hr period on the seventh day at six per hour. Many wavefront segments were observed at each hydrophone depth, and arrival times were tracked and studied at functions

of time and depth. Arrivals within the final section of the pulse are not trackable in time or space at the chosen sampling rates, however. Broadband fluctuations, which are uncorrelated over 10-min sampling and 60-m vertical spacing, are observed with about 40 (ms)² variance. The variance of all other fluctuations (denoted as low frequency) is comparable or smaller than the broadband value; this low-frequency variance can be separated into two parts: a wave front-segment displacement (with vertical correlation length greater than 1 km) that varies substantially between rays with different ray identifiers, and a distortion (with vertical correlation length between 60 m and 1 km) of about 2 (ms)2 variance. The low-frequency variance may be explained as the effect of internal waves, including internal tides. The variance of the broadbound fluctuations is reduced somewhat but not eliminated if only high intensity peaks are selected; this selection does not affect the statistics of the low-frequency fluctuations.

Published in: Journal of the Acoustical Society of America, 92(2) pt. 1:939-955, 1992.

Supported by: ONT contracts N00014-87-K-0670 and N00014-89-K-0120; ONR contracts N00014-87-K-0120, N00014-87-K-0445, N00014-88-K-0263 and N00014-90-J-1022; W.M. Keck Foundation, support from the Institute of Tectonics and support for the first author for completion of this paper by Woods Hole Oceanographic Institution.

WHOI Contribution No. 8061.

A QUANTITATIVE MEASURE OF SIMILARITY FOR TURSIOPS TRUNCATUS SIGNATURE WHISTLES

John R. Buck, Peter L. Tyack

Bottlenose dolphins (Tursiops truncatus) are believed to produce individually distinctive narrowband "signature whistles." These whistles may be differentiated by the structure of their frequency contours. An algorithm is presented for extracting frequency contours from whistles and comparing two such contours. This algorithm performs non-uniform time-dilation to align contours and provides a quantitative distance measure between the contours. Results from two recognition experiments using the algorithm on recorded dolphin whistles are presented.

Submitted to: Journal of the Acoustical Society of America.

Supported by: NAVSEA contract N00140-90-D-1979, NIH grant 5R29 NS252900, ONR N00014-90-J-1628.

WHOI Contribution No. 8062.

TRAPS FOR MEASURING HORIZONTAL LARVAL FLUX

Keith D. Stolzenbach and Cheryl Ann Butman

It is understandable that larval ecologists should search for convenient, reliable and inexpensive ways to quantify the rate at which horizontal water movement transports suspended larvae to potential settlement sites. Even with the advent of moorable zooplankton pumps specifically designed to measure meroplankton concentration (C.A. Butman and K.W. Doherty, unpubl.; R.R. Olson, P. Countway, and J. Maret, unpubl.), the difficulty of computing horizontal fluxes by integrating the product of velocity and concentration measurements has frustrated more than one scientific discipline (e.g., Bush, 1977; Nixon, 1980).

Yund et al. (1991) assert that cylindrical sediment traps can be used to measure the time-average horizontal flux of suspended larvae. They base their conclusion largely on their observation that the number of larvae captured in traps deployed in a laboratory flume increased in direct proportion to both flow velocity and larval concentration. Trap collections in the field are also offered as evidence. It is important to note that the assertion that traps accurately measure horizontal flux of any particle (alive or dead) is an entirely new concept. Traps have been used extensively by oceanographers and limnologists to measure the the vertical flux of particulates through the water column (e.g. reviews of Bloesch and Burns, 1980; Reynolds et al., 1980; Blomqvist and Håkanson, 1981; Butman et al., 1986).

Our comment on the paper of Yund et al. is motivated by several concerns. First, there are severe methodological problems with the flume studies upon which the conclusion is based that traps accurately measure horizontal larval flux. Second, the field measurements provide only weak evidence for extrapolation of the flume results to full-scale situations. And third, the discussion of underlying mechanisms governing accumulation of larvae in traps is both incomplete and confusing. We are concerned that the paper of Yund et al. will send a message to trap users that is oversimplified and, at worst, incorrect.

In Press: Limnology and Oceanography.

Supported by: NSF grant 0CE-8812651.

WHOI Contribution No. 8069.

ANALYSIS OF FINITE-DURATION WIDE-BAND FREQUENCY SWEEP SIGNALS FOR OCEAN TOMOGRAPHY

Timothy F. Duda

A group of amplitude and frequency modulated signals which generate narrow synthesized pulses are described. The pulse-compression properties of these signals should approach those of maximal (M) sequence phase-modulated signals now commonly used in ocean experiments. These amplitude-tapered linear frequency-sweep (chirp) type signals should be accurately reproducible with most acoustic sources, since they have controllable limitedbandwidth frequency content and differentiable phase. The Doppler response of the signals is calculated using a wide-band approach, where the frequency shift from relative motion is not constant throughout the waveform. The resultant Doppler effect on the matched-filter output is a function of the signal duration. The signals are suitable for use with tunable resonant transducers, and have adequate Doppler response for use with Langrangian ocean drifters.

In Press: IEEE Journal of Oceanic Engineering.

Supported by: ONR contracts N00014-91-J-1246 and N00014-92-J-1162.

WHOI Contribution No. 8070.

OPTICAL MEASUREMENTS OF RIPPLES USING A SCANNING LASER SLOPE GAUGE PART I: INSTRUMENTATION AND PRELIMINARY RESULTS

Robert J. Martinsen and Erik J. Bock

We describe the design, implementation, and deployment of a laser slope gauge developed at the Woods Hole Oceanographic Institution for the purpose of studying the propagation characteristics of capillary ripples, and how currents and natural slicks on the ocean surface modify ripple spectra. The laser slope gauge constitutes a nondisruptive optical technique for determining the slope spectrum for the range of waves with wavelengths between 2 mm and 20 cm using both spatial and temporal information. Operation of the sensor and data acquisition system is discussed and a sample data record collected in the Gulf Stream off Cape Hatteras, NC is interpreted and analyzed.

Published in: Optics of the Air-Sea Interface: Theory and Measurement, L. Estep, ed. Sponsored by SPIE, San Diego, CA, July 23-24, 1749:258-271, 1992.

Supported by: MIT Scholarship - Gibbs Brothers Foundation, ONR grant N00014-90-J-1717.

WHOI Contribution No. 8071.

OPTICAL MEASUREMENTS OF RIPPLES USING A SCANNING LASER SLOPE GAUGE PART II: DATA ANALYSIS AND INTERPRETATION FROM A LABORATORY WAVE TANK AND FIELD EXPERIMENTS

Erik J. Bock and Tetsu Hara

A description of a new scanning laser slope gauge is given and the preliminary results obtained from laboratory wave tank measurements are presented. The device relies on the measurements of two components of surface slope to compute spatial and temporal lags used to estimate the full three-dimensional spectrum. The device is capable of resolving frequencies in the range between zero and 63 Hertz, and wavelengths in the range between 0.63 and 20 centimeters. The technique makes use of a two-dimensional laser scanner which samples the perimeter of a 10 centimeter square (an unfilled aperture). The laboratory results show mechanically-generated waves propagating on both distilled water and a one micro-molar solution of Triton-X100 in distilled water. Results indicate the device is well suited to measure the full three dimensional spectra of capillary-gravity waves and is capable of providing ground-truth measurements for the verification of remotely sense 1 cean surface features.

Published in: Optics of the Air-Sea Interface: Theory and Measurement, L. Estep, ed. Sponsored by SPIE, San Diego, CA, July 23-24, 1749:272-282, 1992.

Supported by: ONR grant N00014-91-J-1770. WHOI Contribution No. 8072.

SOLAR-POWERED, TEMPERA-TURE/CONDUCTIVITY/DOPPLER PROFILER MOORINGS FOR COASTAL WATERS WITH ARGOS POSITIONING AND GOES TELEMETRY

J. D. Irish, K. E. Morey and N. R. Pettigrew

Over the past 12 years we have developed and refined instrumented surface buoy systems for our coastal research programs. A buoy consists of a steel ball on which are mounted solar panels, an electronics and battery housing, a radar reflector, guard light and antenna. The system is moored by a Kevlar-core electromechanical cable with an elastic element at the bottom. A microprocessor-

controlled data system switches the power to the sensors, digitizes the output, and transmits the data via GOES. An ARGOS link transmits diagnostic information, and the buoy's location in case it should break loose. Temperature and conductivity are measured at several depths along the mooring, and most recently currents were measured with a downward-looking Acoustic Doppler Current Profiler mounted just below the buoy. Deployments with various configurations have been made in the Gulf of Maine and Massachusetts Bay for periods up to 13 months. Our experience has shown that reliable moorings with telemetry are feasible for at least one year in coastal waters.

Published in: Oceans '92, :730-735, 1992.

Supported by: NSF OCE-8818600 and NOAA, Seagrant R/FM-104, Massachusetts Bays Program through Massachusetts Coastal Zone Management Office, and USGS.

WHOI Contribution No. 8078.

IN-SITU PROCESSING OF ADCM DATA FOR REAL TIME TELEMETRY

Robin C. Singer, Albert J. Plueddemann, Andrea L. Oien and Stephen P. Smith

A Data Processing Module (DPM) has been developed to provide data reduction through real time, in-situ processing of Acoustic Doppler Current Meter (ADCM) data. This enables the transmission of ADCM data from remote locations via satellite, despite the low throughput of such telemetry systems and the high data volume of ADCM's. The DPM was designed for reliability and low power. A DPM-enhanced ADCM can be easily interfaced to buoy systems or instrument packages over at EIA-485 serial link.

The DPM was developed for use in an Ice-Ocean Environmental Buoy (IOEB), an Arctic drifting buoy with large suite of subsurface instruments, a meteorological package, two buoy controllers, and a pair of ARGOS satellite transmitters housed in the surface floatation element. The IOEB was designed for extended deployments in the pack ice. The long deployment duration and limited buoy recovery opportunities dictated the use of satellite telemetry to insure timely data acquisition. The limited ARGOS system throughput necessitated reduction of the ADCM data by a factor of about 170:1.

The DPM can be easily interfaced to buoy systems because it communicates over a standard EIA-485 link and its intelligence is derived from firmware written in "C" and therefore easily modified. The EIA-485 communication is implemented with the SAIL [1] software protocol

which allows a variety of instruments, responding to different SAIL addresses, to communicate on a common link. There are also a variety of features that increase the DPM reliability under adverse conditions and reduce its power consumption to enable long deployments. Self-powered and housed in its own pressure case, the DPM provides a robust tool which can bring ADCM data from remote locations in real time, to scientists in their laboratories.

Published in: Oceans '92, :632-636, 1992.

Supported by: WHOI Vetlesen Fund, ONR grant N00014-89-J-1288.

WHOI Contribution No. 8079.

STATUS OF ACOUSTIC SCATTERING MODELS OF ZOOPLANKTON

Timothy K. Stanton, Dezhang Chu and Kenneth G. Foote

Assessment of zooplankton abundance by use of sonars requires understanding of the acoustic scattering properties of the animals. The scattering properties depend upon the size, acoustic wavelength, shape, orientation, and material properties of the animal. There has been much progress recently toward the understanding of the acoustic properties of the elongated shrimp-like zooplankters. The progress is summarized in this paper. Backscatter data collected from several investigators in the laboratory are presented along with scattering models based, in part, on predictions using the deformed cylinder model (T.K. Stanton, J. Acoust. Soc. Am. 86:691-705 (1989)).

Published in: Oceans '92, :487-491, 1992.

Supported by: ONR grant N90014-89-J-1729.

WHOI Contribution No. 8080.

DETERMINATION OF COMPRESSIONAL WAVE AND SHEAR WAVE SPEED PROFILES IN SEA ICE BY CROSSHOLE TOMOGRAPHY-THEORY AND EXPERIMENT

Subramaniam D. Rajan, George V. Frisk, James A. Doutt and Cynthia J. Sellers

Sea ice is heterogeneous material whose acoustic properties are functions of time and space. Here we present the results of crosshole tomography experiment conducted in multi-year ice with the objective of determining the spatial structure of the compressional and shear wave speeds from travel time measurements made with

high frequency pulses. The results of the experiment indicate that the wave speeds can be determined from such a crosshole experiment with good resolution. The compressional and shear wave speed contour maps indicate that the spatial variations of the wave speeds are complex with regions of low speed. High brine volume is a likely cause for the low speed regions observed. Resolution and variance studies performed on the estimates are also presented. We also present estimates of material properties such as Poisson's ratio, salinity, elastic and shear moduli obtained from the estimates of compressional and shear wave speeds. By measuring the amplitude of the transmitted and received signals along specific paths, estimates of the attenuation coefficients at different depth intervals are obtained. Spatial variability observed in the estimates is believed to be due to scattering by inhomogeneities in the material.

In Press: Journal of the Acoustical Society of America.

Supported by: ONR grant N00014-90-J-1517.

WHOI Contribution No. 8083.

POWER TRANSFORMER DESIGN FOR TETHERED UNDERWATER VEHICLES

Ned C. Forrester

Tethered underwater vehicles benefit from the smallest possible tether through reduction of both tether handling gear and tether drag. If the vehicle is powered through the tether, a transmission voltage in the range of one to three kilovolts usually results in the smallest tether. AC power transmission systems can use transformers for conversion of the high voltage to service levels.

Transformers for underwater vehicles are designed with different goals than conventional transformers. Weight is a prime consideration for any neutrally buoyant vehicle and thus most other constraints, including efficiency, are relaxed in pursuit of lower weight. Design starts with a prioritized list of constraints. Non-linear optimization can then apply these constraints to the basic electro-magnetic and thermal equations governing a transformer. The result is a tentative core and winding design that can be compared with the original goals and iterated to achieve any necessary compromises.

An example design for a 400 Hz, three-phase, oil cooled, pressure compensated, toroidal system delivering 20 kilowatts DC to a vehicle is detailed. The design target and "as manufactured" parameters are compared.

Published in: Oceans '92, :877-882, 1992.

Supported by: ONR contract N000-14-86-C-0038, ONT contract N00014-88-C-0660 and NSF grant OCE-8912891.

WHOI Contribution No. 8084.

A HIERARCHICAL APPROACH TO SEAFLOOR CLASSIFICATION USING NEURAL NETWORKS

W. K. Stewart, M. Marra and M. Jiang

Preliminary progress toward the automated segmentation and classification of undersea terrain is demonstrated with sidescan-sonar imagery from a mid-ocean spreading center. A multi-layer, back-propagation neural network was applied to data from three distinct geoacoustic provinces: axial valley, ridge flank, and sediment pond. A suite of experiments compared the effectiveness of different feature vectors compromising spectral estimates, gray-level run length, and gray-level differences with window sizes and training patterns considered. Run-length features showed the best individual performance across different data sets, while hybrid features appear most promising.

Published in: Oceans '92, :109-113, 1992.

Supported by: ONR grants N00014-90-K-0070, N00014-90-J-1848, N00014-90-J-1912 and OP-23 contract N00014-89-D-0255.

WHOI Contribution No. 8086.

TECHNOLOGY FOR THE MEASUREMENT OF OCEANIC LOW FREQUENCY ELECTRIC FIELDS

Robert A. Petitt, Jr., Jean H. Filloux and Alan D. Chave

Low frequency (<0.01Hz) electric field data from the ocean have wide applications in basic research into the structure of the solid earth, in exploration geophysics, in studies of the depth-averaged velocity structure of ocean currents, and in tactical oceanography. However, a number of unique problems caused by the oceanic environment must be overcome to achieve stable measurements to frequencies as low as 10^{-8} Hz. First, the high conductivity (3-5 S/m) of seawater results in substantially weaker electric fields in the ocean than in other geological materials. This means that precision, low noise electronics must be used and that even the faint fields generated by corrosion of metallic parts may be capable of swamping the signal of interest. Second, even the best non-polarizing electrodes exhibit a time variable offset voltage which is often much larger than that produced by the external electric field.

Finally, the very long period nature of oceanic electric field phenomena places extreme stability requirements on instrument electronics. None of these problems are as important for electric field measurements on land, and a very different approach is required in the oceanic environment. As a case history, this paper will describe instrumentation that has overcome these obstacles in a low power package capable of multivear deployments in the deep ocean. The electric potential is measured between the ends of orthogonal, 3 m long pairs of seawater-filled plastic pipes or salt bridges. The inner ends of the salt bridge are connected to a mechanical DPDT fluid switch or water chopper which physically reverses the electrodes during the measurement cycle. As the switch changes position, a set of non-polarizing silver-silver chloride electrodes are alternately connected to opposite ends of the salt bridge. This not only removes electrode drift, but eases the necessity for ultra stable analog electronics. After amplification by a low power differential amplifier. analog-to-digital conversation is achieved using a voltage controlled oscillator followed by a simple counter. A low power microcontroller handles all basic instrument functions including data storage in EEPROM memory. All of the electronics, including batteries, orientation compass, and a radio transmitter for recovery location, are contained in a single 17 inch glass sphere pressure case. The least count sensitivity of this instrument is 20 nV/m, corresponding to an electric potential of 60 nV across the the 3 m salt bridge. Based on spectral analysis of seafloor records, the real instrument noise level is substantially lower than this figure. The baseline stability over long deployments is comparable.

Published in: *Oceans* '92, :642-647, 1992. Supported by: NSF grant OCE-9196235.

WHOI Contribution No. 8087.

DATA DIRECT FROM THE OCEAN BOTTOM TO THE LABORATORY

Richard L. Koehler and Albert J. Williams 3rd

Data was transmitted in near real time from the ocean bottom to a scientist's desk, and commands were sent back to the ocean bottom. The communication system used a 1185 bits/s acoustic modem to send the data to a nearby surface buoy. VHF packet radio, relayed the data at 1200 bits/s to a shore station where it was stored. The stored data was transferred by telephone modem to the scientist's desk. Commands were sent back to the bottom by a slower reverse channel. The system worked for three weeks until the buoy mooring was damaged.

The difficult parts of the system, the acoustic modem and the packet radio, worked on real data. Some improvements have been made in the acoustic modem, some improvements are necessary to make the data more readable and to correct the mooring fault, and other refinements are desirable.

Published in: Oceans '92, :701-705, 1992.

Supported by: ONR contract N00014-89-J-1058.

WHOI Contribution No. 8088.

A SOFTWARE BASED OPERATION INTERFACE FOR AN UNMANNED UNDERWATER VEHICLE

Roger P. Stokey

There are many advantages to using low cost workstations for the operator interface to an unmanned underwater vehicle. They provide greater design and operational flexibility and can provide more detail to the user. An implementation using a UNIX computer running XWindows is detailed. This computer sends operator commands to the vehicle and displays the status reporting back. Status messages are received at regular intervals and stored in an array, thus allowing the operator to observe performance over time. Vehicle faults are reported via popup windows. Data is sent in a low level format allowing it to be displayed in raw and processed formats. Since the program is event driven, some traditional programming approaches don't work; techniques for circumventing these limitations are discussed. A state free design is used; control items function as both status and command inputs with separate code for each. This allows multiple control stations to be used.

Published in: Oceans '92, :894-899, 1992.

Supported by: ONT contract N00014-88-C-0660 and NSF grant OCE-8912891.

WHOI Contribution No. 8089

A SUBMERSIBLE, ALL ELECTRIC, REMOTELY OPERATED VEHICLE TETHER MANAGEMENT SYSTEM

M. Purcell, T. Austin and R. Stokey

This paper describes the design, construction and performance of a new tether management system (TMS) based on direct drive brushless DC electric motors and capable of operating at unlimited depth. This system was specifically designed to accommodate an electro-optical cable connected to a remotely operated vehicle (ROV). TMS operation is computer controlled with an

operator interface to input instructions. Combining the direct drive electric winch with automatic computer control is a step towards the development of fully automated system for vehicle launch and recovery.

Published in: Oceans '92, :883-887, 1992.

Supported by: ONT contract N00014-88-C-0660.

WHOI Contribution No. 8090.

OCEAN TECHNOLOGY: BENEFICIARY OF AND BENEFACTOR TO ENERGY AND DATA STORAGE, COMMUNICATIONS, AND MATERIAL DEVELOPMENTS IN SISTER FIELDS

Albert J. Williams 3rd

Ocean technology is a subset of technology in general with a few peculiar constraints and a few areas of technological elaboration. Certain commercial developments have been extremely beneficial to ocean technology, such as electronics developments driven by portable calculators and laptop computers. In a few cases such as underwater acoustic telemetry and robotics, ocean applications drive technology that benefit the general field.

Published in: Oceans '92, :25-29, 1992.

WHOI Contribution No. 8096.

LEO-15 AN UNMANNED LONG TERM ENVIRONMENTAL OBSERVATORY

Christopher J. von Alt and J. Frederick Grassle

This paper presents a concept which involves the installation of a series of instrumented seafloor platforms which are linked to shore by an electro-optic cable. The use of an electro-optic cable permits these ocean-based systems to gather data continuously, for a long period of time, and at extended distances from shore. A system life time exceeding 20 years is possible. The electro-optic cable will transfer continuous electrical power and will provide a means of establishing a broad bandwidth fiber-optic link to the seafloor systems. The use of a broad bandwidth bi-directional fiber-optic link facilitates real time interactive control of ocean based experiments, instrumentation, and tethered and free swimming vehicle systems. Once data and control links are transferred to the shore station over the fiber-optic channel, they may then be made accessible for use in world wide education and research programs, through modern computing and communication technologies.

Specifically, this paper examines the design and installation of a Long Term Observatory which will be operated in 15 meters of water (LEO-15). LEO-15 will be located approximately 9 kilometers off the New Jersey Coast at Little Egg Inlet. The observatory will be linked to Rutgers, The State University of New Jersey, Institute of Marine and Coastal Science's shore station at Tuckerton by an electro-optic cable which will be buried in the seafloor.

It has been determined that with some routine maintenance, a reliable long term system may be developed and put into operation. The successful installation and operation of the LEO-15 facility should provide the engineering experience and scientific motivation necessary to install additional sites, worldwide, in both coastal and deep water sites.

Published in: Occans '92, :849-854, 1992.

Supported by: Rutgers, The State University of New Jersey grant NA16RU0370-01 from DOC-NOAA.

WHOI Contribution No. 8097.

A MINMAX APPROACH TO ADAPTIVE MATCHED FIELD PROCESSING IN AN UNCERTAIN PROPAGATION ENVIRONMENT

James C. Preisig

Adaptive array processing algorithms have achieved widespread use because they are very effective at rejecting unwanted signals (i.e., controlling sidelobe levels) and in general have very good resolution (i.e., have narrow mainlobes). However, many adaptive high-resolution array processing algorithms suffer a significant degradation in performance in the presence of environmental mismatch. This sensitivity to environmental mismatch is of particular concern in problems such as long-range acoustic array processing in the ocean where the array processor's knowledge of the propagation characteristics of the ocean is imperfect. An Adaptive Minmax Matched Field Processor is formulated which combines adaptive matched field processing and minmax approximation techniques to achieve the effective interference rejection characteristic of adaptive processors while limiting the sensitivity of the processor to environmental mismatch. An efficient implementation and alternative interpretation of the processor are developed. The performance of the processor is analyzed using numerical simulations.

Submitted to: IEEE Transactions on Signal Processing.

Supported by: ONR grants N00014-89-J-1489 and N00014-91-J-1628.

FURTHER ANALYSIS OF TARGET STRENGTH MEASUREMENTS OF ANTARCTIC KRILL AT 38 KHZ AND 120 KHZ: COMPARISON WITH DEFORMED CYLINDER MODEL AND INFERENCE OF ORIENTATION DISTRIBUTION

Dezhang Chu, Kenneth G. Foote and Timothy K. Stanton

Data collected during the Krill Target Strength Experiment [J. Acoust. Soc. Am. 87:16-24 (1990)] are examined in the light of a recent zooplankton scattering model [J. Acoust. Soc. Am. 86:691-705 (1989)]. Exercise of the model under assumption of an orientation distribution allows absolute predictions of target strength to be made at each frequency. By requiring that the difference between predicted and measured target strengths be a minimum in at least-squares sense, it is possible to infer the orientation distribution. The present agreement may appear crude, at least in some instances, but this may be attributed to shortcomings in the original data, model, and model parameters. Future experiments may be expected to remedy each of these, ultimately contributing to the goal of sonar measurement of zooplankton.

In Press: Journal of the Acoustical Society of America.

Supported by: ONR grant N00014-89-J-1729. WHOI Contribution No. 8108.

EFFECTS OF SEA ICE COVER ON ACOUSTIC RAY TRAVEL TIMES, WITH APPLICATIONS TO THE GREENLAND SEA TOMOGRAPHY EXPERIMENT

Guoliang Jin, James F. Lynch, Richard Pawlowicz and Peter Wadhams

The travel time effects of a sea ice cover on an acoustic pulse are estimated using generalized ray theory. This expands upon the previous work done by Jin and Wadhams [Prog. Oceano., 22:249-275 (1989)] by including the effects of frequency dispersion and different sets of ice parameters. Travel time changes due to single reflections are approximated by plane wave reflection theory, and compared to the generalized ray theory results. Statistical effects for multiple reflections, such as the ice thickness probability distribution function, Fresnel zone averaging, and shadowing are considered. Finally, the effects of ice induced travel time changes on tomographic inversions for water

column oceanography are considered. The implications of this work on the 1988-89 Greenland Sea Tomography experiment are considered in detail.

In Press: Journal of the Acoustical Society of America.

Supported by: ONR grants N00014-91-J-1139 and N00014-92-J-1291.

WHOI Contribution No. 8111.

NEAR OCEAN BOTTOM EXPLOSIVE LAUNCHER NOBEL

Donald E. Koelsch, G. M. Purdy and James E. Broda

A Near Ocean Bottom Explosive Launcher (NOBEL) has been developed by the Woods Hole Oceanographic Institution (WHOI) for measuring structure velocity in the upper most crust with a resolution that is not attainable in any other way. It uses 40 to 50 Hz energy.

In order to determine the structure of thin layers just below the ocean floor, it is necessary to carry out seismic refraction lines with both a sound source and a receiver within a few meters of the ocean bottom. Traditionally, Digital Ocean Bottom Hydrophones (DOBHs) and ocean bottom seismometers have been used as bottom deployed receivers for both passive and active seismic experiments. The sound source for these experiments has been either naturally occurring earthquakes or explosive charges detonated near the surface, limiting the resolving power to a kilometer. Therefore. WHOI embarked on a program to develop a high energy low frequency sound source that would fire 50 shots on command with a shot size of five to ten pounds of high explosives. It would be used with a DOBH as a high resolution seismic system.

Published in: Sea Technology, 33(10):41-47, 1992.

Supported by: NSF grant OCE-8917750.

WHOI Contribution No. 8126.

SOUND SCATTERING BY ROUGH ELONGATED ELASTIC OBJECTS. III. EXPERIMENT

John V. Gurley and Timothy K. Stanton

Acoustical backscattering from randomly rough infinitely long elastic cylinders surrounded by a fluid medium is examined. The cylinder radius is allowed to vary along its lengthwise axis creating one-dimensional rotationally symmetric roughness. Using recently published rough cylinder

formulations [T.K. Stanton, J. Acoust. Soc. Am., 92:1641-1664 (1992) and T.K. Stanton and D. Chu, J. Acoust. Soc. Am., 92:1665-1678 (1992)], explicit approximate expressions are derived for the backscattered field for a laboratory pulse-echo environment: spherically spreading directional source and receiver with arbitrary beam patterns. Efficient numerical integration algorithms are developed to solve for the backscattered field from a specified surface profile. Experimental measurements from dense elastic (stainless steel) cylinders immersed in water are presented to quantitatively illustrate the effects of small scale surface roughness ($\sigma_s/a = 0.0131$ where σ_s is the surface rms roughness and a is the mean cylinder radius) for 4.5 < ka < 30 where k is the acoustic wavenumber. The actual target surface profile is well described and used as an input in the numerical simulations. Agreement is found between measurements and simulation predictions both in the mean field levels and the field fluctuations over a wide range of frequencies.

Submitted to: Journal of the Acoustical Society of America.

Supported by: Oceanographer of the U.S. Navy, MIT/WHOI Joint Program in Oceanography/ Applied Ocean Physics and Engineering, and ONR grant N00014-89-J-1729.

WHOI Contribution No. 8127.

THE DYNAMOOR EXPERIMENT

Henri Berteaux, Alessandro Bocconcelli, Cal Eck, Sean Kery and Pierre Wansek

Under the sponsorship of the Office of Naval Research, the Ocean Systems and Moorings Laboratory (OS&M Lab) of the Woods Hole Oceanographic Institution developed (1990) and deployed (1991) a fully instrumented subsurface buoy in high current waters close to Woods Hole, MA.

The purpose of this engineering experiment, named DYNAMOOR, was to obtain long term, high frequency measurements of the buoy 3D position and of the tension in its mooring line, as a function of prevailing currents and variable, adjustable buoyancy.

Published in: Global Ocean Partnership: MTS '92 Proceedings, Washington Sheraton Hotel, October 19-21, 1992. Marine Technology Society, Washington, DC, 2:931-942, 1992.

Supported by: ONR contract N00014-90-J-1719. WHOI Contribution No. 8129.

SOUND FIELD COMPUTATIONS IN A STRATIFIED, MOVING MEDIUM

D. Keith Wilson

A numerical method for computing the sound field in a stratified, medium is described. The method is quite similar to the well known fast field program (FFP), except that the wave equation is modified to account for fluid and/or source motion. The computation requires a two-dimensional horizontal wavenumber spectrum rather than a one-dimensional radial wavenumber spectrum as required by previous FFP's. As an example, the sound pressure produced by a point source in a neutrally-buoyant atmospheric shear layer is calculated.

In Press: Journal of the Acoustical Society of America.

Supported by: Education Office of the Woods Hole Oceanographic Institution.

WHOI Contribution No. 8131.

ACOUSTIC TOMOGRAPHIC MONITORING OF THE ATMOSPHERIC SURFACE LAYER

D. Keith Wilson and Dennis W. Thomson

During the summer of 1991, tomography of the atmospheric surface layer was implemented at the Pennsylvania State University Meteorology Department's Rock Springs site. In this paper, the results of the experiment which are pertinent to propagation of acoustic signals through the atmospheric surface layer will be emphasized. The transmitted signals were swept sines from 100 to 1000 Hz, with duration 0.1 s. They were detected at the microphones using a cross-correlation technique. Analysis of the measured travel-time and amplitude fluctuations suggests that turbulent eddies having a horizontal characteristic dimension of many hundreds of meters are an important cause of fluctuations in acoustic signals.

Published in: Proceedings of the Fifth International Symposium on Long Range Sound Propagation, The Open University, Milton Keynes, England, :249-262, 1992.

Supported by: Penn State ONR grant
N00014-86-K-06880 and Atmospheric Sciences
Laboratory grant N00039-88-C-0051. The
Woods Hole Oceanographic Institution's
Education Office.

WHO! Contribution No. 8135.

DEVELOPMENT AND EVALUATION OF ELECTROMECHANICAL TERMINATIONS FOR DEEP SEA BUOY APPLICATIONS

Sean Kery and Alessandro Bocconcelli

The Ocean Systems Moorings Laboratory (OS&ML) at the Woods Hole Oceanographic Institution (WHOI) has been developing, and testing electromechanical (EM) cable terminations for real time data telemetry from oceanographic moorings since 1985.

EM cable terminations are needed whenever two lengths of EM cable are joined together, or when an oceanographic sensor is connected to the cable. These terminations consist of a mechanical attachment with full cable strength and watertight electrical connectors that ensure signal continuity.

Several models of EM terminations for steel and kevlar armored cables were developed with the cooperation and technical support of outside manufacturers. Three models were entirely developed and built at WHOI. Their design and performance on deep sea oceanographic moorings is reviewed in this paper. Also given is a step-by-step procedure for implementing EM cable terminations.

Published in: Global Ocean Partnership: MTS '92 Proceedings, Washington Sheraton Hotel, October 19-21, 1992. Marine Technology Society, Washington, DC, 2:971-976, 1992.

Supported by: ONR contract N00014-90-J-1719. WHOI Contribution No. 8137.

ON THE FEASIBILITY OF PURELY TOMOGRAPHIC IMAGING OF FLOW FIELDS

D. Keith Wilson

It has been suggested by Norton that the irrotational part of a flow field cannot be determined from tomographic projections [S.J. Norton, Geophysical Journal, 97:161-168 (1988)]. However, Norton's proof does not apply to the inverse methods typically used for geophysical problems for two important reasons: assumptions regarding the spatial structure of the field are built into geophysical inverses; and, the tomographic projections are interior to the field being imaged. The significance of these points is discussed and illustrated with numerical examples. It is concluded that the tomographic imaging of a flow field presents no special difficulties in comparison to scalar field imaging.

Submitted to: Geophysical Journal International.

Supported by: Woods Hole Oceanographic Institution's Education Office.

WHOI Contribution No. 8144.

PREDICTIONS AND OBSERVATIONS OF SEAFLOOR INFRASONIC NOISE GENERATED BY SEA SURFACE ORBITAL MOTION

Timothy E. Lindstrom and George V. Frisk

A model is developed for the prediction of the seismo-acoustic noise spectrum in the microseism peak region (0.1 to 0.7 Hz). The model uses a theory developed by Cato [J. Acoust. Soc. Am., 89:1096-1112 (1991)] for an infinite depth ocean in which the surface orbital motion caused by gravity waves may produce acoustic waves at twice the gravity wave frequency. Using directional wave spectra as inputs, acoustic source levels are computed and incorporated into a more realistic environment consisting of a horizontally stratified ocean with an elastic bottom. Noise predictions are made using directional wave spectra obtained from the SWADE surface buovs moored off the coast of Virginia and the SAFARI sound propagation code. with a bottom model derived using wave speeds measured in the EDGE deep seismic reflection survey. The predictions are analyzed for noise level variations with frequency, wave height, wind direction, and receiver depth. These predictions are compared to noise measurements made in ECONOMEX using near-bottom receivers located close to the surface buoys. Good agreement is found between the predictions and observations under a variety of environmental conditions.

Submitted to: Journal of the Acoustical Society of America.

Supported by: ONR grant N00014-90-J-1452 and the US Navy support of Lindstrom as a graduate student MTT/WHOL Joint Program.

WHOI Contribution No. 8153.

ACOUSTICAL AND OPTICAL BACKSCATTER MEASUREMENTS OF SEDIMENT TRANSPORT IN THE 1988-89 STRESS EXPERIMENT

James F. Lynch, Thomas F. Gross, Christopher R. Sherwood, James D. Irish and Blair H. Brumley

During the 1988-89 Sediment Transport Events on Shelves and Slopes (STRESS) experiment, a 1 MHz acoustic backscatter system (ABSS) was deployed in 90 m of water off the California coast to measure vertical profiles of suspended sediment concentration from 1.5 to (nominally) 26 m.a.b. An eight week long time series was obtained, showing major sediment transport events (storms) in late December and early January. Comparison of the acoustics measurements, made in the Rayleigh scattering regime, with optical backscatter system (OBS) concentration estimates, made in the geometrical optics regime, allows us to infer some information about the suspended sediment particle size distribution. Correlations between ABSS and OBS concentration measurements and the boundary layer forcing functions (waves, currents, and their non-linear interaction) provided a variety of insights into the nature of the sediment transport at the STRESS site. Transport rates and integrated transport are calculated, and are found to be dominated by the largest storm events.

Submitted to: Continental Shelf Research Special issue on STRESS.

Supported by: ONR contract N00014-89-J-1049. WHOI Contribution No. 8155.

QUANTITATIVE SEAFLOOR CHARACTERIZATION USING A BATHYMETRIC SIDESCAN SONAR

W. Kenneth Stewart, Dezhang Chu, Sandipa Malik, Steve Lerner and Hannuman Singh

Bathymetry and backscatter measurements from a 120-kHz phase-difference sonar are analyzed in terms of statistical and spectral characteristics. Data from a multisensor, multiscale survey of the Juan de Fuca Ridge are compared across three distinct geological provinces: sediment pond, ridge flank, and axial valley. The detrended bathymetry follows a Gaussian distribution; the power spectral density can be approximately described by a power law. The composite multiscale power spectrum demonstrates a similar slope spanning a spatial frequency range from about 0.005 to 50 cyc./m, corresponding to a range of geological features from a few hundred meters down to several centimeters. The backscattering strength and grazing-angle dependencies agree with previous empirical studies; data from a sediment-pond region are shown to match theoretical predictions of the composite-roughness model. Histograms of the echo amplitude are characterized by a multimodal Rayleigh probability density function. For all analyses, the data show distinct differences among the three provinces.

Submitted to: IEEE Journal of Oceanic Engineering.
Supported by: ONR grants N00014-90-K-0070 and N00014-90-J-1848.

WHOI Contribution No. 8156.

RELAXATION-MATCHED MODELLING OF SOUND PROPAGATION IN POROUS MEDIA, INCLUDING FRACTAL PORE SURFACES

D. Keith Wilson

A new model of the complex density (dynamic permeability) and bulk modules for acoustic propagation in porous media is described. The model is based on matching the relaxational characteristics of the viscous and thermal dissipation processes in the pores, rather than exact matching of parameters determined asymptotically in the low and high frequency limits. Furthermore, the model is not derived from any solutions based on a specific pore shape. The relaxation-matched model is simpler than the commonly used Zwikker/Kosten/Attenborough or Biot/Allard models in the sense that it contains no Bessel or Kelvin functions, and requires only three parameters instead of the usual four. Extension of the model to fractal pore surfaces is also discussed.

Submitted to: Journal of the Acoustical Society of America.

Supported by: Woods Hole Oceanographic Institution's Education Office.

WHOI Contribution No. 8158.

AVERAGE ECHOES FROM RANDOMLY-ORIENTED RANDOM-LENGTH FINITE CYLINDERS: ZOOPLANKTON MODELS

Timothy K. Stanton, Dezhang Chu, Peter H. Wiebe and Clarence S. Clay

By heuristically extending the previously developed ray solution (T.K. Stanton et al., submitted to J. Acoust. Soc. Am.) to predict the scattering by cylinders over all angles of incidence. approximate expressions are derived which describe the echo energy due to sound scattered by finite cylinders averaged over orientation and length. Both straight and bent finite length cylinders of high aspect ratio are considered over the full range of frequencies (Rayleigh through geometric scattering). The results show that for a sufficiently broad range of orientation, the average echo is largely independent of the degree of bend that is, the results are essentially the same for both the straight and bent cylinders of various radii of curvature (provided the bend is not too great). Also, in the limit of high frequency (i.e. the accustic wavelength is much smaller than the cross-sectional radius of the object), the averages are independent of frequency. The resultant formulas derived herein are useful in describing the

scattering by elongated zooplankton whose shape may not necessarily be known in the natural ocean environment. The average echo is shown to depend directly upon standard deviation of the angle of orientation as well as size. If independent measurements of size are made (such as from trawling samples), then the properties of the angle distribution and hence behavior may be inferred from the data. Averages over both angle and a narrow distribution of size are shown to only partially smooth out deep nulls in the scatter versus frequency curves. The formulas compare favorably with laboratory data involving aggregations of animals and a broad range of frequencies (38 kHz to 1.2 MHz).

Submitted to: Journal of the Acoustical Society of America.

Supported by: ONR grant N00014-89-J-1729 and ONT through NUWC contract N66604-91-C-5401.

WHOI Contribution No. 8178.

THE IMPORTANCE OF STRATIFICATION ON THE FORMATION OF THE ESTUARINE TURBIDITY MAXIMUM

W. Rockwell Geyer

A simple numerical model demonstrates that the reduction in turbulence due to stratification greatly enhances the trapping of suspended sediment that occurs at the estuarine turbidity maximum. In moderately and highly stratified estuaries, the turbulent diffusivity decreases markedly between the region upstream of the salinity intrusion, where the turbulence is uninhibited by salt stratification, and the stratified regime within the salinity intrusion, where turbulence is reduced by the inhibitory influence of salt stratification. This reduction in turbulent diffusion results in a reduction in the quantity of sediment that can be carried by the flow, causing sediment to be trapped near the landward limit of the salinity intrusion. This trapping process occurs at the same location as that due to the estuarine convergence, but it appears to be many times more effective at trapping silt-sized particles.

A model is formulated that is similar to Festa and Hansen's (1978) model of the estuarine turbidity maximum, with the addition of a stratification-dependent eddy diffusivity. For silt-sized sediment particles, the model indicates as much as a 20-fold increase in the trapping rate with inclusion of the stratification effect. It is likely that this mechanism is important in many partially mixed and highly stratified estuarines.

In Press: Estuaries.

Supported by: NSF grants OCE-8812917 and OCE-9115712.

WHOI Contribution No. 8183.

AMBIENT NOISE MEASUREMENTS IN THE 200-300 HZ BAND FROM THE GREENLAND SEA TOMOGRAPHY EXPERIMENT

J. Lynch, H. X. Wu, R. Pawlowicz, P. Worcester, R. Keenan, H. Graber, P. Wadhams, O. Johannessen and R. Shuchman

Ambient noise in the 200-300 Hz band was measured every four hours from Sept 88 to Sept 89 as part of the Greenland Sea Tomography Experiment (GSP88). Four transceivers, located in the central Greenland Sea gyre, sampled the noise during a wide variety of ice, wind, and wave conditions, revealing large seasonal variations in the noise field. The environmental conditions were obtained from large scale remote sensing and numerical modeling, i.e. operational meteorological forecast models, surface wave models, and microwave and infrared satellite imaging (for ice). To understand the noise field, a number of analyses were performed on the noise, wind, and wave time series, including: regressions, auto-and cross-correlations, spectra, and propagation modeling. As a result, a number of environmental noise effects, particularly as relate to ice edge noise, are observed. The results generally agree well with previous process oriented studies which used in-situ ice, wind, and wave measurements. It is seen that prediction of the Marginal Ice Zone (MIZ) noise field at the acoustic frequencies examined is feasible using large scale environmental information.

In Press: Journal of the Acoustical Society of America.

Supported by: ONR grant N00014-91-J-1246 and NSF support through Scripps.

WHOI Contribution No. 8199.

PASSIVE ACOUSTIC LOCALIZATION OF THE ATLANTIC BOTTLENOSE DOLPHIN USING WHISTLES AND ECHOLOCATION CLICKS

Lee E. Freitag and Peter L. Tyack

A method for localization and tracking of calling marine mammals was tested under realistic field conditions which include noise, multipath and arbitrarily located sensors. Experiments were performed in two locations using four and six hydrophones with captive Atlantic bottlenose

dolphins (Tursiops truncatus). Acoustic signals from the animals were collected in the field using a digital acoustic data acquisition system. The data were then processed off-line to determine relative hydrophone positions and the animal locations. Accurate hydrophone position estimates are achieved by pinging sequentially from each hydrophone to all the others. A two-step least squares algorithm is then used to determine sensor locations from the calibration data. Animal locations are determined by estimating the time differences of arrival of the dolphin signals at the different sensors. The peak of a matched filter output or the first cycle of the observed waveform is used to determine arrival time of an echolocation click. Cross-correlation between hydrophones is used to determine inter-sensor time delays of whistles. Calculation of source location using the time difference of arrival measurements is done using a least squares solution to minimize error. These preliminary experimental results based on a small set of data show that realistic trajectories for moving animals may be generated from consecutive location estimates.

In Press: Journal of the Acoustical Society of America.

Supported by: Mellon Foundation and the National Institute of Health grant 5-R29-DC00429.

WHOI Contribution No. 8200.

A NEURAL-NETWORK APPROACH TO CLASSIFICATION OF SIDESCAN-SONAR IMAGERY FROM A MID-OCEAN-RIDGE AREA

W. Kenneth Stewart, Min Jiang and Martin Marra

A neural-network approach to classification of sidescan-sonar imagery is tested on data from three distinct geoacoustic provinces of a mid-ocean-ridge spreading center: axial valley, ridge flank, and sediment pond. The extraction of representative features from the sidescan imagery is analyzed, and the performances of several commonly used texture measures are compared in terms of classification accuracy using a backpropagation neural network. A suite of experiments compares the effectiveness of different feature vectors, the selection of training patterns, the configuration of the neural network, and two widely used statistical methods: Fisher-pairwise classifier and a nearest-mean algorithm with Maholanobis distance measure. The feature vectors compared here comprise spectral estimates, gray-level run length, spatial gray-level dependence matrix, and gray-level differences. The overall accurate classification rate using the best feature set for the three seafloor types are: sediment ponds, 85.9%;

ridge flanks, 91.2%; and valleys, 80.1%. While most current approaches are statistical, the significant finding in this study is that high performance of seafloor classification in terms of accuracy and computation can be achieved using a neural network with the proper combination of texture features. These are preliminary results of our program toward the automated segmentation and classification of undersea terrain.

Submitted to: IEEE Journal of Oceanic Engineering.

Supported by: ONR grants N00014-90-K-0070, N00014-90-J-1848 and N00014-90-J-1912, OP-23 contract N00014-89-D-0255; and WHOI's Postdoctoral Fellowship of 1991.

WHOI Contribution No. 8209.

IS IT CHEAPER TO MAP ROSSBY WAVES IN THE GLOBAL OCEAN THAN THE GLOBAL ATMOSPHERE?

John L. Spiesberger

Temperatures of planetary and other long waves may be less expensive to monitor in real-time in the ocean than in the atmosphere with new acoustic monitoring technology. The minimum cost, X_{tot} , for acoustically monitoring an ocean region of area A with resolution δa is $2\sqrt{E_sE_r}A^{1/2}/\delta a$ where the total expense for purchasing and maintaining each source and receiver for the system lifetime is given by E_s and E_r respectively. X_{tot} is achieved only when the number of sources and receivers purchased equals $\hat{N}_s = X_{tot}/2E_s$ and $\hat{N}_r = X_{tot}/2E_r$, i.e. where the total monies are split equally between sources and receivers. These choices result in a maximum number of tomographic sections of $X_{tot}^2/4E_sE_r$.

In Press: Journal of Marine Environmental Engineering.

Supported by: ONR contract N00014-86-J-0358 and ONT contract N00014-90-C-0098.

WHOI Contribution No. 8213.

TEMPORAL VARIATION IN BED CONFIGURATION AND ONE-DIMENSIONAL BOTTOM ROUGHNESS AT THE MID-SHELF STRESS SITE

Robert A. Wheateroft

Time-lapse steroephotographs were taken over a 90-d period from mid-November 1990 to late-February 1991 at a 90-m silt-bottom site on the central California shelf as part of the STRESS (Sediment TRansport Events on Shelves and Slopes) project. Five distinct bed configurations were observed during this period, in order of decreasing abundance, these are (1) bioturbated bed, (2) smooth bed, (3) current-rippled bed, (4) scour-pitted bed, and (5) longitudinally-rippled bed. Concurrent measurements of the flow field implicated along-shelf currents, rather than waves, as the primary agent forming the physical bed configurations. The presence of a wave-induced cross-shelf gradient in near-bottom suspended sediment during storm events and the redistribution of this sediment by upwelling or downwelling currents is postulated to control the appearance of depositional current-ripples (NW poleward flow, downwelling) and erosional scour-pits (SE equatorward flow, upwelling). A bed form morphologically similar to longitudinal triangular ripples, observed in the deep ocean, was photographed following a particularly strong along-shelf current event. All physical bed forms were destroyed by bioturbation processes in periods of hours to days.

Analytical photogrammetric techniques were used to extract high-resolution sea floor height data from the stereophotographs. Results indicate maximal relief at this site never exceeded 5 cm. Root-mean-square (RMS) height varies by a factor of three (3.2 to 9.2 mm) and is a weak function of bed configuration. Current ripples have the largest RMS-height, smoothed and scour-pitted beds the smallest. RMS-heights of bioturbated beds are variable and appear to depend on the previously produced physical bed configuration. Changes in RMS-height can be abrupt with factor of two changes observed over a 12-hr period. Horizontal descriptors of roughness such as peak spacing or peak width can not separate bed configurations. Results from slope distributions are broadly coherent with the RMS-height data, in that surfaces with large RMS-heights have broad slope distributions and vice versa. Slope distribution data also indicate that all bed configurations except the current-rippled bed are isotropic. These preliminary data suggest that time series information is needed to adequately resolve both the micro-scale roughness of the sea floor on continental shelves and the presence of short lived, but potentially flow-diagnostic bed configurations.

Submitted to: Continental Shelf Research.

Supported by: ONR subcontract from UW grant N00014-90-J-1926 and WHOI Postdoctoral Scholarship.

WHOI Contribution No. 8222.

BIVALVE FEEDING AND THE BENTHIC BOUNDARY LAYER

Marcel Fréchette, Denis Lefaivre and Cheryl Ann Butman

Benthic suspension feeders, particularly some bivalves, have strong structuring effects on rocky shore communities, which are commonly dominated by the Mytilidae in most oceans (see Paine 1984). This dominance may be related to at least two important aspects of their ecology, the sestonic nature of their food and their sessile mode of life. The food of seston feeders is produced in a three-dimensional environment which flows over the animals. Under favorable conditions, this food is continuously replenished by currents, sinking and reproduction of planktonic organisms. Thus, owing to their sedentary nature and feeding behavior, there is strong coupling between the pelagic and benthic environments through bivalves. Energy from the pelagos is channeled directly to the benthos via the filtering activity of the organisms and is eventually used for various metabolic and growth activities (see Dame and Patten 1981). Given the above, it can be postulated that the biomass of other feeding guilds (e.g. carnivores, which depend directly on primary consumers, and perhaps even grazers, through the elimination of algal growth by sessile animals, Dayton 1973), as well as the overall structure of intertidal communities, is dependent on the "success" or "failure" of the suspension feeders. Thus, given the central position of suspension feeders as structuring agents of the intertidal communities. energy flow from the pelagos to the benthos can be determined by measuring energy flow through this guild. Similar principles hold for subtidal macrofaunal assemblages. Wildish and Peer (1983), for example, reported similar relationships between the pelagos and benthos in the Bay of Fundy, where suspension feeders contributed over 88% of the total macrofaunal production.

Our goal here is to illustrate how local hydrodynamics may modulate energy flow in bivalve suspension feeders. We shall limit our analysis to the study of mechanisms that may explain the positive relationship between current speed and growth in field situations. In particular, we shall analyse different approaches to field studies, and the conceptual framework for these approaches with respect to benthic boundary layer (BBL) processes.

Submitted to: Bivalve Filter Feeders and Marine

Ecosystem Processes, Proceedings of a NATO-Advanced Research Workshop, R. Dame, ed. Springer-Verlag.

Supported by: ONR grant N00014-89-J-1637. WHOI Contribution No. 8223.

FLUME EXPERIMENTS ON FOOD SUPPLY TO THE BLUE MUSSEL MYTILUS EDULIS L. AS A FUNCTION OF BOUNDARY-LAYER FLOW

Cheryl Ann Butman, Marcel Fréchette, W. Rockwell Geyer and Victoria R. Starczak

Toward developing an improved understanding of the mechanisms that control food supply to benthic suspension feeders, three laboratory flume experiments were conducted with a 6.1-m-long by 0.6-m-wide bed of the blue mussel Mytilus edulis L. The experiments tested the hypothesis that phytoplankton depletion above a mussel bed can be predicted adequately by a simple, two-dimensional, advection-diffusion model that incorporates mussel feeding at the bed (Fréchette et al. 1989). Within each experiment, flows with near-surface velocities of about 5 and 15 cm s were tested, and phytoplankton concentrations (as estimated by fluorescence) were measured just upstream of and at four locations in the vertical 5 m downstream of the leading edge of the mussel bed. Detailed vertical profiles of velocity measured along the mussel bed indicated enhanced turbulent mixing due to mussel-bed roughness compared to mixing just upstream of the mussel bed; turbulent stresses were three (slow flow) to ten (fast flow) times higher over the mussel bed compared to the smooth, flat, flume bottom. In Expts. 1 and 3, using natural seawater, initial phytoplankton concentrations were low and there was very little temporal depletion at either flow speed. This may be due to cessation of feeding by the mussels below a threshold concentration. Initial phytoplankton concentration was two to three times higher in Expt. 2, using filtered seawater to which cultured phytoplankton were added, and significant vertical and substantial horizontal gradients in phytoplankton concentration developed during the experiment. Depletion was enhanced in slow flow compared to fast flow, both in the downstream and vertical directions, as qualitatively predicted by the model. Using a range of estimated mussel filtration velocities, that varied by a factor of three, modeled vertical profiles of phytoplankton concentration bracketed the observations in Expt. 2. The results underscore the sensitivity of depletion to filtration velocity and support an hypothesis that filtration velocity in individual blue mussels is flow-speed-dependent. In conclusion, the relatively simple model of Fréchette et al. (1989) appears to be adequate to predict the structure and approximate magnitude of phytoplankton depletion above a mussel bed for a given steady, uniform flow and a known mussel filtration rate.

Submitted to: Limnology and Oceanography.

Supported by: ONR Young Investigator Program

contract N00014-86-K-0579; ONR grant N00014-89-J-1637; Walter A. & Hope Noyes Smith Special Studies Award from WHOI, Department of Fisheries and Oceans, Canada, NSF grant OCE-89817002, and the Coastal Research Center.

WHOI Contribution No. 8224.

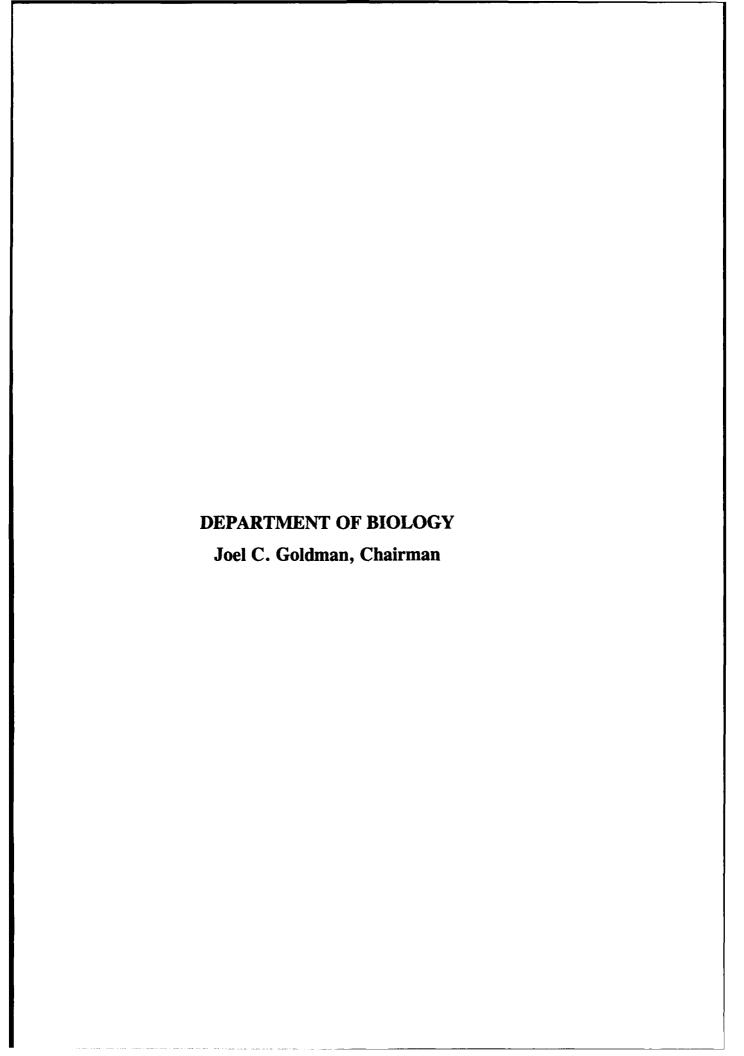
UNDERSEA VISUALIZATION: A TOOL FOR SCIENTIFIC AND ENGINEERING PROGRESS

Lawrence J. Rosenblum, W. Kenneth Stewart and Behzad Kamgar-Parsi

For both remote imaging and on-site measurement the undersea environment is perhaps the most inhospitable one known to man. The inability of most forms of energy to penetrate the ocean sufficiently to provide detailed measurements leads to a reliance on acoustical sensors for remote sensing. Because of the comparatively low acoustical frequencies and often uncertain navigational information, resolution is poor and measurements sparse. This in turn leads to unique problems in visualization and imaging. Overcoming these limitations to obtain reasonable images typically requires an integration of digital imaging with visualization techniques. This paper uses data from several ocean science domains to illustrate how visualization is used to extract knowledge from data.

Submitted to: Animation and Scientific Visualization, Rae Earnshaw, ed. British Computer Society.

WHOI Contribution No. 8231.



AN IMMUNOFLUORESCENT SURVEY OF THE BROWN TIDE CHRYSOPHYTE AUREOCOCCUS ANOPHAGEFFERENS ALONG THE NORTHEAST COAST OF THE UNITED STATES

Donald M. Anderson, Bruce A. Kcafer, David M. Kulis, Robert M. Waters and R. Nuzzi

Surveys were conducted along the northeast coast of the United States between Portsmouth, NH and the Chesapeake Bay in 1988 and 1990 to determine the population distribution of Aureococcus anophagefferens, the chrysophyte responsible for massive and destructive "brown tides" in Long Island and Narragansett Bay beginning in 1985. A species-specific immunofluorescent technique was used to screen water samples, with positive identification possible at cell concentrations as low as 10-20 cells ml⁻¹. Both years, A. anophagefferens was detected at numerous stations in and around Long Island at Barnegat Bay, NJ, typically at high cell concentrations. To the north and south of this "center", nearly half of the remaining stations were positive for A. anophagefferens, but the cells were always at very low cell concentrations. Many of the positive identification in areas distant from Long Island were in waters with no known history of harmful brown tides. The species was present in both open coastal and estuarine locations. The observed population distributions apparently still reflect the massive 1985 outbreak when this species first bloomed, given the number of positive locations and high abundance of A. anophagefferens in the immediate vicinity of Long Island. However, the frequent occurrence of this species in waters far from this population "center" is disturbing. A. anophagefferens is more widely distributed than was previously thought. Numerous areas thus have the potential for destructive brown tides such as those associated with the sudden appearance of the species in 1985.

In Press: Journal of Plankton Research.

Supported by: Suffolk County, (NY), National Sea Grant College Program Office (NA86-AA-D-SG090), (WHOI Sea Grant Project R/P 87-PD and R/B 91 and NA 90-AA-D-SG480 (R/B 100).

WHOI Contribution No. 8119.

DISCRIMINATION BETWEEN DOMOIC-ACID-PRODUCING AND NON-TOXIC FORMS OF THE DIATOM NITZSCHIA PUNGENS USING IMMUNOFLUORESCENCE

S. S. Bates, C. Leger, Bruce A. Keafer and Donald M. Anderson

Separate polyclonal antibodies were developed against cell surface antigens of the two forms of the pennate diatom, Nitzschia pungens, i.e., forma multiseries (the domoic-acid-producing form), and forma pungens (the non-toxic form). Positive antigenic reactions were visualized with epifluorescence microscopy, using a fluorescein isothiocyanate (FITC) indirect immunofluorescence assay. The assay successfully distinguished 31 clones of f. multiseries from the 17 clones of f. pungens tested, with no cross reactions of the antisera between the two forms. The antisera were active against N, pungens cells isolated from Prince Edward Island, Nova Scotia, Massachusetts, Rhode Island, Texas, and Washington, Of the 27 other species tested from the Section Pseudonitzschia two other domoic-acid-producing species (Pseudonitzschia australis and Nitzschia pseudodelicatissima), and the domoic-producing pennate diatom Amphora coffaeiformis showed a slight positive response to the antisera, as did non-toxic N. subcurvata, an Antarctic species, and non-toxic N. fraudulenta. These reactions are not great enough to cause concern about misidentification, but pose questions about phylogenic relationships. Other representatives from the class Bacillariophyceae and from eight other major classes of phytoplankton did not cross react with the antisera. Excellent labelling was obtained with live cells and those frozen at -60°C, or preserved in 2% glutaraldehyde-paraformaldehyde, 2% borate-buffered formalin or 2% paraformaldehyde. Immunofluorescence shows great promise as a technique to distinguish between the two forms of N. pungens for research and monitoring purposes.

Submitted to: Marine Ecology Progress Series.

Supported by: NSF Grant OCE89-11226.

WHOI Contribution No. 8235.

MIXOTROPHIC ALGAE IN THREE ICE-COVERED LAKES OF THE POCONO MOUNTAINS, USA

Ulrike-G. Berninger, David A. Caron and Robert W. Sanders

The occurrence and grazing activity of mixotrophic (phagotrophic) algae in three ice-covered freshwater lakes of different trophic status were examined (oligotrophic Lake Giles, mesotrophic Lake Lacawac, eutrophic Lake Waynewood). Microbial population densities were low $(2.1 \times 10^5 \text{ to } 7.2 \times 10^5 \text{ bacterial ml}^{-1} \text{ and } 1.2 \times 10^3 \text{ to } 2.4 \times 10^3 \text{ nanoplanktonic protists ml}^{-1}). All three nanoplankton communities were dominated by chloroplast-bearing forms (60 to 96%).$

Mixotrophs formed up to 48% of the phototrophic nanoplankton in Lake Lacawac and were responsible for up to ~ 90% of the observed uptake of bacteria-sized particles. The abundance of mixotrophic algae in Lakes Giles and Waynewood were extremely low (3 and 2% of the phototrophic algae, respectively), and heterotrophs dominated nanoplankton bacterivory.

The overall impact of nanoplankton feeding activity of the bacterial assemblage was low under the ice in Lakes Giles and Waynewood. Removal rates of bacteria based on our particle uptake experiments were 1.0 and 4.0% of the bacterial standing stock d⁻¹ in these lakes, respectively. Removal rates were higher in Lake Lacawac and ranged from 4.9 to 11% of the bacterial standing stock d⁻¹ on two successive sampling days.

Published in: Freshwater Biology, 28:268-272.

Supported by: NSF BSR89-19447.

WHOI Contribution No. 7958.

POD-SPECIFIC DEMOGRAPHY OF KILLER WHALES (ORCINUS ORCA)

Solange Brault and Hal Caswell

Killer whales live in stable social groups. It has been suggested that the structure of such groups may influence their demography. Using data from a long-term study by Bigg et al. (1990), we constructed stage-classified matrix population models for the entire population, two sub-populations and individual pods. The population growth rate for the entire population is $\lambda = 1.0247$, with 90% bootstrap confidence interval from 1.0178 to 1.0308. The mean female population stage distribution is not significantly different from the predicted stable stage distribution. Pod-specific growth rates range from $\lambda = 1.0053$ to $\lambda = 1.0699$. Most of the inter-pod

variance in growth rate is due to variance in adult reproductive output. Randomization tests show that this variance is not significantly greater than expected on the basis of variation in individual life histories within the population. We conclude that there is no evidence for an effect of social structure on pod-specific population growth rate. Population growth rate is most sensitive to changes in adult and juvenile survival, followed by fertility. Factors that cause even small changes in survival will thus have a large impact on population growth.

In Press: Ecology.

Supported by: NRC Post-doc Fellowship, EPA R818408-0100 and NSF OCE89-000231.

WHOI Contribution No. 8054.

ENRICHMENT, ISOLATION AND CULTURE OF FREE-LIVING HETEROTROPHIC FLAGELLATES

David A. Caron

Microbiologists traditionally have relied on the study of pure cultures of microorganisms to obtain basic information on the physiology of important species. The culture of a species under carefully controlled conditions provides an experimental framework within which to examine its biology in the absence of potentially confounding interactions with other living organisms. Heterotrophic flagellates are no exception to this maxim, and much of our understanding of flagellate biology has come from laboratory-based studies of cultured species. Studies of cultured flagellates have included examinations of the nutritional modes, feeding rates, growth rates, growth efficiencies, and nutrient remineralization of heterotrophic flagellates. Several simple methods for the enrichment, isolation and routine maintenance of heterotrophic flagellates are described in this chapter. In general, these methods also are applicable for culturing many of the ciliated and amoeboid protozoa.

Submitted to: Current Methods in Aquatic Microbial Ecology, P.F. Kemp, B.F. Sherr, E.B. Sherr and J.J. Cole, eds. Lewis Publishers.

Supported by: NSF Grant OCE89-01005.

WHOI Contribution No. 8036.

LIGHT-DEPENDENT PHAGOTROPHY IN THE FRESHWATER MIXOTROPHIC CHRYSOPHYTE DINOBRYON CYLINDRICUM

David A. Caron, Robert W. Sanders, Ee Lin Lim, Celia Marrasé, Linda A. Amaral, Sheri Whitney, Rika B. Aoki and Karen G. Porter

The mixotrophic (bacterivorous), freshwater, chrysophyte Dinobryon cylindricum was cultured under a variety of light regimes and in bacterized and axenic cultures to investigate the role of phototrophy and heterotrophy for the growth of this alga. D. cylindricum was found to be an obligate phototroph. The alga was unable to survive in continuous darkness even when cultures were supplemented with high concentrations of bacteria, and bacterivory ceased in cultures placed in the dark for a period longer than one day. Axenic growth of the alga, however, was poor even in an optimal light regime. Live bacteria were required for sustained vigorous growth of the algain the light. Carbon, nitrogen and phosphorus budgets determined for the alga during growth in bacterized cultures indicated that bacterial biomass ingested by the alga may have contributed up to 25% of the organic carbon budget of the alga. Photosynthesis was the source of most (>75%) of the organic carbon of the alga. D. cylindricum populations survived but did not grow when cultured in a continuous low light intensity (30 μ Einsteins m⁻² sec⁻¹, or in a light intensity of 150 μ Einsteins m⁻² sec⁻¹ for only two hours each day. Net efficiency of incorporation of bacterial C, N and P into algal biomass under these latter conditions was zero (i.e. no net algal population growth). We conclude that the primary function of bacterivorous behavior in D. cylindricum is to provide essential growth factor(s) or major nutrients for photosynthetic growth. Bacterivorous nutrition, however, may allow for the survival of individuals during periods of very low light intensity or short photoperiod.

In Press: Microbial Ecology.

Supported by: NSF Grant BSR89-19447.

WHOI Contribution No. 8103.

FROM PATCH-OCCUPANCY MODELS TO CELLULAR AUTOMATON MODELS FOR ECOLOGICAL INTERACTIONS

Hal Caswell and Ron J. Etter

The ecological theory of species interactions rests largely on the competition and predator-prey models of Lotka, Volterra, Nicholson, and Gause. These models neglect spatial structure in general,

and patchiness in particular. In this paper we introduce the use of cellular automata (CA) as new class of models for population interactions in space. We will discuss the relations between CA models and the more familiar reaction-diffusion and patch-occupancy formulations, and compare the results of a simple CA competition model to the corresponding Markov chain patch-occupancy model (Caswell and Cohen 1991 a, b).

Patch-occupancy models and ecological cellular automata are both attempts to study spatiotemporal interactions in discrete models. Patch-occupancy models are man-field approximations to CA models. The approach of Caswell and Cohen (1991 a, b), which specifies patch-occupancy models in terms of the time scales of dispersal, disturbance, and local interaction can be adapted directly to the construction of CA models, by defining the state frequencies on which colonization depends in terms of the local neighborhood of a patch rather than in terms of a global average. Comparison of the CA and Markov chain models for competition shows that the latter is a good man-field approximation to the former. The discrepancies between the two seem to be due to inter-neighborhood variance in patch proportions; this variance reduces the effective colonization rate of the losing competition. The patch-occupancy model is a poorer approximation to a CA model with variable disturbance sizes, because the disturbance size distribution introduces a spatial scale intermediate between the single patch and the entire landscape. Similarly, a model with substrate heterogeneity yields spatial patterns that begin to reflect the variability among patches when the pattern becomes sufficiently intense.

In Press: In: Patch Dynamics, S. A. Levin, T. Powell, J. H. Steele eds. Springer-Verlag.

Supported by: NSF Grant OCE89-00231, DOE DE-FG02-89-ERG0882, WHOI Postdoctoral Scholarship, Guggenheim Fellowship.

WHOI Contribution No. 7944.

EVIDENCE FOR METHYLOTROPHIC SYMBIONTS IN A HYDROTHERMAL VENT MUSSEL (BIVALVIA: MYTILIDAE) FROM THE MID-ATLANTIC RIDGE

Colleen M. Cavanaugh, Carl O. Wirsen and H. W. Jannasch

Symbioses between chemolithoautotrophic bacteria and the major macrofaunal species found at hydrothermal vents have been reported from numerous sites in the Pacific Ocean. We present microscopical and enzymatic evidence that

methylotrophic bacteria occur as intracellular symbionts in a new species of mytilid mussel discovered at Mid-Atlantic Ridge (MAR) hydrothermal vents. Two distinct ultrastructural types of Gram-negative procaryotic symbionts were observed by transmission electron microscopy within gill epithelial cells: small coccoid or rod-shaped cells are larger coccoid cells with stacked intracytoplasmic membranes typical of methane-utilizing bacteria. Methanol dehydrogenase, an enzyme unique to methylotrops, was detected in the mytilid gills, while tests for ribulose-1, 5-bisphosphate carboxylase, the enzyme diagnostic of autotrophy via the Calvin cycle, were negative. Stable carbon isotope values (δ 13C) of mytilid tissue (-32.7°/\infty and -32.5°/\infty, for gill and foot tissue respectively) fall within the range of values reported for Pacific vent symbioses, but do not preclude the use of vent derived methane reported to be isotopically heavy (δ 13C) = $\sim -15^{\circ}/_{\infty}$) relative to biogenically produced methane.

Published in: Applied and Environmental Microbiology, 58(12):3799-3803, 1992.

Supported by: NSF Grants OCE89-22854 and OCE92-00458.

WHOI Contribution No. 8095.

PROCHLOROCOCCUS MARINUS NOV. GEN. NOV. SP.: AN OXYPHOTOTROPHIC MARINE PROKARYOTE CONTAINING DIVINYL CHLOROPHYLL A AND B

S. W. Chisholm, S. L. Frankel, R. Goericke, R. J. Olson, P. Palenik, J. B. Waterbury, L. West-Johnsrud and E. R. Zettler

Several years ago, prochlorophyte picoplankton were discovered in the N. Atlantic. They have since been found to be abundant within the euphotic zone of the world's tropical and temperate oceans. The cells are extremely small, lack phycobiliproteins, and contain divinyl chlorophyll a and b as their primary photosynthetic pigments. Phylogenies constructed from DNA sequence data indicate that these cells are more closely related to a cluster of marine cyanobacteria than to their prochlorophyte "relatives" Prochlorothrix and Prochloron. Several strains of this organism have recently been brought into culture, and herewith given the name Prochlorococcus marinus.

Submitted to: Archives for Microbiology.

Supported by: NSF Grants OCE90-12147, OCE90-00043, DSR90-20254, ONR Grant N00014-87-K-0007

WHOI Contribution No. 7938.

SINGLE CELL IDENTIFICATION USING FLUORESCENTLY LABELED, RIBOSOMAL RNA-SPECIFIC PROBES

Edward F. DeLong

In recent years fluorescent DNA stains, used in conjunction with epifluorescence microscopy, have become the standard method for obtaining quantitative information on microbial communities. Most studies to date have utilized DNA and RNA binding fluorochrome stains, such as acridine orange or DAPI, which indiscriminately bind to the nucelic acids of all bacterial cells in a given sample. Field studies using these fluorochrome have provided a wealth of information on total bacterial numbers in a variety of environments, and are particularly well-suited for studying aquatic microbial populations. Though extremely useful, these general fluorochrome stains provide little information on the identity and abundance of specific bacterial population constituents. For detailed analysis of microbial population structure and dynamics. methods for the identification and enumeration of specific microbial taxa are necessary. Recent methodological advances, including the application of fluorescently labeled immunochemical or nucelic acid probes, provide sensitive means to taxonomically identify individual cells present in mixed populations. Though these techniques are relatively new, they have already facilitated rapid identification of culturable and "unculturable" microbial taxa, and the localization of bacterial symbionts in host tissues.

Submitted to: Current Methods in Aquatic Microbial Ecology.

Supported by: ONR Grant No. N00014-90-J-1917. WHOI Contribution No. 7940.

EFFECTS OF NITRATE AND NITRITE ON DISSIMILATORY IRON REDUCTION BY SHEWANELLA PUTREFACIENS 200

Thomas J. DiChristina

The inhibitory effects of nitrate (NO₃-) and nitrite (NO₂-) on dissimilatory iron [Fe³⁺] reduction were examined in a series of electron acceptor competition experiments, using Shewanella putrefaciens strain 200 as a model iron-reducing microorganism. S. putrefaciens was found to express low-rate nitrate-, nitrite- and ferri- reductase activity after growth under highly aerobic conditions, and greatly elevated rates of each reductase activity after growth under microaerobic conditions. The effects of NO₃- and NO₂- on the Fe³⁺ and N-oxide reduction occurred

simultaneously. N-oxide reduction was not affected by the presence of Fe^{3+} , suggesting that S. putrefaciens 200 expressed a set of at least three physiologically distinct terminal reductases that served as electron donors to NO₃-, NO₂- and Fe³⁺, respectively. However, Fe3+ reduction was partially inhibited by the presence of either NO₃or NO₂-. An in situ ferrozine assay was used to distinguish the biological and chemical components of the observed inhibitory effects. Rate data indicated that neither NO₃- nor NO₂- acted as chemical oxidants of bacterially-produced FE²⁺ In addition, the decrease in Fe³⁺ reduction activity observed in the presence of both NO₃- and NO₂was identical to the decrease observed in the presence of only NO2-. these results suggest that bacterially-produced NO2- is responsible for inhibiting electron transport to Fe³⁺.

Published in: Journal of Bacteriology, 174(6)1891-1896, 1992.

Supported by: NSF OCE90-23943.

WHOI Contribution No. 7963.

INTRACELLULAR DISTRIBUTION OF SAXITOXIN IN ALEXANDRIUM FUNDYENSE

Gregory J. Doucette and Donald M. Anderson

The intracellular distribution of saxitoxin (STX) in the marine dinoflagellate Alexandrium fundyense (strain GTCA29) was investigated using immunocytochemical methods. A non-toxic isolate of Alexandrium tamarense (strain PGT183) was included as a control for all experiments. Specimens were prepared using both chemical fixation followed by embedding in either an epoxy-(Spurr) or polar acrylic-based (LR White, Lowicry) K4M) resin, and cryo-fixation techniques. A total of four antibodies against STX (aSTX) were tested. Immunofluorescent labelling of non-osmicated, Spurr-embedded material by all aSTX's was associated with the permanently-condensed chromosomes of A. fundyense. The STX specificity of this staining patterns was verified by negative non-toxic, non-immune and STX pre- incubation controls. Immunocytochemical analysis by electron microscopy confirmed the chromosomal localization of STX. In contrast, LR White-embedded toxic and non-toxic specimens showed labelling of the nucleoplasm. Osmication of either Spurr- or LR White-embedded material climinated virtually all staining. Non-osmicated samples embedded in Lowicryl K4M yielded no nuclear labelling. Both toxic and non-toxic cryo-fixed specimens exhibited labelled chromosomes with not only aSTX but also non-immune serum. We conclude that: 1) STX

occurs in association with the chromosomes of chemically-fixed, Spurr-embedded A. fundyense, 2) osmication and/or embedding in polar acrylic resins precludes immunolabelling of STX, and 3) a non-specific DNA-immunoglobulin interaction prohibits the localization of STX in cryo-fixed dinoflagellates. Because of potential antigen redistribution during chemical fixation, the in vivo distribution of STX remains uncertain.

In Press: Toxic Marine Phytoplankton. T. J. Smayda and Y. Shimizu, eds. Elsevier Science Publishers, Amsterdam.

Supported by: NSF Grant OCE89-11226, NSERC Postdoctoral Fellowship and Florence and John Shumann Foundation.

WHOI Contribution No. 8115.

MECHANISM FOR IRON CONTROL OF THE VIBRIO FISCHERI LUMINESCENCE SYSTEM: INVOLVEMENT OF CYCLIC AMP AND CYCLIC AMP RECEPTOR PROTEIN AND MODULATION OF DNA LEVEL

P. V. Dunlap

Iron controls luminescence in Vibrio fischeri by an indirect but undefined mechanism. To gain insight into that mechanism, the involvement of cyclic AMP (cAMP) and cAMP receptor protein (CRP) and of modulation of DNA levels in iron control of luminescence were examined in V. fischeri and in E. coli containing the cloned V. fischeri lux genes on plasmids. For V. fisheri and E. coli adenylate cyclase (cya) and CRP (crp) mutants containing intact lux genes (luxR luxICDABEG), presence of the iron chelator ethylenediamine-di (o-hydroxyphenyl acetic acid) (EDDHA) increased expression of the luminescence system like in the parent strains only in the cya mutants in the presence of added cAMP In the E. coh strains containing a plasmid with a Mu dI(lacZ) fusion in luxR, levels of β -galactosidase activity (expression from the luxRpromoter) and luciferase activity (expression from the lux operon promoter) were both 2-3 fold higher in the presence of EDDHA in the parent strain. and for the mutants this response to EDDHA was observed only in the cya mutant in the presence of added cAMP. Therefore, cAMP and CRP are required for the iron restriction effect on luminescence, and their involvement in iron control apparently is distinct from the known differential control of transcription from the luxR and LuxICDABEG promoters by cAMP-CRP Furthermore, plasmid and chromosomal DNA levels correlated with an increase in expression of chromosomally encoded β -galactosidase in E. coli

and with a higher level of autoinducer in cultures of V. fischeri. These results implicate cAMP-CRP and modulation of DNA levels in the mechanism of iron control of the V. fischeri luminescence system.

Published in: Journal of Bioluminescence and Chemiluminescence, 7:203-214, 1992.

Supported by: WHOI Independent Study Award. WHOI Contribution No. 7977.

RECENT DEVELOPMENTS IN THE STUDY OF SYMBIOSIS OF LUMINOUS BACTERIA

Paul V. Dunlap

The marine luminous bacteria Vibrio fischeri. Photobacterium leiognathi, and P. phosphoreum form species-specific bioluminescent mutualisms with certain marine fishes and squids. The bacteria are housed as dense pure cultur is in specialized gland-like light organs of the animal host where they obtain nutrients for growth and light production. The host in turn uses the bacterial light for bioluminescence displays involved in feeding, avoiding predators, schooling, and possibly mating. These associations, which can be viewed as controlled bacterial infections, offer special opportunities for studying the interactions between bacteria and marine animals that are involved in symbiosis. Studies of the bacteria in the symbiotic state have indicated that the bacteria grow more slowly in situ than in laboratory culture but produce much higher levels of luminescence. Physiological studies of the bacteria have identified oxygen, iron, and osmolarity as factors that can restrict the growth rate of bacteria, stimulate their luminescence, or do both. These studies have led to a minimal-growth/maximal luminescence model for host control of the symbiotic bacteria. Genetic and molecular approaches are now being used to examine the basis for animal-bacterial interactions in bioluminescent symbiosis. For example, the cloning and expression of the luminescence (lux) genes (luxR luxICDABEG of V. fischeri MJ-1 (from the monocentrid fish Monocentris japonicus) in Escherichia coli, and the recent development of a gene transfer system for V. fischeri, have led to studies of lux gene control in lux::lacZ fusion mutants of this species. The *lux* system of this species is subject to positive and negative genetic autoregulatory control by autoinducer and the LuxR protein and by cyclic AMP (cAMP) and its receptor protein. Glucose and iron (and possibly oxygen) exert additional indirect control over the lux system by undefined mechanisms. How these genetic and physiological factors act and interact in light organ symbiosis is as yet an unresolved issue. Newly developed methods for Transposon

mutagenesis of P. leiognathi LR-1a from the leiognathid fish Leiognathus rivulatus, using pPD104, a broad host range mobilizable plasmid containing transposition-proficient MudI(lacZ, has led to the isolation of different classes of lux dark mutants in this species, including strains defective in luciferase synthesis and strains complemented for luminescence by addition of aldehyde, conditioned medium (ie., autoinducer), and cAMP Transposon mutagenesis of V. fischeri ES-114 from the sepiolid squid Eupryming scolopes using pPD104 has led to the isolation of strains defective in motility. These strains have lost the ability to colonize the squid light organ, which suggests that motility is a molecular determinant of symbiosis in this species. The precision and effectiveness of these modern approaches should rapidly advance our understanding of the molecular basis for how the bioluminescent symbioses are established and maintained.

Submitted to: Microbial Ecology.

Supported by: NSF Grant DCB 91-04653.

WHOI Contribution No. 8180.

CELL DENSITY-DEPENDENT MODULATION OF THE VIBRIO FISCHERI LUMINESCENCE SYSTEM IN THE ABSENCE OF AUTOINDUCER AND LUXR PROTEIN

Paul V. Dunlap and Alan Kuo

Expression of the Vibrio fischeri luminescence genes (luxR luxICDABEG) in Escherichia coli requires autoinducer (N-3-oxo-hexanovl homoserine lactone) and LuxR protein, which activate transcription of luxICDABEG (genes for autoinducer synthase and the luminescence enzymes), and cyclic AMP (cAMP) and cAMP receptor protein (CRP), which activate transcription of the divergently expressed luxR gene. In E. coli and in V. fischeri, the autoinducer-LuxR protein-dependent induction of luxICDABEG transcription (called autoinduction) is delayed by glucose, whereas it is promoted by iron restriction, but the mechanisms for these effects are not clear. To examine in V. fischeri control of lux gene expression by autoinducer, cAMP, glucose, and iron, lur:: Mu dI (lacZ) and lux deletion mutants of V. fischeri were constructed by conjugation and gene replacement procedures. β -galactosidase synthesis in a luxC::lacZ mutant exhibited autoinduction. In a luxR::lacZ mutant, complementation by the luxR gene was necessary for luminescence, and addition of cAMP increased β galactosidase activity 4-6 fold. Furthermore, a luxI::lacZ mutant produced no automducer but responded to its addition with induced syntheses of

 β -galactosidase. These results confirm in V. fischeri key features of lux gene regulation from studies in E. coli. However, β -galactosidase specific activity in the luxI::lacZ mutant, without added autoinducer, exhibited an 8-10-fold decrease and rise back during growth, as did β -galactosidase and luciferase specific activities in the luxR::lacZ mutant and luciferase specific activity in a Δ (luxR luxICD) mutant. The presence of glucose delayed the rise-back in β -galactosidase and luciferase specific activities in these strains, whereas iron restriction promoted it. Thus, in addition to transcriptional control by autoinducer and LuxR protein, the V. fischeri lux system exhibits a cell density-dependent modulation of expression that does not require autoinducer, LuxR protein, or known lux regulatory sites. The response of autoinducer-LuxR-protein-independent modulation to glucose and iron many account for how these environmental factors control lux gene expression.

Published in: Journal of Bacteriology, 174(8):2440-2448, 1992.

Supported by: WHOI Independent Study Award (PVD) and Ocean Ventures Fund (AK).

WHOI Contribution No. 7964.

THE ADVANTAGES OF DISPERSAL IN A PATCH ENVIRONMENT: EFFECTS OF DISTURBANCE IN A CELLULAR AUTOMATON MODEL

Ron J. Etter and Hal Caswell

We use a cellular automaton model to theoretically explore whether long-distance dispersal provides any advantages over local dispersal in a competitive system when the frequency and scale of disturbance varies. We consider a model for a fugitive species capable of persisting regionally if disturbance creates new patches, but excluded by a superior competitor within any patch where they both occur. Only a certain range of disturbance frequencies creates an advantage for global dispersal and this range varies with reproductive output, rate of competitive exclusion, and the extent of disturbance. Local and global dispersal are equally successful when disturbance is rare. If there is not cost to dispersal (global and local dispersers have similar numbers of colonizing propagules), global dispersal is advantageous at intermediate disturbance frequencies. This advantage is considerably higher and extends over a broader range of disturbance frequencies when disturbance varies in size. If there is a cost to dispersal, global dispersal is disadvantageous at high frequencies of disturbance. Bathymetric variation in the proportion of deep-sea prosobranch gastropods with either

planktotrophic or nonplanktotrophic larval development are consistent with the predictions of the model.

In Press: Reproduction, Larval Biology, and Recruitment in the Deep-Sea Benthos. K.J. Eckelbarger and C.M. Young, eds. Columbia University Press.

Supported by: NSF Grant OCE89-00231, DOE Grant DE-FG0289ER6088W.

WHOI Contribution No. 7990.

AROMATIC HYDROCARBON DEGRADING BACTERIA IN THE PETROLEUM RICH SEDIMENTS OF THE GUAYMAS BASIN HYDROTHERMAL VENT SITE: PREFERENCE FOR AROMATIC CARBOXYLIC ACIDS

Frederick E. Goetz and Holger W. Jannasch

Hydrocarbon degrading bacteria in freshly collected petroleum-rich Guaymas Basin sediments were enumerated on mineral base media separately containing the aromatic hydrocarbons naphthalene and biphenyl or the aromatic carboxylic acids benzoate, p- hydroxybcnzoate, mandelate, salicylate, phenylacetate, phthalate or hydrocinnamate. The total numbers of colonies were about 2 orders of magnitude higher on the carboxylic acid media than on the two aromatic hydrocarbons, averaging 105 vs. 103 bacterial per gram of sediment. Of 151 isolates of aerobic. mesophilic marine bacteria, 124 grew on the above carboxylic acids as well as on m-hydroxybenzoate or cinnamate, the rest on naphthalene, biphenyl, dibenzofuran, toluene or phenanthrene. A similarity analysis of 135 of these isolates on the basis of substrate use, sodium chloride requirement, and growth on complex organic marine media, identified 91 metabolically different bacterial strains: 21 belonging to the group of aromatic hydrocarbon utilizers and 70 to the group of carboxylic acid utilizers. Since compounds utilized by organisms of the first group represent end products of petroleum catagenesis, we expected these organisms to predominate. Our results indicate, however, that in Guaymas Basin sediments the majority of hydrocarbon degrading bacteria, numerically and metabolically, appear to be determined by the presence of significant quantities of aromatic carboxylic acids.

In Press: Geomicrobiology Journal.

Supported by: NSF OCE89-22554 and OCE92-00458, ONR N00014-91-J-1751

WHOI Contribution No. 7526.

NUTRIENT AND ENERGY FLOW THROUGH MARINE PLANKTON FOOD CHAINS: IMPACT ON NEW AND REGENERATED PRIMARY PRODUCTION

Joel C. Goldman

There is some controversy regarding the importance of the marine microbial food loop in providing a conduit by which primary production among small phototrophs is channelled up the food chain to higher trophic levels. The question of whether the microbial loop acts as a sink or a source for carbon and nutrients is academic to our understanding of how primary and secondary production are linked together in the ocean. By considering a very simple microbial food chain of only two or three grazing steps, it is a simple exercise to show that the bulk of primarily fixed carbon and acquired nutrients are respired and regenerated well before these materials can become available to support secondary production of larger marine biota. There is now considerable experimental evidence to support this conclusion. Thus if the microbial loop plays a minor role in sustaining the growth of larger marine invertebrate and nekton populations, what are the sources of new production and what are the mechanisms by which primary and secondary production are coupled in the ocean?

There is now accumulating evidence that new production in the ocean, that is primary production that exits the euphotic zone and is supported and balanced by nutrients that are transported across the nutricline from below or from the atmosphere, occurs through the development of relatively simple food chains comprised of larger phytoplankton, zooplankton grazers, and nekton. Although the larger phytoplankton do not grow as fast nor can compete as well for nutrients as cyanobacteria and small eucarvotes that are components of the microbial loop, their success during bloom conditions is the result of imbalances between growth and grazing and the relatively small losses of energy and nutrients that occur in the resulting simple food chains. In nearshore waters and upwelling regions these blooms occur over large spatial and temporal scales and throughout the euphotic zone and thus are easily observed. Blooms in the open ocean, in contrast, can easily go unnoticed. For example, episodic inputs of nutrients into the caphotic zone through mixing events can fuel the rapid growth of very large diatoms (> 50 microns in diameter) in low light regimes, in effect, creating ephemeral eutrophication zones that would be difficult to observe. These cells then can form large aggregates which would sink out rapidly or be transported to

depth by vertically migrating invertebrate and nekton grazers. Only an integrated oxygen signal would be left behind in the euphotic zone as a record of such an event and the resulting energy and nutrient losses would be low. A key factor in trying to record such events is that the appropriate scales of sampling must be employed. For example, measurement of phytoplankton speciation and abundance on discrete, small volume samples could lead to erroneous conclusions regarding the sources of new production. New strategies for oceanographic sampling need to be devised. In addition, it is necessary to understand the processes by which the microbial loop may be linked to new production. Although the microbial loop may not be a source of new production, new nutrients may be funnelled through this system to large phototrophs. Similarly, the microbial loop may be fuelled with energy from the carbonaceous excretion products of large phytoplankton that occur at the end of bloom periods. The complexities of these interactions are poorly known.

Submitted to: Proceedings International Conference on Black Sea Problems.

Supported by: NSF Grants OCE88-18619; and OCE89-22718

WHOI Contribution No. 8196.

CHEMICAL CHARACTERIZATION OF THREE LARGE OCEANIC DIATOMS: POTENTIAL IMPACT ON WATER COLUMN CHEMISTRY

Joel C. Goldman, Dennis A. Hansell and Mark R. Dennett

Three large diatoms, Stephanopyxis palmeriana (Greville) Grunow, Pseudoquinardai recta von Stosch, and Navicula sp. (cell volumes - $1.15 \times 10^5 - 3.83 \times 10^5 \ \mu m^3$), were isolated from the Sargasso Sea and cultivated in batch cultures under low irradiance. Growth rates μ of each species occurred in two phases, an exponential phase where μ varied from 0.72 to 1.12 d⁻¹ and a much slower transition phase that lasted from three to six days. We suspect that diffusion limitation of nutrient transport controlled growth rates during this latter phase. Exponential growth rates were rapid enough to meet the requirements of a bloom scenario whereby total annual new production in a locale such as the Sargasso Sea could be met in a single 21 day bloom. The C:N:P ratio of all three species was close to the Redfield proportions during exponential growth Uncoupling between photosynthesis and nutrient acquisition was evident in one species, S. palmeriana (Greville) Grunow, with carbon

accumulation, both in the form of phytoplankton carbon and dissolved organic carbon, continuing well into the stationary phase, long after nutrients were depleted from the growth medium. In fact, 50% of particulate organic carbon production occurred after the culture entered the station phase. Clearly there is ambiguity in the traditional definition of new production which implies that over a relatively short time scale a balance exists between new nitrogen entering the euphotic zone and new carbon production, assuming a Redfield stoichiometry between cellular carbon and nitrogen. The excess carbon, both particulate and dissolved, could lead to large discrepancies in estimates of new production.

Published in: Marine Ecology Progress Series, 88:257-270, 1992.

Supported by: NSF Grant OCE88-18619.

WHOI Contribution No. 8160.

SIZE-STRUCTURED DEMOGRAPHY OF THE COMPOUND ASCIDIAN PODOCLAVELLA MOLUCCENIS IN A SEASONAL ENVIRONMENT

Nicholas J. Gotelli, Andrew R. Davis and Hal Caswell

We used a size-structured periodic matrix model to study the demography of the annual ascidian Podoclavella moluccensis in a seasonal environment. Two cohorts of ascidians on pier pilings in South Australia were censused approximately every 42 days. Nine censuses throughout the year yielded estimates of the probabilities of growth, persistence, fission and fusion among 4 adult size classes. Podoclavella reproduces sexually only during 6 weeks in November and early December. We incorporated field estimates of rates of larval production, settlement and early juvenile survivorship into the model, and collapsed these terms into a single "recruitment" transition. We used a sensitivity and elasticity analysis to quantify the importance of different transitions to the population growth rate.

The model projected a rapid rate of population increase (1.977 colonies/colony/year), with a corresponding double time of approximately one year. The population growth rate was sensitive to seasonal variation in transition probabilities. Transition probabilities, sensitivities, and elasticities were negatively correlated with sea water temperature, suggesting that small changes in population vital rates during winter months would have the biggest impact on population growth rate. In spite of a variety of potential asexual pathways for reproduction, population growth rate was most sensitive to recruitment

transitions. The contribution of larval processes (brood size, larval settlement, and early juvenile survival) to this recruitment effect was much greater than the contribution of asexual processes (fission, shrinkage, and persistence of small adult colonies). Although *P. moluccensis* produces tadpole larvae for only 6 weeks each year, larval production has important consequences for recruitment and population growth. Our results stand in contrast to demographic analysis of long-lived organisms with delayed reproduction, such as gorgonians (Gotelli 1991) and forest trees (Caswell 1986). For these organisms with perennial life histories, recruitment contributions to population growth rate are negligible.

Submitted to: Ecology.

Supported by: NSF Grant OCE89-00231, EPA Grant R818408-01-0.

WHOI Contribution No. 8006.

MATS OF GIANT SULFUR BACTERIA ON DEEP-SEA SEDIMENTS DUE TO FLUCTUATING HYDROTHERMAL FLOW

Jens K. Gundersen, Bo Barker Jorgensen, Einer Larsen, Holger W. Jannasch

Filamentous sulfide-oxidizing bacteria. Beggiatoa spp., commonly grow as sub-mm thin, white films on anoxic marine sediments. Unusually thick mats (> 1 cm) of giant Beggiatoa filaments, 40-120 μ m wide and 2-1- mm long, were observed at 2000 m water depth in the hydrothermal vent fields of Guaymas Basin, Gulf of California. We were intrigued to explore how such dense communities of the largest known bacterial overcome severe diffusion limitation of their substrate supply, and what advantage they may have by developing such large cell sizes. To understand this, we build a microsensor instrument which could measure vertical gradients of oxygen, sulfide, pH, and temperature through Beggiatoa mats directly on the sea-floor. The instrument was deployed from the submersible ALVIN. We discovered small-scale hydrothermal fluid circulations around patches of the bacteria, causing a pulsatory seawater flow into the mats and thereby enhancing the supply of oxygen and sulfide to the bacteria. The development of giant cells appears to create a loose and strong fabric of filaments which allows this convective flow without the bacteria being swept away.

Published in: Nature, 360(6403):454-456, 1992.

Supported by: NSF OCE92-00458 and ONR N000014-91-J-1751.

WHOI Contribution No. 8164.

CYTOCHROME P4501A INDUCTION AND INHIBITION BY 3,3',4,4'-TETRACHLOROBIPHENYL IN AN AH RECEPTOR-CONTAINING FISH HEPATOMA CELL LINE (PLHC-1)

Mark E. Hahn, Teresa M. Lamb, Mary E. Schultz, Roxanna M. Smolowitz, Alan Poland and John J. Stegeman

The induction of cytochrome P4501A1 (CYP1A1) in rat hepatoma cells has been used by some investigators to determine "dioxin equivalents" in environmental samples, including extracts of fish tissues. However, the relative potency of inducing compounds may vary between species, suggesting the need for taxon-specific model systems. In this paper we present an initial characterization of CYP1A induction in one such system, a telost liver cell line (PLHC-1) derived from a hepatocellular carcinoma of *Poecilionsis* lucida (Hightower & Renfro (1988) J. Exper. Zool. 248:290). Specific binding of the photoaffinity ligand 2-azido-3[125I]iodo- 7,8dibromodibenzo-p-dioxin to proteins in PLHC-1 cytosol indicated the presence of the Ah receptor, which is known to control CYP1A induction in mammals. 3,3',4,4'- Tetrachlorobiphenyl (TCB) induced a microsomal protein in PLHC-1 cells that was recognized by monoclonal antibody (MAb) 1-12-3 to scup CYP1A1 (P450E) on immunoblots. Immunohistochemical staining of whole cells with MAb 1-12-3 showed specific recognition of CYP1A induced by TCB. No staining was seen in untreated or vehicle-treated cells. There was an excellent quantitative correlation between amounts of CYP1A protein detected immunohistochemically and in immunoblots of cell homogenates. In a dose-response experiment, maximal induction of ethoxyresorufin O-deethylase (EROD) activity occurred at 0.1 µM TCB; at higher concentrations (1 and 10 μ M), EROD activity was reduced as compared to the activity at 0.1 µM TCB. In contrast, immunoreactive CYP1A protein increased with increasing TCB concentration up to 10 μ . The loss of EROD activity at high concentrations of TCB did not result from changes in cell number or viability. The apparent inhibition or inactivation of CYP1A catalytic activity by the higher concentrations of halogenated biphenyls has been seen, but not generally recognized, both in vivo and in cultured cells from diverse vertebrate species. PLHC-1 cells may be a good model system for studying Ah receptor- mediated regulation of gene expression, for determining the fish-specific toxic or inducing potency of halogenated aromatic hydrocarbon congeners, and for investigating the mechanism of CYP1A inhibition or inactivation by environmental contaminants such as TCB.

Submitted to: Aquatic Toxicology.

Supported by: PHS Grants ES-05479, ES-04220; EPA R81-7988; Donaldson Charitable Trust

WHOI Contribution No. 8226.

THE ECOLOGY OF BUZZARDS BAY: AN ESTUARINE PROFILE

Brian L. Howes and Dale D. Goehringer

Buzzards Bay, described by Gabriel Archer in an account of Bartholomew Gosnold's discovery in 1602 as "the stateliest sound I was ever in", remains one of the few relatively pristine bays remaining in the metropolitan corridor from Washington to Boston. The Bay and its surrounding marshes and uplands have provided a variety of biotic resources not only to European settlers over the past almost 400 years, but to the native Americans who relied on this estuary for thousands of years before them. Today the uplands are divided between 18 communities and while the Bay is still exploited for its biotic resources, its aesthetic and recreational values add to the growing concern to preserve its environmental quality. At the same time, it has become clear that the health of the Buzzards Bay Ecosystem, like almost all estuarine systems, is controlled not just by processes within the Bay waters themselves, but by inputs from the surrounding upland watershed as well. Therefore, to properly understand and manage this system, it is important to detail activities and land use patterns within the watershed as well as within the tidal reach of the Bay waters. This combined watershed-bay system is referred to as the Buzzards Bay Ecosystem and is the necessary frame of reference for understanding the biotic structure of the Bay and for managing and conserving its resources.

Located in Southeastern Massachusetts, Buzzards Bay and its watershed has long been of interest to biologists for its geographical positioning between several major water masses along the North Atlantic Coast of the United States. This led to the establishment of several major marine research centers, the U.S. Fish Commission (1871, now the National Marine Fisheries Service) and the Marine Biological Laboratory (1888), and later the Woods Hole Oceanographic Institution (1930).

Buzzards Bay's undulating shoreline contains numerous natural harbors and coves, supporting diverse floral and faunal communities as well as commercial and recreational resources. The port of New Bedford, located the southwestern shore, comprises the major industrial and business center within the Buzzards Bay watershed. Well known historically as a hub of the whaling industry in the

early 1800's, it remains an active fishing port (coastal and offshore) for the region and represents the largest revenue-producing fishing port on the East Coast of the United States (Weaver 1984). In the 1980's, New Bedford fisheries landings still ranked as the second most valuable in the United States. The problems facing Buzzards Bay fisheries more than 100 years ago (Baird 1873) (eg. overfishing and restriction of inland waterways) are still with us, however the problem of coastal pollution has been revived as a potential factor in the apparent decline of the areas fisheries. In addition to the historic pollutants (urban runoff, heavy metals), the discovery of PCB pollution in the waters and sediments of New Bedford Harbor in 1976 (Farrington et al. 1984, Weaver 1984) and the rapid growth in the population within the Buzzards Bay watershed have refocused attention resulting in a renewed scientific interest in the Bay and its environs.

The purpose of this community profile is to provide an overview of the ecology of the Buzzards Bay ecosystem. It is not intended to represent an all inclusive review of the literature, but instead an attempt to present key features of the Bay in a readily accessible form and to summarize the dominant ecological processes and parameters which structure the bay environment. Since the current and future environmental health of these types of embayments can be directly influenced by activities within contributing watersheds, understanding the interactions between land and sea is an important component to understanding the ecosystem as a whole. The subjects addressed in this profile, therefore, focus not only on the open bay waters, but also on the ecology of Buzzards Bay within its watershed. After a general introduction to the system, the formation of this bay is discussed in Chapter 2, followed by descriptions of the physical (Chapter 3) and biological (Chapter 4) components of the system and how these interact. Chapter 5 addresses watershed land use and water quality issues within the Bay proper and its circulation restricted coastal embayments. Finally, management issues and the difficulties in balancing demands for access and development while protecting water quality are discussed in Chapter 7.

While Bartholomew Gosnold would certainly be taken aback by the alterations wrought within his stately sound's watershed, areas of the Bay itself remain much as when he sailed almost 400 years ago. However, many activities and increasing pressures of development are beginning to significantly alter this system and only management from a whole system perspective will be effective in protecting this resource which so many are migrating to be near.

Submitted to: U.S. Fish and Wildlife Service.

Supported by: USFWS 84110-83-0269 WHOI Contribution No. 8177.

EQUIVALENCE AND THE ADAPTATIONIST PROGRAM

Edward M. Hulburt

Equivalence guarantees comparison. Thus, one may make a legitimate comparison of all species which, if responding, are adapted to a certain condition with all species which, if not adapted, do not respond to this condition. Several ways in which this theme is elaborated are presented.

An insight into the way in which equivalence works is illustrated as follows. When an eastern woodchuck has a low elevation habitat, has a long growing season, has sexual maturation in the second year, has annual reproduction, and has an aggressive intolerant social system, this bundle of traits is adaptive of, maximizes the fitness of. woodchuck x. And the equivalent to "If x has the woodchuck bundle of traits, then this bundle is adaptive of x" is 'If this bundle is not adaptive of x, then x does not have the woodchuck bundle of traits'. So there are two steps wherein x stays the same: x has the woodchuck bundle: x does not have the woodchuck bundle. But there is a third step wherein an Olympic marmot as a different 'x' has an opposite bundle of traits and thus does affirm the second equivalent "if the woodchuck bundle is not adaptive of x, then x does not have this bundle".

The process of adaptation, as when bird, adapted for flight, came from reptile, not adapted for flight, is really a three step process: x is adapted for flight, the same x is conceived as not adapted for flight, a different x (reptile) really is not adapted for flight. But this evolutionary metamorphosis of 'adapted' from 'not adapted' rests squarely on the mechanics of an equivalence, just like the one just mentioned for the woodchuck-marmot case.

The adaptationist program says this: "each aspect of an organism's morphology, physiology and behavior has been molded by natural selection as a solution to a problem posed by the environment" (Lewontin 1978). But the "wholesale reconstruction of a reptile to make a bird is considered a process of major adaptation by which birds solved the problem of flight" (Lewontin 1978). The first quoted sentence says that each organism (or group or organisms) solved a problem and thus endorses only affirmation of "adapted". The equivalence analysis behind the second quote endorses both affirmation and denial of "adapted" in the process of adaptation. Thus, there is contradiction in the presentation of the adaptationist program by Lewontin.

Submitted to: Ecological Modelling.
WHOI Contribution No. 8030.

MICROBIAL GROWTH KINETICS: A HISTORICAL ACCOUNT

Holger W. Jannasch and Thomas Egli

In the early 1940s Hinshelwood's unhesitating parallels between chemical reaction kinetics and microbial growth have often been credited with the origin of ideas that subsequently led to the mathematical description of processes and parameters in batch and continuous culture. The conception of the chemostat, the steady-state-attaining continuous culture, in 1950 by Monod in Paris and simultaneously by Novick and Szilard in Chicago was preceded by a tradition of using continuous culture systems in microbial technology, especially in Prague by a group then headed by Málek. This discussion concentrates primarily on work done during the 1950s and 1960s when developments in various applications of microbial growth kinetics went through an "exponential phase" mediated by the mathematical treatment by Herbert and his co-workers at Porton. In a number of international symposia and the well organized annual reviews in the Czech journal Folia Microbiologia, a wealth of new ideas were efficiently made available to the international community of microbiologists. From a large number of innovative applications in "homocontinuous" culture, major advances occurred in the areas of cell mass production, growth and cell division, DNA/RNA ratio and cell size, microbial selection and enrichment processes, rates of mutation and the periodic accumulation of mutants, metabolic regulation and enzyme synthesis, especially derepression, etc. Besides the enforced steady state conditions of the chemostat, "heterocontinuous" single- and multi-stage systems provided intriguing experimental possibilities in biotechnology as well as the study of natural microbial processes at increasing complexity.

In Press: Antonie van Leeuwenhoek special issue. Symposium Proceedings, Zürich.

Supported by: NSF Grant OCE92-00458.

WHOI Contribution No. 8166.

COMPARATIVE PHYSIOLOGICAL STUDIES ON HYPERTHERMOPHILIC ARCHAEA ISOLATED FROM DEEP-SEA HOT VENTS WITH EMPHASIS ON PYROCOCCUS STRAIN GB-D

Holger W. Jannasch, Carl O. Wirsen, Stephen J. Molyneaux and Thomas A. Langworthy

Three new sulfur- or non-sulfur-dependent archaeal isolates, including a Pyrococcus strain, from Guaymas Basin hydrothermal vents (Gulf of California, depth 2010 m) were characterized and physiologically compared to four known hyperthermophiles, previously isolated from other vent sites, with emphasis on growth and survival under the conditions particular to the natural habitat. Incubation under in situ pressure (200 atm) did not increase the maximum growth temperature by more than 1°C for any of the organisms, but did result in increases of growth rates up to 15% at optimum growth temperatures. At in situ pressure, temperatures considerably higher than those limiting growth (i.e., >105°C) were survived best by isolates with highest maximum growth temperatures, but none of the organisms survived 150°C or higher for 5 minutes. Free oxygen was toxic to all isolates at growth range temperatures, but at ambient deep sea temperature (3-4°C) the effect varied in different isolates, the non-sulfur-dependent isolate being the most oxygen tolerant. Hyperthermophiles could be isolated from refrigerated and oxygenated samples after a 5 years' storage. Cu, Zn and Pb ions were found to be toxic under non-growth conditions (absence of organic substrate), again the non-sulfur-dependent isolate being the most tolerant.

Published in: Applied and Environmental Microbiology, 58(11):3472-3481, 1992.

Supported by: NSF Grants OCE89-22854 and OCE92-00548, ONR Grant N00014-91-J-1751.

WHOI Contribution No. 8128.

BACTERIAL SULFATE REDUCTION ABOVE 100°C IN DEEP-SEA HYDROTHERMAL VENT SEDIMENTS

Bo Barker Jorgensen, Mai F. Isaksen and Holger W. Jannasch

The currently known upper temperature limit for growth of organisms, a number of archaebacteria, is 100°C, but among the sulfate-reducing bacteria growth temperatures of greater than 100°C have not been found. A search for high-temperature activity of sulfate-reducing

bacteria was done in hot deep-sea sediments at the hydrothermal vents of the Guaymas Basin tectonic spreading center in the Gulf of California. Radio-tracer studies revealed that sulfate reduction can occur at temperatures up to 110°C with an optimum rate at 103°to 106°C. This observation expands the upper temperature limit of this process in deep ocean sediments by 20°C and indicates the existence of an unknown group of hyperthermophilic bacteria with a potential importance for the biogeochemistry of sulfur above 100°C.

Published in: Science, 258(5089):1756-1757, 1992. Supported by: NSF OCE92-00458 and ONR N00014-91-J-1751.

WHOI Contribution No. 8165.

AMPHIPODS ON A DEEP-SEA HYDROTHERMAL TREADMILL

S. Kaartvedt, C. L. Van Dover, L. S. Mullineaux, P. H. Wiebe, and S. M. Bollens

Conspicuous swarms of a pardaliscid amphipod were observed at about 2520 and 2580 m depth in the East Pacific Rise vent field during dives with the submersible ALVIN. Swarms occurred in association with mussels, clams and tubeworms, and were located above, and immediately downstream of cracks with emanating hydrothermal water. Numerical density sometimes exceeded 10000 individuals 1^{-1} , which is three orders of magnitude higher than any previous report on pelagic crustaceans from the deep-sea. The amphipods were, however, not obligatory swarmers, and thin-layered shoals and scattered individuals were observed. Orientation of individuals was often polarized as they headed into the venting flow, swimming vigorously at 5-10 cm s⁻¹ to maintain their position in the current. Retention within the preferred habitat requires an average swimming speed corresponding to the average current speed, suggesting a sustained swimming of >10 body lengths s^{-1} . These observations contrast with the general concept of low swimming activity in deep sea crustaceans. Submitted to: Deep Sea Research.

Supported by: NSF Grant OCE90-19575 WIIOI Contribution No. 8193.

USE OF REMOTELY-SENSED SEA SURFACE TEMPERATURES IN STUDIES OF ALEXANDRIUM TAMARENSE BLOOM DYNAMICS

Bruce A. Keafer and Donald M. Anderson

Remote sensing of sea surface temperatures

(SST) has proven to be a useful tool in studies of the bloom dynamics of Alexandrium tamarense and the onset of PSP in the southwestern Gulf of Maine. A warm coastal current (= plume) formed from spring runoff that is believed to be responsible for the southerly transport of A. tamarense along the coast in this region was easily resolved in SST imagery. Coastal upwelling, which moved the warmer A. tamarense containing buoyant plume offshore and away from nearshore shellfish, was detected in two of the three years of this study. The imagery provides valuable insights into the short-term oceanographic processes responsible for the development and behavior of the plume and the distribution of A. tamarense. Remotely-sensed SST has great promise as a tool to provide early warning of the conditions conducive for bloom development, transport and the initiation of PSP in this region.

In Press: Toxic Marine Phytoplankton, T.J. Smayda and Y. Shimizu, eds. Elsevier, Amsterdam.

Supported by: National Sea Grant College Program
Office (NA90-AA-D-SG480), and ONR Grant
N00014-89-J-111.

WHOI Contribution No. 8114.

ISOTOPIC FRACTIONATION OF OXYGEN BY RESPIRING MARINE ORGANISMS

John Kiddon, Michael Bender, Joe Orchardo, Joel Goldman, David A. Caron and Mark Dennett

We measured the respiratory isotope effect, ε_{resp} , for nine representative unicellular marine organisms. The bacterium Pseudomonas halodurans, the diatoms Skeletonema costatum and Phaeodactylum tricornutum, the phytoflagellates Cryptomonas baltica, Dunaliella tertiolecta, the heterotrophic flagellates Paraphysomonas imperforata and Bodo sp., and the ciliate Uronema sp. exhibit ε_{resp} , values in the range -14 to -26°/ ∞ . We also measured ε_{resp} for three metazoans. The ε_{resp} for the copepod Acartia tonsa ranged from -17 to -25°/ ∞ , while two larger organisms, the mollusk Mercenaria mercenaria and the salmon Salmo salmar, respire with a smaller ε_{resp} , from -5 to -10°/ ∞ .

The average respiratory isotope effect of the dominant marine respirers (the bacteria, microalgae and zooplankton) is about $-20 \pm 3^{\circ}/_{\infty}$. An ε_{resp} of this magnitude supports the hypothesis that the photosynthesis-respiration cycle is responsible for the $23.5^{\circ}/_{\infty}$ enrichment in the $\delta^{18}0$ ratio of atmospheric 0_2 relative to seawater (the Dole effect). The large value and high variability in the average ε_{resp} limits the usefulness of a proposed method using the $\delta^{18}0$ of

naturally fractionated dissolved 0_2 in seawater as a tracer of primary production in the oligotrophic ocean.

Submitted to: Global Biogeochemcial Cycles.

Supported by: NSF Grant OCE-85-11283, WHOI Independent Study Award.

WHOI Contribution No. 8245.

EFFECTS OF TEMPERATURE ACCLIMATION ON THE EXPRESSION OF HEPATIC CYTOCHROME P4501A AND MRNA AND PROTEIN IN THE FISH FUNDULUS HETEROCLITUS

Pamela J. Kloepper-Sams and John J. Stegeman

Previous studies showed that hydrocarbon induction of hepatic microsomal monooxygenase activity is attenuated in the telost fish Fundulus heteroclitus acclimated to low temperature. The basis of that attenuation, and the effects of temperature on monooxygenase activity, were examined by analyzing liver cytochrome P4501A (CYP1A) mRNA, protein, and catalytic activity in control and β -naphtholflavone (BNF)-treated F. heteroclitus acclimated to 6°C or 16°C. There were no temperature-related differences in total P450 content, NADPH-cytochrome c (P450) reductase activity, ethoxyresorufin O-deethylase (EROD) activity, or in immunoquantified CYP1A content in hepatic microsomes of untreated fish. Fish acclimated to 16°C and given a single intraperitoneal injection of BNF exhibited a rapid rise and fall in CYP1A mRNA content, and an induction of EROD activity and CYP1A protein that was undiminished over 7 days. Similarly treated fish acclimated at 6°C showed an increase in EROD activity or CYP1A content over 7 days. Examined over a longer term, microsomal EROD activity was significantly induced by BNF in fish at both temperatures; activity peaked at 5-7 days in 16° fish, while in 6° fish (0.68 nmol/min/mg) was less than half that seen in the warmer animals (1.46 nmol/min/mg). Immunodetectable CYP1A content showed the same trend as EROD activity, and the catalytic efficiency (nmol product formed/min/nmol CYP1A) for EROD activity was about the same in all groups, indicating that concentration of the catalyst alone could account for the different patterns of microsomal activity. CYP1A mRNA content was again induced to a similar degree by BNF in both the 6° and 16° fish: the apparent half-life of the mRNA was substantially longer in cold-acclimated than in warm-acclimated BNF-treated fish. Comparing the levels of CYP1A mRNA and protein at the two acclimation temperatures following BNF treatment indicates that translational activity, rather than

transcriptional activity, is the sensitive point in the effect of temperature on CYP1A induction in these fish.

Published in: Archives of Biochemistry & Biophysics, 299 (1):38-46, 1992.

Supported by: PHS Grants ES-04220 and CA-44306. WHOI Contribution No. 8028.

ELEVATED ORNITHINE
DECARBOXYLASE ACTIVITY,
POLYAMINES AND CELL
PROLIFERATION IN NEOPLASTIC AND
VACUOLATED LIVER CELLS OF
WINTER FLOUNDER (PLEURONECTES
AMERICANUS)

Robert A. Koza, Michael J. Moore and John J. Stegeman

Liver neoplasms, including hepatocellular and cholangiocellular carcinomas, commonly occur in winter flounder (Pleuronectes americanus) caught from chemically-contaminated areas such as Boston Harbor. Hydropically vacuolated cells, very often associated with neoplasia in winter flounder liver, appear to represent the first cellular abnormality in animals that later develop frank neoplasms. The proliferative capacity of hydropically vacuolated cells was studied by analyzing both ornithine decarboxylase (ODC) activity and bromodeoxyuridine (BrdU) labeling indices. Liver of winter flounder with vacuolated cellular lesions had ODC activity more than 5-12 fold greater than that in liver that lacked such vacuolation, whether caught from Boston Harbor or Georges Bank. Large focal areas of hydropically vacuolated cells dissected from severely affected livers had ODC activity as high or higher than surrounding parenchymal tissue. Significant elevations in hepatic polyamine levels and ratios of putrescine/spermidine were also present in all Boston Harbor animals studied, especially those exhibiting vacuolated cellular lesions, as compared to George Bank fish. BrdU labeling techniques indicate that hydropically vacuolated cells, along with perivacuolar small basophilic cells and neoplastic cholangiocytes, appear to have the capacity to synthesize DNA and undergo mitosis. The frequent association of hydropically vacuolated cells with hepatic neoplasia, along with high ODC activity and DNA synthesis capability, suggest that the vacuolated cells and/or perivacuolar basophilic cells may be integral to the development of many neoplastic phenotypes in winter flounder liver.

Submitted to: Carcinogenesis.

Supported by: PHS Grant CA 44306; NOAA COP Grant NA-90-AA-D-SG480

WHOI Contribution No. 8203.

INITIATION AND PROMOTION OF HEMATOPOIETIC NEOPLASIA IN SOFT SHELL CLAMS EXPOSED TO NATURAL SEDIMENT

D. F. Leavitt, D. Miosky Dragos, B. A. Lancaster, A. C. Craig, C. L. Reinisch and J. McDowell Capuzzo

Field studies have shown that soft shell clams (Mya arenaria) living in contaminated sediments in New Bedford Harbor, MA., have a higher prevalence of hematopoietic neoplasia than clams living in less contaminated sediments. To determine the mechanism by which this phenomenon occurs, either initiation of the neoplasia or promotion of an endemic problem, a protocol modified from rat liver neoplasia studies was undertaken. Previously diagnosed clams (using an immunoperoxidase technique) were distributed into individual pots (10 clams per pot) containing sediment collected from New Bedford Harbor or a control site. The clams were distributed into 3 disease groups; clams with no evidence of the disease (stage 0 group), clams with a disease state where less than 15% of the circulating hemocytes were neoplastic (stage 1 group), and clams that were diagnosed disease-free but were then challenged with an injection of 10⁵ neoplastic cells in filtered seawater (transmitted group). Disease state, mortality, and growth rates of each group were monitored over a 4 month period. The results indicate that clams which were originally diagnosed with no disease developed leukemia at about the same rate regardless of the sediment type of the experiment. Those clams that were challenged with the diseased cells developed leukemia at a significantly higher rate when exposed to contaminated sediment, indicating that the contaminants in sediment from New Bedford Harbor assist in promoting the development of the disease once it has been initiated. This observation was supported by the stage 1 clams exposed to New Bedford Harbor sediment. These data suggest that the significantly higher prevalences of hematopoietic neoplasia observed in New Bedford Harbor are due to the promotional properties of the contaminants (including PAHs, PCBs, and trace metals) rather than initiation of the leukemia.

Submitted to: Proceedings, Workshop on Invertebrate Neoplasia, World Congress on Cell and Tissue Culture, Washington, DC.

Supported by: Tufts University, Center for Environmental Management, US EPA CR813481.

WHOI Contribution No. 8242.

TEMPORAL VARIATION IN POPULATIONS OF THE MARINE ISOPOD EXCIROLANA: HOW STABLE ARE GENE FREQUENCIES AND MORPHOLOGY?

H. A. Lessios, James R. Weinberg and Victoria R. Starczak

Excirolana braziliensis is a dioeceous marine isopod that lives in the high intertidal zone on both sides of tropical America. It lacks a dispersal phase and displays a remarkable degree of genetic divergence even between localities less than 1 km apart. Nine populations of this species from both sides of the Isthmus of Panama and one population of the closely allied species, E. chamensis, from the eastern Pacific were studied over the period of two years for allozymic temporal variation in thirteen loci and over three to four years for morphological variation in nine characters. Genetic and morphological constitution variation in nine characters. Genetic and morphological constitution of 9 out of 10 populations remained stable. Allele frequencies at two loci and overall morphology in a tenth beach occupied by E. braziliensis changed drastically and significantly between 1986 and 1988. The change in gene frequency is too great to be explained by genetic drift occurring over a maximum of 14 generations regardless of assumed effective population size; drift is also unlikely to have caused changes in morphology. Selective survival of a previously rare genotype is more plausible, but still not probable. The most credible explanation is that the resident population at this locality went extinct and that the beach was recolonized by immigrants from another locality. Such infrequent episodes of extinction and recolonization from a single source may account for the large amount of genetic divergence between local populations of E. braziliensis. However, the low probability of large temporal genetic change even in a species such as this, in which gene flow between local demes is limited and generation time is short, suggests that a single sample through time is usually adequate for reconstructing the genetic history of populations.

Submitted to: Evolution.

Supported by: Smithsonian Institution; National Geographic Society; and WHOI.

WHOI Contribution No. 8016.

THE LAW OF THE FISHES

Phillip S. Lobel

The generalization that deep-bodied fish are rarely eaten by larger predatory fishes was examined for the Caribbean coral reef community using Randall's (1967) data on fishes food habits. The largest proportions (63/piscivores (N = 58 spp.) were fusiform with body depth to standard length ratios of 20 to 40%. Anecdotal observations illustrate exceptions; sometimes prey are too large to swallow or are ingested tail first.

Supported by: NOAA; Office of Sea Grant NA90-AA-D-SG535, ONR Grant N00014-91-J-1591, NOAA NURP Grant 89-09-NA88A-H-URD20.

WHOI Contribution No. 8159.

SEASONAL AND DAILY CHANGES IN BACTERIVORY IN A COASTAL PLANKTON COMMUNITY

Celia Marrasé, Ee Lin Lim and David A. Caron

Flourescently labeled bacteria (FLB) were used to examine the long-term changes (monthly for eight months) and short-term changes (daily for ten days) of bacterial grazing in a natural plankton community. Two preliminary experiments also were performed to evaluate the effect of sample volume, incubation time, and light regime on the results. The experimental results indicated a "bottle effect" for the three smallest sample volumes employed (100, 200 and 500 ml), and lower grazing rates were always observed during 24 h incubations than during 48 h incubations. The light regime (continuous darkness, continuous light, 12L:12D) did not affect the grazing rates during a 48 h experimental period. Bacterivory in the seasonal study in Vineyard Sound, Massachusetts was highly responsive to water temperature and was the primary factor determining grazing pressure over the winter-summer period. Samples incubated at 20°C during the winter months consistently exhibited higher rates of consumption of bacterial than a triplicate set of samples incubated at ambient water temperature of 5°C. Daily fluctuations in the rates of bacterivory during a ten-day period in May were significant, but were approximately 1/10 the magnitude of the seasonal fluctuation. Maximal rates of bacterivory removed up to 60% of the bacterial assemblage daily.

Published in: Marine Ecology Progress Series, 82:281-289, 1992.

Supported by: NSF OCE86-00510, NSF OCE89-01005, the Florence and John Schumann Foundation and a Fulbright Fellowship.

WHOI Contribution No. 7987.

MATRIX METHODS FOR AVIAN DEMOGRAPHY

David B. McDonald and Hal Caswell

Population studies of birds have a long history. Demographic methods for such studies were last reviewed by Ricklefs (1973). That review focused on methods derived from classical age-structured demography, using the life table (survivorship (l_x) and maternity (m_x) functions; we will refer to this combination as an (l_x) m_x table as the framework for analysis. Most avian demographic studies have used these methods, or simplifications which take advantage of particular aspects of avian life cycles (e.g., Mertz, 1971).

In the nearly two decades since Ricklefs' review matrix population models have been developed into a powerful general framework for demographic analysis. They subsume classical life table analysis as a special case, but have capabilities that go far beyond that analysis:

(1) They are not limited to classifying individuals by age; instead, they can accommodate classifications by stages that describe social status, spatial location, developmental stage, habitat quality or other variables of biological interest.

(2) They lead easily to sensitivity analysis, which pinpoints the most ecologically and evolutionarily important portions of the life history

- (3) They can be constructed using the life cycle graph, an intuitively appealing graphical description of the life cycle, which helps to assure correct parameterization of the model and provides a mechanism for evaluating alternative life histories
- (4) They are easily extended to include stochastic variation and density-dependent nonlinearities, forming the basis of complex simulation models, if desired.

Matrix models were initially developed by Leslie (1945, 1948). They have been thoroughly reviewed in Caswell (1989b); this paper is based largely on, and intended as an introduction to, that book.

In Press: Current Ornithology.

Supported by: NSF Grant OCE89-00231, DOE Grant DE-FG02-89ER60882, EPA Grant R818408-01-0.

WHOI Contribution No. 7937.

THE BIOACCUMULATION AND BIOLOGICAL EFFECTS OF LIPOPHILIC ORGANIC CONTAMINANTS IN OYSTERS

Judith McDowell Capuzzo

Bioaccumulation of lipophilic organic contaminants in oysters are consistent with patterns of bioaccumulation predicted from general patterns observed in other species of marine bivalve molluscs. The major factors controlling the distribution of organic contaminants are the relative concentrations of individual contaminants in ambient waters and pore waters of benthic habitats, modified to some extent by differences in partitioning between organisms and water (as indicated by differences in K-ow), and seasonal variations in lipid content. For some contaminants, such as tributyltin, both physical-chemical factors and non-specific binding may influence the ultimate fate. Although the range of studies on biological responses of oysters to organic contaminants is more limited in scope than studies using species such as the mussel Mytilus edulis, patterns of response at various levels of biological hierarchy are consistent and suggest that our understanding of toxic mechanisms may be transferred from one species to another.

Specific questions that remain unanswered are:

- (1) What are the mechanisms by which neoplastic conditions of bivalve molluscs are induced by lipophilic organic contaminants?
- (2) To what extent is biotransformation of contaminants involved in the responses of bivalve molluscs at different levels of biological hierarchy?
- (3) How does exposure to multiple classes of contaminants alter biological responses of bivalve molluscs?
- (4) Are responses in bivalve molluscs reversible with depuration of organic contaminants?

The oyster Crassostrea virginica may serve as an ideal test species to resolve these questions, particularly in estuarine habitats and the Gulf of Mexico where ambient levels of organic contaminants have been well documented.

Submitted to: The Eastern Oyster, Crassostrea virginica, A. Eble, V. S. Kennedy and R. I. E. Newell, eds. Maryland Sea Grant.

Supported by: NOAA Grant No. NA87AA-0-0M093 and Grant No. NA260A0462-01.

WHOI Contribution No. 8243.

RESPONSES OF MOLLUSCS TO CHEMICAL CONTAMINANTS IN COASTAL ENVIRONMENTS

Judith McDowell Capuzzo

Uptake and bioconcentration of organic contaminants by marine bivalves are dependent on the bioavailability of specific compounds, the duration of exposure, and the physiological condition of populations. Species differ in rate the of uptake due to differences in filtration rates, lipid content, and habitat. Biological effects associated with bioconcentration of lipophilic contaminants have been attributed to the uptake of specific compounds and/or their metabolites, rather than the total body burden of hydrocarbons or chlorinated hydrocarbons. Empirical data suggest that linkages exist between: (1) developmental and reproductive abnormalities; (2) the physiological and molecular processes involved in uptake, retention and loss of contaminants; and (3) the toxicity and/or transformation of lipophilic contaminants. Biological responses that may contribute to the impairment of reproductive and developmental processes include responses that can be categorized as interfering with bioenergetic processes such as feeding and nutrient allocation; biosynthetic processes, such as the synthesis of energy stores; and morphogenic processes such as those involved in structural development. An understanding of the relationship between bioavailability, bioconcentration, and mechanisms of biological damage warrants further consideration.

Submitted to: Proceedings, Northeast Shelf
Ecosystem: Stress, Mitigation and Sustainability,
Large Marine Ecosystems Series.

Supported by: NOAA Grant No. NA87AA-0-0M093 and Office of Sea Grant NA86AA-D-S6090 (RP/22 and RP/17).

WHOI Contribution No. 8244.

INDUCED CYTOCHROME P450IA IN WINTER FLOUNDER FROM GEORGES BANK AND COASTAL SITES OF THE NORTHEASTERN UNITED STATES AND CANADA

Emily Monosson and John J. Stegeman

The content of hydrocarbon-inducible liver microsomal cytochrome P450IA was measured in winter flounder collected from the coastal sites Boston Harbor, MA; Hempsted Harbor, NY and Niantic, CT, adjacent to heavily populated areas, from Passamaquoddy Bay, New Brunswick, Canada (less populated than the former sites) and

from one offshore site, Georges Bank. Hepatic concentrations of Aroclor 1254 (A1254) and 3,3',4,4'-tetrachlorobiphenyl (3,3',4,4'-TCB) were also measured in fish from each site. Concentrations of A1254 were the least in fish from Georges Bank and New Brunswick (ranging from $0.002 - 0.003 \text{ ug g}^{-1} \text{ dry weight)}$, as were 3,3',4,4'-TCB concentrations (ranging from 0.002 -0.003 ug g⁻¹ dry weight). Concentrations of both A1254 and 3,3',4,4'-TCB were much higher in fish from Boston, Niantic and Hempsted Harbor (ranging from $7.6 - 11.3 \text{ ug g}^{-1}$ for Aroclor, and from 0.013 - 0.024 mg·g⁻¹ for 3,3',4,4'-TCB). Immunoblot analysis with monoclonal antibody 1-12-3 revealed P4501A protein content of 0.17 and 0.19 nmol mg⁻¹ in liver mocrosomes of fish from Georges Bank and New Brunswick. Microsomal P4501A content in fish from Boston, Niantic and Hempsted ranged from 0.25 to 0.41 nmol mg⁻¹. Ethoxyresorufin- O-deethylase (EROD) specific activities were also greater in fish from Boston, Niantic and Hempsted, compared to flounder from Georges Bank or New Brunswick. These data, together with data on PCB content, P4501A content and/or EROD activity reported in previous studies of winter flounder indicate that strong induction of P4501A protein occurs in these fish along the majority of the industrialized east coast. The results also show that induction of P4501A is common, but less strong at sites removed from the urban centers of the east, and that for the sites included in this study, the degree of hepatic induction of P4501A correlates well with hepatic A1254 and 3,3',4,4'-TCB concentrations.

Submitted to: Canadian Journal of Fisheries and Aquatic Science.

Supported by: EPA Cooperative Agreement CR-813155.

WHOI Contribution No. 8148.

BROMODEOXYURIDINE UPTAKE IN HYDROPIC VACUOLATION AND NEOPLASMS IN WINTER FLOUNDER LIVER

Michael J. Moore and John J. Stegeman

Winter flounder (Pleuronectes americanus) from Boston Harbor, MA., undergo a progressive series of hepatic changes involving hydropic vacuolation of epithelial cells, biliary hyperplasia, and hepatocellular and cholangiocellular neoplasia. Several affected fish often exhibit grossly visible lesions. To examine cell proliferation associated with these conditions, evidence for DNA synthesis was sought. Boston winter flounder livers were screened endoscopically to select fish with and without grossly visible hepatic lesions, and then

injected intraperitoneally with bromodeoxyuridine (BrdU) 3 hours before sacrifice. Incorporation of this nucleotide analog was visualized immunohistochemically in formalin-fixed, paraffin-embedded tissues. Basal epithelia in the gill and intestine stained strongly, as did renal hemopoietic epithelia. In contrast, renal tubular epithelia and cardiomyocytes did not stain. Normal appearing hepatocytes stained occasionally, whilst more frequent staining was observed in vacuolated and neoplastic hepatic epithelia. We conclude: 1) that the BrdU assay as described here has potentially widespread application to the study of cell proliferation in fish tissues: 2) that vacuolated cells may actively proliferate in winter flounder liver from Boston Harbor and 3) vacuolated cells may be involved in the neoplastic transformation of hepatic epithelia.

Submitted to: Marine Environmental Research.

Supported by: PHS Grant CA/ES44306, and Donaldson Charitable Trust.

WHOI Contribution No. 8008.

IMPLICATIONS OF MESOSCALE FLOWS FOR DISPERSAL OF DEEP-SEA LARVAE

Lauren S. Mullineaux

Dispersal of larvae between isolated benthic habitats in the deep sea may be strongly influenced by mesoscale (10's to 1000's of meters) flows. For instance, mesoscale flow features near seamounts, such as eddies and Taylor Caps, are capable of retaining water parcels for periods of weeks to months. These flow features are likely to retain and accumulate larvae spawned by the seamount benthos, increasing the probability that they recolonize their source habitats. When topographic flow features become unstable and advect away from the seamount, they may transport the larvae to remote habitats as discrete concentrated patches. At hydrothermal vents, hot water released at the seafloor forms bouyant plumes that entrain large volumes of near-bottom water. Zooplankton, including larvae of benthic invertebrates, may thereby be transported 10's of kilometers away from the source vent communities. If the vertical velocity of the buoyant plume is sufficiently strong it may form vortices, retaining vent fluids and their associated fauna in the vicinity of the vent. These vortices, and the benthic larvae entrained into them, may then advect away as discrete patches. Thus, dispersal of larvae from vents and seamounts may occur infrequently, but in concentrated patches, causing episodic recruitment to remote habitats.

Submitted to: Reproduction, Larval Biology and Recruitment in the Deep-Sea Benthos. K.J. Eckelbarger and C.M. Young, eds. Columbia University Press.

Supported by: ONR N00014-89-J-1431 and NSF OCE91-810575.

WHOI Contribution No. 7956.

LARVAL RECRUITMENT IN RESPONSE TO MANIPULATED FIELD FLOWS

Lauren S. Mullineaux and Elizabeth D. Garland

Settlement responses of several invertebrate taxa, including the hydroid Tubularia crocea, the bryozoans Bugula turrita and Schizoporella unicornis, and the tube-building polychaete Hydroides dianthus were studied in manipulated field flows. During three experiments in 1989 and two in 1980, densities of newly-recruited larvae were measured on flat plates, whose flow regimes had been manipulated by altering the leading edge configurations. Settlement responses to flow were strongly species specific, with T. crocea preferring regions with both high turbulence and strong shear stress, and S. unicornis settling almost exclusively in regions with high shear stress. B. turrita settled most prominently in regions of reduced shear stress, exhibiting settlement patterns that closely approximated predictions from a passive particle contact model. H. dianthus showed a moderate avoidance of regions with high shear stress. These results indicate that boundary-layer flows affect settlement of several common encrusting species, a probable consequence of larval behaviors such as substrate rejection or exploration in response to flow. These responses are likely to generate patchiness during initial colonization of natural habitats, and certainly affect colonization of settlement panels commonly used in marine ecological studies.

Submitted to: Marine Biology.

Supported by: ONR Grants N00014-89-J-1341 and N00014-89-J-1112 and Coastal Research Center.

WHOI Contribution No. 8110.

INTERLABORATORY COMPARISON AND OPTIMIZATION OF HEPATIC MICROSOMAL ETHOXYRESORUFIN O-DEETHYLASE ACTIVITY IN WHITE SUCKER (CATOSTOMUS COMMERSONI) EXPOSED TO BLEACHED KRAFT PULP MILL EFFLUENT

K. R. Munkittrick, M. R. van den Heuvel, D. A. Metner, W. L. Lockhart and J. J. Stegeman

Twelve samples of minced liver from white

sucker (Catostomus commersoni) were delivered to 14 laboratories in Canada and the USA for the analysis of hepatic ethoxyresorufin-O-deethylase (EROD). Samples were collected from a site exposed to bleached kraft pulp mill effluent (BKME) and from a reference site. All laboratories analyzing EROD activity successfully differentiated between effluent exposed fish (high activity) and reference samples (low activity). Absolute activity detected in samples from the induced site varied greatly with analysis method; assay conditions at most laboratories were sub-optimal; for white sucker microsomes, and absolute activity of the samples was most affected by pH, temperature and substrate limitation. The type of protein analysis used was also thought to contribute greatly to the variability observed. However, the induction level (mean exposed divided by mean reference values) was similar. Relative induction did not appear to be affected by storage time, pH, buffer, assay time, or assay temperature. The induction level was not affected by whether post- mitochondrial supernatant (PMS; 10,000xg) or microsomal fractions (100,000xg) were used in analysis, although absolute activity was 3.5 times higher using microsomal preparations. There was a statistically significant agreement in the rankings of high activity samples using microsomal preparations; a corresponding ranking of PMS values was non-significant. The presence of cytochrome P450 1A enzyme was detected using monoclonal antibody 1-12-3 against scup P450 1A1. Immunoblotting showed 8.4-fold differences in the measured levels of the single cross-reacting band, confirming the distinction between exposed and reference fish determined by EROD assay.

Submitted to: Environmental Toxicology ℓ^g Chemistry.

Supported by: NOAA Office of Sea Grant NA910-AA-DFG480, R/P 37.

WHOI Contribution No. 8181.

SALT MARSH DEVELOPMENT STUDIES AT WAQUOIT BAY, MASSACHUSETTS: INFLUENCE OF GEOMORPHOLOGY ON LONG-TERM PLANT COMMUNITY STRUCTURE

Richard R. Orson and Brian L. Howes

Stochastic events related to beach formation and inlet dynamics have been the major factors influencing the development of the Waquoit Bay tidal marshes. This results from the physical structure of the Waquoit Bay system where tidal exchange is limited to one or two small inlets and is in contrast to marsh development in nearby Barnstable Marsh where direct unrestricted

exchange with Cape Cod Bay has smoothed the effects of stochastic events on vegetation development. We contend that vegetation development in salt marshes where connections to adjacent waters are restricted will be dominated by abiotic factors (eg; storms, sedimentation rates, etc.) while those marshes directly linked to open bodies of water and where alterations to hydrodynamic factors are gradual, autecological processes (eg: interspecific competition) will dominate long-term plant community development.

The results from the five marsh systems within the Waquoit Bay complex suggest that once a vegetation change occurs the new community tended to persist for long periods of time (100's -1000's years). Stability of the "new" community appeared to depend upon the stability of the physical structure of the system and/or time between perturbations necessary to allow the slower auteocological process to have a discernable effect. In order for the plant community to persist as long as observed, the vegetation must also be exerting an influence on the processes of development. Increased production of roots and rhizomes and growth characteristics (density of culms) are some of the factors which help to maintain long-term species dominance.

It is clear from this investigation that the structure of the plant community at any one point in time is dependent upon numerous factors including historical developmental influences. To properly assess changes to the present plant community or determine recent rates of accretion, historic developmental trends must be considered. The factors that have influenced the development of marsh in the past will be important in understanding and formulating predictive models in the future.

Published in: Estuarine Coastal and Shelf Science, 35: 453-471, 1992.

Supported by: NOAA Grants NA87AA-DC2030 and NA88AA-DC2014.

WHOI Contribution No. 7968.

DIFFUSION-INDUCED CHAOS IN A SPATIAL PREDATOR-PREY SYSTEM

Mercedes Pascual

A continuous predator-prey model in which both species diffuse along a spatial gradient is shown to exhibit temporal chaos at a fixed point in space. The model incorporates a nonlinear functional response of the predator and a logistic growth of the prey; the intrinsic growth rate of the prey varies linearly with space. Numerical results demonstrate that low diffusion values drive an otherwise periodic system into aperiod behavior

with sensitivity to initial conditions. Evidence is provided for a quasiperiodic route to chaos as the diffusion rate decreases. These results suggest that complex temporal dynamics in natural communities may arise through the spatial dimension. Spatially induced chaos may play an important role in spatial pattern generation in heterogeneous environments.

Published in: Proceedings of the Royal Society, Series B., 251:107, 1993.

Supported by: Ocean Ventures Fund Grant, NSF Grant OCE89-00231, ONR Grant N00014-92-J-1527.

WHOI Contribution No. 8219.

NOVEL INTERVENING SEQUENCES IN AN ARCHAEA DNA POLYMERASE GENE

F. B. Perler, D. G. Comb, W. E. Jack, L. S. Moran, B. Qiang, R. B. Kucera, J. Benner, B. E. Slatko, D. O. Nwankwo, S. K. Hempstead, C. K. Carlow and H. W. Jannasch

The DNA polymerase gene from the Archaea, Thermocooccus literalis, has been cloned and expressed in E. coli. It is split by two novel intervening sequences (IVS) which form one continuous open reading frame (ORF) with the three polymerase exons. Neither IVS is similar to previously described introns. However, the deduced amino acid sequences of both IVSs are similar to ORFs present in mobile group I introns. The second IVS (IVS2) encodes an endonuclease, I-ThI, which cleaves at the exon2/exon3 junction after IVS2 has been deleted. IVS2 self-splices in E. coli yielding active polymerase, but processing is abolished if the IVS2 reading frame is disrupted. Silent changes in the DNA sequence at the exon2/IVS2 junction which maintain the original protein sequence do not inhibit splicing. These data suggest that protein rather than mRNA splicing may be responsible for production of the mature polymerase.

Published in: Proceedings National Academy Science, 89:5577-5581, 1992.

Supported by: NSF OCE92-0047 "d ONR N00014-91-J-1751.

WHOI Contribution No. 8045.

HARBOUR PORPOISES AND GILL NETS IN THE GULF OF MAINE

A. J. Read, S. D. Kraus, K. D. Bisack and D. Palka

This paper reviews the current status of harbour porpoises, *Phocoena phocoena*, in the Gulf

of Maine. Large numbers of perpoises are killed each year in commercial fisheries in this area, but until recently there have been no reliable estimates of the magnitude of this mortality or of population abundance. The magnitude of incidental mortality was estimated from the product of incidental catch rates, documented by observers aboard commercial fishing vessels, and indirect measures of fishing effort, such as fish landings. Estimated porpoise catches by the Gulf of Maine groundfish gill net fishery, which is responsible for most of the mortality, range from 1,700 in 1991 to 2,400 in 1990. A shipboard survey of the Gulf of Maine conducted in the summer of 1991 produced an abundance estimate of approximately 45,000 porpoises. At the present time, the population growth rate of harbour porpoises is unknown, but knowledge of the vital rates of other cetacean species suggests that the population is unlikely to be able to sustain present catch levels. Innovative management measures are required to reduce the incidental mortality of harbour porpoises while maintaining a viable groundfish gill net fishery.

In Press: Conservation Biology, Vol. 7.

Supported by: National Sciences and Engineering Research Council of Canada.

WHOI Contribution No. 8185.

PATTERNS OF GROWTH IN WILD BOTTLENOSE DOLPHINS, TURSIOPS TRUNCATUS

A. J. Read, R. S. Wells, A. A. Hohn and M. D. Scott

The growth of bottlenose dolphins is described from observations made during a capture-release program that has operated in coastal waters of the eastern Gulf of Mexico from 1970 to the present. Measurements of standard length, girth and body mass were recorded from 47 female and 49 male dolphins, some captured as many as nine times. Ages were known from approximate birth dates or estimated from counts of dentinal growth layers. In all three measurements, females grew at a faster initial rate than males, but reached asymptotic size at an earlier age. This extended period of growth in males resulted in significant sexual dimorphism in length, girth, and mass at physical maturity. The growth of both sexes was well described by three-parameter Gompertz models using either cross-sectional data or a mixture of longitudinal and cross-sectional data. There was considerable variation in size-at-age for both sexes in all year classes. Residuals of size measurements were used to derive measures of relative size for individual dolphins; most dolphins demonstrated little ontogenetic change in relative size. Body mass was

adequately predicted by multiple regression equations that incorporated both length and girth as independent variables.

In Press: Journal of Zoology, London.

Supported by: Center for Field Research; Natural Sciences and Engineering Research Council of Canada.

WHOI Contribution No. 8186.

RELATIONSHIPS BETWEEN BACTERIA AND HETEROTROPHIC NANOPLANKTON IN MARINE AND FRESH WATERS: AN INTER-ECOSYSTEM COMPARISON

Robert W. Sanders, David A. Caron and Ulrike-G. Berninger

Despite differences in the species compositions and absolute abundances of planktonic microorganisms in fresh- and salt water, there are broad similarities in microbial food webs across systems. Relative abundances of bacteria and nanoplanktonic protozoa (HNAN, primarily heterotrophic flagellates) are similar in marine and freshwater environments, which suggests analogous trophic relationships. Ranges of microbe abundances in marine and fresh waters overlap. and seasonal changes in abundances within an ecosystem are often as great as difference in abundances between freshwater and marine systems of similar productivities. Densities of bacteria and heterotrophic nanoplankton, therefore, are strongly related to the degree of eutrophication, and not salt per se. Thus it is more appropriate to examine the relationship of heterotrophic nanoplankton to their prey along a gradient of productivity rather than along a gradient of salinity. Based on the results of a simple food web model involving bacterial growth, bacterial removal by HNAN, predation on HNAN, and the observed relationships between bacterial and HNAN abundances in natural ecosystems, it is possible to demonstrate that bottom-up control (food supply) is more important in regulating bacterial abundances in oligotrophic environments while top-down control (predation) is more important in eutrophic environments.

Published in: Marine Ecology Progress Series, 86:1-14, 1992.

Supported by: NSF Grants BSR89-19447 and OCE89-01005.

WHOI Contribution No. 8102.

RECORDING UNDERWATER SOUNDS OF FREE-RANGING DOLPHINS WHILE UNDERWAY IN A SMALL BOAT

Lacla S. Sayigh, Peter L. Tyack and Randall S. Wells

Few studies of vocalizations of free-ranging cetaceans have successfully linked continuous, underwater recordings with ongoing behavioral observations. Noise from engines and/or water flowing around the hydrophone generally limited researchers to recording sounds from stationary sites or from boats with their engines turned off, especially if the sounds of interest were in the same frequency ranges as that of engine or flow noise. But unless the animals stay in one place, these techniques do not allow for long-term recording sessions, or for simultaneous detailed behavioral observations. Therefore, we designed an inexpensive, portable system tailored to record whistles (ranging from about 5 to 25 kHz) of bottlenose dolphins (Tursiops truncatus), while they are being followed in a small boat. We utilized this technique in studies of free-ranging bottlenose dolphins in waters near Sarasota, Florida. Our understanding of the natural contexts of dolphin vocalizations was enhanced by combining this technique with simultaneous behavioral observations and with background information on the dolphins being recorded.

Submitted to: Marine Mammal Science.

Supported by: Ocean Ventures Fund; NSF Grant BN5-9014545, PHS Grant 1R29NS25290, ONR Grant N00014-87-K-0236.

WHOI Contribution No. 8092.

APLACOPHORA AS PROGENETIC ACULIFERANS AND THE COELOMATE ORIGIN OF MOLLUSKS AS SISTER TAXON TO SIPUNCULA

Amélie II. Scheltema

Evidence is presented in support of the following phylogenetic hypotheses: (1) Sipuncula are sister group to Mollusca; (2) the two aplacophoran taxa, Neomeniomorpha (= neomenioids) and Chaetodermomorpha (= chaetoderms), are monophyletic with a common neomenioid-like ancestor, and of the two taxa. Chaetodermomorpha are more derived; (3) Aplacophora and Polyplacophora are sister taxa and form a clade, Aculifera; (1) Aculifera are sister group to remaining extant mollusks, Conchifera, and (5) Aplacophora are progenetic Aculifera

The evidence is based on homologies of early and late embryological development, adult

morphologies, and molecular analyses. Embryological development in sipunculans and mollusks shows a close relationship between them, and embryological development of shell separates Aculifera and Conchifera. Adult morphologies indicate (1) monophyly of Aplacophora; (2) sister-group relationship between Aplacophora and Polyplacophora; (3) a molluscan plesiomorphy of nonsegmented serial replication of organs; and (4) progenesis in Aplacophora. Molecular evidence supports embryological and morphological relationships of Sipuncula and Mollusca.

Mollusca are thus hypothesized to be coelomate Eutrochozoa, which share an ancestor that probably had serial replication of organs. Differences in size and structure of coelom among Eutrochozoa are hypothesized to have been brought about by changes in timing and process of cavitation of mesodermal bands, which arise from cell 4d. Through the process of progenesis Aplacophora retained an ovoid embryological shape and several internal structures that, although they appear to be in a primitive state, are actually secondarily derived as is quadrant D specification during early cleavage.

Submitted to: Biological Bulletin.
WHOI Contribution No. 8205.

ADAPTATIONS FOR REPRODUCTION AMONG DEEP-SEA BENTHIC MOLLUSCS: AN APPRAISAL OF THE EXISTING EVIDENCE

Rudolf S. Scheltema

Adaptations for reproduction among deep-sea Mollusca are fully as varied as those found among their shoal-water counterparts. Such wide diversity of adaptations for reproduction can be related to a corresponding wide diversity in the deep-sea benthic environment, until recently largely unexpected and mostly unknown. With a few exception most deep-sea molluses that have been studies have no obvious evidence for a coupling between periodicity of reproduction and primary productivity at the sea-surface, nor any evidence of any seasonal periodicity in reproduction. Fertility among deep-sea bivalve molluses varies widely (2-30,000 eggs at once), but lifetime fecundity cannot be precisely determined since neither the rate of gametogenesis nor the age or length of life can be readily ascertained for most iteroparous species. The mode of development among deep-sea molluses may be direct, without a planktonic stage, or indirect, either with a short non-feeding. lecithotrophic larva or a planktotrophic veliger stage feeding as it is passively dispersed by ocean currents. "Ontogenetic vertical imgration" has

been proposed for planktotrophic molluscan larvae. Although some indirect evidence has been advanced, up to now the veligers of only two species of eurybathyal deep-sea gastropods are known to actually occur in the near-surface waters. The mode of development will have important consequences for (1) colonization or recruitment, (2) genetic exchange between populations and (3) the biogeography of deep-sea molluscs, but studies on such aspects of molluscan life-history have only just begun.

Submitted to: Reproduction, larval biology and recruitment in the deep sea benthos. Columbia University Press.

Supported by: NSF OCE84-10262.

WHOI Contribution No. 8354.

POPULATION ANALYSIS OF TOXIC AND NONTOXIC ALEXANDRIUM SPECIES USING RIBOSOMAL RNA SIGNATURE SEQUENCES

Christopher A. Scholin and Donald M. Anderson

Sequence analysis was used to determine if small-subunit(Ss) and large-subunit (Ls) ribosomal RNA (rRNA) genes (rDNA) can provide distinct molecular markers for Alexandrium species. Analysis of the entire SsrDNA for one North American A. fundyense culture unexpectedly revealed the presence of two distinct genes, one of which we believe to be a pseudogene. An assay developed to detect these two sequences in PCRamplified material was used to screen 27 globally-distributed, toxic and nontoxic Alexandrium species. Results indicate that the putative pseudogene occurs only in toxic North American isolates, irrespective of their species designation, but does not occur in other toxic and nontoxic forms from other regions of the world. Analysis of a portion of the LsrDNA has revealed hypervariable domains which are likely to provide highly specific signature sequences useful in delineating genetically similar populations.

In Press: Toxic Marine Phytoplankton, T.J. Smayda and Y. Shimizu eds. Elsevier, Amsterdam.

Supported by: NSF Grant OCE89-11226, Ocean Ventures Fund.

WHOI Contribution No. 8113.

THE EXISTENCE OF TWO DISTINCT SMALL-SUBUNIT RRNA GENES IN THE NORTH AMERICAN TOXIC DINOFLAGELLATE ALEXANDRIUM FUNDYENSE (DINOPHYCEAE)

Christopher A. Scholin, Donald M. Anderson and Mitchell L. Sogin

Two distinct small-subunit rRNA genes (16S-like rDNAs), termed the "gene" and "B gene," have been detected in a clonal isolate of the toxic dinoflagellate, Alexandrium fundyense (Halim) Balech. The two sequences, which occur in roughly a 1:1 ratio in PCR- amplified material, differ at approximately 40 positions scattered throughout the length of the molecule. Transcripts of the B sequence were not detected in total RNA extracts from nutrient replete and ammonium starved (sexually induced) cultures, as well as nutrient replete log-phase cultures harvested at two hour intervals over a complete circadian cycle. Many of the position changes exhibited by the B gene deviate from universally- and eukaryotic-conserved small- subunit rRNA sequences. In contrast, the A gene is expressed under all culture conditions tested and does not violate any conserved sequence positions. It is thus likely that the B sequence is a pseudogene which is not represented by stable transcripts. The B gene may serve as a useful marker for fine-scale population and taxonomic analyses of some Alexandrium species.

In Press: Journal of Phycology.

Supported by: NSF Grant OCE89-11226, Ocean Ventures Fund, NIH Grant GM 32964.

WHOI Contribution No. 7992.

CYTOCHROME P4501A INDUCTION IN TISSUES, INCLUDING OLFACTORY EPITHELIUM, OF TOPMINNOWS (POECILIOPSIS SPP.) BY WATERBORNE BENZO(A)PYRENE

Roxanna M. Smolowitz, Mary E. Schultz and John J. Stegeman

Topminnows of the genus *Poecihopsis* are susceptible to hepatocarcinogenesis by waterborne exposure to procarcinogenic polynuclear aromatic hydrocarbons (PAH). We examined induction of cytochrome P4501A (CYP1A) in liver and other organs of the species *P. monacha* and *P. lucida* exposed to benzo(a)pyrene (BaP) in water (added in acetone carrier) at 1 mg/1 for 48 and 90 hours. Fish were fixed whole in formalin, and CYP1A was examined immunohistochemically in sagittal

sections of whole animals by staining with monoclonal antibody 1-12-3, which recognizes a single cross-reacting CYP1A protein in *Poeciliopsis* liver microsomes. Fish exposed to BaP for 48 hours showed moderate staining, and those exposed for 90 hours showed strong specific staining in various epithelial cells in both species. These included hepatocytes, pancreatic cells, epithelial cells in gill, enterocytes of the gut, and kidney tubular epithelium. Endothelial cells in several organs, including gill pillar cells and endocardial cells in the heart, showed strong staining. Staining was stronger in P. monacha than in P. lucida. Untreated animals of both species showed mild staining of the same cells stained in BaP-treated fish. In P. monacha carrier (acetone) elicited moderate increase in staining in most cell types, including those of liver and gill; the basis for this acetone effect is not known. There was a very strong specific induction by BaP in olfactory epithelium and epidermal taste bud epithelium of P. monacha, the first demonstration of strong CYP1A induction in chemosensory epithelia exposed to inducer in a physiologically relevant way. This study clearly established that waterborne polynuclear aromatic hydrocarbons can elicit induction of P4501A proteins in multiple cell types in many organs of fish, with some site of induction (olfactory epithelium) possibly related directly to the route of exposure. The species difference in the induction response, with induction in liver and some other organs generally being greater in P. monacha than in P. lucida, could be related to previously recognized species differences in PAH toxicities in Poeciliopsis.

CYP1A induction in olfactory cells could be significant in several ways. Induction of CYP1A proteins in the sensory cells could be important in facilitating clearance of hydrocarbons from those cells. However, CYP1A enzymes might also activate protoxicants or promutagens in the nasal system, as has been suggested in mammals (32). In this regard, a search for cellular lesions in nasal mucosa of fish from contaminated environments should prove interesting. Full conclusions regarding the biological significance of the induction will await determination of whether the stained cells are sensory or sustentacular, a focus of further studies.

In summary, waterborne polynuclear aromatic hydrocarbons are very capable of inducing CYP1A in various cells, including sensory epithelium, of *Pocciliopsis* spp. and probably other fish. The cellular localization of induction in gill and internal organs of topminnows exposed to waterborne inducer is similar to localization detected both in experimentally induced (i.p) and environmentally induced (wild caught) fish of other species. *Pocciliopsis* or other small fish used in carcinogenesis studies, such as medaka *Oryzias*

latipes (35), can be examined whole in sagittal section on a single slide. Such fish thus offer a convenient system for study of various aspects of CYP1A function and regulation, including the regulation of olfactory CYP1A, and for studies relating induction to PAH carcinogenesis and/or cytotoxicity in liver or other organs.

Submitted to: Carcinogenesis.

Supported by: PHS Grant ES-04220.

WHOI Contribution No. 8104.

ANIMAL-SEDIMENT RELATIONSHIPS REVISITED: WHAT DO WE REALLY KNOW ABOUT CAUSE AND EFFECT?

Paul V. R. Snelgrove and Cheryl Ann Butman

Over the last few decades, many studies have correlated infaunal invertebrate distributions with sediment grain size, leading to the generalization of distinct associations between animals and sediments. The most touted associations were deposit feeders with muddy sediments and suspension feeders with sandy sediments. Proposed causative factors have included grain size per $s\epsilon$, organic content, microbial content, trophic- and species-specific interactions and food supply. An early predominant hypothesis to explain the association of suspension feeders with sandy sediments was that they are excluded from muddy habitats by amensalistic interactions with deposit feeders. There is, in fact, little evidence for the pattern that this hypothesis purports to explain and the proposed underlying mechanism oversimplifies sediment-transport dynamics. Animal-sediment relationships have been evaluated using sediment and biological samples that have been integrated over vertical scales within the bed that are larger than those relevant to most organisms. Moreover, sediment grain size was usually determined on completely disaggregated samples and these grain-size distributions may not be biologically or hydrodynamically meaningful. Critical re-examination of data on animal-sediment relationships suggests that many species are not always associated with a single sediment type, and that suspension and deposit feeders often co-occur in large numbers. Furthermore, because of recent demonstrations of feeding plasticity in a number of infaunal species, the simple dichotomy of suspension versus deposit feeding is no longer valid. Likewise, in most studies that have tested or evaluated trophic-group amensalism, the hypothesis generally was qualified to such a degree that it is no longer meaningful. We suggest that the complexity of soft-sediment communities may defy any simple paradigm. As examples, we summarize existing information on the distribution

and ecology of two infaunal species that are better studied than most, the bivalve Mercenaria mercenaria and the polychaete Owenia fusiformis. Distributional and experimental data on these two species do not consistently support the amensalism hypothesis. These data also illustrate the complexity of animal-sediment relationships and the modest level of our present understanding of the role of the near-bed flow and sedimentary environment in determining infaunal distributions.

Most studies of animal-sediment associations were conducted at a time when the complex, dynamic relationship between bottom sediments and near-bed hydrodynamics were poorly understood, and the recently expanding interest in coastal sediment transport and its controlling mechanisms has created an entirely new framework for studying organism-sediment interactions. We re-evaluate animal-sediment relationships in this light, reviewing what is known about factors that we believe are more likely to limit or delimit distributions of infaunal organisms - physical factors (hydrodynamic regime and sediment-transport regime) that directly correlate with and are the causative processes responsible for sediment distributions, and factors (food supply and larval supply) that indirectly correlated with sediment distributions. A multidisciplinary study of the biology, geology, hydrodynamics and sediment transport on George Bank, USA, is used to illustrate the complexity and dynamic nature of near-shore, sedimentary environments and animal-sediment relationships therein. In conclusion we recommend research directions that may help clarify cause and effect, emphasizing manipulative experiments and sampling that is more biologically and physically meaningful as compared to previous correlative studies.

Submitted to: Oceanography and Marine Biology, an Annual Review.

Supported by: Ocean Ventures, NSF Grant OCE88-12651, ONR Grant N00014-89-J-1637, NSERC (Canada).

WHOI Contribution No. 8112.

HYDRODYNAMIC ENHANCEMENT OF LARVAL SETTLEMENT OF THE BIVALVE MULINIA LATERALIS (SAY) AND THE POLYCHAETE CAPITELLA SP. I IN MICRODEPOSITIONAL ENVIRONMENTS

Paul V. R. Snelgrove, Cheryl Ann Butman and Judith P. Grassle

To test whether larval settlement of the opportunistic bivalve *Mulina lateralis* (Say) and the polychaete *Capitella* sp. 1 is modified by

near-bottom flow, laboratory still-water and flume-flow experiments were conducted using a sediment array consisting of depressions (2.8 cm deep, 3.8 cm diameter) and flush compartments filled with organic-rich mud or a low-organic, glass bead mixture of a comparable grain size. Previous flume experiments have shown preference for mud over glass beads by both species. Depressions create a microdepositional environment that traps passive particles so that the relative importance of active selection versus passive deposition of larvae may be tested. Capitella sp. I larvae consistently selected the organic-rich mud over the glass bead mixture regardless of whether treatments were flush or depressions, though enhanced numbers were observed in depressions. Mulinia lateralis larvae also chose mud over glass beads but, in some instances, were found in higher numbers in glass bead depressions (a "poor" choice) compared to flush mud (a "good" choice). These results suggest that near-bottom flow modifies settlement in both species (i.e. settlement enhancement in depressions), but the effect is greater for M. lateralis larvae. Higher settlement generally observed in mud depressions compared with glass bead depressions suggests that escape from depressions was possible for both species if the substrate was unsuitable, though M. lateralis was more vulnerable to passive "trapping". Similar experiments with much smaller depressions showed no settlement enhancement in depressions for Capitella sp. I and enhancement only in some cases for M. lateralis larvae, suggesting that the hydrodynamic effect may be scale dependent for both species.

Submitted to: Journal of Experimental Marine Biology and Ecology.

Supported by Ocean Ventures, NSERC (Canada); and NSF Grants OCE88-12651 and OCE88-13584.

WHOI Contribution No. 8004

THE CYTOCHROMES P450 IN FISH

John J. Stegeman

Diverse catalytic activities commonly associated with P450 in other systems appear also in fish. Functions include synthesis and degradation of endogenous substrates including steroids, and xenobiotic metabolism. Some steroidogenic reactions involve catalysts similar in structure and function and possibly number to those in mammals, but reactions specific to some fish, such as the formation of oocyte final maturation steroids, could involve novel P450 gene products. Fish P450s in gene families 1 to 4 that metabolize xenobiotics are also similar to some

mammalian forms, but they may be fewer in number. Whether the diversity or lack thereof in these telost P450 gene families is related to the diversity of marine natural products is unknown. but possible. The regulation of P450 genes, the nature of receptors and association with other elements such as the heat-shock proteins, are poorly known in fish, yet the regulation of P450 genes in fish has aspects that appear to be distinct from those in mammals. Fish may therefore be important subjects for the study of the evolution of the regulatory systems as well as the P450 genes themselves. Furthermore, there are practical benefits, such as the analysis of pollutant effect, to be gained from knowledge of telost P450 systems. As the diversity and regulatory mechanisms become known, P450s will be increasingly useful for dissecting environmental influences on regulation of structural genes, as well as establishing the role of monooxygenases in the physiology and environmental health of fish.

Published in: Biochemistry and Molecular Biology of Fish. P. Hochaka and T. Mommsen, eds.

Supported by: USPHS (NIH) Grant ES-04220, the Donaldson Charitable Trust and the Stanley Watson Chair.

WHOI Contribution No. 8147.

EFFECT OF SAMPLING FREQUENCY ON MEASUREMENTS OF SEASONAL PRIMARY PRODUCTION AND OXYGEN STATUS IN NEAR-SHORE COASTAL ECOSYSTEMS

Craig D. Taylor and B. L. Howes

New automated in situ techniques were used for high resolution time series measurement of primary production and water column oxygen concentration in nearshore coastal marine embayments. Results revealed two-fold day to day large fluctuations in measured phytoplankton production and periodic changes in water column oxygen concentration as great as 100 µM occurring in a matter of a few hours. Effects of sampling frequency upon the determination of seasonal primary production and water column oxygen status was assessed by down-sampling of high resolution measurements at various intervals and rc-analysis of the desired parameters using the lower resolution data. Results indicate that ecosystem studies using classic measurement intervals (e.g., 30 days) may be under-sampled 5-30 fold with respect to both primary production and oxygen concentration, and that serious inaccuracies in data crucial to ecological and water quality studies may result.

Submitted to: Limnology and Oceanography.

Supported by: NOAA, Sea Grants NA86-AA-D-SG090 R/B-95-PD and R/P-34; NA90-AA-D-SG480 R/P-38.

WHOI Contribution No. 8044.

NUTRIENT PROCESSING IN AN ARTIFICIAL WETLAND ENGINEERED FOR HIGH LOADING: A SEPTAGE TREATMENT EXAMPLE

J. M. Teal, B. L. Howes, S. B. Peterson, J. E. Petersen, and A. Armstrong

A greenhouse enclosed wetland system treated septage on Cape Cod, MA from March 1990 to December, 1992. Treatment time (avg. flow) was 11 days at temperatures from 9 to 27 °C. Processing occurred in tanks with floating wetland plants and algae coupled with artificial marshes with rooted macrophytes. Significant removal of all major waste components was observed: average BOD-5 was reduced from 1600 to 8.8 mg/l, TSS from 8300 to 20 mg/l, and after the final marsh configuration, TN from 210 to 5.6 mg/l, DON from 160 to 4.3 mg/l, PO4 from 45 to 3.8 mg/l, effluent NO3 was 1.1mg/l. Residual DON appeared to be highly resistant to degradation. Denitrification occurred in the marshes where loading was low. Organic decomposition, nitrification and denitrification all occurred in initial tanks where dissolved and particulate organic loading remained high. This co-occurrence of processes through much of the SAS brings its N cycle closer to a natural marsh system in both complexity and function and may make it more efficient in N transformations than conventional wastewater treatment systems.

Submitted to: Wetlands of the World Biogeochemistry, Ecological Engineering,
Modelling and Management, INTECOL Wetland
Symposium.

Supported by: Island Foundation, C.S. Mott. WHOI Contribution No. 8232.

SIGNATURE WHISTLE DEVELOPMENT OF THREE CAPTIVE BOTTLENOSE DOLPHINS, TURSIOPS TRUNCATUS

Peter L. Tyack, Kurt Fristrup and Janet S. McIntosh

Whistles of three dolphin calves at the Miami Seaquarium were recorded during their first six to nine months of life in order to study the development of stereotyped, individually-distinctive whistles, called signature whistles. Quantitative analysis of calf whistles

demonstrates that their variability decreased with age. None of the calves developed signature whistles similar to those of their parents. All three calves incorporated elements resembling sound prevalent in the newborn's environment, including artificial sounds. This provides evidence for vocal learning in signature whistle development.

Submitted to: Animal Behaviour.

Supported by: PHS Grant 5R29 NS25290

WHOI Contribution No. 8100.

MARINE MAMMALS, OCEAN ACOUSTICS AND THE CURRENT REGULATORY ENVIRONMENT

Peter Tyack, William A. Watkins and Kurt M. Fristrup

Man-made underwater sounds represent a potentially serious problem for marine mammals. This paper summarizes our own research and available literature on the behavioral responses of marine mammals to man-made underwater sounds. Most baleen whales tested in playback experiments avoided levels of continuous sounds louder than 120 dB re 1 μ Pa. The impact of these sounds depends on their acoustic structure, sound propagation in the local environment, and animal sensitivity, which may very with species and behavioral context. Ignorance of the impact of noise on marine mammals couples with legal requirements for conservation management to create the danger of excessive regulation for many seagoing activities.

Submitted to: Science.

Supported by: ONT Contract N00014-90-C-0098.

WHOI Contribution No. 8134.

RESISTANCE TO CO-OCCURRING PHAGES ENABLES MARINE SYNECHOCOCCUS TO CO-EXIST WITH CYANOPHAGES ABUNDANT IN SEAWATER

John B. Waterbury and Frederica W. Valois

Recent reports highlighting very high viral abundances in seawater have led to an increased interest in the role of viruses in aquatic environments and a resurgence of the hypothesis that viruses are significant agents of bacterial mortality. Synechococcus, a small unicellular cyanobacterium that is an important primary producer at the base of the marine food web, was used to assess this hypothesis. We present evidence that cyanophages of Synechococcus, that

are often present in seawater at concentrations between 10³ and 10⁴ phages/ml⁻¹, have a negligible effect on Synechococcus mortality because natural populations of Synechococcus were found to be largely resistant to their co-occurring phages. Cyanophages are maintained by scavenging relatively rare sensitive cells present in the Synechococcus community.

Submitted to: Science.

Supported by: Gift from Stanley W. Watson to WHOI.

WHOI Contribution No. 8241.

UNDERWATER SOUND RECORDING OF ANIMALS

William A. Watkins and Mary Ann Daher

Underwater sound recording of animals uses specialized techniques to obtain faithful copies of sounds produced by animals during their normal activities underwater. Techniques have to be unobtrusive as well as nondisturbing to avoid changing the animal behaviors. The first scientific recording of underwater sounds from a marine mammal at sea was by William E. Schevell and Barbara Lawrence in 1948. Although the equipment has changed considerably since then, the techniques, approaches to animals, and environmental impediments have remained essentially the same. However, the frequency and dynamic ranges of underwater sounds can easily exceed terrestrial sounds, so the selection of suitable equipment is critical. The elements of a useful system for bioacoustic recording of marine animals include the hydrophone, impedance transformer/preamplifier, cable, signal amplifier, recorder, and sound monitor. The important criteria for each of these is discussed, along with directional listening systems, and the need for calibrations to verify the performance of the entire underwater recording system. For each situation, the ideal system is the one with the best compromise of interactive components to record that particular sound spectrum.

Published in: Bioacoustics, 4:195-209, 1992.

Supported by: ONR Grant N00014-91-J-1445.

WHOI Contribution No. 8033.

OBSERVATIONS OF LAGENODELPHIS HOSEI, FRASER'S DOLPHIN, OFF DOMINICA IN THE SOUTHEAST CARIBBEAN

William A. Watkins, Mary Ann Daher, Kurt Fristrup, and Giuseppe Notarbartolo di Sciara

Two pods of Lagenodelphis hosei, Fraser 1956 (Fraser's dolphin), were observed in the southeast Caribbean, off Dominica. On 26 October 1991 a pod of about 60 dolphins including small calves was observed for 2.5 hrs, and on 28 October 1991 a pod of about 80 mostly larger dolphins was observed for more than 1 hr. The pod of 26 October was composed of a number of groups; individuals from many of those groups cooperated in herding fish identified as "rainbow runner" (Elagatis bipinnulatus (Quoy and Gaimard) 1824, family Carangidae) that were schooled near the surface. The pod of 28 October operated as one large, relatively tight group which separated for only short periods into two or three smaller groups which also chased near-surface schools of (unidentified) fish. Recordings of underwater sounds were made by three-dimensional hydrophone array. Events were followed acoustically and visually, and video and photographs were taken of surface activities. The dolphins used broadband clicks in apparent echolocation, and communicative whistles with fundamentals ranging from 4 to 24 kHz, lasting from 0.1 to 2 sec. Repetitive sounds with distinctive frequency contours were produced by individuals.

Submitted to: Caribbean Journal of Science.

Supported by: ONR Grant N00014-91-J-1445; NSF Grant BNS 8508047; Nat'l Geographic Society Grant 3745-88.

WHOI Contribution No. 8206.

INTRODUCTION TO INTERDISCIPLINARY STUDIES OF KUROSHIO AND GULF STREAM RINGS

Peter H. Wiebe and Terrence M. Joyce

As a final facet in the synthesis phase of the NSF sponsored Warm-Core Rings Program, a U.S.-Japan workshop on warm-core rings was held at the Woods Hole Oceanographic Institution from 3 to 7 October 1988, the third such workshop promoting cooperative research and exchange of information on warm-core rings.

While the principal focus of the third workshop was on the Gulf Stream of Kuroshio regions, information about rings in other western boundary current regions was presented. Published in: Deep-Sea Research, 39 (Suppl. 1):v-vi, 1992.

Supported by: NSF Grants, OCE80-12748, OCE85-08350 and OCE87-9962.

WHOI Contribution No. 7878.

MICROBIAL DEGRADATION OF A STARCH-BASED BIOPOLYMER IN THE MARINE ENVIRONMENT

Carl O. Wirsen and Holger W. Jannasch

Microbial degradation of a starch-based biopolymer was studied in marine environments under varied conditions. Starch and other complex carbohydrates were degraded much slower under deep-sea conditions than in control experiments at comparable temperatures but at 1 atm. Supplementation with nitrogen and phosphate significantly enhanced the degradation activity. Closed systems were required for these quantitative analytical studies. Semiquantitative studies using open systems in the natural marine environment confirmed the observation of reduced microbial activities under deep-sea conditions and also demonstrated the importance of the macrofaunal component in substrate removal. Starch-based biopolymer contains 13 percent soluble growth supporting carbohydrate-type material. Laboratory incubations, using this material, demonstrated higher rates of degradation when it was in contact with sediment rather than suspended in seawater alone. Biopolymer thickness and incubation temperature were significant factors in the level of biodegradation that occurred. Limiting marcrofaunal access by varied screen sizes had negligible effect on biopolymer degradation in shallow water. Scanning electron microscopy of incubated samples revealed a great diversity of morphological types of bacteria. Pure cultures of marine organisms were isolated from actively degrading biopolymers for future physiological studies of specific bacterial activities.

In Press: Fundamentals of Biodegradable Materials and Packaging, Technomic Publishers. U.S. Army Natick.

Supported by: U.S. Army Natick R D & E, Contract Number DAAK60-91-C-0096.

WHOI Contribution No. 8060.

CHEMOSYNTHETIC MICROBIAL ACTIVITY AT MID-ATLANTIC RIDGE HYDROTHERMAL VENT SITES

Carl O. Wirsen, Holger W. Jannasch and Stephen J. Molyneaux

Chemosynthetic production of microbial biomass, determined by ¹⁴CO₂ fixation and enzymatic (RuBisCo) activity, at the Mid-Atlantic Ridge (MAR) 23° and 26° N vent sites was found in various niches: warm water emissions, loosely rock-attached flocculent material, dense morphologically diverse bacterial mats covering the surfaces of polymetal sulfide deposits, and filamentous microbes on the carapaces of shrimp (Rimicarus exoculats). The bacterial mats on polymetal sulfide surfaces contained unicellular and filamentous bacteria which appeared to use as their chemolithotropic electron or energy source either dissolved reduced minerals from vent emissions, mainly sulfur compounds, or solid metal sulfide deposits, mainly pyrite. Moderately thermophilic chemosynthetic activity was observed in carbon dioxide fixation experiments and in enrichments, but no thermophilic aerobic sulfur oxidizers could be isolated. Both obligate and facultative chemoautotrophs growing at mesophilic temperatures were isolated from all chemosynthetically active surface scrapings. The obligate autotrophs could oxidize sterilized MAR natural sulfide deposits as well as technical pyrite at near neutral pH, in addition to dissolved reduced sulfur compounds. While the grazing by shrimp on the surface mats of MAR metal sulfide deposits was observed and deemed important, the animals primary occurrence in dense swarms near vent emissions suggests that they were feeding at these sites, where conditions for chemosynthetic growth of their filamentous microbial epiflora were optimal. The data show that the transformation of geothermal energy at the massive polymetal sulfide deposits of the MAR is based on the lithoautotrophic oxidation of soluble sulfides and pyrites into microbial biomass.

In Press: Journal of Geophysical Research, Solid Earth Special Section - "Atlantic Hydrothermal Activity".

Supported by: NSF Grants OCE89-22854 and OCE92-00458.

WHOI Contribution No. 8076.

INDUCTION OF P4501A IN INTERTIDAL FISH IN PRINCE WILLIAM SOUND AS A RESULT OF THE EXXON VALDEZ OIL SPILL

Bruce R. Woodin and John J. Stegeman

Cytochrome P4501A induction is a sensitive and specific adaptive response in fish exposed to a wide variety of xenobiotics, including the polycyclic aromatic hydrocarbon components of crude oil. The intertidal fish, Anoplarchus purpurescens, was collected from two reference sites and three sites oiled to varying degrees by the 1989 Exxon Valdez oil spill in Prince William Sound. Animals collected from a reference site were subsequently caged at that site and at two oiled sites. In laboratory experiments, A. purpurescens from a reference site were injected with BNF, a known inducer of P4501A, or were exposed to sediments and/or were fed amphipods from an oiled site. Immunoblotting of hepatic microsomes showed that P4501A was induced up to six-fold in field-sampled and caged fish from all oiled sites when compared to fish from reference sites. By comparison, BNF-treated fish showed nearly 40-fold induction compared to fish from reference sites. By comparison, BNF-treated fish showed nearly 40-fold induction of P4501A over control values. Laboratory exposure to oiled sediments induced levels of P4501A to 20-fold greater than controls within 3 weeks. These levels dropped rapidly to control levels 3 weeks after removal of oil exposure. Feeding of oiled foods increased P4501A levels, but not significantly (p≤0.05) over 3 weeks. Our results clearly show that the sediment-entrained and weathered oil present 14 months after the spill is capable of altering P4501A levels in intertidal fish. The degree of response observed in the field was only 15% of the level produced by BNF. The rapid return to control levels when fish are removed from oiled sediments and the caging experiments indicate that the induction of P4501A in field samples was due to pollutants in the ecosystem at that time.

Submitted to: Scries of Environmental Quality and Ecosystem Stability.

Supported by: Alaska Department of Environmental Conservation.

WHOI Contribution No. 8068.

SUBJECT HEADING INDEX Department of Biology 1992

ANIMAL BEHAVIOR	
S. Kaartvedt, C. L. Van Dover, L. S. Mullineaux, P. H. Wiebe, and S. M. Bollens	В-13
Phillip S. Lobel	B-16
Laela S. Sayigh, Peter L. Tyack and Randall S. Wells	B-22
Peter L. Tyack, Kurt Fristrup, Janet S. McIntosh	B-26
William A. Walkins and Mary Ann Daher	B-27
William A. Walkins, Mary Ann Daher, Kurt Fristrup, and Giuseppe Notarbartolo di Sciara	B-28
BENTHIC ECOLOGY	
S. Kaartvedt, C. L. Van Dover, L. S. Mullineaux, P. H. Wiebe, and S. M. Bollens	B-13
H. A. Lessios, James R. Weinberg and Victoria R. Starczak	B-15
Lauren S. Mullineaux	B-18
Lauren S. Mullineaux and Elizabeth D. Garland	B-19
Rudolf S. Scheltema	B-22
Paul V. R. Snelgrove and Cheryl Ann Butman	B-24
<u>BENTHOS</u>	
Ron J. Etter and Hal Caswell	В-7
Nicholas J. Gotelli, Andrew R. Davis and Hal Caswell	B-9
H. A. Lessios, James R. Weinberg and Victoria R. Starczak	B-15
Lauren S. Mullineaux	B-18
Lauren S. Mullineaux and Elizabeth D. Garland	B-19
Rudolf S. Scheltema	B-22
Paul V. R. Snelgrove and Cheryl Ann Butman	B-24
Paul V. R. Snelgrove, Cheryl Ann Butman and Judith P. Grassle	B-25
BIOACOUSTICS	
Emily Monosson and John J. Stegeman	B-17
Laela S. Sayigh, Peter L. Tyack and Randall S. Wells	B-22
William A. Watkins and Mary Ann Daher	B-27
William A. Walkins, Mary Ann Daher, Kurt Fristrup, and Giuseppe Notarbartolo di Sciare	3 B-28
BIOCHEMISTRY	
Mark E. Hahn, Teresa M. Lamb, Mary E. Schultz, Rozanna M. Smolowitz, Alan Poland and John J. Stegeman	B-10
Pamela J. Kloepper-Sams and John J. Stegeman	B-14
K. R. Munkittrick, M. R. van den Heuvel, D. A. Metner, W. L. Lockhart and J. J. Steger	
Roxanna M. Smolowitz, Mary E. Schultz and John J. Stegeman	B-23
John J. Stegeman	
Bruce R. Woodin and John J. Stegeman	

BIOGEOCHEMISTRY	
Frederick E. Goetz and Holger W. Jannasch	B-7
John Kiddon, Michael Bender, Joe Orchardo, Joel Goldman, David A. Caron and Mark Dennett	B-13
Paul V. R. Snelgrove and Cheryl Ann Butman	
J. M. Teal, B. L. Howes, S. B. Peterson, J. E. Petersen and A. Armstrong	
Carl O. Wirsen, Holger W. Jannasch and Stephen J. Molyneaux	
Bruce R. Woodin and John J. Stegeman	
BIOGEOGRAPHY	
Donald M. Anderson, Bruce A. Keafer, David M. Kulis, Robert M. Waters and R. Nuzzi	B-1
Robert A. Koza, Michael J. Moore and John J. Stegeman	B-14
Richard A. Orson and Brian L. Howes	B-19
H. A. Lessios, James R. Weinberg and Victoria R. Starczak	B-15
Rudolf S. Scheltema	B-22
Christopher A. Scholin, Donald M. Anderson and Mitchell L.Sogin	B-23
BIOLOGICAL/CHEMICAL/PHYSICAL INTERACTIONS	
Mark E. Hahn, Teresa M. Lamb, Mary E. Schultz, Rozanna M. Smolowitz, Alan Poland and John J. Stegeman	B-10
S. Kaartvedt, C. L. Van Dover, L. S. Mullineaux, P. H. Wiebe, and S. M. Bollens	B-13
Pamela J. Kloepper-Sams and John J. Stegeman	B-14
Michael J. Moore and John J. Stegeman	B-18
Lauren S. Mullineaux	B-18
Lauren S. Mullineaux and Elizabeth D. Garland	B-19
Mercedes Pascual	B-20
Roxanna M. Smolowitz, Mary E. Schultz and John J. Stegeman	B-23
BIOTECHNOLOGY	
S. S. Bates, C. Leger, Bruce A. Keafer and Donald M. Anderson	B-1
Edward F. DeLong	B-4
Christopher A. Scholin and Donald M. Anderson	B-23
COMMUNITY ECOLOGY	
Hal Caswell and Ron J. Etter	B -3
Ron J. Etter and Hal Caswell	B-7
Phillip S. Lobel	B-16
Lauren S. Mullineaux and Elizabeth D. Garland	B-19
Richard A. Orson and Brian L. Howes	B-19
Robert W. Sanders, David A. Caron and Ulrike-G. Berninger	B-21
DESCRIPTIVE/FUNCTIONAL/MORPHOLOGY	
Colleen M. Cavanaugh, Carl O. Wirsen and H. W. Jannasch	B -3
Amélie H. Scheltema	
Roxanna M. Smolowitz, Mary E. Schultz and John J. Stegeman	
Paul V. R. Svelgrove and Cheryl Ann Rytman	B.24

ECOSYSTEM STUDIES	
Brian L. Howes and Dale D. Goehringer	B-10
S. Kaartvedt, C. L. Van Dover, L. S. Mullineaux, P. H. Wiebe, and S. M. Bollens	B-13
Robert A. Koza, Michael J. Moore and John J. Stegeman	B-14
Richard A. Orson and Brian L. Howes	B-19
Craig D. Taylor and B. L. Howes	B-26
Peter H. Wiebe and Terrence M. Joyce	B-28
Bruce R. Woodin and John J. Stegeman	B -29
EVOLUTION	
Edward M. Hulburt	B-11
H. A. Lessios, James R. Weinberg and Victoria R. Starczak	B-15
Amélie II. Scheltema	B-22
John J. Stegeman	B-25
FISHERIES	
Phillip S. Lobel	B-16
A. J. Read, S. D. Kraus, K. D. Bisack and D. Palka	B-20
Bruce R. Woodin and John J. Stegeman	B-29
FISHES	
Mark E. Hahn, Teresa M. Lamb, Mary E. Schultz, Rozanna M. Smolowitz, Alan Poland and John J. Stegeman	B-1 0
Pamela J. Kloepper-Sams and John J. Stegeman	B-14
Robert A. Koza, Michael J. Moore and John J. Stegeman	B-14
Phillip S. Lobel	B-16
Emily Monosson and John J. Stegeman	B-17
Michael J. Moore and John J. Stegeman	B-18
K. R. Munkittrick, M. R. van den Heuvel, D. A. Metner, W. L. Lockhart and J. J. Stegeman	B-19
Roxanna M. Smolowitz, Mary E. Schultz and John J. Stegeman	B-23
John J. Stegeman	B-25
Bruce R. Woodin and John J. Stegeman	B-29
GENETICS	
P. V. Dunlap	B-5
H. A. Lessios, James R. Weinberg and Victoria R. Starczak	B-15
Rudolf S. Scheltema	B-22
INSTRUMENTATION	
Bruce A. Keafer and Donald M. Anderson	
Laela S. Sayigh, Peter L. Tyack and Randall S. Wells	B-22
Craig D. Taylor and B. L. Howes	B-26
William A. Watkins and Mary Ann Daher	B-27

LARVAL ECOLOGY	
Lauren S. Mullineaux	B-18
Lauren S. Mullineaux and Elizabeth D. Garland	B-19
Rudolf S. Scheltema	В-22
Paul V. R. Snelgrove and Cheryl Ann Butman	B-24
Paul V. R. Snelgrove, Cheryl Ann Butman and Judith P. Grassle	B-25
LIFE HISTORY	
Solange Brault and Hal Caswell	B-2
David A. Caron, Robert W. Sanders, Ee Lin Lim, Celia Marrasé, Linda A. Amaral, Sheri Whitney, Rika B. Aoki and Karen G. Porter	B-3
Nicholas J. Gotelli, Andrew R. Davis and Hal Caswell	B-9
David B. McDonald and Hal Caswell	B-16
Rudolf S. Scheltema	B-22
Paul V. R. Snelgrove and Cheryl Ann Butman	B-24
MARINE MAMMALS	
Solange Brault and Hal Caswell	B-2
A. J. Read, S. D. Kraus, K. D. Bisack and D. Palka	B-20
A. J. Read, R. S. Wells, A. A. Hohn, and M. D. Scott	B-21
Laela S. Sayigh, Peter L. Tyack and Randall S. Wells	B-22
Peter L. Tyack, Kurt Fristrup, Janet S. McIntosh	B-26
Peter Tyack, William A. Watkins and Kurt M. Fristrup	B-27
William A. Watkins and Mary Ann Daher	B-27
William A. Watkins, Mary Ann Daher, Kurt Fristrup, and Giuseppe Notarbartolo di Sciara	B-28
MARINE POLLUTION	
Mark E. Hahn, Teresa M. Lamb, Mary E. Schultz, Rozanna M. Smolowitz, Alan Poland and John J. Stegeman	B-10
Pamela J. Kloepper-Sams and John J. Stegeman	B-14
Robert A. Koza, Michael J. Moore and John J. Stegeman	B-14
D. F. Leavitt, D. Miosky Dragos, B. A. Lancaster, A. C. Craig, C. L. Rcinisch and J. McDowell Capuzzo	B-15
Judith McDowell Capuzzo	
Judith McDowell Capuzzo	
Emily Monosson and John J. Stegeman	B-17
Michael J. Moore and John J. Stegeman	B-18
K. R. Munkittrick, M. R. van den Heuvel, D. A. Metner, W. L. Lockhart and J. J. Stegeman	
Roxanna M. Smolowitz, Mary E. Schultz and John J. Stegeman	
Carl O. Wirsen and Holger W. Jannasch	B-28
Bruce R. Woodin and John J. Stegeman	В-29
MATHEMATICAL ECOLOGY	
Solange Brault and Hal Caswell	B-2
Hal Caswell and Ron J. Etter	
Ron J. Etter and Hal Caswell	B-7
David B. McDonald and Hal Caswell	B-16
Marcalas Paraud	D 00

MICROBIAL ECOLOGY	
Ulrike-G. Berninger, David A. Caron and Robert W. Sanders	B-2
David A. Caron	B-2
David A. Caron, Robert W. Sanders, Ee Lin Lim, Celia Marrasé, Linda A. Amaral, Sheri Whitney, Rika B. Aoki and Karen G. Porter	B-3
S. W. Chisholm, S. L. Frankel, R. Goericke, R. J. Olson, P. Palenik, J. B. Waterbury, L. West-Johnsrud and E. R. Zettler	B-4
Edward F. DeLong	
Frederick E. Goetz and Holger W. Jannasch	B-7
Joel C. Goldman	B-8
Holger W. Jannasch, Carl O. Wirsen, Stephen J. Molyneaux and Thomas A. Langworthy	B-12
Bo Barker Jorgensen, Mai F. Isaksen and Holger W. Jannasch	B-12
John Kiddon, Michael Bender, Joe Orchardo, Joel Goldman, David A. Caron and Mark Dennett	B-13
Celia Marrasé, Ee Lin Lim and David A. Caron	B-16
Robert W. Sanders, David A. Caron and Ulrike-G. Berninger	B-21
John B. Waterbury and Frederica W. Valois	B-27
Carl O. Wirsen and Holger W. Jannasch	B-28
Carl O. Wirsen, Holger W. Jannasch and Stephen J. Molyneaux	B-29
MICROBIAL GENETICS	
P. V. Dunlap	B-5
Paul V. Dunlap	B-6
Paul V. Dunlap and Alan Kuo	B-6
F. B. Perler, D. G. Comb, W. E. Jack, L. S. Moran, B. Qiang, R. B. Kucera, J. Benner, B. E. D. O. Nwankwo, S. K. Hempstead, C. K. Carlow and H. W. Jannasch	7. Slatko, B-20
MICROBIOLOGY	
David A. Caron	B-23
Colleen M. Cavanaugh, Carl O. Wirsen and H. W. Jannasch	B-3
S. W. Chisholm, S. L. Frankel, R. Goericke, R. J. Olson, P. Palenik, J. B. Waterbury, L. West-Johnsrud and E. R. Zettler	B-4
P. V. Dunlap	B-5
Paul V. Dunlap	B-6
Paul V. Dunlap and Alan Kuo	B-6
Edward F. DeLong	B-4
Thomas J, DiChristina	B-4
Frederick E. Goetz and Holger W. Jannasch	B-7
Holger W. Jannasch, Carl O. Wirsen, Stephen J. Molyneaux and Thomas A. Langworthy	B-12
Bo Barker Jorgensen, Mai F. Isaksen and Holger W. Jannasch	B-12
Celia Marrasé, Ee Lin Lim and David A. Caron	B-16
F. B. Perler, D. G. Comb, W. E. Jack, L. S. Moran, B. Qiang, R. B. Kucera, J. Benner, B. E. D. O. Nwankwo, S. K. Hempstead, C. K. Carlow and H. W. Jannasch	Slatko, B-20
John B. Waterbury and Frederica W. Valois	B-27
Carl O. Wirsen and Holger W. Jannasch	B-28
Carl O. Wirsen, Holger W. Jannasch and Stephen J. Moluneaux	B-29

<u>MODELLING</u>	
Solange Brault and Hal Caswell	B-2
Hal Caswell and Ron J. Etter	В-3
Ron J. Etter and Hat Caswell	B-7
David B. McDonald and Hal Caswell	B-16
Mercedes Pascual	B-20
Robert W. Sanders, David A. Caron and Ulrike-G. Berninger	B-21
MOLECULAR BIOLOGY	
S. S. Bates, J. Leger, B. A. Keafer and D. M. Anderson	B-1
Edward F. DeLong.	
P. V. Dunlap	
Paul V. Dunlap	
Paul V. Dunlap and Alan Kuo	
Mark E. Hahn, Teresa M. Lamb, Mary E. Schultz, Rozanna M. Smolowitz, Alan Poland and	Б-0
John J. Stegeman	
Pamela J. Kloepper-Sams and John J. Stegeman	
Amélie H. Scheltema	
Christopher A. Scholin and Donald M. Anderson	Б-23
Christopher A. Scholin, Donald M. Anaerson and Mitchell L. Sogin	B-23
PATHOLOGY	
Robert A. Koza, Michael J. Moore and John J. Stegeman	B-14
D. F. Leavitt, D. Miosky Dragos, B. A. Lancaster, A. C. Craig, C. L. Reinisch and J. McDowell Capuzzo	B-15
Michael J. Moore and John J. Stegeman	
Rozanna M. Smolowitz, Mary E. Schultz and John J. Stegeman	
PHYSIOLOGY	
Thomas J. DiChristina	B-4
Gregory J. Doucette and Donald M. Anderson	
P. V. Dunlap	
Paul V. Dunlap and Alan Kuo	
D. F. Leavitt, D. Miosky Dragos, B. A. Lancaster, A. C. Craig.	
C. L. Reinisch and J. McDowell Capuzzo	
Judith McDowell Capuzzo	B-17
Judith McDowell Capuzzo	B-17
Roxanna M. Smolowitz, Mary E. Schultz and John J. Stegeman	B-23
PHYTOPLANKTON	
Donald M. Anderson, Bruce A. Keafer, David M. Kulis, Robert M. Waters and R. Nuzzi	B-1
Ulrike-G. Berninger, David A. Caron and Robert W. Sanders	B-2
David A. Caron, Robert W. Sanders, Ee Lin Lim, Celia Marrasé, Linda A. Amaral, Sheri Whitney, Rika B. Aoki and Karen G. Porter	B-3
S. W. Chisholm, S. L. Frankel, R. Goericke, R. J. Olson, P. Palenik, J. B. Waterbury, L. West-Johnsrud and E. R. Zettler	
Joel C. Goldman, Dennis A. Hansell and Mark R. Dennett	
Bruce A. Keafer and Donald M. Anderson	
Christopher A. Scholin, Donald M. Anderson and Mitchell L. Sogin	
Craig D. Taylor and B. L. Howes	

PHYTOPLANKTON ECOLOGY	_
Donald M. Anderson, Bruce A. Keafer, David M. Kulis, Robert M. Waters and	
S. S. Bates, C. Leger, Bruce A. Keafer and Donald M. Anderson	
Ulrike-G. Berninger, David A. Caron and Robert W. Sanders	
Joel C. Goldman	
Joel C. Goldman, Dennis A. Hansell and Mark R. Dennett	B-8
Bruce A. Keafer and Donald M. Anderson	B-13
Mercedes Pascual	B-20
Christoper A. Scholin and Donald M. Anderson	B -23
Christoper A. Scholin and Donald M. Anderson and Mitchell L. Sogin	B-23
POPULATION ECOLOGY	
Solange Brault and Hal Caswell	B-7
Hal Caswell and Ron J. Etter	B-3
Edward F. DeLong	B-4
Gregory J. Doucette and Donald M. Anderson	B-5
Nicholas J. Gotelli, Andrew R. Davis and Hal Caswell	
Edward M. Hulburt	
H. A. Lessios, James R. Weinberg and Victoria R. Starczak	
David B. McDonald and Hal Caswell	
A. J. Read, S. D. Kraus, K. D. Bisack and D. Palka	
A. J. Read, R. S. Wells, A. A. Hohn, and M. D. Scott	
Christopher A. Scholin, Donald M. Anderson and Mitchell L. Sogin	
Paul V. R. Snelgrove and Cheryl Ann Butman	
John B. Waterbury and Frederica W. Valois	
RECRUITMENT	
Ron J. Etter and Hal Caswell	B-7
Nicholas J. Gotelli, Andrew R. Davis and Hal Caswell	
Lauren S. Mullineaux and Elizabeth D. Garland	
Rudolf S. Scheltema	
Paul V. R. Snelgrove and Cheryl Ann Butman	
P. V. R. Snelgrove, C. A. Butman and J. P. Grassle	
DEMOTE CENSING	
REMOTE SENSING	D 11
Bruce A. Keafer and Donald M. Anderson	D-10
SYSTEMATICS	
S. S. Bates, C. Leger, Bruce A. Keafer and Donald M. Anderson	B-1
S. W. Chisholm, S. L. Frankel, R. Goericke, R. J. Olson, P. Palenik, J. B. Waterbury, L. West-Johnsrud and E. R. Zettler	
H. A. Lessios, James R. Weinberg and Victoria R. Starczak	
Amélie H. Scheltema	B-22
Christopher A. Scholin, Donald M. Anderson and Mitchell L. Sogin	B-23
TAXONOMY	
S. S. Bates, C. Leger, Bruce A. Keafer and Donald M. Anderson	B -1
Edward F. DeLong	
H. A. Lessios, James R. Weinberg and Victoria R. Starczak	
Christoper A. Scholin and Donald M. Anderson	

<u>TOXICOLOGY</u>	
Gregory J. Doucette and Donald M. Anderson	B-5
Mark E. Hahn, Teresa M. Lamb, Mary E. Schultz, Rozanna M. Smolowitz, Alan Poland and John J. Stegeman	B-10
Pamela J. Kloepper-Sams and John J. Stegeman	B-14
Robert A. Koza, Michael J. Moore and John J. Stegeman	B-14
Judith McDowell Capuzzo	B-17
Judith McDowell Capuzzo	B-17
K. R. Munkittrick, M. R. van den Heuvel, D. A. Metner, W. L. Lockhart and J. J. Stegeman	B-19
Rozanna M. Smolowitz, Mary E. Schultz and John J. Stegeman	B-23
Bruce R. Woodin and John J. Stegeman	В-29
ZOOPLANKTON ECOLOGY	
Ulrike-G. Berninger, David A. Caron and Robert W. Sanders	B-2
David A. Caron	B-2
S. Kaartvedt, C. L. Van Dover, L. S. Mullineaux, P. H. Wiebe, and S. M. Bollens	B-13
Celia Marrasé, Ee Lin Lim and David A. Caron	B-16
Robert W. Sanders, David A. Caron and Ulrike-G. Berninger	B-21
VIRUSES	
John B. Waterbury and Frederica W. Valois	B-27

DEPARTMENT OF GEOLOGY AND GEOPHYSICS G. Michael Purdy, Chairman

ACCELERATOR MASS SPECTROMETRY

AMS-GRAPHITE TARGET PRODUCTION METHODS AT THE WOODS HOLE OCEANOGRAPHIC INSTITUTION DURING 1986-1991

Alan R. Gagnon and Glenn A. Jones

In July 1986 an AMS radiocarbon target preparation laboratory was established at the Woods Hole Oceanographic Institution for the purpose of producing graphite to be analyzed at the NSF-Accelerator Facility for Radioisotope Analysis at the University of Arizona (Tucson). By June 1991, 924 graphite targets had been prepared and 845 analyzed. Our lab procedures during this time included the careful documentation of weights of all starting samples, catalysts, and final graphite yields, as well as the volume of CO₂ gas evolved during CaCO₃ hydrolysis or closed tube organic carbon combustions. These numbers allow us to evaluate the methods used in general and our lab in particular.

In Press: Radiocarbon.

Supported by: ONR Contract N00014-85-C-0714, the Mellon Foundation, and NOAA NA84AA-D-SG033.

WHOI Contribution No. 8136.

A SHELL-DERIVED TIME HISTORY OF BOMB-¹⁴C ON GEORGES BANK AND ITS LABRADOR SEA IMPLICATIONS

Christopher R. Weidman and Glenn A. Jones

Bomb-produced radiocarbon has been used in the past as an important tracer of ocean circulation and as a valuable tool for calculating CO₂ air-sea exchange. However, previous studies of the ocean's time-varying bomb-14C record have been confined exclusively to analyzing banded corals, and thus, their application has been limited to the lower latitudes. The first time history of bomb-14C from the high-latitude oceans is obtained from a 54-year old mollusc specimen, (Bivalvia) Arctica islandica, which was collected live from Georges Bank (41°N) in 1990. The annual growth bands of its shell were analyzed for Δ^{14} C using accelerator mass spectrometry (AMS), producing a Δ^{14} C time history from 1939-1990. The depleted condition of the Georges Bank bomb-14C signal relative to two coral-derived North Atlantic Δ^{14} C time histories suggests a significant deep-water source for the waters on Georges Bank. This evidence supports previous

work linking the origin of waters on Georges Bank to the $^{\rm T}$ abrador Sea, and also allows a time history of bomb- $^{14}{\rm C}$ for the Labrador Sea to be estimated. Pre-bomb $\Delta^{14}{\rm C}$ values calculated for the Labrador Sea are lower than earlier estimates, suggesting a greater inventory of bomb- $^{14}{\rm C}$ has accumulated here than previously reported. Deduced variations in the ventilation and/or $^{14}{\rm CO}_2$ uptake rates in the Labrador Sea correspond with observed changes in surface salinity of the Labrador Sea.

In Press: Journal of Geophysical Research.

Supported by: DOE Fellowship, Global Climate Change Program and NOAA NA16RC0080-02.

WHOI Contribution No. 8152.

RADIOCARBON CHRONOLOGY OF BLACK SEA SEDIMENTS

Glenn A. Jones and Alan R. Gagnon

Accelerator Mass Spectrometer (AMS) radiocarbon analyses have been made on 102 samples from twelve sediment cores and 23 samples from two water column profiles. These materials were collected during the first leg of the 1988 joint U.S.-Turkish Black Sea Expedition and provide the most comprehensive radiocarbon chronology of Black Sea sediments yet attempted. Radiocarbon analyses from carefully collected box cores suggest a maximum detrital correction for radiocarbon ages of Unit I sediments of 480 years for the organic carbon and 380 years for the carbonate fractions. Evidence does not support the 1430-to-2000 year detrital corrections argued for in past studies. The best estimates for the age of the beginning of the final invasion of the coccolithophore Emiliania huxleyii (Unit 1/2 boundary of Ross and Degans, 1974) and the age of the first invasion of E. huxleyii (Unit I/II boundary of Hay et al., 1991) are 1660 and 2700 yBP respectively. Sapropel formation began at 8200 yBP at all depths in the basin, a pattern in disagreement with those predicted by existing time-evolution models of sapropel formation for this basin. Our data suggests the oxic/anoxic interface has remained relatively stable throughout the Holocene, is controlled largely by the physical oceanography of the basin, and has not evolved over time as assumed by previous workers.

In Press: Deep-Sea Research.

Supported by: NSF Grant OCE-8712181.

WHOI Contribution No. 8174.

GEOCHEMISTRY

FLUID CIRCULATION IN THE OCEANIC CRUST: CONTRAST BETWEEN VOLCANIC AND PLUTONIC REGIMES

Stanley R. Hart, Jerzy Blusztajn, Henry J. B. Dick and James R. Lawrence

Vein carbonates from a variety of ocean crust environments have been analyzed for Sr contents and Sr and oxygen isotopic compositions. Veins from upper crustal lithologies typically have low formation temperatures (<100°C) and form within 10-15 m.y. after crust formation, from solutions containing a basaltic component of very high Ca/Sr (>30 times that of hot smoker vent fluids). Veins from the gabbro lithologies at site 735B show both high (>50°C) and very low (<10°C) formation temperatures. The high temperature carbonate veins have a large basaltic component (low 87/86 Sr) with low Ca/Sr and probably formed before unroofing c this deep crustal block. The low temperature veis have only a minor basaltic component, and formed after unroofing, but within 10 m.y. of crust formation. Hot smoker vent fluids represent the low Ca/Sr limit of fluids represented by carbonate veins and thus cannot represent the totality of the seawater-ocean crust Ca/Sr exchange budget.

In Press: Journal of Geophysical Research.

Supported by: NSF Grant OCE-8400794 and OCE-9101340.

WHOI Contribution No. 8210.

EXPERIMENTAL CPX/MELT PARTITIONING OF 24 TRACE ELEMENTS

Stanley R. Hart and Todd Dunn

Cpx/melt partition coefficients have been determined by ion probe for 24 trace elements at natural levels in an alkali basalt experimentally equilibrated at 1380°C and 3 Gpa. One goal was to intercompare D's for both HFSE and REE in a single experiment. Relative to the REE spidergram, Hf and Ti show virtually no anomaly, whereas Zr exhibits a major negative anomaly. Other incompatible elements (Ba, K, Nb) fall in the range of published values, as do elements such as Sr, Y, Sc, Cr and V. Pb shows a value intermediate between La and Ce. Values for Be, Li and Ga are reported for the first time, and show that Be is as incompatible as the light REE's whereas Li and Ga are somewhat more compatible than the heavy REE.

Published in: Contributions to Mineral Petrology, 113:1-8, 1993.

Supported by: NSF Grant EAR-8708372 and EAR-8805221.

WHOI Contribution No. 8146.

MANTLE PLUMES AND ENTRAINMENT: ISOTOPIC EVIDENCE

S. R. Hart, E. H. Hauri, L. A. Oschmann and J. A. Whitehead

Many oceanic island basalts show sublinear subparallel arrays in Sr-Nd-Pb isotopic space. The depleted upper mantle is rarely a mixing end-member of these arrays, as would be expected if mantle plumes originated at a 670 km boundary layer and entrained upper mantle during ascent. Instead, the arrays are fan-shaped and appear to converge on a volume in isotopic space characterized by low ⁸⁷Sr/⁸⁶Sr and high ¹⁴³Nd/¹⁴⁴Nd, ²⁰⁶Pb/²⁰⁴Pb and ³He/⁴He ratios. This new isotopic component may be the lower mantle, entrained into plumes originating from the core-mantle boundary layer.

Published in: Science, 256:517-520, 1992.

Supported by: NSF Grant EAR-9096194, and a Mellon Independent Study Award.

WHOI Contribution No. 8015.

RESPONSE: "MANTLE PLUMES AND MANTLE SOURCES. K.A. FARLEY AND H. CRAIG"

S. R. Hart, E. H. Hauri, L. A. Oschmann and J. A. Whitehead

Response: In our paper on evidence for lower mantle plume entrainment, we stressed the potential role that He isotopes could play in supporting or rejecting our theory. We noted the lack of published He data on many key islands, so we welcome the comment by Farley and Craig.

Unfortunately, data are needed for He and Sr, Nd, and Pb isotopes on the same samples, and figure 1 of the comment by Farley and Craig does not help in this respect. Pitcairn shows enormous variations in Sr, Nd, and Pb, and we need to know if all basalts from Pitcairn are high He 3/4 and if there is a correlation such that He increases in one direction or the other along the Sr, Nd, Pb array. The Cameroon line is marked by volcanoes stretching for 1500 km, yet it is labeled "low He" by Farley and Craig, with no reference to which volcanoes were sampled or where the data can be found (the data are not in their references 2 or 3, nor is the Fernando data to be found there). There

are additional high He islands (figure 1) which extend the high He domain more toward our FOZO component.

Farley and Craig locate their PHEM mantle component from the array which their Samoa (Tutuila) data (1) makes on He-Sr, He-Nd, and He-206/204 PB plots. The observed data scatter and possible curvature in these arrays would seem to allow a PHEM location near our FOZO component.

Finally, we address what appear to be several remarkable features touched on by Farley and Craig. The first is that no single island shows He isotope values both higher and lower than the typical value of 8 Ra inferred for the upper mantle from MORB. If this finding holds as additional He data are generated, it may implicate mixing of upper mantle as an important plume entrainment process. The second is the general left-right division of the DMM-EMI-HIMU mantle plane (figure 1 of the comment by Farley and Craig) into high and low He regions. If this feature "holds up," it may argue not only for the low He 3/4 signature for HIMU, established by Graham et al. (2) but also for a relatively high He concentration in HIMU, so that this component is able to overwhelm the He from other mixing and members.

Published in: Science, 258:821-822, 1992. Supported by: NSF Grant EAR-9101340. WHOI Contribution No. 8172.

GEOLOGY

COASTAL BENCH FORMATION AT HANAUMA BAY, OAHU, HAWAII

Wilfred B. Bryan and Robert A. Stephens

A coastal bench developed from one to six meters above sea level in basaltic tuff at Hana 'ma Bay conforms to the upper limit of wetting by wave wash at high tides associated with present sea level; it does not constitute evidence for a recent Holocene high stand on Oahu. Variations in bench width and elevation are related to differences both in exposure to waves and to exposure to daily heating and drying of the cliff behind the bench. Salt weathering of the sort usually invoked to explain weathering effects in deserts is a major factor in the retreat of the cliff and the consequent formation of the bench. The waves do not "cut" the bench but instead, by daily wetting protect it from desiccation. The bench forms as a result of the disintegration and retreat of the unprotected cliff. The same process can satisfactorily explain the formation of Koko Bench, presently submerged at -5 m along the north shore of Hanauma Bay. Use of similar benches as geological indicators of past sea levels requires a detailed understanding of the coastal setting and exposure to waves, and the different responses of specific rock types at and above the air-sea interface.

In Press: Bulletin of the Geological Society of America.

Supported by: NOAA NA86-AA-D-SG090. WHOI Contribution No. 8123.

UNCONTROLLED GROWTH OF HUMAN POPULATIONS, GEOLOGICAL BACKGROUND, AND FUTURE PROSPECTS

K. O. Emery

The geological history of the Earth is replete with examples of animals proliferating to numbers that exceeded the ability of their environments to provide support. Enormous numbers and widespread distributions of many animals sometimes have been followed by drastic reductions in numbers of individuals and even by complete extinction of species. Humans of many nations are following the same trend of population growth beyond the ability of resources to insure adequate food, clothing, shelter, safety, and transport and beyond the ability of the Earth to accommodate the wastes. Human population is now 5.4 billion, with a present doubling time estimated at about 35 years. Is this uncontrolled proliferation also to be followed by severe reduction or even extinction? If not, how may human population be stabilized or reduced to a level commensurate with resources and waste disposal - more effective contraceptives, increased abortion, high taxes on procreation? An approach more effective than religion or political control may be through better education (increased percentage literacy) that is known to correlate with lower birth rates and increased national income per capita in the about 167 nations of the world. If leadership cannot soon rise to face this situation, human inhabitation of the Earth may become much more complicated in the not too distant future.

In Press: Population and Environment.

WHOI Contribution No. 7798.

MORPHOTECTONICS OF THE MID-ATLANTIC RIDGE (24°- 30°N)

J. Escartin Guiral and J. Lin

The Mid-Atlantic Ridge between the Kane and Atlantis Fracture Zones (24° N-30° N) is a slow-spreading ridge (half-spreading rates between 10 and 14 km/My) intersected by 17 non-transform discontinuities (offsets between 0 and 30 km). These discontinuities, together with the two fracture zones, bind 18 different segments, 50 km long in average. The location of these non-transform offsets has been mapped from both gravity and SeaBeam bathymetric data covering an area 60 km wide and 800 km long over the ridge axis. The absence of a thick sediment cover that tend to obliterate the original seafloor morphology has allowed us to assemble a map of seafloor faults for this region. Faulting of the oceanic crust is initiated away from the axial valley floor, where volcanic processes dominate. Variations in faulting style along the strike of the ridge are related to ridge segmentation, with long segments showing long faults oriented 15°E, while short segments containing shorter faults are oriented 30°E.

The along-axis variations in faulting style are accompanied by variations of the asymmetry of the axial rift valley. The axial valley tends to be symmetric in the center of the segment (small amount of crustal extension) and becomes an asymmetrical half-graben (greater crustal extension) in the proximity of the bounding discontinuities. Since the spreading rate does not vary consideraably along the single segments, this tectonic variability reflects a drecrease of the magma supply rate along each segment axis away from the center towards the distal ends. Gravity anomaly profiles show that crustal thickness decreases from the center of the segment towards the discontinuities and/or that the density of the underlying mantle increases away from the segment center. The data also shows that along-axis topography is isostatically compensated, while across-axis relief is dynamically maintained by internal stresses in the oceanic crust.

The gravity data and morphological observations suggest that convection in the upper mantle is segmented, with the presence of upwelling plumes centered in each of the segments. The plumes would be responsible for higher melt supply rates in the center of the plume than near the discontinuities. Consequently, the rate of crustal extension will also increase away from the segment center. This accreting structure is also responsible for the variations in crustal thickness inferred from the gravity structure.

In Press: Acta Geologica Hispanica.

Supported by: Student Fellowship from Caja de

Pensiones "La Caixa", NSF Grant OCE-9012576 and ONR Contract N00014-91-J-1433.

WHOI Contribution No. 8118.

PRACTICAL GEOLOGICAL COMPARISON OF SEAFLOOR SURVEY INSTRUMENTS

Martin C. Kleinrock, R. N. Hey and A. E. Theberge, Jr.

Seafloor survey instruments are integral to the study of marine geology. Because understanding their resolution and limitations is critical, we compare how different survey systems represent the seafloor. Coincident data collected at the Galapagos propagator (GLORIA, SeaMARC II, Sea Beam, Deep-Tow, camera sled, and Alvin) allow comparisons of how well seafloor features observed and characterized in high resolution data are represented in lower-resolution, coarser-scale data sets. Our reported values for the minimum sizes of detectable and well-representable features of several types (e.g., faults, volcanoes, etc.) for different systems show that theoretical resolutions often grossly overestimate the capabilities of systems; care must be taken in evaluating which system to use to address a particular problem.

Published in: Geophysical Research Letters, 19(13):1407-1410, 1992.

Supported by: ONR Contracts N00014-90-J-1434 and N00014-89-J-1021.

WHOI Contribution No. 8058.

A DETAILED CHRONOLOGY OF THE AUSTRALASIAN IMPACT EVENT, THE BRUNHES-MATUYAMA POLARITY REVERSAL, AND GLOBAL CLIMATE CHANGE

David A. Schneider, Dennis V. Kent and Gilberto A. Mello

A mechanism had been recently proposed to show how an impact event can trigger a geomagnetic polarity reversal by means of rapid climate cooling. We test the proposed mechanism by examining the record from 2 high sedimentation rate (8-11 cm/kYr) deep-sea sediment cores (ODP Sites 767 and 769) from marginal seas of the Indonesian archipelago, which record the Australasian impact with well-defined microtektite layers, the Brunhes-Matuyama polarity reversal with strong and stable remanent magnetizations, and global climate with oxygen isotope variations in planktonic foraminifera. Both ODP cores show the impact to have preceded the reversal of

magnetic field directions by about 12 kYr. Both records indicate that the field intensity was increasing near the time of impact and that it continued to increase for about 4 kYr afterward. Furthermore, the oxygen isotope record available from sediments at ODP Site 769 shows no indication of discernible climate cooling following the impact: the microtektite event occurred in the later part of glacial Stage 20 and was followed by a smooth warming trend to interglacial Stage 19. Thus the detailed chronology does not support the previously proposed model which would redict that a decrease in geomagnetic field intensity resulted from a minor glaciation following the impact event. We conclude that the evidence for a causal link between impacts and geomagnetic reversals remains insufficient to demonstrate a physical connection.

Published in: Earth and Planetary Science Letters, 111:395-405, 1992.

Supported by: WHOI Postdoctoral Fellowship. WHOI Contribution No. 8043.

GEOPHYSICS

GEOTHERMAL HEAT FLUX FROM HYDROTHERMAL PLUMES ON THE JUAN DE FUCA RIDGE

Karen G. Bemis, Richard P. Von Herzen and Michael J. Mottl

Estimates of the heat output of hydrothermal vents, identified along the Endeavor and Southern Segments of the Juan de Fuca Ridge, are used to evaluate the total heat flux associated with hydrothermal circulation for the ridge segment. A 50 m array carried by DSV Alvin sampled the temperature and vertical velocity structure of hydrothermal plumes from individual vents. These measurements are used to estimate the thermal flux associated with such plumes. The maximum heat flux calculated for a single vent is 50 MW (1 $MW = 1x10^6$ watts). The average heat flux per vent is 13 MW and 4 MW, respectively, for the Endeavour Segment (18 vents) and Southern Segment (18 vents). The estimates for any given vent may vary over an order of magnitude. This uncertainty is due mainly to the difficulty of locating the centerline of the plume relative to the point of measurement, although the uncertainties in the constants for the appropriate equations based on laboratory experiments also contribute significantly to the net error. For the Endeavour Segment, the minimum total geothermal heat flux due to hydrothermal circulation exceeds 70 MW. The minimum estimate for the Southern Segment

is 16 MW. The maximum estimate is probably closer to the total heat flux from high temperature venting (239 MW and 66 MW respectively). High temperature hydrothermal venting accounts for only a small fraction of the heat available according to steady-state predictions of conductive heat flux; other hydrothermal innomena (e.g., diffuse flow) probably account or a greater proportion of the total hydrothermal heat flux.

In Press: Journal of Geophysical Research.

Supported by: NSF Grant OCE-8714511 and WHOI Education.

WHOI Contribution No. 8133.

ACOUSTIC AND ELASTIC SCATTERING FROM SEAMOUNTS IN THREE DIMENSIONS - A NUMERICAL MODELLING STUDY

Daniel R. Burns

A three dimensional (3-D) finite difference elastic wave propagation numerical model is used to study the acoustic scattering in the water column and the elastic scattering in the subbottom from seamounts (conical hills) located on the ocean floor. Two models are investigated: scattering from a single seamount located on a flat seafloor, and scattering from two seamounts on an otherwise flat seafloor. In both cases a point source of acoustic energy is introduced in the water column, and particular attention is paid to the backscattered acoustic energy which emanates from the seamount features. The results indicate that in addition to the expected scattering off the front and back faces of the seamount, additional energy is radiated into the water column from reverberations inside the seamount and the related interface energy which propagates around the circumference of the seamount. Comparison of the single seamount and two seamount models suggests that the effect of multiple features is an increase in the overall level of backscattered acoustic energy. A comparison between the 3-D single seamount model and a two dimensional (2-D) simplification is also presented. The 3-D model results in a more complicated backscattered wavefield due to the effects of the seamount resonant and circumferential modes which are lost in 2-D representations. Elastic scattering in the subbottom due to seamount features is also illustrated.

Published in: Journal of the Acoustical Society of America, 92(5):2784-2791, 1992.

Supported by: ONR Contract N00014-90-J-1493 and N00014-90-C-0098.

WHOI Contribution No. 8082.

GEOELECTRIC FIELD MEASUREMENTS ON A PLANETARY SCALE: OCEANIC AND GEOPHYSICAL APPLICATIONS

A. D. Chave, D. S. Luther, L. J. Lanzerotti and L. V. Medford

The characteristics of an initial year of electric field measurements obtained from a long (≈3900 km), unpowered submarine cable extending from Point Arena, California, to Hanauma Bay, Hawaii are reported. The power spectrum estimated from the cable time series is similar to that from seafloor point electric field sensors at frequencies above 1 cpb, but differs at lower frequencies by decreasing monotonically down to at least 0.02 cpd. The multiple squared coherence between the cable data and three component geomagnetic fluctuations measured at Fresno, CA, is high $(\gamma^2 \gamma 0.9)$ from 1.0-0.09 cpd, then declines slowly with decreasing frequency. Maps of the squared coherence between the cable voltage and the surface air pressure, wind stress, and wind stress curl derived from the FNOC product over the entire eastern North Pacific show no significant relationships at frequencies above ≈0.05 cpd, but strong nonlocal coherence with the wind stress curl forcing obtains at lower frequencies. Taken together, these observations support a transition from high frequency dominance by external sources to low frequency dominance by oceanic motional sources at 0.05-0.1 cpd, a considerably smaller value than has previously been observed with point electric field sensors on the ocean bottom. The difference is caused by horizontal averaging of the short spatial scale motional component over the long submarine cable.

Published in: Geophysical Research Letters, 19(13):1411-1414, 1992.

Supported by: NSF Grant OCE-9119493.

WHOI Contribution No. 8017.

STRUCTURE OF YOUNG UPPER CRUST AT THE EAST PACIFIC RISE NEAR 9°30'N

G. L. Christeson, G. M. Purdy and G. J. Fryer

Eight on-bottom seismic refraction experiments are analyzed in an effort to resolve the structure of the emplacement zone of lavas and dikes at a fast-spreading ridge segment. The results suggest that the thickness of the lava and sill section doubles in thickness over an across-axis distance of ~1 km due to the emplacement of lava that either overflows the ASC or travels through

lateral tube conduits, and that the depth to the top of the sheeted dikes increases from ~ 160 m within the ASC to ~ 340 m for the crust ~ 1 km to the west

Published in: Geophysical Research Letters, 19(10):1045-1048, 1992.

Supported by: NSF Grants OCE-8917750 and OCE-8917988 and ONR Contract N00014-90-J-1622.

WHOI Contribution No. 7989.

SEISMIC STRUCTURE OF THE SOUTHERN EAST PACIFIC RISE

R. S. Detrick, A. J. Harding, G. M. Kent, J. A. Orcutt, J. C. Mutter and P. Buhl

Seismic data from the ultrafast spreading (150-162 millimeters per year) southern East Pacific Rise show that the rise axis is underlain by a thin (less than 200 meters thick) extrusive volcanic layer (seismic layer 2A) that thickens rapidly off-axis. Also beneath the rise axis is a narrow (less than 1 kilometer wide), melt sill that is in some places less than 1000 meters below the sea floor. The small dimensions of this molten body indicate that the magma chamber size does not depend strongly on spreading rate aspredicted by many ridge-crest thermal models. However, the shallow depth of this body is consistent with an inverse correlation between magma chamber depth and spreading rate. These observations indicate that the paradigm of ridge crest magma chambers as small, sill-like, mid-crustal bodies is applicable to a wide range of intermediate and fast spreading ridges.

Published in: Science, 259:499-503, 1993.
Supported by: NSF Grant OCE-9012707.

WHOI Contribution No. 8204.

A UTILITARIAN APPROACH TO MODELING NON-GAUSSIAN CHARACTERISTICS OF A TOPOGRAPHIC FIELD

John A. Goff

This paper develops a general framework for the analysis of the moments of a topographic field greater than 2. This framework uses "iterated" expectation to reduce a statistical moment function to component parts involving the vertical (disjoint) moment of the same order, lower moments, and two-point conditional expectations. In this way it is possible to isolate the unique informational contribution of each moment. Use of this framework necessitates a "bootstrap" or perturbation method, where lower moments are modeled first, and then used as constraints in the modeling of higher moments. Functional modeling of any moment is thus reducible to characterization of the disjoint moment (e.g., skewness, kurtosis) and the two point conditional expectation. In this paper, I demonstrate how it is possible to "design" a statistical model most sensitive to specific non-Gaussian topographic characteristics by solving for the two-point conditional expectation under an invertible mapping between Gaussian and non-Gaussian fields of interest. Mappings of this sort are useful both for profact that they can be very intuitive descriptions of non-Gaussian characteristics, and for their utility in generating non-Gaussian synthetic topography. The primary intent of this methodology is to forge a link between physical topographic characteristics, the information we want to know, and statistical moments, our tool for quantitatively measuring topographic fields. In addition, mapping models can be used to calculate the skewness and kurtosis (or higher moments) of topographic slopes directly. The applicability of these methods is demonstrated for mapping models which create vertical and lateral asymmetry and peakiness in a topographic field.

Supported by: ONR Contract N00014-90-J-1584. WHOI Contribution No. 8217.

QUANTITATIVE CHARACTERIZATION OF ABYSSAL HILL MORPHOLOGY ALONG FLOW LINES IN THE ATLANTIC OCEAN

John A. Goff

The morphology of the seafloor, when sampled along flow lines of relative plate motion, represents an indirect geologic time series record of the processes which form it. Eventually we hope to be able to interpret this information so that we may improve our understanding of the workings of ridge-crest and off-ridge processes through time. This study takes an important step toward that goal by quantitatively characterizing, through stochastic modeling, the abyssal hill morphology along the available Sea Beam flow line data sets in the Atlantic. The six Sea Beam flow line data sets used in this study include two near the Kane Fracture Zone and four near the Rio Grande and Moore Fracture Zones. Stochastic parameters estimated from these flow lines, such as the rms height, lineament azimuth, characteristic widths, and plan-view aspect ratio, are plotted as a function of crustal age. In addition to testing available hypotheses, the purpose of this work is to investigate how the abyssal hill morphology changes with age and to correlate this behavior to known changes in ridge characteristics with age. These results place important constraints on our understanding of the process of seafloor creation, and begin to establish a baseline against which morphology may be interpreted in the absence of other information.

Along the Kane Fracture Zone, variations in the estimated abyssal hill lineament azimuth. rms height, and plan-view aspect ratio with crustal age appear to be correlated in various ways with the segmentation history and also possibly with large changes in plate motion direction that have occurred there within the past 80 m.v. Along the Rio Grande and Moore Fracture Zones, variations in the lineament azimuth, rms height and other parameters as a function of crustal age are often significant on a ~ 5 -10 m.y. time scale. These variations are difficult to interpret as vet. To emphasize longer time scale variations, the estimated rms heights from the South Atlantic flow lines are averaged over common age bins. This demonstrates a strong negative correlation of rms height with the spreading rate. However, when characteristic widths are averaged in this manner. no strong correlation with spreading rate is found. Large variations in this parameter occur on a \sim 25 m.y. time scale.

Published in: Journal of Geophysical Research, 97:9183-9202, 1992.

Supported by: ONR Contract N00014-90-J-1584. WHOI Contribution No. 8025.

THE WILKES TRANSFORM SYSTEM AND "NANNOPLATE"

John A. Goff, Daniel J. Fornari, James R. Cochran, Christopher Keeley, and Alberto Malinverno

A recent Hydrosweep survey of the Wilkes transform system, the second fastest-slipping transform on the world's ocean ridge system, shows it to be a highly complex and continually evolving plate boundary. A $\sim \! 50$ km x 50 km area north of the eastern portion of the Wilkes transform appears to be rotating in accordance with the theory of edge-driven microplate kinematics. We have called this region a "nannoplate" to distinguish it both as a separate small area of lithosphere between the Pacific and Nazca plates, and as a smaller and less stable phenomenon than a microplate.

In Press: Geology.

Supported by: NSF Grant OCE-9019741.

WHOI Contribution No. 8221.

ABYSSAL HILL SEGMENTATION: QUANTITATIVE ANALYSIS OF THE EAST PACIFIC RISE FLANKS 7°S-9°S

John A. Goff, Alberto Malinverno, Daniel J. Fornari and James R. Cochran

The recent R/V Ewing EW9105 survey of the East Pacific Rise (EPR) and adjacent flanks between 9°S-7°S provides an excellent opportunity to explore the casual relationship between the ridge and the abyssal hills which form on its flanks. This data covers 100% of the flanking abyssal hills out to 115 km on either side of the axis. We apply the methodology of Goff and Jordan [1988] for estimating statistical characteristics of abyssal hill morphology (rms height, characteristic lengths and widths, plan view aspect ratio, azimuthal orientation, and fractal dimension). Principal observations include (1) the rms height of abyssal hill morphology as negatively correlated with the width of the 5-10 km wide crestal high, consistent with the observations of Goff [1991] for northern EPR abyssal hill morphology; (2) the characteristic abyssal hill width displays no systematic variation with position relative to ridge segmentation within the EW9105 survey area, in contrast with observations of Goff [1991] for northern EPR abyssal hill morphology, in which characteristic widths tend to be smallest at segment ends and largest toward the middle of segments; (3) abyssal hill rms heights and characteristic widths are very large just north of a 50 km-offset overlapping spreading center (OSC), suggesting that the overlap region is being pushed northward, perhaps in response to microplate-style tectonics; and (4) within the 8°38'S-7°12'S segment, abyssal hill lineaments are generally parallel to the ridge axis, while south of this area, abyssal hill lineaments rotate with a larger "radius of curvature" than does the EPR axis approaching the EPR-Wilkes ridge-transform intersection.

Supported by: NSF Grant OCE-9019741.

WHOI Contribution No. 8220.

THE ROLE OF DENSITY IN THE ACCUMULATION AND ERUPTABILITY OF BASALTIC MELTS AT MID-OCEAN RIDGES

E. E. Hooft and R. S. Detrick

It is commonly assumed that magma ponds at a level of neutral buoyancy in the shallow crust where melt densities are equal to the bulk density of the surrounding crust. However, at the East Pacific Rise this neutral buoyancy level lies only 500 ± 250 m below the sea floor, significantly

shallower than the depth (1-2 km) of the magma bodies imaged in multichannel reflection data, suggesting that other factors must control the collection of melt in these reservoirs. Ridge crest magma chambers lie at or below the critical depth where lithostatic pressure due to the integrated weight of the overlying crustal column is sufficient to force a column of magma from this reservoir to the sea floor. Magma chamber depths beneath intermediate and fast spreading ridges vary inversely with spreading rate and the accumulation of melt in these bodies appears to be controlled thermally by the balance of magmatic heat input and heat loss due to conductive and hydrothermal cooling.

In Press: Geophysical Research Letters.

Supported by: NSF Grant OCE-9012707.

WHOI Contribution No. 8176.

GEOELECTROMAGNETISM

L. J. Lanzerotti, R. A. Langel and A. D. Chave

Earth's magnetic field and the electric currents flowing in Earth and above it in the ionized space plasma environment are of intrinsic scientific interest, as well as of practical importance to fields such as mineral prospecting and communications. Four sources contribute to the electromagnetic field near Earth: electric currents in the core, permanent magnetization in the crust and upper mantle, motion of conducting seawater in Earth's main field, and electric currents in the space plasmas (the ionosphere and magnetosphere). The core (main) magnetic field is the strongest, and studies of this field and its time and spatial variations provide information on the region of the field generation and on the electrical conductivity of Earth's mantle. Studies of the external currents and magnetic fields by ground- and space-based techniques provide information on the plasma-filled space that surrounds the planet. Analysis of the induced electric currents in Earth yield further information on the conductivity structure of the crust and mantle or on ocean currents.

In Press: Encyclopedia of Applied Physics, VCH Publishers, NY, G.L. Trigg, ed.

Supported by: NSF Grant EAR-9121278.

WHOI Contribution No. 8216.

TWO-DIMENSIONAL VELOCITY INVERSION/IMAGING OF LARGE OFFSET SEISMIC DATA VIA THE TAU-P DOMAIN

Edmund C. Reiter, G. M. Purdy and M. N. Toksoz

We describe a method for determining a two-dimensional (2-D) velocity field from refraction data that has been decomposed into some function of slowness. The most common decomposition, intercept time - slowness or τ - p, is used as an intermediate step in an iterative wavefield continuation procedure previously applied to one-dimensional (1-D) velocity inversions. We extend the 1-D approach to 2-D by performing the downward continuation along numerically computed raypaths. Synthetic data are used to demonstrate how this approach can compensate for the effects of known lateral inhomogeneities whi e determining an underlying 1-D velocity field. 'Ve also use synthetic data to show how multiple refraction lines may be used to determine a general 2-D velocity model. Large offset field data collected with an Ocean Bottom Hydrophone are used to illustrate this technique in an area of significant lateral heterogeneity caused by a sloping seafloor. At present, limitations of this 2-D approach are caused primarily by the sparseness of typical refraction surveys, but hopefully may be overcome in the future with more appropriate acquisition geometries.

In Press: Geophysics.

Supported by: NSF Grant OCE-8917628.

WHOI Contribution No. 8116.

A SEMBLANCE GUIDED MEDIAN FILTER

Edmund C. Reiter, M. N. Toksoz and G. M. Purdy

We describe and implement a slowness selective median filter based on information from a local set of traces. The filter is constructed in two steps with the first being an estimation of a preferred slowness and the second the selection of a median or trimmed mean value to replace the original data point. A symmetric window of traces is selected about each trace to be filtered and the filter repeatedly applied to each time point. The preferred slowness is determined by scanning a range of linear moveouts within the user specified slowness passband. Semblance is computed for each trial slowness and the preferred slowness selected from the peak semblance value. Data points collected along this preferred slowness are then sorted from lowest to highest and in the case

of a pure median filter, the middle point(s) selected to replace the original data point. The output of the filter is therefore quite insensitive to large amplitude noise bursts, retaining the well known beneficial properties of traditional one-dimensional median filter. Energy which is either incoherent over the filter width or lies outside the slowness passband, may be additionally suppressed by weighting the filter output by the measured peak semblance. A low pass filtered version of the computed peak semblance envelope should be used in order to avoid pulse distortion in the vicinity of wavelet zero crossings.

This approach may be used as a velocity filter to estimate coherent signal within a specified slowness passband and reject coherent energy outside this range. For applications of this type, other velocity estimators may be used in place of our semblance measure to provide improved velocity estimation and better filter performance. The filter width may also be extended to provide increased velocity estimation, but will result in additional lateral smearing of signal. A minimum filter width should be more than twice the width of the noise which is to be suppressed in order to allow the median filter to provide an adequate estimate of the signal. We show that in addition to a velocity filter, our approach may be used to improve signal to noise ratios in noisy data. The median filter tends to suppress the amplitude of random background noise and semblance weighting may be used to further reduce the amplitude of background noise while enhancing coherent signal.

In Press: Geophysical Prospecting.

Supported by: NSF Grant OCE-8917628.

WHOI Contribution No. 8117.

PALEOMAGNETISM OF SOME OCEAN DRILLING PROGRAM LEG 138 SEDIMENTS: DETAILING MIOCENE MAGNETOSTRATIGRAPHY

David A. Schneider

The aims of this study are twofold. Firstly, the study tries to provide the most reliable chronology possible for two critical sections by correlating the magnetic polarity stratigraphy measured in these sediments with a newly revised geomagnetic polarity timescale. Secondly, this study attempts to examine in detail the nature of 7 short events not included in the shipboard standard timescale, but for which there was abundant magnetostratigraphic evidence obtained during the

Results presented here force some modifications to the shipboard interpretations of the magnetostratigraphy of Sites 845 and 844 on

the basis of new data generated using discrete samples, and from a greater appreciation of the magnetostratigraphic signature of Miocene-age short events. Those short events can be classified into two groups: those that likely reflect short full-polarity intervals, and those that more likely represent an interval of diminished geomagnetic intensity. Three of the 7 events documented here correspond well with 3 subtle features, as seen in marine magnetic profiles, that have been newly included in the geomagnetic polarity timescale as short, full-polarity subchrons. One of the 7 events corresponds to a poorly defined feature of the marine magnetic record which has also been newly included in the geomagnetic polarity timescale, but which was considered of enigmatic origin. The 3 remaining events investigated here, although they have not been identified with features in the sea-floor magnetic record, are suggested to be events of a similar nature, most likely times of anomalously low geomagnetic intensity.

In addition to the Miocene magnetostratigraphic results given, several sets of averaged paleomagnetic inclinations are presented. Although these results clearly show the effects of a residual coring overprint, they demonstrate that paleomagnetic estimates of paleolatitudes can be made which are in good general agreement with ancient site positions calculated using hotspot-based plate reconstructions.

Supported by: Ocean Drilling Program and a WHOI Postdoctoral Fellowship.

WHOI Contribution No. 8211.

AGE VARIATIONS OF OCEANIC CRUST POISSON'S RATIO: INVERSION AND A POROSITY EVOLUTION MODEL

Peter R. Shaw

Porosity in the oceanic crust is one of the most important factors influencing measured seismic velocities. Porosity is particularly important in the uppermost young crust, where rapid variations in velocities with depth and crustal age are observed. Knowledge of the concentration and aspect ratios of inferred crack populations can be improved considerably if estimates of Poisson's ratio are available from observations of compressional and shear seismic velocities v_p and v_s . In this paper I present a joint seismic waveform inversion for v_p and v_s : velocities are found while maximizing or minimizing Poisson's ratio using a hypothesis-testing mechanism. I apply this method to OBII data in 140 Ma Atlantic crust; the resulting solution corridor agrees with laboratory measurements without the low Poisson's ratio anomalies at depths of 0.8-1.5 km found by Spudich and Orcutt [1980] and Au and Clowes [1984] on

younger (< 15 Ma) Pacific crust. Compiling other published v_p and v_s solutions, an age-dependent pattern emerges: none of the solutions for crust older than 60 Ma display the Poisson's ratio anomaly. I propose a simple crustal evolution model, using thin and thick cracks, to explain these observations: thin cracks preferentially close at shallow depths in the crust, producing the localized Poisson's ratio anomaly. Sealing of all cracks by hydrothermal deposits as the crust ages restores the seismic velocities to be consistent with the laboratory measurements. This model is consistent with similar models of crack populations and their evolution from shallow measurements.

In Press: Journal of Geophysical Research.

Supported by: ONR Contract N00014-89-J-1018.

WHOI Contribution No. 7978.

RIDGE SEGMENTATION, FAULTING, AND CRUSTAL THICKNESS IN THE ATLANTIC

Peter R. Shaw

The Mid-Atlantic Ridge (MA) between the Kane and Atlantis fracture zon - consists of segments 20-85 km in length; bull's-eye patterns in the mantle Bouguer gravity anomaly field centered on several segments associated with narrow rift valleys have been interpreted as centers of strong mantle upwelling and thick crust. Here I present a map of normal faults inferred from $\sim 5x10^4$ km² of Sea Beam bathymetry along the Mid-Atlantic Ridge between 28°N and the Atlantis fracture zone. Faults are mapped both on- and off-ridge using a criterion that distinguishes them from volcanic topography. Abyssal hill lineations seem to form at the rift valley walls through the growth of the normal faults; towards ridge segment ends these faults are more widely spaced, with larger throws than those at segment centers, and often define the boundaries of the gravity bull's-eyes. These two different faulting styles, which probably reflect changes in lithospheric strength, are preserved into the rift mountains. Large-throw faults are highly correlated with the mantle Bouguer highs, suggesting that amagmatic extension on the large faults contributes to the crustal thinning inferred towards the segment ends.

Published in: Nature, 358(6386):490-493, 1992.

Supported by: ONR Contracts N00014-89-J-1021, N00014-90-J-1615 and N00014-91-J-1433.

WHOI Contribution No. 8009.

QUANTITATIVE COMPARISON OF SEISMIC DATA SETS WITH WAVEFORM INVERSION: TESTING THE AGE-DEPENDENT EVOLUTION OF CRUSTAL STRUCTURE

Peter R. Shaw

Studies of seismic variability play a more important role in the understanding of processes that form oceanic crust and individual velocity-depth solutions found in isolation. For such variability studies, solutions must be contrasted with one another; this is normally not straightforward owing to the lack of rigorous uncertainty estimates available for solutions. Here I present a method for the direct comparison of such solutions by hypothesis testing. A null hypothesis is proposed that a single velocity solution is consistent with two sets of data. The hypothesis is tested by seeking such a model using waveform inversion and comparing its misfit against the misfit from fully independent solutions. The degree of similarity of the velocity structures can be further quantified by solving for the pair of solutions that are as similar as possible but consistent with each set of data; the F test is used to evaluate the significance of each additional effective model parameter as it lends independence to the two solutions. The method posses advantages of a hypothetical Monte Carlo search of all models because the complete forward problem is carried out at each step, yet it is tractable because the search direction is well defined. The method is applied to two data sets collected near the Mid-Atlantic Ridge on 0 and 7 m.y. crust in order to quantify the differences between the solutions. The comparison finds quantifiable differences in both layers 2 and 3 between these two regions, suggesting that significant evolution of the entire crustal section has taken place in the first 7 m.y.

Published in: Journal of Geophysical Research, 97(B13):19,981-19,991, 1992.

Supported by: ONR Contract N00014-89-J-1018. WHOI Contribution No. 8139.

CHANGE IN FAILURE STRESS ON THE SOUTHERN AN ANDREAS FAULT SYSTEM CAUSED BY THE 1992 MAGNITUDE=7.4 LANDERS EARTHQUAKE

Ross S. Stein, Geoffrey C. P. King and Jian Lin

The 28 June Landers earthquake brought the San Andreas fault significantly closer to failure near San Bernadino, a site that has not sustained a

large earthquake since at least 1812. Stress also increased on the San Andreas fault near San Bernardino and on the San Andreas fault southeast of Palm Springs. Unless creep or moderate earthquakes relieve these stress changes, the next great earthquake on the southern San Andreas fault is likely to be advanced by one to two decades. In contrast, stress on the San Andreas north of Los Angeles dropped, potentially delaying the next great earthquake there by 2 to 10 years.

Published in: Science, 258:1328-1332, 1992.

Supported by: Southern California Earthquake Center Fellowship.

WHOI Contribution No. 8149.

A NUMERICAL SCATTERING CHAMBER FOR STUDYING REVERBERATION IN THE SEAFLOOR

R. A. Stephen

A numerical scattering chamber, based on the finite difference solution to the two-way elastic (or anelastic) wave equation in the time domain, is a powerful and convenient approach to studying the physics of surface and volume reverberation at the seafloor. Scattering from both surface roughness and volume heterogeneities at scale lengths comparable to wavelengths can be treated. The method includes all shear wave and interface wave effects and all multiple interactions between scatterers. Bottom parameters varying from soft sediments (with shear wave velocities much less than water velocity) to hard basalts (with shear velocities higher than water velocity) are studied. We use a Gaussian pulse-beam as the incident field and we compute the resultant scattered field (in compressional and shear wave energy density) on arrays of receivers surrounding the scattering region. Backscatter coefficients, defined as the ratio of the energy in the scattered beam at a given angle to the energy in the incident beam, can be computed. For example, for an incident beam at fifteen degrees grazing angle, the coefficient for direct backscattering from a very rough, basaltic seafloor is 17dB.

Published in: Ocean Reverberation, H. Urban, ed. Kluwer Academic Publishers, Dordrecht, The Netherlands.

Supported by: ONR Contract N00014-90-J-1493. WHOI Contribution No. 8052.

HOW MUCH GABBRO IS IN OCEAN SEISMIC LAYER 3?

Stephen A. Swift and Ralph A. Stephen

Ocean seismic layer 3 is distinguished from layer 2 by higher velocities, lower variability, and lower gradients in velocity with depth. Based on studies of rocks recovered from ophiolites and walls of fracture zones, most models of lower ocean crust correlate seismic layer 3 with sequences of gabbroic lithologies. The average velocity (6.5 km/s) for a vertical seismic profile in a gabbro sequence at Ocean Drilling Program (ODP) Hole 735B is consistent with refraction values for layer 3. However, the Q (inverse attenuation) obtained from these data, after correction to temperature and pressure conditions in lower crust, are too low to be consistent with amplitudes of signals observed in refraction experiments. Laboratory measurements of Q on gabbros from Hole 735B and ophiolites are also one to two orders of magnitude lower than seismic refraction Q. These results indicate that the gabbro sequence at ODP Hole 735B cannot be typical of seismic layer 3. Based on Q, upper layer 3 may be metadolerite, and lower layer 3 may include interbedded gabbros and ultramafics. Serpentine is highly attenuating and is unlikely to be a major component.

Published in: Geophysical Research Letters, 19(18):1871-1874, 1992.

Supported by: NSF Grant OCE-8922762.

WHOI Contribution No. 8138.

COMMENT ON "THE ELECTRICAL CONDUCTIVITY OF THE OCEANIC UPPER MANTLE" BY G. HEINSON AND S. CONSTABLE

Pascal Tarits, Alan D. Chave and Adam Schultz

In a recent paper, Heinson and Constable (1992; hereafter HC) have attempted to construct an oceanic upper mantle electrical conductivity model by combining laboratory measurements on dry olivine as a function of temperature with a geotherm inferred from a variety of geophysical and petrological data. HC argue that the 1D magnetotelluric (MT) response computed from their model structure is not compatible with three sets of seafloor electromagnetic (EM) data collected in the late 1970's, and proceed to examine those data in more detail. They infer that some of the EM data are not consistent with a 1D structure on the basis of several statistical tests, and further conclude that the presence of an upper mantle high conductivity zone is not required by

the data. Finally, HC attempt to reconcile these disparate observations by suggesting that a highly resistive upper mantle (which is required by their model) combined with the presence of resistive coastlines will result in significant distortion of the EM response at points in the ocean's interior. They construct sample MT responses by combining their mantle conductivity model with some simple coastline geometries using a thin sheet algorithm, and maintain that the results bear resemblance to the seafloor EM observations.

We will discuss three categories of objections to the approach taken by and conclusions of HC in the next three sections of this commentary. First, HC's assertion that the addition of coastlines with various geometries to their very resistive mantle conductivity model can reconcile the seafloor MT data is questionable, contrary to the conclusions of HC, the existence of weakly conductive vertical paths between the ocean and deep mantle or horizontal electrical connections between oceans through continents have a zeroth order effect on the MT response by dramatically reducing the size of the coastal boundary layer even when part of the upper mantle is extremely resistive. This is demonstrated with some simple 3D thin sheet and 2D numerical models. Given the ubiquitous presence of vertical and horizontal electrical connections in the real oceans, the seafloor MT response in the ocean's interior is unlikely to be highly sensitive to edge conditions. Because small conductivity perturbations result in large changes in the model MT response, the resemblance between seafloor MT data and models which include coastlines reported by HC cannot be regarded as well-established.

Second the EM response functions used by HC were taken from among the earliest seafloor soundings, while their associated error estimates were not derived from the original source, but rather are the product of extensive ad hoc manipulation. In light of the considerable recent advances in our understanding of magnetotelluric data analysis, inferences should be derived from such old results only with considerable caution. In particular, the response functions used by HC, which were not computed using the remote reference method, are probably biased at high frequencies by magnetometer noise, and the response function error estimates are certainly too small, yet all of the statistical deductions presented by them depend heavily upon the accuracy of these parameters. Similarly, their conclusions about the presence or absence of a high conductivity zone in the mantle depend upon meaningful MT responses (including the confidence limits) and hence must be correspondingly discounted.

Third, their synthesis of predictions from laboratory data is based on very uncertain petrologic and thermodynamic data and models.

Dry olivine data establishes only a minimum conductivity for the rock matrix under subsolidus conditions, and the addition of trace amounts of volatiles can result in dramatic increases in the bulk subsolidus conductivity without requiring extensive partial melting. As a result, we regard the C model as extremal and speculative rather than conservative and well-founded.

In Press: Geophysical Journal International.

Supported by: NSF Grant OCE-9219493.

WHOI Contribution No. 8067.

PHYSICAL PROPERTIES AND LOGGING OF THE LOWER OCEANIC CRUST: HOLE 735B

R. P. Von Herzen, D. Goldberg and M. Manghnani

Results from downhole logging instrumentation and physical properties measurements on samples recovered from a 500-m-thick section of gabbros at Site 735 on the SW Indian Ridge are compared. Here we emphasize particularly the seismic, electrical, and nuclear logging measurements to deduce the physical state and evolution of this crustal section over the 11-12 M.y. since its formation. Various seismic methods give compressional velocities ranging from 6.5 to >7 km/s, typical of lower oceanic crustal velocities determined from marine refraction measurements. Except for the unusually low intrinsic electrical resistivity (<10 ohm-m) of some Fe-Ti-oxide gabbros, the relatively high range of resistivities (~3x10² - 2x10⁴ ohm-m) for most of the section deeper than 150 m sub-seafloor is consistent with low porosities (few percent) derived from the neuron log. The decrease with depth of thin, relatively high porosity (20-25%) zones, low temperature (sea water) rock alteration, and fluid permeability suggests that overburden stress is an important factor maintaining closed fractures in young ocean crust.

Published in: The Indian Ocean: A Synthesis of Results from the Ocean Drilling Program, Geophys. Monograph 70, American Geophysical Union (Washington, D.C.), 41-56, 1992.

Supported by: Joint Oceanographic Institutions, Inc. WHOI Contribution No. 8042.

THE NEW NATIONAL OCEAN SCIENCES ACCELERATOR MASS SPECTROMETER FACILITY AT WOODS HOLE OCEANOGRAPHIC INSTITUTION - PROGRESS AND FIRST RESULTS

K. F. Von Reden, G. A. Jones, R. J. Schneider, A. P. McNichol, G. J. Cohen, and K. H. Purser

Start-up performance and first results of the new Woods Hole Accelerator Mass Spectrometer are discussed. Special attention is given to the hemispherical ionizer sputter source and the triple-isotope injector design.

Published in: Radiocarbon, 34:3:478-482, 1992.

Supported by: NSF Cooperative Agreement OCE-8802509.

WHOI Centribution No. 8091.

SEISMIC PROPAGATION ACROSS THE THE EAST PACIFIC RISE: FINITE DIFFERENCE EXPERIMENTS AND IMPLICATIONS FOR SEISMIC TOMOGRAPHY

William S. D. Wilcock, Martin E. Dougherty, Sean C. Solomon, G. M. Purdy, and Douglas R. Toomey

We use a full-waveform finite-difference technique to investigate seismic propagation across the East Pacific Rise at 9°30'N for a two-dimensional velocity model based on that proposed by Vera and others. The primary feature of the model is an upper crustal low velocity region, corresponding to the axial magma chamber, which includes a small magma body located 1.6 km beneath the seafloor at the rise axis. The high velocity gradients in this region result in a complex pattern of propagation which includes considerable scattering and diffraction of energy above and below the magma chamber. A qualitative comparison of finite-difference solutions with data collected by receivers located 9 km and 20 km off-axis during a tomography experiment at 9°30'N shows generally good agreement. For paths that cross the rise axis, the first arrival in the finite-difference solutions diffracts above the magma chamber, although the amplitude of this phase is very low and falls below ambient noise levels in the observed data. In such cases, the first arrival with significant energy is a diffraction below the magma chamber. A strong PP phase in the finite-difference solutions is not prominent in the data, a discrepancy that may result from a simplified seafloor velocity structure and the

absence of attenuation in the finite-difference algorithm. A high-amplitude Moho-turning (PmP) phase which results from the large velocity change across the Moho beneath the rise axis is apparent in both the finite difference solution and the observations. Synthetic delay-time inversions for velocity demonstrate the importance of ensuring that picked arrival times are assigned to ray paths that pass to the correct side of the magma body. Synthetic inversions of spectral estimates of t* show that Q⁻¹ models are compromised not only if the ray paths are incorrect, but also if t* estimates include significant contributions from more than one phase. Deterministic scattering from the magma chamber may contribute noticeably to spectral estimates of t*, but the results of the finite-difference experiments suggest that the high levels of attenuation observed for phases passing below the magma chamber are predominantly the result of intrinsic attenuation.

Supported by: NSF Grants OCE-9000458. WHOI Contribution No. 8246.

MICROEARTHQUAKES ON AND NEAR THE EAST PACIFIC RISE, 9-10°N

William S. D. Wilcock, G. M. Purdy, Sean C. Solomon, David L. DuBois, and Douglas R. Toomey

Records from a seismic network deployed as part of an active tomography experiment at 9°30'N on the East Pacific Rise provide an opportunity to characterize local microearthquake activity over an 8-day period. With the exception of the region around the 9°03' overlapping spreading center (OSC), no events were located on the rise axis. One microearthquake, located from P and S-wave arrival times, lies adjacent to the network, 18 km to the west of the rise axis. Five more events, located from P-wave and T-phase data, are to the south of the network. Three cluster around the western arm of the 9°03'OSC. while two are located 25-30 km to the east of the OSC. The seismic moments of the microearthquakes range from 4×10^{10} to 4×10^{20} dyn cm, several orders of magnitude larger than those reported in other studies of shallow events along the axis of the East Pacific Rise. These results suggest that overlapping center may be the locus of substantial microearthquake activity and that at this location the normal faults that form on the young flanks of the East Pacific Rise are active off-axis to distances of at least 20 km.

Published in: Geophysical Research Letters, 19:2131-2134, 1992.

Supported by: NSF Grants OCE-8615797, OCE-8615892, OCE-9000177 and OCE-9106233 WHOI Contribution No. 8171.

THE SEISMIC ATTENUATION STRUCTURE OF A FAST-SPREADING MID-OCEAN RIDGE

William S. D. Wilcock, Sean C. Solomon, G. M. Purdy and Douglas R. Toomey

The two-dimensional P-wave attenuation structure of the axial crust of the East Pacific Rise, obtained from an inversion of waveform spectra collected during an active-source seismic tomography experiment, shows that attenuation near the surface is high everywhere but decreases markedly within 1 to 3 kilometers of the rise axis. The near-axis variation is attributed to the thickening of the surface basalt layer and possibly to in situ changes in porosity related to hydrothermal circulation. High attenuation is also observed beneath the rise axis at depths ranging from about 2 kilometers (less than 1 kilometer beneath the axial magma lens) to the base of the crust. The levels of attenuation in this deeper region require at most only a small fraction of partial melt.

Published in: Science, 258:1470-1747, 1992. Supported by: NSF Grant OCE-8615797 WHOI Contribution No. 8150.

HYDROTHERMAL

PROCESS OF BRINE GENERATION AND CIRCULATION IN THE OCEANIC CRUST: FLUID INCLUSION EVIDENCE FROM THE TROODOS OPHIOLITE, CYPRUS

Deborah S. Kelley, Paul T. Robinson and John G. Malpas

Detailed temporal, thermal, and compositional data on aqueous fluid inclusions from a suite of plutonic and diabase samples from the Troodos ophiolite, Cyprus provide the first documentation that generation of high-temperature brines may be common at depth in the oceanic crust.

Anastomosing arrays of fluid inclusions in rocks of the upper intrusive sequence record episodic fracturing events. The earliest fracturing event, at temperatures <450-600°C resulted in entrapment of brine-rich aqueous fluids with salinities of 36-61 wt% NaCl equivalent. Homogenization of the brine inclusions by halite dissolution, the virtual absence of vapor-rich fluid inclusions throughout the upper level plutonic sequence, and the restriction of brine

inclusions to the most evolved plutonic rocks suggests that exsolution of brines off of the late stage gabbro and plagiogranite melts played a significant role in generating the quartz-hosted, high-salinity inclusions. Cooling of the fluids during pulses of fluid migration associated with episodic fracturing events, resulted in entrapment of the brines in the deep-seated, high-temperature portion of the hydrothermal system. In localized areas, the high-temperature brines (NaCl±Kcl±CaCl2 caused extreme alteration of the plagiogranite bodies and in the formation of podiform epidosites.

Arrays of low-temperature, low-salinity fluid inclusions, which in some samples crosscut fractures dominated by brine inclusions, indicate downward propagation of a cracking front subsequent to collapse of the high-temperature magmatic system, resulting in penetration of seawater-like fluids into the plutonic sequence at temperatures >200-400°C. Hydration reactions under greenschist facies conditions, or limited mixing with brine-rich fluids, may have resulted in salinity variations from 70% below to 200% above seawater concentrations. Temperatures and compositions of the low-salinity inclusions are similar to those found in stockwork systems beneath Troodos ore deposits and to those of fluids exiting active submarine hydrothermal vents at mid-ocean ridge spreading centers. The low-temperature fracture networks may represent an extensive deep-seated feeder system which coalesced to form zones of concentrated hydrothermal upflow.

Published in: Journal of Geophysical Research, 97(B6):9307-9322, 1992.

Supported by: Natural Sciences and Engineering Research Council of Canada and a WHOI Postdoctoral Fellowship.

WHOI Contribution No. 7959.

OCEAN ACOUSTICS

MEAN AND RMS SCATTERING STRENGTH FORMULATION UNDER AN INTRINSIC SEPARATION OF SCALES HYPOTHESIS

John A. Goff

The intrinsic separation of scales hypothesis asserts that a scattering surface, irrespective of its roughness properties, is separated by the acoustic wavelength into two scale regimes; features larger than the separation scale act to specularly reflect rays in different directions, whereas features smaller than the separation scale act to scatter

acoustic energy in all directions. This paper explores the consequences of this hypothesis by formulating the relationship, given the probability density for illuminated slopes, between a local-scale scattering strength function and three global-scale (i.e., the entire surface) scattering functions. The latter include the mean and rms global scattering strength and a grain ratio scattering strength function which is applicable to anisotropic surfaces. The following applications are envisioned for these formulations: (1) prediction of global scattering properties given the separation-scale slope distribution and the local scattering strength function (the latter may be derived by an empirical fit to ensemble numerical solutions); (2) evaluation of the suitability of an assumed local scattering strength function in the analysis of experimental results; and (3) formulation of an inverse problem to estimate local scattering strength from experimentally derived global scattering properties. In addition to building an intuition regarding the relationship between local and global scattering properties, two interesting conclusions can be derived from examples presented in this paper. First, the highly diffuse $\sin \theta_L$ model for local scattering strength appears to be a special case: $\sin \theta_L$ local scattering strength produced sin θ_G mean global scattering strength. Second, the Lambertian local scattering strength model ($\sin^2\theta_L$) did not produce Lambertian global scattering strength. In fact, none of the simple local scattering strength models used here resulted in a global scattering strength model which compared favorably with the Lambertian model. This implies that Lambert's Law, as it may apply to global scattering strength, is not a simplistic phenomenon; i.e., it will take a more complex local scattering function than those considered here to produce the seemingly simple $\sin^2 \theta_G$ relationship at the global scale.

Supported by: ONR Contract N00014-90-J-1584.

WHOI Contribution No. 8218.

MONOSTATIC SHADOWING OF HOMOGENEOUS FRACTAL PROFILES

John A. Goff

The effect of shadowing on the probability density of illuminated slopes is investigated for a class of homogeneous fractal profiles. Unlike smoother surfaces, the shadowing of slopes for a fractal surface will depend strongly on the horizontal scale over which slopes are determined. Under the approach taken, the analytic solution is difficult to solve, if not intractable. However, this approach gives rise to an approximate form to the solution which is dependent on a single parameter

 α . It is found that for a large range in surface morphology an α can always be found which yields a satisfactory fit to numerical solutions of the shadowing problem. An analytic form for α is proposed whose coefficients, dependent on morphological parameters and the grazing angle, are determined by an inversion of empirical fits to the numerical solution. This analytic form successfully predicts α to within 18% of its numerically determined value, which is likely accurate enough for most acoustic backscatter applications.

Published in: Journal of the Acoustical Society of America, 92(2), pt. 1:1008-1016, 1992.

Supported by: ONR Contract N00014-92-J-1214.

WHOI Contribution No. 8026.

PALEOCEANOGRAPHY

FORAMINIFERAL PRODUCTION AND MONSOONAL UPWELLING IN THE ARABIAN SEA: EVIDENCE FROM SEDIMENT TRAPS

W. B. Curry, D. R. Ostermann, M. V. S. Guptha and V. Ittekkot

Planktonic foraminifera collected in sediment traps in the Arabian Sea during 1986 and 1987 responded to the southern Asian monsoon with changes in productivity, relative abundance of species and isotopic shell chemistry. Most species of foraminifera increased in flux shortly after the advent of the southwest monsoon. G. bulloides increased its production rate by three orders of magnitude. The isotopic chemistry of G. ruber recorded the increase in monsoon upwelling by increasing its δ^{13} O values by about $1^{\circ}/_{\infty}$ accurately reflecting the average 4°C sea surface temperature decrease associated with the upwelling. The mean value of δ^{18} O for G. ruber was greater in the western Arabian Sea than in the central or eastern basins because upwelling in that region cools surface water. The carbon isotopic composition of G. ruber does not have a clear temporal or geographic relationship to upwelling. While its $\delta^{13}\mathrm{C}$ values decreased in the western Arabian Sea during the upwelling event, the mean δ^{13} C values remained higher in the western than in the eastern and central Arabian Sea. This longitudinal gradient is opposite to that expected from the geographic gradient of upwelling: the region with the most intense upwelling should have lower δ^{13} C values in surface waters because of the upwelling of low- δ^{13} C water to the surface.

Published in: Upwelling Systems: Evolution Since the Early Mioocene, C.P. Summerhayes, W.L. Prell and K.C. Emeis, eds. Geological Society of London, Special Publication, 64:93-106, 1992.

Supported by: NSF Grant ATM-9115619.

WHOI Contribution No. 7975.

ASSESSING THE COMPLETENESS OF THE DEGLACIAL-MARINE STRATIGRAPHIC RECORD ON WEST SPITSBERGEN BY ACCELERATOR MASS SPECTROMETRY RADIOCARBON DATING: IMPLICATIONS FOR CORRELATION TO DEEP-SEA RECORDS

Steven L. Forman, Scott J. Lehman and William Briggs

The record of Quaternary glaciations of coastal areas is frequently preserved as a raised deglacial-emergence sequence. Detailed radiocarbon dating of forams and marine macro-fossils from a representative deglacial sequence on west Spitsbergen document two periods of sedimentation at ca. 11,400 yr B.P. and at 9,500 yr B.P. that together, span <500 years. The incompleteness of this record (<25%), the highly episodic nature of sedimentation, the dominance of local glacial and environmental effects and the presence of allochthonous forams precludes confident correlation of the raised-marine stratigraphy to more complete records from the deep sea. The late Weichselian and older deglacial sequences on west Spitsbergen have a similar sedimentologic succession. Thus, one possibility is that older raised-marine deglacial sequences on Svalbard and other Arctic areas may represent similar brief intervals confounding correlations across the Arctic and with well established events (i.e. Eemian Interglacial) at lower latitudes.

Published in: Geology.

Supported by: NSF Grants DPP-8813875 and OCE-9019660.

WHOI Contribution No. 7930.

MID-DEPTH CIRCULATION OF THE SUBPOLAR NORTH ATLANTIC DURING THE LAST GLACIAL MAXIMUM

D. W. Oppo and S. J. Lehman

Holocene and glacial carbon isotope data of benthic foraminifera from shallow to mid-depth cores from the northeastern subpolar Atlantic show that this region was strongly stratified, with carbon-13-enriched glacial North Atlantic intermediate water (GNAIW) overlying carbon-13-depleted Southern Ocean water (SOW). The data suggest that GNAIW originated north of the polar front and define GNAIW end-member carbon isotope values for studies of water-mass mixing in the open Atlantic. Identical carbon isotope values in the core of GNAIW and below the subtropical thermocline are consistent with rapid cycling of GNAIW through the northern Atlantic. The high carbon isotope values below the thermocline indicate that enhanced nutrient leakage in response to increased ventilation may have extended into intermediate waters. Geochemical box models show that the atmospheric carbon dioxide response to nutrient leakage that results from an increase in ventilation rate may be greater than the response to nutrient redistribution by conversion of North Atlantic deep water into GNAIW. These results underscore the potential role of Atlantic Ocean circulation changes in influencing past atmospheric carbon dioxide values.

Published in: Science, 259:1148-1150, 1993.
Supported by: NSF Grant OCE-91625900.

WHOI Contribution No. 8151.

ENHANCED VENTILATION OF THE NORTH ATLANTIC SUBTROPICAL GYRE THERMOCLINE DURING THE LAST GLACIATION

Niall C. Slowey, and William B. Curry

Although studies have shown that the ocean's intermediate and deep circulation changed from the last glaciation to today, the history of the subtropical gyres has remained a mystery. Variations of gyre processes and global climate should be intimately linked because gyre circulation is driven by air-sea interactions and directly reflects the climate at the ocean's surface. The gyres are also a significant reservoir of carbon and nutrients, and gyre processes affect the distribution of nutrients and carbon within the oceans and so atmospheric CO2. Here we use Bahamian for a miniferal δ^{13} C and δ^{18} O values to produce the first detailed reconstruction of glacial thermocline nutrient and temperature profiles. These data show that thermocline waters of the glacial North Atlantic subtropical gyre lacked the oxygen minimum which is characteristic of the modern ocean and were depleted of nutrients, indicating greater, more uniform thermocline ventilation at that time. Therefore not only intermediate-depth waters but the entire upper water column within the glacial North Atlantic

was depleted of nutrients. Moreover, glacial thermocline waters were cooler, had a greater temperature gradient and a shallower base. Both thermocline ventilation and thermal structure during the last glaciation are in accord with glacial climate.

Published in: Nature, 358(6388):665-668, 1992.

Supported by: NSF Grants OCE-8813307 and OCE-9102438.

WHOI Contribution No. 8066.

PALEONTOLOGY

CRETACEOUS RADIOLARIA FROM THE ONTONG-JAVA PLATEAU, WESTERN PACIFIC: HOLES 803D AND 807C OF ODP LEG 130

Kozo Takahashi and Hsin Yi Ling

Among the five drilled sites of ODP Leg 130, two deep holes, 803D and 807C, penetrated through Cretaceous sediments overlying the basaltic pillows, flows, and possibly basement rocks. Although abundant, but poorly preserved, radiolarians with limited diversity were recovered from a few horizons within the sediments proximal to the basalt, they are age diagnostic and provided useful information to the geology of the equatorial western Pacific. At Hole 803D, four thin layers of radiolarites interbedded with claystone and clayey siltstone yielded radiolarian assemblages of the late Albian age. Layers of limestone below claystone and siltstone were recovered at Hole 807C, which contain Aptian radiolarian fauna. The radiolarian ages for these two holes are in accord with those from planktonic foraminiferal and paleomagnetic considerations.

In Press: Proceedings of the Ocean Drilling Program
Leg 130 Scientific Results, Volume 30:93-102,
1992.

Supported by: Ocean Drilling Program.

WHOI Contribution No. 7960.

PETROLOGY

THE PLUTONIC FOUNDATION OF A SLOW-SPREADING RIDGE

Henry J. B. Dick, all Robinson and Peter S. Meyer

Hole 735B drilled 500 m of gabbroic layer 3 at the SW Indian Ridge. The section consists of small intrusions with no evidence for a large steady-state magma chamber. The complex stratigraphy represents multiple phases of magmatism, alteration, and ongoing deformation in the zone of lithospheric necking and crustal accretion beneath a slow spreading ocean ridge. Magma evolution was by fractional crystallization of intercumulus melt in crystal mush, by melt-rock reaction and wall rock assimilation as batches of melt migrated upward through the crust. The major form of igneous layering, undeformed olivine gabbro cut by numerous layers of sheared ferrogabbro, formed by synkinematic differentiation in deforming partially molten gabbro. This process drove late intercumulus melt into shear zones, where reaction, crystallization, oxide precipitation and melt trapping transformed the rock to ferrogabbro.

The section underwent extensive brittle-ductile deformation, with shear zones forming while the section was still partially molten, under anhydrous granulite conditions, and at higher water-rock ratios in the amphibolite facies. The shear zones extensively controlled both magmatic and subsolidus fluid flow and alteration. Alteration and circulation of seawater was tectonically enhanced, with extension and lithospheric necking superimposed on the dilational thermal stress available for cracking resulting in high

permeabilities.

Alteration decreased abruptly in mid-amphibolite facies with the end of brittle-ductile deformation as the section was transferred into the rift valley wall and the zone of block uplift. Alteration conditions then closely resembled those of the statically cooled Skaergaard Intrusion, with diopside replacing amphibole as the principal mafic hydrothermal vein mineral. This is attributed to low permeability and more reacted fluid with cracking driven only by thermal dilation during static cooling.

Late trondhjemite veins formed by fractional crystallization and by wall rock anatexis of amphibolites during reintrusion of the section. This provides direct evidence that the section underwent multiple alteration and magmatic events as magmatism waxed and waned.

Published in: The Indian Ocean: A Synthesis of Results from the Ocean Drilling Program, American Geophysical Union Monograph 70, American Geophysical Union (Washington, D.C.), 1-39, 1992.

Supported by: NSF Grant OCE-9101340. WHOI Contribution No. 8154.

RE-OS ISOTOPE SYSTEMATICS OF HIMU AND EMII OCEANIC ISLAND BASALTS FROM THE SOUTH PACIFIC OCEAN

Erik H. Hauri and Stanley R. Hart

The Re-Os and complementary Sr, Nd and Pb systematics of 24 oceanic island basalts from the islands of Savaii, Tahaa, Rarotonga, Rurutu, Tubuai and Mangaia are investigated. Re concentrations range from 100-1621 ppt (parts per trillion), while Os concentrations vary from 26 to 750 ppt. The Re and Os concentration variations suggest that fractionation and accumulation of olivine, or a low Re/Os phase in conjunction with olivine, is important in determining the Os concentration and the Re/Os ratio of the erupted basalt.

¹⁸⁷Os/¹⁸⁶Os in EMII basalts from Samoa and Tahaa varies from 1.0261 to 1.1275. These ratios are mostly within estimates for depleted upper mantle, and do not constrain the involvement of recycled continental crust in the origin of the EMII signature. ¹⁸⁷Os/¹⁸⁶Os ratios in HIMU basalts from Rurutu, Tubuai and Mangaia range from 1.1159 to 1.2473, and provide strong evidence for the role of subducted oceanic crust in the HIMU source. The Pb-Pb systematics constrain the range of possible ages, ²³⁸U/²⁰⁴Pb, and Th/U ratios of the subducted crust; this crust is estimated to pass through the subduction zone with Rb/Sr, Sm/Nd, Lu/Hf and Th/U ratios similar to fresh MORB. The homogeneity of the Os isotopic compositions in the Tubuai and Mangaia basalts indicates that interaction of these basalts with low ¹⁸⁷Os/¹⁸⁶Os mantle had an insignificant effect on the Os isotopic composition of the erupted magmas. This requires a network of channels, veins or cracks capable of delivering melt from the source region (plume) to the surface fast enough to avoid interaction with the depleted upper mantle and the oceanic lithosphere.

The possible identification of the HIMU signature (high ²⁰⁶Pb/²⁰⁴Pb, low ⁸⁷Sr/⁸⁶Sr) with recycled oceanic crust suggests the possible presence of segments of recycled crust, with independent histories, in other oceanic mantle sources, including that of some mid-ocean ridge basalts.

In Press: Earth and Planetary Science Letters, 114:353-371, 1993.

Supported by: NSF Grant EAR-8708372. WHOI Contribution No. 8225.

SEDIMENTOLOGY

ANNUAL BIOGENIC PARTICLE FLUXES TO THE INTERIOR OF THE NORTH ATLANTIC OCEAN; STUDIED AT 34°N 21°W AND 48°N 21°W

Susumu Honjo and Stephen J. Manganini

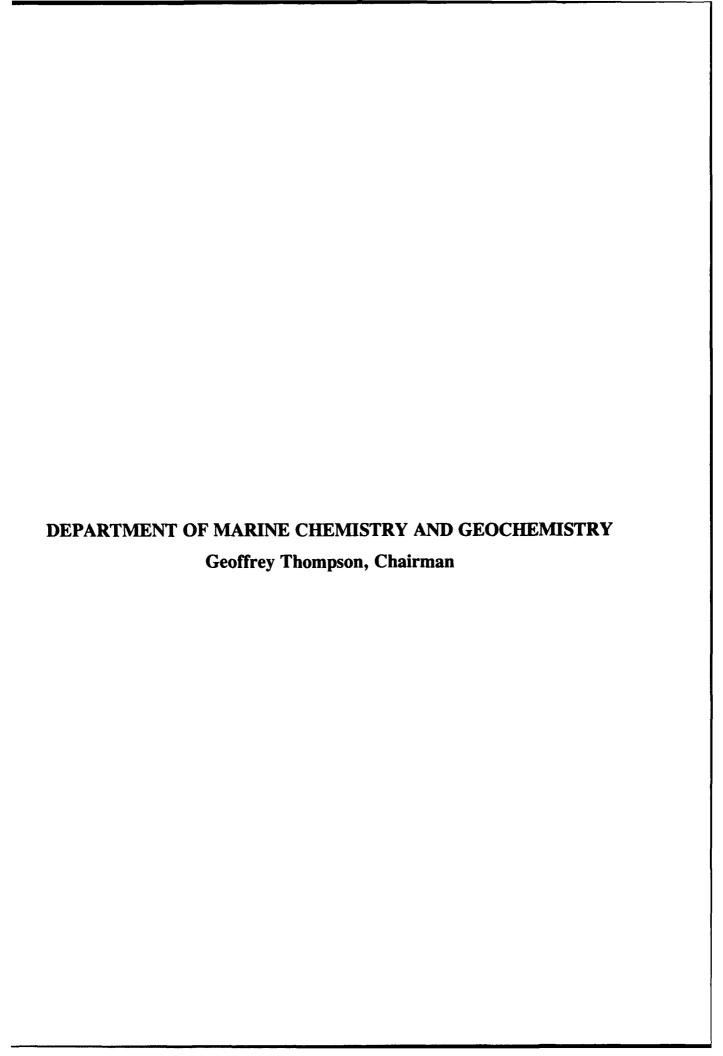
In order to clarify the annual quality, quantity and export process of biogenic particles from the euphotic zone to the deep ocean interior, an array of automated time-series sediment traps were deployed for 1 year from April 4, 1989 to April 17, 1990 at 34°N 21°W and 48°N 21°W as a part of JGOFS' North Atlantic Bloom Experiment (NABE). Three sediment traps with 13 time-series sediment collectors were placed at both stations approximately 1 km and 2 km below the surface and 0.7 km above the bottom. They collected settling particles during twenty-six 14-day intervals for 376 days with an 20-day hiatus in September/October 1989 for changeover of the trap moorings. The collection periods of the six traps were synchronized, forming a spatio-temporal matrix of 156 samples. The annual mass flux at about 2 km deep during this experiment was 22 and 27 g m⁻² yr⁻¹ at the 34°N and 48°N stations, consisting of biogenic particles with traceable quantities of lithogenic particle flux. The spring particle bloom, characterized by the sedimentation of particles relatively enriched by Norg, began in January at the 34°N station and in March at the 48°N station. The bloom continued for 4.5 and 3 months and provided 62 and 50% of the annual biogenic particle mass flux at 2 km at the 34 and 48°N stations. The surface bloom penetrated to the ocean interior within a few weeks, with apparently accelerated settling speed at deeper layers. The order of susceptibility of biogenic elements to mineralization while settling in the 1-0.7 km a.b. water column was, from least to most resistant: P, N_{org}, org, Si and Ca. The C/N/P ratio at 0.7 km a.b. was 154: 18: 1 at the 34°N station and 148: 18: 1 at the 48°N station.

Published in: Deep-Sea Research, 40(1/2):587-607, 1993.

Supported by: NSF Grant OCE-8814228.

WHOI Contribution No. 7961.

GG-20



BIOGEOCHEMISTRY

SEDIMENTARY NITROGEN ISOTOPIC RATIO RECORDS SURFACE OCEAN NITRATE UTILIZATION

Mark A. Altabet and Roger Francois

In two contrasting regions of the ocean, the equatorial Pacific and the Southern Ocean, the δ^{15} N of core top sediments were strongly related to [NO₃] in surface waters. In the equatorial Pacific along 135°W longitude, surface [NO3] decreases poleward from about 5 to 0 µmol/kg and underlying core top δ^{15} N increases from 7 to $16^{\circ}/_{\infty}$. In the southeast Indian Ocean between 60° and 30°S latitude, [NO₃] decreases from 25 to 0 μ mol/kg and core top δ^{15} N increases from 5 to 11°/∞. These results are consistent with water column and laboratory observations of substantial isotopic fractionation in the utilization of NO₃ by phytoplankton. Our observations indicate that the surface water relationship of increased $\delta^{15}N$ with increased NO3 utilization is transmitted to and preserved in the sediments. Sedimentary $\delta^{15}N$ can thus be used as recorder of past changes in surface NO₃ utilization; an important parameter for understanding changes in ocean biogeochemistry over geologic time. The quantitative relationship between surface [NO₃] and core top δ^{15} N appears damped relative to expectations in the equatorial Pacific, but this observation can be accounted for by a number of mechanisms. This and the diagenetic processes that appear to elevate sediment $\delta^{15}N$ relative to sinking particulate nitrogen require further study.

Supported by: NSF Grant OCE-9115641.

WHOI Contribution No. 7941.

INDICATORS OF SEWAGE CONTAMINATION IN SEDIMENTS BENEATH A DEEP-OCEAN DUMP SITE OFF NEW YORK

M. H. Bothner, H. Takada, I. T. Knight, R. T. Hill, B. Butman, J. W. Farrington, R. R. Colwell, and J. F. Grassle

The world's largest discharge of municipal sewage sludge to the surface waters of the deep sea has caused measurable changes in the concentration of sludge indicators in sea-floor sediments. Silver, linear alkylbenzenes, coprostanol, and spores of the bacterium Clostridium perfringens, in bottom sediments and in near-bottom suspended sediment, provide evidence for rapid settling of a portion of

discharged solids, accumulation on the sea floor, and biological mixing beneath the water-sediment interface. Biological effects include an increase in 1989 of two species of benthic polychaete worm not abundant at the dump site before sludge dumping began in 1986. These changes in benthic ecology are attributed to the increased deposition of utilizable food in the form of sludge-derived organic matter.

In Press: Marine Environmental Research.
Supported by: NOAA's NURP Program.
WHOI Contribution No. 7995.

THORIUM ISOTOPES AS INDICATORS OF PARTICLE DYNAMICS IN THE UPPER OCEAN: RESULTS FROM THE JGOFS NORTH ATLANTIC BLOOM EXPERIMENT

J. Kirk Cochran, Ken O. Buesseler, Michael P. Bacon, and Hugh D. Livingston

Measurements of ²³⁴Th and ²²⁸Th in suspended and sinking particles made during the 1989 JGOFS North Atlantic Bloom Experiment permit estimation of the rates of particle cycling. Using a simple model of thorium-particle interactions applied to water column and floating sediment trap data at 150 and 300 m, the rate constant, β_2 , for aggregation of small suspended particles into large rapidly sinking (~150 m/d) particles increases from ~ 0 to ~ 30 y⁻¹ over the course of the bloom. The rate constant for disaggregation of sinking particles, β_{-2} , similarly increases from ~100 to ~300 y⁻¹ over the same period. These values suggest that small particle residence times (relative to packaging or aggregation) decrease to ~15 days and that large particle residence times (relative to disaggregation) decrease to ~ 1 day as the bloom progresses. Late in the bloom, particles are cycled such that aggregation of suspended particles ($\sim 2 \mu g/l/d$) is comparable to particle break-up ($\sim 3 \mu g/1/d$). Errors on the rate constants, calculated by propagating estimated errors on the individual terms in the model, are large and arise principally from uncertainty in the gradient in activity and mass fluxes between the two trap depths. However, the values calculated independently from the two tracers (234Th and 228Th) generally agree to within 30%. The ²³⁴Th balance for the upper water column (Buesseler et al., 1992) suggests that a substantial portion of the thorium and mass flux is not recorded by the traps. If it is assumed that this flux is carried on more slowly sinking particles $(\sim 50 \text{ m/d})$ that are not trapped efficiently, and these particles directly interact with the suspended particles pool in the same fashion as the trapped

sinking particles, calculation of aggregaton and disaggregation rate constants late in the bloom shows a higher value for β_2 but a comparable value for β_{-2} relative to the values determined for the trapped particles. This suggests that the slowly sinking material (e.g. marine snow) is more effective at aggregating small, suspended particles than are the rapidly sinking particles. Temporal increases in β_2 and β_{-2} for the trapped particles are matched by increases in the rate constants for decomposition of particulate organic carbon and nitrogen (3 to 35 y⁻¹ for C; 5 to 40 y⁻¹ for N), suggesting that increases in microbial activity are directly reflected in rates of particle aggregation and disaggregation.

In Press: Deep-Sea Research.

Supported by: NSF Grants OCE-8817836 and OCE-9016494 to WHOI and OCE-8818544 and OCE-9016832 to SUNY.

WHOI Contribution No. 8202.

CYCLING OF DISSOLVED AND PARTICULATE ORGANIC MATTER IN THE OPEN OCEAN

Ellen R. M. Druffel, Peter M. Williams, James E. Bauer, and John R. Ertel

Radiocarbon (Δ^{14} C), δ^{13} C, bulk carbon and organic constituent concentration measurements are presented for dissolved and particulate carbon pools from the North Central Pacific Ocean (NCP) and the Sargasso Sea (SS). We operationally define three overlapping pools of dissolved organic carbon (DOC): (1) DOC that is oxidizable by UV radiation (DOC_{uv}); (2) "extra" DOC measured by Co/CoO flow-through high-temperature catalytic oxidation (DOC_{Ft-htc}), which also has low Δ^{14} C values like DOC_{uv} (Bauer et al., 1992a); and (3) a potential residual DOC fraction that is the difference between DOC measured by discrete-injection high-temperature catalytic oxidation (DOC_{htc}) and DOC_{Ft-htc}, and which has unknown Δ^{14} C signature. The distribution of a large fraction of DOC appears to be controlled by circulation of deep ocean waters between major oceans. The DOC in the SS is slightly younger than would be expected if circulation was the sole process controlling DOC cycling. We propose that there is more bomb ¹⁴C in the deep SS DOC to account for this difference. The Δ^{14} C values of suspended, and to a lesser extent sinking particulate organic carbon (POC), decrease with depth, with the suspended POC displaying a much steeper gradient in the SS than in the NCP. These data reflect the incorporation of low-activity organic matter into the POC pool, possibly through incorporation of DOC by physical adsorption and/or biological heterotrophy.

Published in: Journal of Geophysical Research, 97(C10):15,639-15,659, 1992.

Supported by: NSF Grants OCE-8416632, OCE-8716590 and OCE-9101183.

WHOI Contribution No. 8239.

CHANGES IN THE δ^{13} C OF SURFACE WATER PARTICULATE ORGANIC MATTER ACROSS THE SUBTROPICAL CONVERGENCE IN THE S.W. INDIAN OCEAN

Roger Francois, Mark A. Altabet, Ralf Goericke, Daniel C. McCorkle, Christian Brunet, and Alain Poisson

We have measured the carbon isotopic composition of particulate organic matter suspended in surface waters (POM) between 59°S and 30°S in the SW Indian ocean during austral summer. In an attempt to further document the pattern of covariance between POC-δ¹³C and [CO_{2aq}], we concurrently measured surface water pCO₂, temperature, salinity, nitrate concentration, POM concentration, chlorophyll-a and the δ^{13} C of total dissolved inorganic carbon. We found the previously reported negative correlation between POC- δ^{13} C and [CO_{2aq}]. In addition to this general trend, however, we report a prominent maximum in POC- δ^{13} C in the region immediately north of the Subtropical Convergence, which also coincides with a maximum in [POM] and a minimum in pCO₂. The increase in POC-δ¹³C between 50°S and the Subtropical Convergence is consistent with the trend expected if [CO2aq] were the main factor controlling the isotopic composition of POM. In contrast, data from the region north of the subtropical Convergence clearly illustrate that POC-δ¹³C can also very independently of [CO_{2aq}], as a 5 per mil decrease in POC- δ^{13} C was found in a region characterized by nearly constant [CO_{2aq}]. We review several physiological factors which may account for these observations and discuss their implications for paleoceanographic reconstruction of [CO_{2aq}] from the carbon isotopic composition of sedimentary organic matter.

Supported by: NSF Grant DPP-9118031.

WHOI Contribution No. 8237.

DYNAMICS OF THE TRANSITION ZONE IN CZCS-SENSED OCEAN COLOR IN THE NORTH PACIFIC DURING OCEANOGRAPHIC SPRING

David M. Glover, J. S. Wroblewski, and Charles R. McClain

A transition zone in phytoplankton concentration running across the North Pacific basin at 30° to 40° north latitude corresponds to a basin wide front in surface chlorophyll observed in a composite of Coastal Zone Color Scanner images for May, June and July 1979-1986. This transition zone with low chlorophyll to the south and higher chlorophyll to the north can be simulated by a simple model of the concentration of phytoplankton, zooplankton and dissolved nutrient (nitrate) in the surface mixed layer of the ocean applied to the North Pacific basin for the climatological conditions during oceanographic springtime (May, June and July). The model is initialized with a 1° × 1° gridded estimate of wintertime (February, March and April) mixed layer nitrate concentrations calculated from an extensive nutrient database and a similarly gridded mixed layer depth data set. Comparison of model predictions with CZCS data provides a means to evaluate the dynamics of the transition zone. We conclude that in the North Pacific, away from major boundary currents and coastal upwelling zones, wintertime vertical mixing determines the total nutrient available to the plankton ecosystem in the spring. The transition zone seen in basin-scale CZCS images is a reflection of the geographic variation in the wintertime mixed layer depth and the nitracline, leading to a latitudinal gradient in phytoplankton chlorophyll.

Supported by: NSF Grants OCE-8701461 and OCE-8811375, and NASA Grants NAGW-1314 and NAGW-2431.

WHOI Contribution No. 8169.

BIOCHEMICAL PROPERTIES OF THE OCEANIC CARBON CYCLE

Catherine Goyet and Peter G. Brewer

This chapter describes and documents the recent advances in CO₂ measurement technology, and presents current observations and understanding of the ocean response to global warming due to the atmospheric CO₂ increase. For the sake of teaching course integrity, this chapter also includes a summary of the CO₂ chemistry in seawater

Supported by: NSF Grant OCE-871461. WIIOI Contribution No. 8065.

DISSOLVED ORGANIC CARBON CONCENTRATIONS IN MARINE PORE WATERS DETERMINED BY HIGH-TEMPERATURE OXIDATION

William R. Martin and Daniel C. McCorkle

We have developed sampling methods and an analytical system to determine the concentration of dissolved organic carbon in marine pore waters. Our analytical approach modifies the high-temperature, platinum catalyzed method of Sugimura and Suzuki (1988), by using chromatographic trapping of the DOC-derived CO₂, followed by reduction to CH₄ and flame ionization detection. Sampling experiments using nearshore sediments indicate that pore water separation by whole core squeezing causes artificially elevated DOC concentrations, while pore water recovery by sectioning and centrifugation does not appear to introduce DOC artifacts. Results from a set of northwestern Atlantic continental slope cores suggest that DOC production may account for more than 50% of the organic carbon which is recycled at the sediment-water interface.

Supported by: NSF Grants OCE-8900105, OCE-9012473 and OCE-9115669.

WHOI Contribution No. 8173.

THE RELATIONSHIP BETWEEN CERIUM AND MANGANESE OXIDATION IN THE MARINE ENVIRONMENT

James W. Moffett

The microbially mediated oxidation of Ce(III) and Mn(II) in surface waters of Vineyard Sound, Massachusetts, has been studied to evaluate the relationship between these two processes under different experimental conditions. Oxidation of Ce(III) and Mn(II) under different conditions of oxygen concentration, pH and concentrations of Mn(II), Ce(III), and Pr(III) was studied using radiotracers as described in Moffett (1990). Results indicate that the two processes are closely related, with the ratio of specific rates being approximately 3:1 over a wide range of absolute rates and environments. They show similar trends in oxygen dependence. Ce(III) oxidation is inhibited by Mn(II), and Mn(II) oxidation is inhibited by Ce(III) and Pr(III). The data indicate that both elements are processed by the same enzymatic pathway. The implications of this study for the geochemistry of Ce, the interpretation of Ce anomalies and the role of manganese oxides in trace metal scavenging is discussed.

Supported by: NSF Grants OCE-8817401. WHOI Contribution No. 8228.

KINETICS OF THE REMOVAL OF DISSOLVED ALUMINUM BY DIATOMS IN SEAWATER: A COMPARISON WITH THORIUM

S. B. Moran and R. M. Moore

Kinetic experiments were conducted using batch systems to investigate the removal of dissolved Al and ²³⁴Th tracer by dead Phaeodactulum tricornutum diatoms in seawater. Experiments were conducted at constant temperature (2°C), pH (7.8), and salinity (30 psu), using realistic oceanic concentrations of dissolved Al (50 nM), and 1, 2.5, 5, and 10 mg/L suspensions of dead diatoms in ultrafiltered (<10,000 NMW) seawater. Results are characterized by a rapid initial removal followed by slower sorption of dissolved Al and ²³⁴Th by the diatoms on time-scales ranging from hours to days. Both the removal rate and the percentage of Al and ²³⁴Th removed are strong functions of the particle concentration (C_p) . Modelling the kinetic data as a reversible exchange of metal between solution and particles indicates a first-order dependence of the forward rate constants for Al and ²³⁴Th on C_p. Extending these results to oceanic scavenging, it is shown that a first-order dependence exists between oceanic scavening rate constants for Al and Th and suspended particle concentration for $C_p \sim 0.01-1$ mg/L. This relationship is suggested to reflect the importance of physicochemical removal mechanisms (surface-adsorption, coagulation/sedimentation) rather than active biological uptake of dissolved Al and Th in oceanic waters. Oceanic scavenging rate constants for Al and Th qualitatively agree with removal rate constants predicted by the Brownian-pumping model for reactive metal scavenging.

Published in: Geochimica et Cosmochimica Acta, 56:3365-3374, 1992.

Supported by: WHOI and NSERC of Canada Postdoctoral Fellowships.

WHOI Contribution No. 8081.

SHORT RESIDENCE TIME OF COLLOIDS IN THE UPPER OCEAN ESTIMATED FROM ²³⁸U/²³⁴TH DISEQUILIBRIA

S. Bradley Moran and Ken O. Buesseler

Recent observations of abundant, non-living, sub-micrometre particles in the upper ocean and

new measurements of "dissolved" organic carbon have fuelled speculation concerning the role of colloidal matter in ocean chemistry and biology. Colloids may act as reactive intermediates in the marine geochemistry of trace metals, and a biologically labile pool of colloidal matter would affect contemporary models of ocean carbon cycling. Here we report the use of naturally occurring 234 Th as an in situ tracer to estimate the residence time of colloidal matter in the surface waters near Bermuda. The 234Th activity of colloidal matter (size range 10,000 nominal molecular weight to $0.2 \mu m$) is similar to that of small particles (0.2-53 μ m). Modelling of our results indicates a mean residence time of colloidal ²³⁴Th with respect to aggregation into small particles of 10 days, which is approximately the same as for small particle 234 Th, yet a factor of ~ 6 less than for the dissolved pool. These results suggest that, more generally, macromolecular colloidal matter has a short residence time and hence a rapid turnover rate in the upper open ocean.

Published in: Nature, 359(6392):221-223, 1992.

Supported by: WHOI and NSERC of Canada Postdoctoral Scholarships, NSF Grant OCE-8915760, NOAA Sea Grant NA90-AA-D-SG480, WHOI Coastal Research Center Grant 250003.13.

WHOI Contribution No. 8120

THE RELATIONSHIP BETWEEN δ^{13} C OF ORGANIC MATTER AND [CO₂(AQ)] IN OCEAN SURFACE WATER: DATA FROM A JGOFS SITE IN THE NORTHEAST ATLANTIC OCEAN AND A MODEL

G. H. Rau, T. Takahashi, D. J. Des Marais, D. J. Repeta, and J. H. Martin

The δ^{13} C of suspended particulate organic matter (SPOM) in surface waters increased from -22.9 to -18.1% during April 25-May 31, 1989 at the JGOFS North Atlantic Bloom Experiment Site (NABE Site; 47°N, 20°W). During the same period, nearly parallel increases in sinking POM δ^{13} C were also found, although these values were usually lower than those of the corresponding SPOM. Consistent with the hypothesis that plankton δ^{13} C and [CO₂(aq)] are inversely related. the increases in both sinking and suspended POM δ^{13} C were highly negatively correlated with mixed-layer [CO2(aq)] that generally decreased from 13.2–10.1 μ moles/kg during the five weeks. The change in SPOM δ^{13} C per change in [CO₂(aq)], however, appears to be somewhat greater than that expected from previous, though less direct, ocean and laboratory evidence. By

adapting a model of plant δ^{13} C by Farquhar et al. (1982), it is shown that under a constant phytoplankton demand for CO2 an inverse, nonlinear SPOM δ^{13} C response to ambient [CO₂(aq)] is expected. Such trends are unlike the negative linear relationships indicated by data from the NABE Site and/or f-om Southern Hemisphere waters. Such differences between predicted and observed SPOM δ^{13} C vs. [CO₂(aq)] trends and among observed relationships can be reconciled, however, if biological CO2 demand is allow to vary. This has significant implications for the use of the $\delta^{13}\mathrm{C}$ of plankton (or their organic subfractions or sedimentary remains) as a proxy for past or present ocean CO₂ concentrations and biological productivity.

Published in: Geochimica et Cosmochimica Acta, 56:1413-1419, 1992.

Supported by: NSF Grant OCE-8814920.

WHOI Contribution No. 8063.

IMPROVED HPLC METHOD FOR THE ANALYSIS OF CHLOROPHYLLS AND CAROTENOIDS FROM MARINE PHYTOPLANKTON

S. W. Wright, S. W. Jeffrey, R. F. C. Mantoura, C. A. Llewellyn, T. Bjørnland, D. Repeta, and N. Welschmeyer

Using a ternary gradient system, over 50 carotenoids, chlorophylls and their derivatives were separated from marine phytoplankton. Only 2 pairs of carotenoid pigments (19'-butanoyloxy-fucoxanthin and siphonaxanthin, and 19'-hexanoyloxyfucoxanthin and 9'-cis-neoxanthin) and 3 chlorophylls (chlorophylls C_1 , C_2 , and Mg2,4 divinyl pheoporphyrin a_5 monomethyl ester [Mg2,4D]) were not resolved. Pigment chromatograms are presented for 12 unialgal cultures from 10 algal classes important in the marine environment: Amphidinium carterae Hulbert (Dinophyceae); Chroomaonas salina (Wislouch) Butcher (Cryptophyceae); Dunaliella tertiolecta Butcher (Chlorophyceae); Emiliania huxleyi (Lohmann) Hay et Mohler and Pavlova lutheri (Droop) Green (Prymnesiophyceae); Euglena gracilis Klebs (Euglenophyceae); Micromonas pulsilla (Butcher) Manton et Parke and Pucnococcus provasolii Guillard (Prasinophyceae); Pelagococcus subviridis Norris (Chrysophyceae); Phaeodactylum tricornutum Bohlin (Bacillariophyceae); Porphyridium cruentum (Bory) Drew et Ross (Rhodophyceae), and Synechococcus sp. (Cyanophyceae). A chromatogram is also given of a complex mixture of over 50 algal pigments such as might be found in a phytoplankton field sample. This method is useful

for analysis of phytoplankton pigments in seawater samples and other instances where separations of complex pigment mixtures are required.

Published in: Marine Ecology Progress Series, 77:183-196, 1991.

Supported by: NSF Grant OCE-8814920 WHOI Contribution No. 8075.

ORGANIC GEOCHEMISTRY

ASPARTIC ACID RACEMIZATION AND PROTEIN DIAGENESIS IN CORALS OVER THE LAST 350 YEARS

Glenn A. Goodfriend, P. E. Hare, and Ellen R. M. Druffel

D/L aspartic acid values from a 350-year time series of annual growth bands of a living colony of the coral Porites australiensis show a very regular pattern of increase with age. The initial rate of racemization is extraordinarily rapid (0.6% per year) but slows in older growth bands to 0.04% per year (4% per century). The skeletal proteins show progressive hydrolysis with increasing age, with free aspartic acid comprising 16% of the total aspartic acid in the 350-year-old band. The proteins are unusually rich in aspartic acid (nearly 50 mol%). The relative weakness of the peptide bonds formed by aspartic acid moieties is probably responsible for the rapid hydrolysis and consequent rapid racemization of aspartic acid. Racemization analysis provides a means of checking for sections of missing bands in corals and for screening of prospective samples for U-Th dating.

Published in: Geochimica et Cosmochimica Acta, 56:3857-3850, 1992.

Supported by: NSF Grant OCE-8915919.

WHOI Contribution No. 8240.

QUANTIFYING EARLY DIAGENESIS OF FATTY ACIDS IN A RAPIDLY ACCUMULATING COASTAL MARINE SEDIMENT

Robert I. Haddad, Christopher S. Martens, and John W. Farrington

We report here the results of a quantitative study designed to (i) evaluate the rates of early diagenesis of unbound fatty acids in an organic-rich, coastal marine sediment and (ii) address the relative importance of incorporation of baterial biomass within the sedimentary organic

matter surviving microbially mediated early diagenesis. Radiochronometric tracer studies at the sampling site, Cape Lookout Bight, N.C., U.S.A., prove that sediment accumulation has occurred at a constant rate of 10.3±1.7 cm yr⁻¹ since at least 1971. Higher plant and labile plankton-derived organic materials driving early diagenesis appear to have accumulated at constant annual rates since at least the mid 1970s. Change in the unbound fatty acid concentrations are thus known to result primarily from diagenetic processes. While these data cannot discriminate between the diagenetic processes of (a) complete remineralization and (b) incorporation into a "non-extractable" bound fatty acid fraction, it is nonetheless significant that the measured decrease could account for as much as 8.2% of the production $\sum CO_2$ and CH_4 at this site (assuming complete remineralization to these end products). These results also indicate the following reactivity relationships: unsaturated fatty acids > branched fatty acids > saturated fatty acids. Furthermore, within the saturated fatty acid fraction, medium chain length compounds (C₁₄-C₁₉) are degraded at "apparent" rates 6-7 times faster than long chain length compounds (C₂₀-C₃₄). Results of kinetic modelling indicate that no simple relationship exists between remineralization rates and molecular weight (or carbon chain length) and suggest that the preferential preservation of terrestrially derived long chain length fatty acids results from their inclusion into microbially inaccessible matrices.

Published in: Organic Geochemistry, 19(1-3):205-216, 1992.

Supported by: NSF Grants OCE-8416963, OCE-8716528, and OCE-8509858.

WHOI Contribution No. 8012.

PRESSURE SEALS—INTERACTIONS WITH ORGANIC MATTER, EXPERIMENTAL OBSERVATIONS. RELATION TO A "HYDROCARBON PLUGGING" HYPOTHESIS FOR PRESSURE SEAL FORMATION

Jean K. Whelan, Lorraine Buxton Eglinton, and Larry Cathles

Organic geochemical characteristics diagnostic of pressure seals have been determined for two wells in the Moore-Sams Field of the Tuscaloosa Trend, Louisiana Gulf Coast (Mix and Bizette wells) and one well penetrating a much weaker pressure transition zone of the Anadarko Basin, Oklahoma (Weaver Well). Preliminary data suggest these characteristics of organic matter in zones of pressure seals: a rapid increase in vitrinite reflectance near the top of the pressure seal;

fractionation of bitumens through the pressure seal with a gradual change from lighter to heavier n-alkanes with increasing depth in the pressure seal; a build up of hydrocarbons just beneath the pressure seal; and an enhancement of asphalt (or asphaltene) throughout the general zone of the pressure seal. For all three wells, very tight associations of carbonate cement, fine pyrite, asphaltenes, and micrinite (generally considered to be a residual product of hydrocarbon generation) were observed in the general zone of pressure seals, suggesting that interactions of organic and inorganic materials may be required for pressure seal formation and maintenance, even in fairly organic lean wells such as Weaver. A rapid increase in thermal maturity, as measured by vitrinite reflectance, occurs through the top of the Mix pressure transition zone reaching levels typical of the gas thermal window, suggesting that gas formation within and below this (seal) zone is contributing both to overpressuring and sealing of pressure seals investigated here. A "hydrocarbon plugging hypothesis" of pressure seal formation is presented which accommodates all of these observations. It is proposed that the pressure drop across the pressure transition zone causes precipitation of oil and asphalt which has been carried to it by an upward streaming gas and that both the gas and the precipitated oil aid in creating pressure seals impermeable enough to survive over geologic time.

Supported by: Gas Research Institute Grants 5088-260-1746 and 5091-260-2298.

WHOI Contribution No. 7984.

$\begin{array}{c} \textit{GEOCHEMISTRY-INORGANIC},\\ \textit{ISOTOPIC} \end{array}$

LARGE VARIATIONS OF SURFACE OCEAN RADIOCARBON: EVIDENCE OF CIRCULATION CHANGES IN THE SW PACIFIC

Ellen R. M. Druffel and Sheila Griffin

The El Niño-Southern Oscillation (ENSO) is the most prominent interannual climate signal. Occurring every few years, it is characterized by increased sea surface temperature (SST) in the central and eastern tropical Pacific, and anomalously low southeast trade winds between the Easter Islands and Darwin, Australia. ENSO years in the southwestern Pacific have historically been marked by periods of drought in Australia and low SST in the North Coral Sea, although long-term oceanic records of such events have not been available. We have measured large

interannual changes of surface ocean ¹⁴C/¹²C during AD 1635-1957 as recorded in annually-banded corals from the southern Great Barrier Reef, Australia. Low ¹⁴C/¹²C coincide with recorded ENSO events, suggesting increased upwelling or advection of ¹⁴C-depleted source waters to this location during ENSO events. During the 17th and early 18th centuries, the coral ¹⁴C/¹²C excursions were larger than those during the 19th and 20th centuries, suggesting a change in the effect of ENSO events on the 14C-cycle at our southwestern Pacific site. No Suess effect (decrease) in ¹⁴C/¹²C levels during the input of 14C-free fossil fuel CO2 in the 20th century) was observed in these corals. We propose these data record changes in oceanic circulation that may be long-term manifestations of the southerly excursions recently observed of the subtropical gyre during ENSO.

In Press: Journal of Geophysical Research.

Supported by: NSF Grants OCE-9015919 and OCE-8715910.

WHOI Contribution No. 8073.

A LARGE DROP IN ATMOSPHERIC ¹⁴C/¹²C AND GREATLY REDUCED GLACIAL MELTING DURING THE YOUNGER DRYAS, DOCUMENTED WITH ²³⁰TH AGES OF CORALS

R. Lawrence Edwards, J. Warren Beck, G. Burr, D. Donahue, J. M. A. Chappell, A. L. Bloom, E. R. M. Druffel, and F. W. Taylor

In order to calibrate part of the ¹⁴C time scale and estimate rates of sea level rise during deglaciation, we determined ¹⁴C and ²³⁰Th ages on fossil corals from the Huon Peninsula, Papua New Guinea. Results show that globally averaged rates of melting may have been high at the beginning of the Younger Dryas (YD), consistent with the idea that the diversion of melt water from the Mississippi to the St. Lawrence River triggered the YD event. During the latter part of the YD and after the YD, the atmospheric ¹⁴C/¹²C ratio dropped by 15%. This prominent drop coincides with greatly reduced rates of sea level rise. Reduction of melt water flux because of cooler conditions during the YD may have caused an increase in ocean ventilation rate, which caused the atmospheric ¹⁴C/¹²C ratio to fall.

In Press: Science.

Supported by: NSF Grant OCE-8915919.

WHOI Contribution No. 8238.

GLACIAL/INTERGLACIAL CHANGES IN SEDIMENT RAIN RATE IN THE S.W. INDIAN SECTOR OF SUBANTARCTIC WATER AS RECORDED BY 230 TH, 231 PA, U AND 615 N

Roger Francois, Michael P. Bacon, Mark A. Altabet, and Laurent D. Labeyrie

High-resolution records of opal, carbonate and terrigenous fluxes have been obtained from a high-sedimentation rate core (MD84-527: 45°50′S; 51°19′E) by normalization to $^{230}\mathrm{Th}$. This method estimates paleofluxes to the seafloor on a point-by-point basis and distinguishes changes in sediment accumulation due to variations in vertical rain rates from changes in syndepositional sediment redistribution by bottom currents. We also measured sediment $\delta^{15}\mathrm{N}$ to evaluate the changes in nitrate utilization in the overlying surface waters associated with paleoflux variations.

Our results show that opal vertical rain rates during the Holocene and stage 3 were much lower than the rates of opal accumulation on the seafloor based on ¹⁴C dating. At this particular location, changes in opal accumulation on the seafloor appear to be mainly controlled by changes in sediment redistribution by bottom currents rather than reflecting variations in opal rain rates from the overlying water column. Correction for syndepositional sediment redistribution and the improved time resolution that can be achieved by normalization to ²³⁰Th disclose important variations in opal rain rates. We found relatively high but variable opal paleoflux during stage 3, with two maxima centered around 36 ky and 30 ky B.P., low opal paleoflux during stage 2 and deglaciation and a pronounced maximum during the early Holocene. We interpret this record as reflecting variations in opal production rates associated with climate-induced latitudinal migration of the Southern Ocean frontal system. Sediments deposited during periods of high opal paleoflux also have high authigenic U concentrations, suggesting more reducing conditions in the sediment, and high Pa-231/Th-230 ratios, suggesting increased scavenging from the water column.

Sediment $\delta^{15}N$ is ca. 1.5 per mil higher during isotopic stage 2 and deglaciation. The low opal rain rates recorded during that period appear to have been associated with increased nitrate depletion. This suggests that opal paleofluxes do not simply reflect latitudinal migration of the frontal system, but also changes in the structure of the upper water column. Increased stratification during isotopic stage 2 could have been produced by a meltwater lid, leading to lower nitrate supply

rates to surface waters.

Supported by: NSF Grant OCE-8922707, DPP-9118031.

WHOI Contribution No. 8201.

METABASALTS FROM THE MID-ATLANTIC RIDGE: NEW INSIGHTS INTO HYDROTHERMAL SYSTEMS IN SLOW SPREADING CRUST

Kathryn M. Gillis and Geoffrey Thompson

An extensive suite of hydrothermally altered rocks has been recovered along the Mid-Atlantic Ridge, south of the Kane Fracture Zone (23°-24°N). This suite was collected by ALVIN and dredging primarily along the western rift valley walls where detachment faulting has provided a window into the crustal component of hydrothermal systems. Rocks of basaltic composition are altered to two assemblages with these characteristics: (i) Type I: albitic plagioclase (An_{02-10}) + mixed-layer smectite/chlorite or chlorite ± actinolite ± quartz ± sphene, <10% of the clinopyroxene is altered, and there is no trace metal mobility; and (ii) Type II: plagioclase (An_{10-30}) + amphibole (actinolite - magnesio-hornblende) + chlorite + sphene, >20% of the clinopyroxene is altered, and Cu and Zn are leached. Although both types include samples with variolitic, intersertal, intergranular, and diabasic textures, intergranular and diabasic textures are most commin in Type II samples. The geochemical signature of these alteration types reflect the relative proportion and composition of secondary minerals, and the degree of alteration of primary phases, and does not show simple predictive relationships. Element mobilities indicate that both alteration types formed at low water/rock ratios.

The MARK assemblages are typical of the greenshist and transition to the amphibolite facies and represent two distinct, albeit overlapping, temperature regimes: Type I - 180° to 300°C and Type II - 300° to >450°C. By analogy with DSDP/ODP Hole 504B and many ophiolites, the MARK metabasalts were altered within the downwelling limb of a hydrothermal cell and Type I and II samples formed in the upper and lower portions of the sheeted dike complex, respectively. The distribution of these types along a south to north transect along the western rift valley wall indicates that deeper crustal levels are exposed toward the ridge-transform intersection. Episodic magmatic and hydrothermal events documented at slow-spreading ridges suggest that these observed mineral assemblages represent the

cumulative effects of more than one hydrothermal event. Groundmass and vein assemblages in the MARK metabasalts indicate wither that alteration conditions did not change during successive hydrothermal events or that these assemblages record only the highest temperature event. Lack of retrograde reactions or overprinting of lower temperature assemblages (e.g., zeolites) suggests that there is a continuum in alteration conditions while crustal segments remain in the ridge environment, prior to uplift and emplacement into the rift valley walls or movement off-axis.

The Type II samples may be representative of the reaction zone where compositions of hydrothermal fluids actively venting at the seafloor today become fixed. This prediction necessitates interaction between hydrothermal fluids and intersertal glass and/or mafic phases, in addition to plagioclase, in order to produce the observed range in vented fluid pH.

In Press: Contribution to Mineralogy and Petrology.

Supported by: NSF Grant OCE-8917352.

WHOI Contribution No. 8142.

COMPARISON OF THE 1991 PCO₂ DISTRIBUTION IN THE EQUATORIAL PACIFIC OCEAN ALONG 150°W WITH THAT MEASURED IN 1979: AN INDICATION OF GLOBAL CHANGE?

Catherine Goyet and Edward T. Peltzer

Measurements of the partial pressure of CO₂ (pCO₂) in surface seawater and marine air along the cruise track of the WOCE leg P-16c from 15°N to 15°S along 150°W) during the period from August 29, 1991 to September 29, 1991, were performed continuously. The automated underway pCO2 system was composed of a small "shower-head" equilibrator and a non-dispersive infra-red analyzer with a cooled lead selenide solid state detector. The observed latitudinal variation of surface pCO2 were typical of a non-ENSO year; with a maximum of 445 μ atm near the equator, this ocean area remains a large source of CO2 gas for the atmosphere. Compared with a data set measured twelve years earlier at these same latitudes along 150°W during another non-ENSO year, these recent results provide new insights into the continuous rise of CO2 gas in the surface ocean due to fossil fuel CO2 invasion.

Supported by: DOE Grant DE-FG02-ER60980, NASA Grant NAGW-2431.

WHOI Contribution No. 8198.

HELIUM ISOTOPE GEOCHEMISTRY OF SOME VOLCANIC ROCKS FROM SAINT HELENA

David W. Graham, Susan E. Humphris, William J. Jenkins and Mark D. Kurz

 3 He/ 4 He ratios have been measured for olivine and clinopyroxene phenocrysts in 7-15 million year old basaltic lavas from the island of St. Helena. Magmatic helium was effectively resolved from post-eruptive radiogenic helium by employing different extraction techniques, including in vacuo crushing, and stepwise heating or fusion of the powders following crushing. The inherited 3 He/ 4 He ratio at St. Helena is 4.3-5.9 R_A. Helium isotope disequilibrium is present within the phenocrysts, with lower 3 He/ 4 He upon heating and fusion of the powders following crushing, duitoradiogenic ingrowth or to α -particle implantation from the surrounding (U+Th)-rich lavas.

A single crushing analysis for clinopyroxene in a basalt from Tubuaii gave ${}^{3}\text{He}/{}^{4}\text{He} = 7.1 \text{ R}_{A}$ ³He/⁴He ratios at St. Helena and Tubuaii (HIMU hotspots characterized by radiogenic Pb isotope signatures are similar to ³He/⁴He ratios previously measured at Tristan da Cunha and Gough Island (EM hotspots characterized by low ²⁰⁶Pb/²⁰⁴Pb). Overall, the He-Sr-Pb isotope systematics at these islands are consistent with a mantle origin as contiguous, heterogeneous materials, such as recycled crust and/or lithosphere. ³He/⁴He ratios at HIMU hotspots are similar to mantle xenoliths which display nearly the entire range of Pb isotope compositions found at ocean islands, and are only slightly less than values found in mid-ocean ridge basalts (7-9 R_A). This suggests that the recycled materials were injected into the mantle within the last 10 y^9 .

Published in: Earth and Planetary Science Letters, 110:121-131, 1992.

Supported by: NSF Grants OCE-8516082, OCE-8812078 and OCE-8911505.

WHOI Contribution No. 7997.

HELIUM ISOTOPE GEOCHEMISTRY OF MID-OCEAN RIDGE BASALTS FROM THE SOUTH ATLANTIC

David W. Graham, William J. Jenkins, Jean-Guy Schilling, Geoffrey Thompson, Mark D. Kurz and Susan E. Humphris

We report new helium isotope results for 49 basalt glass samples from the Mid-Atlantic Ridge between 1°N-47°S. 3 He/ 4 He in South Atlantic MORB varies between 6.5-9.0 R_A (R_A is the atmospheric ratio of 1.39 × 10⁻⁶), encompassing

the range of of previously reported values for MORB erupted away from high ³He/⁴He hotspots such as Iceland. He, Sr and Pb isotopes show systematic relationships along the ridge axis. The ridge axis is segmented with respect to geochemical variations, and local spike-like anomalies in ³He/⁴He, Pb and Sr isotopes, and trace element ratios such as $(La/Sm)_N$ are prevalent at the latitudes of the islands of St. Helena, Tristan da Cunha and Gough to the east of the ridge. The isotope systematics are consistent with injection beneath the ridge of mantle "blobs" enriched in radiogenic He, Pb and Sr, derived from off-axis hotspot sources. The variability in ³He/⁴He along the ridge can be used to refine the hotspot source—migrating-ridge sink model.

MORB from the 2-7°S segment are systematically the least radiogenic samples found along the mid-ocean ridge system to date. Here the depleted mantle source is characterized by 87Sr/86Sr of ~0.7022, Pb isotopes close to the geochron and with $^{206}\text{Pb}/^{204}\text{Pb}$ of ~ 17.7 , and $^{3}\text{He}/^{4}\text{He}$ of 8.6-8.9 R_A. The "background" contamination" of the subridge mantle, by radiogenic helium derived from off-ridge hotspots, displays a maximum between ~20-24°S. The He-Pb and He-Sr isotope relations along the ridge indicate that the ³He/⁴He ratios are lower for the hotspot sources of St. Helena, Tristan da Cunha and Gough than for the MORB source, consistent with direct measurements of ³He/⁴He ratios in the island lavas. Details of the He-Sr-Pb isotope systematics between 12-22°S are consistent with early, widespread dispersion of the St. Helena plume into the asthenosphere, probably during flattening of the plume head beneath the thick lithosphere prior to continental breakup. The geographical variation of He/Pb ratio deduced from the isotope systematics suggests only minor degassing of the plume during this stage. Subsequently, it appears that the plume component reaching the MAR was partially outgassed of He during off-ridge hotspot volcanism

Overall, the similar behavior of He and Pb isotopes along the ridge indicates that the respective mantle sources have evolved under conditions which produced related He and Pb isotope variations.

Published in: Earth and Planetary Science Letters, 110:133-147, 1992.

Supported by: NSF Grants OCE-8516082, OCE-8812078 and OCE-8911505.

WHOI Contribution No. 7996.

and related melting activity.

ANNUAL CYCLES OF MASS FLUX AND ISOTOPIC COMPOSITION OF PTEROPOD SHELLS SETTLING INTO THE DEEP SARGASSO SEA

John P. Jasper and Werner G. Deuser

Mass fluxes and stable isotopic compositions $(\delta^{18}O)$ and $\delta^{13}C$) of pteropod shells collected during a six-year series of two-month sediment-trap deployments in the deep (3.2 km) Sargasso Sea provide information on annual population changes, habitat depths, and life spans of thecosome pteropods (Euthecosomata). The flux of pteropod shells responds to the annual cycle of primary production in the upper ocean. Flux maxima of the shells (>1 mm) of eight species occur from late winter through autumn. Seasonal changes in the hydrography of the upper water column are quite accurately recorded in the δ^{18} O variations of six perennial species, which generally confirm the distinction between non-migratory (Creseis acicula, Creseis virgula conica, and Diacria quadridentata) and diurnally migratory taxa (Styliola subula, Cuvierina columnella, and Clio pyramidata). Isotopic records of C. acicula and C. virgula conica are consistent with shell formation above 50 m. The records of the migratory species reflect what appear to be average calcification depths of 50-75 m. Average annual δ^{13} C variations reveal the annual cycles of primary production and stratification of near-surface waters. Adult life spans of the species studied appear to be no more than a few months. The results of this study should be useful in paleoceanographic reconstructions based on isotopic measurements of sedimentary pteropod shells.

In Press: Deep-Sea Research.

Supported by: NSF Grant OCE-9017114.

WHOI Contribution No. 7946.

MANTLE HETEROGENEITY BENEATH OCEANIC ISLANDS: SOME INFERENCES FROM ISOTOPES

Mark D. Kurz

The radiogenic isotopes in oceanic basalts are extremely useful as tracers of long lived heterogeneities in the earth's mantle, and therefore in understanding mantle melting. The helium isotopes provide unique information in that high $^3\mathrm{He}/^4\mathrm{He}$ ratios are indicative of relatively undegassed mantle reservoirs (i.e., having had high time integrated $^3\mathrm{He}/(\mathrm{Th}+\mathrm{U})$ ratios. An alternative hypothesis is that high $^3\mathrm{He}/^4\mathrm{He}$ may have been produced by ancient melting events, if

the solid/melt partition coefficient (K_d) for He is greater than for Th and U (i.e., yielding high He/(Th + U) in the residue of melting). The distribution of helium within basaltic phenocrysts, and olivine/glass helium partitioning within mid-ocean ridge basalts, suggest that helium behaves as an incompatible element upon melting $(K_d \text{ (olivine/glass)} < 0.0055)$, which strongly supports the hypothesis that high ${}^3\text{He}/{}^4\text{He}$ ratios are derived from undegassed mantle reservoirs.

New stratigraphic studies of Hawaiian volcanoes, demonatrates that the mantle sources have changed on extremely short time scales, between 100 to 10,000 years before present. The preferred explanation for these variations is that they represent heterogeneities within the Hawaiian mantle plume, combined with late stage melting in the lithosphere. The alternative hypothesis, that the variations are produced by melt percolation effects is considered less likely due to the essentially continuous supply of magma to Hawaiian volcanoes, but is impossible to rule out completely.

In Press: Melting and Melt-Movement in the Earth.

Supported by: NSF Grant OCE-817833.

WHOI Contribution No. 8074.

A RADIOTRACER STUDY OF CERIUM AND MANGANESE UPTAKE ON TO SUSPENDED PARTICLES IN CHESAPEAKE BAY

James W. Moffett

The oxidation kinetics of Ce(III) and Mn(II) were studied in Chesapeake Bay in March and July 1990 to establish the role of water column redox processes in contributing to Ce anomalies observed in this estuary (Sholkovitz and Elderfield, 1988; Sholkovitz et al., 1992). Oxidation was measured by adding Mn(II) and Ce(III) to freshly collected water samples as radiotracers, and measuring their uptake on to the ambient suspended particle assemblage. Mn(II) oxidation was measured by following the uptake of ⁵⁴Mn(II) onto suspended particles and utilizing protocols established by other workers to distinguish oxidation from Mn(II) adsorption. The same protocols were applicable to Ce(III), using ¹³⁹Ce(III), and were supported by the use of ¹⁵²Eu(III) as a non-redox reactive control.

Specific rates of Ce(III) and Mn(II) oxidation measured at station 1 (depth = 4 m) in July were 1296% per day and 4032% per day respectively. In March at the same station, the specific rate of Mn(II) oxidation was only 10% per day, and Ce(III) oxidation was undetectable. Both Ce(III) and Mn(II) oxidation processes were inhibited by azide, indicating that they were microbially

mediated. The seasonal differences probably reflect strong seasonal variation in the abundance of Mn oxidizing bacteria. No Ce(III) oxidation occurred in samples collected below the oxic/anoxic interface in July. The specific rate constants for both elements were over 1000 times higher than those measured in the Sargasso Sea. However, the ratio of Mn(II) to Ce(III) specific oxidation rates was approximately 3:1 in the oxic samples collected in July, very similar to the ratio determined in previous studies of the Sargasso Sea and Vineyard Sound, Massachusetts. This suggests a common mechanism of oxidation of both elements which may be significant in a wide range of marine environments.

Supported by: NSF Grant OCE-8817401.

WHOI Contribution No. 8227.

COMMENTS ON "REDOX CYCLING OF RARE EARTH ELEMENTS IN THE SUBOXIC ZONE OF THE BLACK SEA" BY C. R. GERMAN, B. P. HOLLIDAY AND H. ELDERFIELD, GEOCHIMICA ET COSMOCHIMICA ACTA, 55:3553-3558, 1991

Edward R. Sholkovitz

German et al. (1991) utilized the existence of a suboxic layer in the water column of the Black Sea to determine if the large changes in the concentration of dissolved rare earth element (REEs) across redox boundaries are controlled by the Mn redox cycle or the Fe redox cycle. They concluded that the Mn redox cycle is controlling the vertical profiles and fractionation of REEs. Their main conclusion can be summarized by quoting directly from their paper: (1) "Clearly then redox cycling of the REEs in the Black Sea is not associated with the suboxic/anoxic interface" and (2) Detailed sampling across this boundary layer has provided an equivocal test of whether REE cycling in a stable anoxic basin is associated with the oxic/suboxic interface along with Mn...or with the suboxic/anoxic interface."

Here I argue that German et al.'s (1991) conclusion is not supported by the data. The focus will be on the trivalent REEs which do not have a redox chemistry of their own but are indirectly affected by the redox cycles of Fe and Mn. The redox cycle of Ce will not be addressed.

Supported by: NSF Grant OCE-9016894 WHOI Contribution No. 7998.

CHEMICAL EVOLUTION OF RARE EARTH ELEMENTS: FRACTIONATION BETWEEN COLLOIDAL AND SOLUTION PHASES OF FILTERED RIVER WATER

Edward R. Sholkovitz

A study of Connecticut River water demonstrates that low temperature geochemical reactions lead to large scale fractionation of rare earth elements (REE) between dissolved, colloidal and solution phases. Filtration through progressively smaller pore-sized filters (0.45, 0.22 and 0.025 µm) results in filtrates which have lower absolute REE concentrations and which are progressively more fractionated relative to the crust. With decreasing pore size, the filtrates have shale normalized abundances which become systematically more depleted in the light REE relative to the heaviest REE (Lu). Hence, the solution phase is more fractionated relative to the crust as particles and colloids are removed from river water. When compared to the REE composition of the dissolved phase, the colloidal phase is progressively enriched in a systematic pattern in going from the heaviest to lightest REE. In addition, river colloids are preferentially enriched in the redox-active REE cerium, leaving the solution phase with a more negative Ce-anomaly than the dissolved phase.

Colloidal particles carry a large part of the dissolved REE pool (colloidal phase + solution phase) in river waters and are highly fractionated relative to the REE composition of the solution phase. These observations establish that colloids play a major role in explaining and linking the geochemistry of REE in fresh waters, estuaries and the ocean. If river colloids are coagulated during estuarine mixing (as they are for REE) and if the solution phase of rivers is the major source of REE to the oceans, then extensive fractionation within the oceanic geochemical cycle doesn't need to be invoked to explain the evolved REE patterns of seawater. Instead, the REE composition of the solution phase is evolved on the continents as fractionation occurs between rocks, soils and freshwaters. The fractionation of REE(III) between phases of the Connecticut River water is consistent with solution-ligand models. Similarly, some significant portion of the seawater's pronounced negative Ce-anomaly, previously attributed to oceanic redox processes, has its source in the solution phase of river waters.

Published in: Earth and Planetary Science Letters, 114:77-84, 1992.

Supported by: NSF Grant OCE-9016894. WHOI Contribution No. 8037.

THE GEOCHEMISTRY OF RARE EARTH ELEMENTS IN THE AMAZON RIVER ESTUARY

Edward R. Sholkovitz

Both the concentration and relative abundance of rare earth elements (REE) in river and estuarine waters are greatly modified by several different types of biogeochemical reactions in estuaries. This paper presents a detailed study of these reactions in the Amazon River Estuary using samples collected on an "AmasSeds" (Amazon Shelf Sediment Study) cruise in August 1989. Extensive removal of dissolved (0.22 mm filtered) REE from river water occurs in the low (0-6) salinity region due to salt-induced coagulation of river colloids. This removel leads to large scale fractionation of the REE(III) and the development of large (more negative) cerium anomalies. In the transition zone between terrigenous suspended particles and biological particles at about a salinity of 22, only Ce exhibits a sharp decrease in the concentration. This leads to the development of large (more negative) anomalies, caused by the biologically-mediated oxidation of Ce(III) to Ce(IV) in the zone of high productivity. A comparison of REE concentrations of deep and surface water suggests that dissolved REE are released to deep waters from sediments and/or resuspended particles.

Coagulation of river colloids, biologically-mediated oxidation in zone of high biological production and release from sediments all lead to significant fractionation of REE(III) and redox modification of cerium (preferential removal of Ce relative to La(III) and Nd(III).) These processes result in the composition of dissolved REE becoming fractionated relative to the crust (e.g., LREE depleted and negative Ce anomalies) and more evolved toward the REE composition of the oceans. Hence, estuarine chemistry plays a key role in controlling the REE composition of the oceans.

In Press: Geochimica et Cosmochimica Acta.
Supported by: NSF Grant OCE-8711032.

WHOI Contribution No. 8105.

EXPERIMENTAL MEASUREMENTS OF ³HE AND ⁴HE MOBILITY IN OLIVINE AND CLINOPYROXENE AT MAGMATIC TEMPERATURES

T. W. Trull and M. D. Kurz

In Vacuo heating of 0.5-0.7 mm olivine and clinopyroxene grains separated from Hawaiian ultramafic xenoliths leads to complete He loss within hours to days for temperatures of 700-1400°C. Diffusivities calculated from the observed release rates assuming spherical grains and initially homogeneous He distributions define Arrhenius relations with activations energies of 420±20 and 290±40 Kj/mole and log₁₀ D_o of $+5.1\pm0.7$ and $+2.1\pm1.2$ cm²/s in olivine and pyroxene, respectively. Values at 1350°C are 5.3×10^{-9} cm² in olivine and 10 times faster in pyroxene $(4.7 \times 10^{-8} \text{ cm}^2/\text{s})$. These values include small corrections for grain size variations and, in the case of olivine, about 15% prior diffusive He loss

However, an important factor that has not been considered in previous studies of this type, as that the xenolith He resides predominantly within CO₂ rich fluid inclusions. Theoretical description of He loss in such a case demonstrates that the diffusivities calculated using the standard approach actually represent the product of the true volume diffusivity (D) and the helium solubility, as represented by the distribution coefficient K_{Dv} (defined by C_{crystal}/C_{fluid}). Although He solubility in crystals is not well determined, estimates based on the CO₂ concentrations in these samples suggest that it is very low K_{Dv} of 3×10^{-4} for pyroxene and 6×10^{-6} for olivine; which also implies low crystal-melt distribution coefficients of 0.05 and 0.001). The resultant corrected diffusion rates are significantly faster than those obtained by the standard approach (~10⁻⁴ cm²/s at 1350°C and are thus higher than basaltic melt values). The most reasonable interpretation of this result is that He release is enhanced by internal grain fractures, including the planar healed cracks along which most fluid inclusions are arrayed. This treatment illustrates the difficulties involved in extrapolating laboratory He release measurements to nature, in particular the strong influence of mineral defects. The diffusivities reported here probably represent upper limits for mantle He transport or magma-phenocryst He exchange. As such, they imply that He transport over kilometer length scales in the mantle is dominated by convection rather than diffusion, and that phenocrysts in extrusive rocks will retain most of their pre-eruption helium contents. In combination with the observation that ³He diffuses only marginally faster than 4He (4±4% faster in

pyroxene and 9±4% faster in olivine), this implies that significant isotopic fractionation of residual helium contents is unlikely to occur.

Supported by: NSF Grant OCE-8716970.

WHOI Contribution No. 8229.

VENTILATION AND TRANSPORT OF THERMOCLINE AND INTERMEDIATE WATERS IN THE NORTHEAST PACIFIC DURING RECENT EL NIÑOS

Kim A. Van Scoy and Ellen R. M. Druffel

We present time series of tritium (³H) concentrations in seawater from stations in the eastern subpolar (50°N, 145°W) and subtropical (28°N, 122°W) North Pacific. In the eastern subpolar North Pacific the tritium gradient between surface water and North Pacific Intermediate Water (NPIW) is smallest during years which coincide with El Niño events. In the eastern subtropical North Pacific between 200 and 400 m the tritium signature suggests the water is of subpolar origin during non-El Niño years. During El Niño years the water at this location is devoid of tritium. We hypothesize that the El Niño phenomenon alters both the ventilation of thermocline and intermediate waters in the eastern subpolar North Pacific, as well as the transport of this water to the eastern subtropical gyre. Combined with satellite altimeter data, these results offer both a mechanism and a time frame by which subpolar water ventilates the vast reservoir of the subtropical North Pacific.

In Press: Journal of Geophysical Research (Oceans).

Supported by: Postdoctoral Fellowship from the Woods Hole Oceanographic Institution.

WHOI Contribution No. 8167.

A COMPARISON OF DISSOLVED AND PARTICULATE MN AND AL DISTRIBUTIONS IN THE WESTERN NORTH ATLANTIC

Philip A. Yeats, John A. Dalziel and S. Bradley Moran

The dissolved Mn distribution on an oceanographic section along 50°W in the western North Atlantic shows decreasing concentrations in the offshore direction in the surface layer and with depth at the deep water stations. Leachable particulate Mn concentrations are low in the open ocean surface waters and elevated at intermediate depths. Dissolved Al concentrations in the surface layer are highe in the open ocean than on the shelf

and the vertical distributions are characterized by surface maxima, a subsurface minimum at ≈1000 m and increasing concentrations in the deep waters. Leachable particulate Al concentrations are elevated on the shelf and in open ocean surface waters compared to the intermediate and deep waters. The Deep Western Boundary Current has high levels of dissolved Al and leachable particulate Mn and Al, and low levels of dissolved Mn.

The distribution of dissolved Al is controlled primarily by inputs from atmospheric dust and removal onto biogenic particles. Both fluvial and atmospheric inputs affect dissolved Mn levels with removal occurring primarily by oxidation of Mn²⁺. The Al distribution is characterized by short residence times in shelf and surface waters and relatively constant distribution coefficients. The Mn distribution is characterized by longer surface water residence times, shorter deep water residence times, and on widely varying distribution coefficients than Al. Removal of Al by a surface-adsorption mechanism and Mn by slower oxidation of Mn²⁺ are consistent with these observations. A model of Mn oxidation kinetics accurately predicts the intermediate depth leachable particulate Mn maximum.

Published in: Oceanologica Acta, 15:609-619, 1992.

Supported by: Postdoctoral Fellowship from the Woods Hole Oceanographic Institution and NSERC of Canada.

WHOI Contribution No. 8064.

MARINE CHEMISTRY

TEMPERATURE DEPENDENCE OF CO₂ PARTIAL PRESSURE IN SEAWATER

Catherine Goyet, Frank J. Millero, Alain Poisson, and Deborah K. Shafer

The flux of CO_2 across the air-sea interface is controlled by the difference in the partial pressure of carbon dioxide (pCO_2) in the atmosphere and in the surface seawater. The partial pressure of CO_2 in seawater is frequently measured at a temperature that is higher or lower than the in-situ temperature. Consequently, one of the key factors in an accurate determination of the partial pressure of CO_2 in seawater is not only the knowledge of both the temperature of the measurement (T_m) and the in-situ temperature (T_{in}) , but also of the accuracy of the temperature correction. Ideally, this correction should be made by using known parameters $(pH - A_T, pH - C_T)$ $pCO_2 - C_T$, $A_T - C_T$, etc.), and reliable constants for carbonic acid. Since they are frequently not available and pCO_2 is measured alone, one must

make an estimate of the effect of temperature on seawater pCO2 from the accurate knowledge of seawater salinity and temperature and the approximate knowledge of the carbonate parameters. In this paper we give an empirical relationship that can be used to estimate the effect of temperature on the fugacity of CO_2 (fCO_2 ; the fugacity of a real gas is defined as the pressure an ideal gas would have at the same temperature and pressure, to have the same free energy. In practice, the correction for the non-ideal nature of CO_2 gas is negligible (<1 μ atm) and pCO_2 is often treated identically to fCO_2), as a function of the measured temperature and salinity and the estimated ratio $X = C_T/A_T$ (total inorganic carbon/total alkalinity). The equation is of the form:

 $fCO_{2[t]} - fCO_{2[20]} = A + Bt + Ct^2 + Dt^3 + Et^4$ where $fCO_{2[t]}$ and $fCO_{2[20]}$ represent fCO_2 at temperatures t°C and 20°C, respectively; the parameters A, B, etc., are functions of X and

salinity (S):

 $A = (a_o + a_2X + a_4X^2)/(1 + a_1X + a_3X^2)$ $B = (b_o + b_2X + b_4X^2)/(1 + b_1X + b_3X^2)$ $C = (c_o + c_2X + c_4X^2)/(1 + c_1X + c_3X^2)$ $D = (d_o + d_2X + d_4X^2)/(1 + d_1X + d_3X^2)$

 $E = e_o + e_1 X + e_2 X^2 ln(X) + e_3 exp(X) + e_4 / ln(X)$ the parameters a, b, etc., are functions of salinity.

The 25 parameter equation fits the calculated values of fCO_2 calculated from the constants of Goyet and Poisson (1989), when X varies from 0.8 to 1.2, t varies from -1°C to 40°C, and S varies from 30 to 40. Direct measurements on the effect of temperature on the pCO_2 of seawater from -1°C to 30°C were found to be in good agreement (standard error better than 5 μ atm) with the values determined from the equation.

Supported by: NSF Grant OCE-91815137, DOE Grant De-FGO2-ER60980, and NASA Grant NAGW-2431.

WHOI Contribution No. 8234.

LANTHANIDE LUMINESCENCE IN SEAWATER: APPLICATION TO A STUDY OF CERIUM REDOX **CHEMISTRY**

James W. Moffett

The luminescence properties of the lanthanides Ce(III), Tb(III), and Pr(III) in seawater have been studied and applied to a study of the redox chemistry of cerium in seawater in model systems in order to evaluate the role of non-biological processes in the marine geochemistry of cerium. Reactions were followed by direct spectrofluorimetric assay of Ce(III) in seawater. For reactions involving particle surfaces, redox reactions were distinguished from simple

adsorption using Pr(III) and Tb(III), which can also be measured spectrofluorimetrically, as non-redox reactive controls. No Ce(III) oxidation was observed in the absence of added particles in seawater or in NaCl media up to pH 10. Adsorption of Ce(III) was observed in suspensions of iron oxides, manganese oxides, and aragonite in seawater. However, Ce(III) oxidation occurred only on manganese oxides. The reaction was not oxygen dependent, indicating that Mn oxide was the oxidant. The influence of pH, Mn(II), Pr(III) and Ce(III) concentrations, sodium azide (a metabolic inhibitor) and ascorbate (a mild reducing agent) were also studied. The results set upper limits on the importance of nonbiological reactions in Ce oxidation and are useful in designing experiments to distinguish these reactions from biologically mediated ones at natural Ce concentrations.

The fluorescent properties of these elements make them useful for studying lanthanide solution chemistry. The principal limitations are the apparent quenching of fluorescence by adsorption onto particle surfaces, and the relatively weak fluorescence intensities of Pr(III) and Tb(III) under our experimental conditions.

Supported by: NSF Grant OCE-8817409. WHOI Contribution No. 8077.

AUTHIGENIC APATITE FORMATION AND BURIAL IN SEDIMENTS FROM NON-UPWELLING, CONTINENTAL MARGIN ENVIRONMENTS

Kathleen C. Ruttenberg and Robert A. Berner

Evidence for precipitation of authogenic carbonate fluorapatite (CFA) in Long Island Sound and Mississippi Delta sediments suggests that formation of CFA is not restricted to environments of active coastal upwelling. We present porewater data suggestive of CFA formation in both these areas. Application of a sequential leaching procedure, designed specifically to separate authigenic carbonate fluorapatite from other phosphorus-containing phases, including detrital apatite of igneous or metamorphic origin, provides strong supporting evidence for authigenic apatite formation in these sediments. The size of the authigenic apatite reservoir increases with depth, indicating continued formation of CFA during early diagenesis. This depth increase is mirrored by a decrease in solid-phase organic P at both sites, suggesting that CFA is forming at the expense of organic P. Mass balance considerations. application of diagenetic models to interstitial water nutrient data, and the saturation state of the interstitial water are consistent with this interpretation. Diagenetic redistribution of

phosphorus among the different solid-phase reservoirs is observed at both sites, and results in near perfect retention of P by these sediments over the depth intervals sampled. Formation of CFA in continental margins which do not conform to the classically defined regions of phosphorite formation renders CFA a quantitatively more important sink than has previously been recognized. Including this reservoir as a newly identified sink for reactive P in the ocean, the residence time of P in the modern ocean must be revised downward. The implication for ancient oceans of CFA formation in continental margin sediments other than phosphorites is that phosphorite formation may be less a representation of episodicity in removal of reactive P from the oceans than of localized concentration of CFA in phosphatic sediments by secondary physical processes.

Published in: Geochimica et Cosmochimica Acta, 57:991-1007, 1993.

Supported by: NSF Grants OCE-9101495, EAR-8420334, EAR-8617600, and OCE-8917409.

WHOI Contribution No. 8356.

INSTRUMENTS AND METHODS

MEASUREMENT OF SEAWATER PCO₂ USING A RENEWABLE-REAGENT FIBER OPTIC SENSOR WITH COLORIMETRIC DETECTION

Michael D. DeGrandpre

A new method, based on a renewable-reagent fiber optic sensor, for measuring the partial pressure of CO₂ (pCO₂) in seawater is presented. The sensor operates by measuring the light intensity at the absorbing wavelengths of a colorimetric acid-base indicator which is continuously delivered to the fiber tips through capillary tubing. The light intensity is modulated by pH changes that occur when CO₂ diffuses across a gas-permeable membrane. The sensor operates both in a diffusion-dependent steady state and equilibrium regime depending upon the indicator flow rate. At low flow rates, an equilibrium model can be used to predict the response of the sensor. The results indicate that the sensor operates within the steady-state regime at flow rates higher than approximately $0.2 \mu L/minute$. The optimal precision is $\pm 0.8 \ \mu atm$ from 300-550 μatm CO₂, calculated from the response sensitivity and 3x the root mean square noise. Response times (100%) range from 11 to 26 minutes and depend upon the indicator flow rate. Sensitivity to temperature and sample hydrodynamics is also discussed. The sensor performance was tested on a

research cruise and these results are compared to the underway pCO₂ measured simultaneously by an infrared CO₂ analyzer.

Published in: Analytical Chemistry, 65:331-337, 1993.

Supported by: DOE Grant DE FG02-92ER61437.

WHOI Contribution No. 8168.

THE CHLOROPHYLL-LABELING METHOD: THE RADIOCHEMICAL PURITY OF CHLOROPHYLL A—A RESPONSE TO JESPERSEN ET AL., 1992, J. PLANKTON RES.

Ralf Goericke

Jespersen et al. (1992) recently published a critique of the chlorophyll-labeling method which allows the measurement of phytoplankton carbon-biomass and growth rates in the field (Redalje and Laws, 1981). Jespersen et al. (1992) observed that microalgae incorporated [14C] bicarbonate much more rapidly into chl a than into particulate algal carbon in six out of seven ¹⁴C-labeling experiments. They argued that contamination was not a likely cause of the observed labeling patterns, and concluded that 'real variations in the labeling patterns of the carbon pools' were responsible for their results and pointed out that such labeling patterns question the central assumption of the chl-labeling method, i.e., 'that, after a sufficiently long incubation, the specific activity of the chl a carbon is identical to the specific activity of the total phytoplankton carbon' (Redalje and Laws, 1981). Jespersen et al. (1992) concluded that such labeling patterns will lead to an overestimation of phytoplankton growth rates and an underestimation of carbon biomass when using the chl-labeling method in the field.

I have encountered similar ¹⁴C-labeling patterns while developing methods for the preparation of radiochemically clean chl a for the measurement of chl a turnover in microalgae. However, the observed labeling patterns were an artifact due to contamination of chl a preparations by colorless radiolabeled compounds. The simple high-pressure-liquid chromatography (HPLC) procedure initially used, did not remove these contaminants from the chl a preparations. It is likely that the chl a preparations of Jespersen ct al (1992) were similarly contaminated. Here, I present those data that demonstrate presence of contaminants in preparations of chl a and discuss the methods for the isolation of radiochemically pure chl a developed by Goericke and Welschmeyer (1992a).

Published in: Journal of Plankton Research, 14(12):1781-1785, 1992.

Supported by: NSF Grant OCE-9101384. WHOI Contribution No. 8182.

HIGH ACCURACY MEASUREMENTS OF TOTAL DISSOLVED INORGANIC CARBON IN THE OCEAN: COMPARISON OF ALTERNATE DETECTION METHODS

C. Goyet and A. K. Snover

High accuracy measurements of total dissolved inorganic carbon in the ocean are currently performed using an automated coulometric system based on that described by Johnson et al. (1987). These measurements require highly trained technicians and the manipulation of expensive and hazardous chemicals. We tested an alternate detection method based on non-dispersive infra-red analysis. All the dissolved carbonate species from a seawater sample are extracted as CO2 gas by acidification and nitrogen stripping The CO2 gas was then quantitatively detected alternately with a coulometric system and an infra-red analyzer. The reproducibility of both detection methods is very similar, better than 1.5 μ mol/kg. The detection of the CO₂ gas by infra-red analysis presents several advantages over the coulometric detection: it simplifies and reduces the cost of the measurements, it shortens the analysis time, it reduces the sample size requirement by at least a factor 5, and it allows us to consider complete automation of the system for underway surface seawater measurements.

Supported by: NSF Grant OCE-9115317, DOE Grant DE-FGO2-ER60980, and a Summer Student Fellowship from the Arthur Vining Davis Foundation.

WHOI Contribution No. 8233.

INHERENT OPTICAL PROPERTIES OF THE OCEAN: RETRIEVAL OF THE ABSORPTION COEFFICIENT OF CHROMOPHORIC DISSOLVED ORGANIC MATTER FROM FLUORESCENCE MEASUREMENTS

Frank E. Hoge, Anthony Vodacek and Neil V. Blough

The quantitative relationship between the absorption and fluorescence emission of chromophoric (colored) dissolved organic matter (CDOM) has been determined along 5 cruise tracks in the western North Atlantic Ocean, the Gulf of Mexico, and Monterey Bay, and includes Gulf Stream, Loop Current, slope, shelf, and coastal waters. We present a protocol for the determination of CDOM fluorescence that will

allow both interlaboratory comparisons and the calibration of airborne fluorescence measurements. This protocol is based on the use of the water Raman signal as an internal radiometric standard and quinine sulfate as an external standard. This study demonstrates that when an appropriate and consistent procedure is employed to standardize the fluorescence measurements, the fluorescence per unit absorption exhibits surprisingly little variation for diverse waters. The maximum variability observed between all sites was 36% and within the western North Atlantic the variability was only 12%. Algorithms are presented for retrieval of the absorption coefficient of CDOM at 355 and 337 nm from shipboard or airborne measurements of the water-Raman-normalized fluorescence emission resulting from 335 and 337 nm excitation.

 In Press: Limnology and Oceanography.
 Supported by: NASA/EOS Interdisciplinary Grant NAGW-2431 and ONR Grant N00014-89-J-1260.
 WHOI Contribution No. 8011.

DEVELOPMENT OF A SEQUENTIAL EXTRACTION METHOD FOR DIFFERENT FORMS OF PHOSPHORUS IN MARINE SEDIMENTS

Kathleen C. Ruttenberg

A sequential extraction method (SEDEX) has been developed to separately quantify five sedimentary P reservoirs: loosely sorbed P; ferric iron-bound P; authigenic carbonate fluorapatite + biogenic apatite + CaCO₃-associated P; detrital apatite P; and organic P. The SEDEX method successfully separates two of the main categories of authigenic phosphate phases called upon most often as sedimentary sinks for diagenetically mobilized P: ferric oxyhydroxide-associated P and authigenic carbonate fluorapatite (CFAP). It offers a means of separating authigenic CFAP from detrital apatite of igneous or metamorphic origin. The importance of this distinction is that CFAP represents an oceanic sink for reactive P, whereas detrital apatite does not. In addition, a means of reversing secondary adsorption of P onto residual solid surfaces during extraction has been developed.

Extensive standardization of the SEDEX method for application to marine sediments has been performed with analogs for naturally occurring phosphatic phases.

Published in: Limnology and Oceanography, 37(7):1460-1482, 1992.

Supported by: NSF Grants OCE-9101495, EAR-8420334, EAR-8617600, and OCE-8917409. WHOI Contribution No. 8355.

DEPARTMENT OF PHYSICAL OCEANOGRAPHY James Luyten, Chairman

OCEAN CIRCULATION & LOW FREQUENCY VARIABILITY

EVIDENCE FOR BAROTROPIC WAVE RADIATION FROM THE GULF STREAM

Amy S. Bower and Nelson G. Hogg

Highly energetic velocity fluctuations associated with topographic Rossby waves have frequently been observed over the continental slope and rise off the US east coast. It has been suggested that the energy source for these waves could be eastward propagating Gulf Stream meanders, which can couple to the westward propagating Rossby waves if the meander shape is time-dependent. In this study, a historical archive of all available current meter data from the western North Atlantic has been examined for evidence of energy radiation from the Gulf Stream via barotropic/topographic Rossby waves. Horizontal maps of abyssal (> 2000 m) eddy kinetic energy and Reynolds stress were constructed for four frequency bands. The maps are compared qualitatively with similar maps generated from a stochastic wave radiation model.

The eddy energy maps have many interesting features but bear little resemblance to the model-generated maps. This is most likely due to the oversimplified basin geometry used in the model. Observed energy levels reach maximum values over the mean position of the Gulf Stream at low frequencies, but this maximum migrates northwestward to a location over the rise and slope south of New England at higher frequencies. Energy levels may be enhanced here due to refraction of Rossby waves emanating from the Gulf Stream.

The Reynolds stress maps show strong evidence of radiating waves north of the Gulf Stream over a large geographical area and at all frequencies considered. The velocity components are found to be statistically coherent and 180° out of phase at many locations when viewed in a coordinate system aligned with the local ambient potential vorticity gradient. Since we expect that energy is radiated symmetrically from the Gulf Stream, radiated waves are most likely present south of the stream as well. However, their presence is not apparent in the observations, perhaps due to the dominance of other eddy-generating mechanisms there such as baroclinic instability of the re-circulation.

Published in: Journal of Physical Oceanography, 22(1):42-61, 1992.

Supported by: NSF Grant OCE86-08258; ONR Contract N00014-85-C-0001.

WHOI Contribution No. 7587.

OCEAN HEAT TRANSPORT ACROSS 24°N LATITUDE

Harry L. Bryden

Direct estimates of ocean heat transport indicate that the meridional circulation across 24°N carries 1.2 PW of heat northward in the Atlantic Ocean and 0.8 PW of heat northward in the Pacific Ocean. The total ocean heat transport across 24°N of 2.0 PW is substantially less than recent indirect estimates of ocean transport based on satellite radiation measurements and atmospheric energy transport estimates. Heat transports in the Atlantic and Pacific Oceans are accomplished by two different mechanisms. In the Atlantic, a deep vertical-meridional circulation cell with northward flowing warm surface waters and southward flowing cold deep waters effects the northward heat transport across 24° N. In the Pacific, a horizontal circulation cell in the upper waters with northward flowing warm waters on the western side of the ocean and southward flowing colder waters in the central and eastern parts of the ocean effect the northward heat transport across 24°N. Prospects for direct determination of the ocean heat transport as a function of latitude are described with emphasis on the need to identify the principal mechanisms of ocean heat transport in each ocean basin.

Submitted to: Hann Symposium Volume of AGU Geophysical Monograph Series.

Supported by: NSF Grant OCE91-01493.

WHOI Contribution No. 7954.

SILL EXCHANGE TO AND FROM ENCLOSED SEAS

Harry L. Bryden

Recent theoretical developments in modelling the two-layer exchange across a sill are applied to predict the maximal exchange possible through the Strait of Gibraltar. Predictions of the outflow of Mediterranean water, the inflow of Atlantic water and the salinity difference between the two water masses are made as a function of the net evaporation over the Mediterranean basin. Time series current and salinity measurements on the Gibraltar sill during 1985-86 are then used to determine the observed outflow, inflow, outflow salinity transport, and salinity difference. The observed outflow salinity transport provides a nearly direct estimate for the net evaporation over the Mediterranean basin of 52 cm yr⁻¹, that may be more accurate than the usual climatological estimates. The observed outflow of Mediterranean

water is -0.68 Sv \pm 0.17 Sv and it agrees with the predicted outflow of -0.84 Sv for a net evaporation of 52 cm yr⁻¹ within its estimated error. The best estimate of the observed inflow is 0.72 Sv and again it agrees well with the predicted inflow of 0.88 Sv. The observed salinity difference between the Mediterranean and Atlantic waters of $2.21^{\circ}/_{\circ o}$ is about 20% higher than the theoretically predicted salinity difference of $1.80^{\circ}/_{\circ o}$. Given that the present hydraulics theory does not include important dynamical effects such as rotation and friction that could lower the predicted maximal exchange, the agreement within 20% between the observed and predicted exchanges through the Strait of Gibraltar must be considered encouraging.

Submitted to: Proceedings, "Mediterranean Sea 2000" Symposium.

Supported by: ONR Contract N00014-92-J-1273. WHOI Contribution No. 8019.

GENERATION OF INTERNAL LEE WAVES TRAPPED OVER A TALL ISOLATED SEAMOUNT

David C. Chapman and Dale B. Haidvogel

A primitive equation numerical model is used to study the generation of internal lee waves in a steady, rotating, uniformly stratified flow past an isolated seamount. We find that large-amplitude internal lee waves can form over the seamount even when the imposed steady flow is too weak to support the internal lee waves away from the seamount (i.e. low Froude and Rossby numbers). These internal lee waves are trapped over the flank of the seamount where nonlinear advection of momentum leads to a large local acceleration of the flow. As the flow decelerates downstream of the seamount, the internal lee wave amplitude and wavelength are reduced to the point where parameterized subgridscale mixing quickly dissipates the waves. This contrasts with the traditional case of internal lee waves in rapid background flows where the local acceleration over the seamount is relatively unimportant and the waves continue well downstream of the seamount The model results also indicate that the trapped internal lee waves form within a few days following flow initiation, suggesting that they may be excited by more realistic temporally varying oceanic flows.

Submitted to: Geophysical & Astrophysical Fluid Dynamics.

Supported by: ONR Contract N00014-89-J-1106.

WHOI Contribution No. 8048.

ENERGETICS OF GRAVITATIONAL ADJUSTMENT FOR MESOSCALE CHIMNEYS

Albert J. Hermann and W. Brechner Owens

The rates of energy flux out of newly formed circular patches of dense water ("chimneys") are considered as a function of patch size on an f-plane. The dense fluid resulting from a rapid deep convective process serves as a powerful reservoir of both mass and energy. Energy flux due to superinertial waves precedes mass flux. Both mass and energy are ultimately carried away from the local site of convection through baroclinic instability. Analytical and numerical methods are employed to investigate the relative amounts of potential energy radiated to the far field by either process, and the rates at which this is accomplished. An analytical solution is developed for the superinertial transients generated during linear, axisymmetric gravitational adjustment of a unit step. Initial energy decay by axisymmetric gravitational collapse is greater for a narrow chimney than for a wide one, but ultimately this is equalled and surpassed by the steady spreading of the wide chimney via its baroclinic breakup into smaller structures.

Submitted to: Journal of Physical Oceanography.
Supported by: ONR Contract N00014-86-K-0751.
WHOI Contribution No. 7965.

TOWARD PARAMETERIZATION OF THE EDDY FIELD NEAR THE GULF STREAM

Nelson G. Hogg

Analysis of measurements from two long-term moored arrays in and near the Gulf Stream suggests a simple parameterization of eddy spatial covariance statistics: a parameterization that can be referred to as "quasi-homogeneous and isotropic." Taking the normalized covariance function (i.e. the correlation function) for streamfunction to be homogeneous and isotropic and assuming motions to be horizontally nondivergent and hydrostatic permits the velocity and temperature covariances to be derived from the streamfunction covariance. Statistical tests indicate that deviations from these assumptions are indistinguishable from gaussian random noise. The spatial correlation function used is gaussian with a decay scale of about 140 km which is only weakly depth dependent. A simple form is also suggested for the vertical lag dependence.

This parameterization permits calculation of derived quantities such as the eddy vorticity flux

divergence which is discussed in the context of the mean potential vorticity balances for the depth integrated circulation and for the subthermocline layer. The divergence of the relative vorticity flux is found capable of driving two counter-rotating gyres of strength 30-40 Sv on either side of the Stream, as are observed. The "thickness flux" dominates the lower layer eddy potential vorticity flux and is of the correct sign to make the recirculation more barotropic. The lower layer eddy forcing is weak and the gyres exist in a region of nearly uniform mean potential vorticity.

Submitted to: Deep-Sea Research.

Supported by: ONR Contract N00014-85-C-0001; NSF Grant OCE86-08258.

WHOI Contribution No. 8192.

REAL FRESH WATER FLUX AS THE UPPER BOUNDARY CONDITION FOR THE SALINITY BALANCE AND THERMOHALINE CIRCULATION FORCED BY EVAPORATION AND PRECIPITATION

Rui Xin Huang

Fresh water flux used as the boundary condition for the salinity balance is applied to a primitive equation model of the oceanic general circulation. Instead of the relaxation condition or the virtual salt flux boundary conditions used in the previous models, the real fresh water flux across the upper surface is specified as the vertical velocity boundary condition for the continuity equation, and the salinity flux is set to identically zero at the sea surface. Preliminary numerical experiments show that a model with the new boundary conditions runs smoothly.

Much important physics involving the fresh water flux emerge from the new model. The barotropic Goldsbrough gyres driven by the precipitation and evaporation, which were excluded in the previous numerical models, are reproduced. In addition, the model's results reveal extremely complex structure of the three-dimensional circulation driven by the fresh water flux. In fact, a relatively small amount of fresh water flux drives very strong meridional and zonal cells and baroclinic gyres, which are 100 times stronger than the driving fresh water flux. Salt oscillation appears as the result of interaction between mixing and dissipation. It is suggested that the real fresh water flux should be used as the correct boundary condition in oceanic general circulation models, including the mixed layer models, the ice-ocean coupling models, and atmosphere-ocean coupling models.

Submitted to: Journal of Physical Oceanography.

Supported by: NSF Grant OCE90-17158; ONR Contract N00014-90-1518.

WHOI Contribution No. 8002.

PARAMETER SENSITIVITY STUDY OF THE HALINE CIRCULATION

Rui Xin Huang and Ru Ling Chou

Haline circulation forced by fresh water alone is studied for a broad region of parameter space by varying the amplitude of evaporation minus precipitation, the vertical and horizontal mixing of salt, horizontal dissipation of momentum, and the horizontal resolution. When the amplitude of freshwater flux is increased from 0.01 m year-1 to 1 m year -1 with other parameters fixed, the system evolves from a steady state of no oscillation to a state of periodic oscillation whose frequency increases almost linearly with the supercriticality. When the freshwater flux is fixed and the vertical mixing coefficient is increased from 0.5 to 3.0 cm²s⁻¹, the system evolves from a steady state to a state of single-period oscillation, period doubling, a single period, and finally to a chaotic state when $k_s > 2$ cm² s⁻¹. The strength of the meridional overturning and the mean sea surface salinity (deviation from mean) increases with the square-root of the vertical mixing.

Submitted to: Journal of Geophysical Research.

Supported by: U.S. World Ocean Circulation Experiments; NSF Grant OCE90-17158; and the Environmental Protection Agency.

WHOI Contribution No. 8191.

THE GOLDSBROUGH-STOMMEL CIRCULATION OF THE WORLD OCEANS

Rui Xin Huang and Raymond W. Schmitt

Goldsbrough (1933) first showed how the mass flux at the ocean surface due to the difference between evaporation and precipitation could induce barotropic flow in the ocean interior through the requirement of vorticity conservation. Here we present a first order description of the Goldsbrough circulation for the world oceans, using available climatologies. While such flows are an order of magnitude smaller than the wind-driven circulation, the interaction between the Goldsbrough gyres and the wind-driven and thermally driven circulation determines the salinity distribution of the world oceans. Therefore, it is important to study the Goldsbrough circulation and its interaction with motions driven by other forcings. In addition, the western boundary

currents required to close the Goldsbrough interior and to satisfy inter-basin mass transport (Wijffels et al., 1992) can be substantial. In the Atlantic the southward western boundary current reaches two Sverdrups at 35°N. It is suggested that this adverse current causes a southward shift in the separation point of the Gulf Stream; a simple model indicates that the displacement is about 75 Km.

Submitted to: Journal of Physical Oceanography.

Supported by: NSF Grant OCE90-17158; Atlantic Climate Change Program of NOAA Grant NA16RC0521-01.

WHOI Contribution No. 7991.

CONVECTIVE FLOW PATTERNS IN AN EIGHT-BOX CUBE DRIVEN BY COMBINED WIND STRESS, THERMAL, AND SALINE FORCING

Rui Xin Huang and Henry M. Stommel

An eight-box cube model ocean, simulating the subpolar gyre in the North Atlantic, is formulated in order to understand how the wind-induced horizontal gyre affects the thermohaline circulation and its catastrophe. The model is forced from above by thermal conduction and freshwater flux. The structure of the thermohaline circulation and its catastrophe during the process of gradually increasing or reducing the evaporation/precipitation are examined. The results indicate that, although adding the third dimension and a wind-driven horizontal gyre of medium strength splits the catastrophe into several separate ones, only some of these catastrophes remain of significant amplitude. With choice of parameters appropriate for the North Atlantic, the model predicts a single stable state, circulating in the thermal sense (sinking at the pole). This can be driven smoothly to a reversed saline sense (sinking at the equator), without catastrophe, by increasing the precipitation/evaporation rate beyond 3 times the present-day value.

Published in: Journal of Geophysical Research, 97(C2):2347-2364, 1992.

Supported by: NSF Grants OCE88-08076 and OCE89-13128; ONR Contract N00014-90-J-1518. WHOI Contribution No. 7605.

WIND-FORCED VARIATIONS IN SEA SURFACE HEIGHT IN THE NORTHEAST PACIFIC OCEAN

Kathryn A. Kelly, Michael J. Caruso and Jay A. Austin

Sea surface height (SSH) anomalies from the Geosat altimeter for the northeast Pacific Ocean

were analyzed to determine their annual and interannual fluctuations over a 2.5-year period. The interannual anomalies suggested a large-scale response to changes in the North Pacific wind field, with weaker wind stress curl in the Gulf of Alaska corresponding to a weakening and eastward migration of the Alaskan Gyre, and increased transport in the California Current. Uncertainties in the inverse barometer correction cast some doubt on the accuracy of the observed SSH in the Gulf of Alaska. The annual fluctuations in SSH showed a westward phase propagation in the California Current between about 36°N and 46°N. These observations were successfully modeled using a linearized potential vorticity equation with one active layer. The model was forced by realistic wind stress curl, which resembled a standing wave, based on an analysis of a gridded wind product. The annual fluctuations in SSH were produced by a combination of Ekman pumping and a Rossby wave, which suggests that the California Current core propagates offshore during the year.

Submitted to: Journal of Physical Oceanography.
Supported by: NASA Contracts 957652 and
NAGW-1666.

WHOI Contribution No. 8122.

NOTE ON THE SOURCES OF NORTH ATLANTIC DEEP WATER

James Luyten, Michael McCartney, Henry Stommel, Robert Dickson and Ed Gmitrowicz

Because the volumetric census of deep and bottom water in the North Atlantic Ocean consists of three isolated linear ridges along which heat and salt flow through the main volumetric mode (and point of intersection), it is possible to deduce the expected ratio of heat flux and ratio of salt fluxes measured in the Denmark Strait Overflow off Greenland and in the Antarctic Bottom Water near the equator. The weakly stratified layers of Upper North Atlantic Deep Water fall on the nearly linear ridge at temperatures above that of the mode.

There is an incompatibility between observed ratio and deduced ratio. It is made worse by resorting to double diffusion in the theory. We predict that a remeasurement of the flux of Antarctic Bottom Water near the equator will show that the previous determination at 4°N is unrepresentatively low.

Submitted to: Journal of Physical Oceanography.

Supported by: ONR Contracts N00014-90-J-1508 and N00014-90-J-1425; NSF Grants OCE86-14486 and OCE89-13128.

WHOI Contribution No. 7943.

THE CROSSING OF THE EQUATOR BY THE DEEP WESTERN BOUNDARY CURRENT IN THE WESTERN ATLANTIC OCEAN

Michael S. McCartney

Property distributions and geostrophic shear from a hydrographic section near 37°W in the Atlantic ocean show the deep western boundary current (DWBC) in the North Atlantic Deep Water (NADW) established against the western boundary of the Brazil Basin immediately south of the equator (between 2°S and 5°S). The DWBC thus has directly crossed the equator to the South Atlantic following the east-southeast trend of the continental slope isobaths. The estimated DWBC transport of NADW is $34 \times 10^6 m^3 s^{-1}$, similar to other estimates from the tropics. These large DWBC transports are opposed by flow of deep water to the North Atlantic immediately off-shore of the DWBC, with as much as two thirds of the DWBC transport being part of these recirculations. One recirculation center is over the Demerara Abyssal Plain north of the equator, another is near 11°S in the Brazil Basin; with the degree of their recirculation connection not established. These recirculations spread the northern source influences over the width of the recirculation (rather than the DWBC width), and efficiently dilute the northern source concentration with South Atlantic influences, with the self-mixing of the recirculation complicating the interpretation of tracer distributions. A further complication occurs for the uppermost levels of the NADW, for the DWBC flows to the southern hemisphere beneath an opposing western be ary current of Antarctic Intermediate Water (AAIW), and down gradient property fluxes mutually erode the upper NADW and the AAIW core characteristics. This causes a displacement of the axis of maximum northern source concentration offshore from the axis of maximum transport of upper NADW in the DWBC, a demonstration that the relationship between a tracer tongue and the flow field can be obsure.

Submitted to: Journal of Physical Oceanography.

Supported by: NSF Grants OCE86-14486, OCE91-05834; NOAA Grant NA16RC0528-01.

WHOI Contribution No. 8039.

THE TRANSPORT OF ANTARCTIC BOTTOM WATER AT 4°N IN THE WESTERN BASIN OF THE NORTH ATLANTIC OCEAN

Michael S. McCartney

In 1982 Whitehead and Worthington published the results of a field program examining the transport of Antarctic Bottom Water (AABW) at 4°N in the western basin of the North Atlantic Ocean. Two estimates of the transport below 1.9°C were made: a current meter based estimate of 0.8×10^6 m³ s⁻¹, and a geostrophic estimate from hydrographic data of $1.98 \times 10^6 \text{ m}^3 \text{ s}^{-1}$. The present study reexamines their data and calculations, rejects both transport estimates and gives a new estimate of 4.3×10^6 m³ s⁻¹. It is argued that the current meters, purported to represent the total flow, are unlikely to because they sampled only 14% of the area of AABW at 4°N. Their geostrophic estimate involves several systematic errors and a substantial error at one station pair. When these are corrected for, their original estimate $1.98 \times 10^6 \text{m}^3 \text{ s}^{-1}$ estimate is revised to 3.16×10^6 m³ s⁻¹. Considerable flow is suggested for the "bottom triangles" of the station pairs at 4°N (where the bottom is very rough), and the present treatment of them gives $1.14 \times 10^6 \text{ m}^3\text{s}^{-1}$ more transport than the (corrected) Whitehead and Worthington estimate, giving the new estimate of $4.3 \times 10^6 \text{ m}^3\text{s}^{-1}$ At 4°N the more robust part of the transport estimate is 2.65×10^6 m³s⁻¹, for this amount is the transport below 1.9°C but above the deepest common level, and thus independent of the extrapolation procedure for the bottom triangles.

Submitted to: Journal of Geophysical Research.

Supported by: NSF Grants OCE86-14486 and OCE91-05834; the Climate Change Program NOAA Grant NA16RC0528-01.

WHOI Contribution No. 7929.

TRANS-EQUATORIAL FLOW OF ANTARCTIC BOTTOM WATER IN THE WESTERN ATLANTIC OCEAN: ABYSSAL GEOSTROPHY AT THE EQUATOR

Michael S. McCartney and Ruth A. Curry

In its general northward flow along the western trough of the Atlantic, Antarctic Bottom Water (AABW) must pass over several sills separating the various abyssal basins. At the equator, the western trough is deformed by major east-west offsets of the Mid-Atlantic Ridge and the

continental margin of Brazil forming a nearly zonal channel about 250 km wide, centered at the equator, and extending approximately 1000 km along its axis. Thus the general northward flow of AABW is topographically constrained to be westward as it crosses the equator. A hydrographic section across this channel at 37°W shows the AABW isopycnals to be "bowl" shaped within and beneath the level of the channel walls. The equatorial geostrophic relation permits us to compute a zonal velocity from the well-defined parabolic distribution of dynamic height, relative to a reference level at the transition between AABW and the overlying deep water. We estimate $4.6 \times 10^6 \text{ m}^3\text{s}^{-1}$ for the westward - and ultimately northward - transport of AABW. Although this value exceeds previous estimates of net northward transport in the Brazil and Guiana Basins made from IGY data of the late 1950's, it fits well into the overall scenario constructed from transport estimates made from section data collected during the 1980s. This scenario has about $6-7 \times 10^6$ m³ s⁻¹ flowing northwards in the Brazil Basin, of which 2×10^6 m³ s⁻¹ exits to the eastern basin through the Romanche Fracture Zone, and the remainder, about $4-5 \times 10^6$ m³ s⁻¹, continues northwards into the Guiana Basin. About 2 × 106 m³ s⁻¹ exits to the eastern basin through the Vema Fracture Zone at 11°N and about 2 × 106 m³ s⁻¹ continues northward in the western basin.

In Press: Journal of Physical Oceanography.

Supported by: NSF Grant OCE86-14486 and OCE91-05834; NOAA Grant NA16RC0528-01.

WHOI Contribution No. 7973.

ON THE BAROCLINIC STRUCTURE OF THE ABYSSAL CIRCULATION AND THE ROLE OF TOPOGRAPHY

Joseph Pedlosky and David C. Chapman

A simple linear model of the abyssal circulation is studied in which a north-south topographic slope influences the interior and boundary layer flow. As in an earlier study, the reversals of the meridional velocity in the abyssal interior are related to the longitudinal variation of upwelling into the main thermocline.

When the topography slopes in the anti- β sense (down to the north in the northern hemisphere) an eastern boundary current appears regardless of the magnitude of the slope. If the slope is weak, the eastern boundary current is broad and bottom-trapped. As the slope becomes steeper, the current narrows and stretches vertically. At a critical value of the slope, for which the barotropic potential vorticity gradient

changes sign, the eastern boundary current metamorphoses into a modified Munk layer.

For all the values of the slope, a system of broad, baroclinic western boundary currents exist whose effects reach rather far into the interior.

In Press: Journal of Physical Oceanography.

Supported by: NSF Grant OCE88-16015 and from the Division of Atmospheric Sciences.

WHOI Contribution No. 8094.

SELF-SUSTAINED INERTIAL OSCILLATIONS

Joseph Pedlosky and Henry Stommel

We describe a self-sustaining baroclinic inertial oscillation whose energy source rests in a uniform horizontal temperature gradient. This energy is released through the agency of a temperature-dependent mixing law which is meant to crudely model the occurrence of enhanced mixing when the stratification weakens. The mixing is chosen to be negligible over most of the cycle and large only when the stratification is small.

Sustained inertial oscillations are shown to be the natural end-state of the instability of possible steady solutions when the decrease of the mixing rate with temperature exceeds a critical value. If the variation of the mixing rate with temperature is abrupt, a finite-amplitude oscillation is sustained although a possible steady solution is linearly stable.

Submitted to: Journal of Physical Oceanography.

Supported by: NSF Grant OCE89-13128 and from the Division of Atmospheric Sciences.

WHOI Contribution No. 7999.

HOW DOES THE DEEP WESTERN BOUNDARY CURRENT CROSS THE GULF STREAM?

Robert S. Pickart and William M. Smethie, Jr.

The manner in which the Deep Western Boundary Current (DWBC) crosses the Gulf Stream is investigated using data from a hydrographic survey conducted in 1990. Absolute geostrophic velocity vectors are computed using in-situ float data to obtain the reference level. Three density layers are considered in detail: two mid-depth layers which together comprise the shallowest water mass component of the DWBC (500-1200 m), and a deep layer consisting of the Norwegian-Greenland overflow water (2500-3500 m). The shallowest layer does not

make it through the crossover and is completely entrained by the Gulf Stream; however, the resulting deficit in equatorward transport is almost completely replenished by offshore entrainment just south of the crossover. In the layer below, which is denser than the Gulf Stream coming off the shelf, a portion of the DWBC recirculates to the northeast while the onshore-most portion continues equatorward. In the deep layer only a small amount recirculates. Maps of potential vorticity reveal a Q-barrier associated with the Gulf Stream in the mid-depth layers, which is lessened to allow the equatorward continuation in the deepest layer while maintaining its potential vorticity through the crossover.

Submitted to: Journal of Physical Oceanography.

Supported by: NSF Grant OCE90-09464.

WHOI Contribution No. 8040.

RECIRCULATION AND SEASONAL CHANGE OF THE KUROSHIO FROM ALTIMETRY OBSERVATIONS

Bo Qiu

Surface height fluctuations across an eastward flowing boundary current, such as the Gulf Stream and the Kuroshio, can be caused by changes both in the upstream inflow and in the neighboring recirculation gyres. Clarifying these causes is important in understanding the time-dependent nature of the boundary currents and their relationship to the surface wind and buoyancy forcing. Using satellite altimetry data to identify these causes, however, requires mean surface height field information, which is not readily available from the altimetry observation owing to lack of accurate geoid data. The present study presents a method to estimate the mean surface height profile across a boundary current system (includig recirculation gyres) by combining altimetrically measured residual height data and historical hydrographic data. Applying this method to the Kuroshio revealed that the absolute surface height profiles thus estimated agree well with the results from quarterly, in-situ hydrographic observations. By separating the signals of the surface height fluctuations into those of the eastward flowing jet and the recirculation gyres, we found that the seasonal cycle in the surface transport of the Kuroshio, which has a maximum in July and August, is primarily due to the seasonal change in the intensity of the recirculation gyre south of the Kuroshio.

Published in: Journal of Geophysical Research, 97(C11):17,801-17,811, 1992.

Supported by: ONR Contract N00014-92-J-1656. WHOI Contribution No. 7939.

A CENSUS OF EDDIES OBSERVED IN NORTH ATLANTIC SOFAR FLOAT DATA

Philip L. Richardson

SOFAR floats that looped in discrete eddies were studied in order to map and describe the distribution and characteristics of eddies in the North Atlantic. One hundred eighteen individual float trajectories in eddies (loopers) were identified, each consisting of 2 or more consecutive loops. The highest percentage of float days in loopers occurred at 700 m in the Newfoundland Basin, where roughly half of the data were in eddies, mostly cyclones. In the Gulf Stream region, approximately 20% of the float days recorded at 700 m are loopers, again mostly cyclones. Overall, 21% of 700 m data and 6% of 2000 m data are loopers.

The fastest swirl speeds, >40 cm/sec, were in cyclones (Gulf Stream rings) south of the Stream, but numerous swift ~35 cm/sec anticyclones were found there, too. Swirl velocity decreased with depth, to roughly half as swift at 2000 m as at 700 m for three eddies measured simultaneously with floats at these two depths in the Sargasso Sea. In the western North Atlantic, the average swirl velocity of cyclones and anticyclones was the same. The slowest swirl speeds, ~6 cm/sec, were found in anticyclones in the eastern Atlantic at 1100 m.

Advection velocity of eddies was generally westward to southwestward at a few cm/sec. The mean advection velocity of 39 eddies in the Sargasso Sea was $\bar{u}=-2.8\pm0.4$ cm/sec, $\bar{v}=-0.4\pm0.4$ cm/sec, compared to a nearly zero mean velocity of nonlooping floats. Near the Gulf Stream and along its extension in the Newfoundland Basin, eddies were often advected downstream with speeds up to 15–20 cm/sec and eddy trajectories were often complicated. South of 30N, and near the western boundary 700 m eddies were advected northwestward and 1300 m and 2000 m eddies southeastward by boundary currents there.

Numerous energetic anticyclones were observed south of the Gulf Stream; one was tracked for 430 days and its properties well measured. The formation of these eddies has not been documented, but they are inferred to have formed near and by the Gulf Stream and to consist of a thick layer of 18° water lying above a depression in the thermocline. Analogous anticyclones were observed in the Newfoundland Basin seaward of the Gulf Stream extension there.

Submitted to: Progress in Oceanography.

Supported by: NSF Grants OCE90-09463 and OCE89-16082.

WHOI Contribution No. 7933.

DEEP CROSS EQUATORIAL FLOW IN THE ATLANTIC MEASURED WITH SOFAR FLOATS

Philip L. Richardson and William J. Schmitz, Jr.

Neutrally buoyant SOFAR floats at nominal depths of 800, 1800, and 3300 m were tracked for 21 months in the vicinity of western boundary currents near 6N and at several sites in the Atlantic near 11N and along the equator. Trajectories at 1800 m show a swift (; 50 cm/sec). narrow (100 km wide) southward-flowing deep western boundary current (DWBC) extending from 7N to the equator. The average transport per unit depth in the North Atlantic DWBC was estimated to be 13.8×10^3 m²/s. Coupling this value with mean velocities measured in the DWBC by current meters in depths from 1400 to 2700 m (C. Colin) gave a volume transport of around 15 x 10^6 m³/s. Approximately 6×10^6 m³/s recirculated northward between the DWBC and the Mid-Atlantic Ridge, leaving 9×10^6 m³/s as cross-equatorial transport. No obvious DWBC nor swift equatorial current was observed by 3300 m floats, because a low mean velocity at this depth lay between higher freon and higher velocity cores above and below. Additional cross-equatorial transport presumably occurs below the 3300 m level.

The trajectories suggest that at times (February-March 1989) DWBC water turned castward and flowed along the equator and at other times (August-September 1990) the DWBC crossed the equator and continued southward. The velocity near the equator, calculated by grouping floats in a box along the equator, was eastward at 4.1 cm/sec from February 1989 to February 1990 and westward at 4.6 cm/sec from March 1990 to November 1990. Thus the amount of cross-equatorial flow in the DWBC appeared to be linked to the direction of equatorial current which varied over periods of more than a year.

Eight-hundred-meter floats revealed a northwestward intermediate level western boundary current although flow patterns were complicated. Three floats that significantly contributed to the northwestward flow looped in anticyclonic eddies that translated up the coast at 8 cm/sec. Six 800 m floats drifted eastward along the equator between 5S and 6N at a mean velocity of 11 cm/sec; one reached 5W in the Gulf of Guinea, suggesting that the equatorial current extended at least 35-40° along the equator. Three of these floats reversed direction near the end of the tracking period, implying low frequency fluctuations.

Submitted to: Journal of Geophysical Research.

Supported by: NSF Grants OCE85-21082 and OCE91-14656.

WHOI Contribution No. 8093.

MAN-INDUCED SALINITY AND TEMPERATURE INCREASES IN WESTERN MEDITERRANEAN DEEP WATER

Eelco J. Rohling and Harry L. Bryden

The historical data base is used to study property changes in both the Western Mediterranean Deep Water (WMDW) and the Levantine Intermediate Water (LIW). Changes in WMDW properties during the past century have been described previously, although on a more limited data base. We are not aware of any previous study of changes in LIW properties. In the extensive data base we used, increases appear in both WMDW temperature and salinity, from 1909 to the present, which substantiate previously reported observations. In addition, we find that the density of WMDW seems to have increased as well, which disagrees with previous suggestions that it has remained constant. We observe that the WMDW temperature increase displays a distinct acceleration starting about 1955 and that a similar, although less conspicuous, acceleration occurs in the WMDW salinity increase. From our study of historical data on LIW properties, the LIW salinity also appears to have increased since 1909. We argue that the warming trend in WMDW may well be a response to the salinity increase, which seems to be imported from the eastern Mediterranean by LIW, and as such our observations endorse a recently published hypothesis. The increase in LIW salinity, in turn, is attributed to changes in the eastern Mediterranean freshwater budget, resulting from damming of major rivers that drain either directly or indirectly into the eastern Mediterranean. Finally, we demonstrate that the basin has not yet reached a new steady state after this freshwater disturbance and that the response time of the system seems to be in the order of 100 years.

Published in: Journal of Geophysical Research, 97(C7):11,191-11,198, 1992.

Supported by: ONR Contract N00014-89-J-1085. WHOI Contribution No. 8020.

VARIATIONS IN SEA LEVEL, FRESHWATER BUDGET, AND HYDROGRAPHY IN THE MEDITERRANEAN

Eelco J. Rohling and Harry L. Bryden

The present paper focuses on changes in the Mediterranean hydrography related to glacial-interglacial sea level fluctuations and variations in the Mediterranean freshwater budget. First we discuss the influences of sea level change on the exchange transport through the Strait of Gibraltar, on the Atlantic-Mediterranean salinity contrast, and on the depth of the ir flow-outflow interface in the eastern end of the Strait of Gibraltar (at the narrows). These variations are studied with a recently developed hydraulic control model for that strait. The exchange transport and the interface depth at the narrows appear to decrease quasilinearly, whereas the salinity contrast shows a distinctly non-linear increase, with falling sea level. Subsequently, the results of the hydraulic control model are combined with recently developed two-layered models for the eastern Mediterranean, giving a model which describes how sea level fluctuations and variations in the eastern Mediterranean freshwater budget interact to determine depth variations of the eastern Mediterranean pycnocline. The sensitivity of that pycnocline depth model to literature-based discrepancies in the estimates of the present-day surface water inflow and excess evaporation is discussed. We conclude that the model results, which are presented in the form of ratios with respect to present-day values, remain valid as long as the ratio between the present-day estimates of surface water inflow and excess evaporation remains consistent. Applied to assess the eastern Mediterranean conditions at the Pleistocene-Holocene transition, when sea level stood 50 m below the present, the model suggests that excess evaporation was nearly 20% higher than today, that the Atlantic-Mediterranean salinity contrast and the salinity contrast across the eastern Mediterranean pycnocline were both about 50% higher than today, and that the inflow-outflow interface in the eastern end of the Strait of Gibraltar (at the narrows) resided at approximately 0.8 times its present depth.

Submitted to: Paleoceanography.

Supported by: ONR Contract N00014-89-J-1085.

WHOI Contribution No. 8001.

SURFACE-INTENSIFIED ROSSBY WAVES OVER ROUGH TOPOGRAPHY

R. M. Samelson

Observations and numerical experiments that suggest that sea-floor roughness can enhance the ratio of thermocline to abyssal eddy kinetic energy. motivate the study of linear free wave modes in a two layer quasi-geostrophic model for several cases of idealized variable bottom topography. The focus is on topography with horizontal scale comparable to that of the waves, that is, on "rough" small-amplitude topography. Surface-intensified modes are found to exist at frequencies greater than the flat-bottom baroclinic cut-off frequency. These modes exist for topography that varies in both one and two horizontal dimensions. An approximate bound indicates that the maximum frequency of the surface-intensified modes is greater than the baroclinic cut-off by a factor equal to the total fluid depth divided by the lower layer depth. For fixed topographic wavenumber, there is not a simple dependence of the degree of surface-intensification on topographic amplitude, but rather a resonant structure with sharp peaks at certain topographic amplitudes. These modes may be resonantly excited by surface forcing.

Published in: Journal of Marine Research, 50(3):367-384, 1992.

Supported by: ONR Contract N00014-91-J-1570. WHOI Contribution No. 8005.

TRIANGULAR AND ASYMMETRIC PLANFORMS FOR SALT FINGERS

Raymond W. Schmitt

Solutions are given for a rich variety. 'salt finger planforms. By using the two dimensional nature of the horizontal diffusion in the fingers, it is possible to combine sheet and rectangular base functions when specific relationships are maintained between the component wavenumbers. Some patterns are quite elaborate and seem unlikely to be realized. However, equilateral and right triangles are sufficiently simple that they might be observed in the laboratory. The solutions also allow fingers with asymmetric or "squarish" cross-section. The asymmetric modes appear to be consistent with the near-surface salt fountains reported by Osborn (1991).

Submitted to: Iournal of Physical Oceanography.

Supported by: NSF Grant OCE89-11053; ONR Contract N00014-89-J-1073.

WHOI Contribution No. 8207.

THE ROLE OF THE OCEANS IN THE GLOBAL WATER CYCLE

Raymond W. Schmitt and Susan E. Wijffels

An assessment is made of the contribution of the oceans to the global water cycle. Because of the multiply-connected nature of the world ocean, it is not possible to infer the transport of water by the oceans from surface forcing (E-P) and runoff alone. Direct ocean measurements are required to provide the constants of integration for summations of surface flux divergence in order to determine transports. The only inter-ocean transport known with any confidence is that through Bering Straits; it allows us to estimate the freshwater and salt transports in the North Pacific and Atlantic basins. An ocean transport picture emerges that is surprisingly different from that proposed by Baumgartner and Reichel (1975), who assumed zero freshwater transport across the Atlantic equator. Given the great uncertainties in evaporation and precipitation estimates over the oceans, direct ocean transport measurements provide important constraints on the global water cycle and must be more fully utilized in future research programs.

Submitted to: Hann Symposium Volume of AGU Geophysical Monograph Series.

Supported by: NOAA Grant NA16RC0522-01.

WHOI Contribution No. 7979.

ON THE FLORIDA CURRENT T/S ENVELOPE

William J. Schmitz, Jr., James R. Luyten and Raymond W. Schmitt

According to a recent study, the 30 Sv transported by the Florida Current through the Straits of Florida off Miami may consist of a wind-driven contribution of 17 Sv from the North Atlantic, along with a thermohaline component of 13 Sv from the South Atlantic. Here we examine this possibility in terms of temperature-salinity (T-S) and temperature-oxygen (T- 0_2) distributions. It is demonstrated that only part of the Temperature-Salinity Envelope for the Florida Current can be advectively traced back to the interior Atlantic along 24N. The fresh contribution, especially near the sea surface, can mostly be found to the south along 52W, and into the tropical South Atlantic. The salty contribution is present along 24N, although there are also fresh contributions from the Canary Current and from Continental Edge Water formed in the Gulf of Mexico. The T-S characteristics of the coldest

segment of the Florida Current (7–12°C) could be a product of comparatively fresh water of South Atlantic origin becoming slightly saltier by vertical mixing due to salt fingers in the tropical Atlantic and Caribbean. In the Caribbean passages there is an interesting partitioning of the Florida Current T-S envelope with Windward Passage dominating the salty segment and Anegada Passage playing a crucial role in the low temperature fresh segment. The South Atlantic contribution can be traced into the Caribbean and out of the Florida Straits in oxygen range as well.

Submitted to: Bulletin of Marine Science.

Supported by: NSF Grants OCE85-21082 and OCE89-11053; ONR Contracts N00014-89-J-1039, N00014-90-J-1425 and N00014-89-J-1073.

WHOI Contribution No. 8140.

A MECHANISM FOR LOW FREQUENCY VARIABILITY AND SALT FLUX IN THE MEDITERRANEAN SALT TONGUE

Michael A. Spall

A theory for low frequency variability in the interior of ocean subtropical gyres and its role in the zonal flux of salt within the Mediterranean salt tongue is presented The observed zonal enhancement of the low frequency variability is interpreted as the signature of baroclinic instability of the primarily meridional wind driven flow. The near zonal orientation results from the relatively weak vertical shear of the large scale upper ocean flow and the stabilizing influence of the planetary vorticity gradient. With regards to the dynamics of the Mediterranean salt tongue, there is a reversal of the vertical shear of velocity at mid-depths in the eastern basin of the North Atlantic which results in a local mid-depth maximum in the zonal eddy flux of density. Linear theory predicts a vertical structure of this density flux which is nearly coincident with the observed vertical distribution of the warm, salty water of the Mediterranean salt tongue. A nonlinear primitive equation model is used to investigate the large amplitude behavior of the instabilities and to obtain a quantitative estimate of the eddy density flux over the life cycle of the waves and the horizontal density ratio is used to convert this density flux into a consistent flux of salt. The waves carry an offshore flux of anomalous salt between 25°W and 10°W of approximately 1 Sv ppt, which accounts for a significant portion of the total estimated anomalous salt flux through the Strait of Gibraltar.

Submitted to: Journal of Physical Oceanography.

Supported by: NSF Grant OCE90-09463. WHOI Contribution No. 8049.

VARIABILITY OF SEA SURFACE SALINITY IN STOCHASTICALLY FORCED SYSTEMS

Michael A. Spall

The influences of horizontal advection and horizontal diffusion on the variability of sea surface salinity in stochastically forced systems are investigated. This problem is motivated by the sensitivity of the ocean thermohaline circulation to surface sainity and the resulting implications on the global heat budget and climate system. Basic ideas are developed using a two dimensional box model and then applied to a more realistic three dimensional ocean general circulation model. It is shown that, in the absence of advection and diffusion, the ocean response is essentially that predicted by Taylor's random walk model. Advection becomes important when the advective time scale is less than the response time of the mixed layer to the stochastic forcing amplitude, $\tau_a > 1$. Advection of parcels from regions of upwelling into regions of downwelling limits their exposure time to the stochastic forcing and thus the maximum attainable variance in the system (variance increases linearly with time). Regions of upwelling and downwelling may be introduced through the thermohaline overturning circulation or by the wind driven Ekman transport, depending on the specific model configuration. Horizontal diffusion is found to be important when the diffusive time scale is less than the mixed layer response time, $\tau_d > 1$. The primary role of diffusion is to reduce the effective stochastic forcing through rapid mixing of uncorrelated surface forcing events. Accurate knowledge of the stochastic forcing amplitude, decorrelation time, and length scale and distribution are critical to model the variance of sea surface salinity. Important aspects of the ocean model include the surface velocity, horizontal diffusivity, and the mixed layer depth. Implications on modeling of the ocean and coupled ocean-atmosphere systems are discussed.

Published in: Climate Dynamics, 8:151-160, 1993.
Supported by: NOAA Grant NA90AA-D-AC498.

WHOI Contribution No. 7952.

DIANEUTRAL MOTION, WATER-MASS CONVERSION AND NON-LINEAR EFFECTS ON THE DENSITY RATIO IN THE PACIFIC THERMOCLINE

Yuzhu You, Trevor J. McDougall and Raymond W. Schmitt

The averaged hydrography of Levitus (1982) has been used to form maps of various quantities that contribute to dianeutral advection in the Pacific thermocline. On much of the "26.50" neutral surface cabling and thermobaricity contribute between -0.2×10^{-7} m s⁻¹ and -2×10^{-7} m s⁻¹ to the total dianeutral velocity. The dianeutral advection caused by vertical turbulent mixing is also mapped on several surfaces in the Pacific Ocean. The upwelling across the "26.20" neutral surface, at an average depth of about 200 m, is positive and quite strong throughout the whole equatorial region. There is a striking pattern of strong dianeutral upwelling in the central Pacific on the "26.50" neutral surface, while in the eastern Pacific on the same surface there is a large region of downwelling. Subsurface water-mass conversion is defined as the rate at which fluid properties change on a neutral surface, and the contribution of vertical turbulent mixing to water-mass conversion is also evaluated and mapped in the Pacific thermocline.

In addition, we build on the work of Schmitt (1990) who first drew attention to the source term in the R_{ρ} equation caused by the action of vertical shear on the epineutral gradient of salinity or potential temperature. This term is shown to be similar to the term responsible for the path-dependence of neutral surfaces since both involve the expression $\nabla_n \bar{p} \times \nabla_n \bar{\theta}$. k. This term is evaluated on several surfaces in the Pacific and found to be small on basin scales, consistent with the relatively high density ratios found in the Pacific. We also derive several terms in the R_{ρ} equation which arise because of the nonlinear equation of state; these can be as large as the other terms in the equation.

Submitted to: Journal of Physical Oceanography.

Supported by: NSF Grant OCE89-11053.

WHOI Contribution No. 8161.

THEORETICAL AND LABORATORY MODELS

A GENERAL THEORY FOR EQUIVALENT BAROTROPIC THIN JETS

Benoit Cushman-Roisin, Larry Pratt and Elise Ralph

The so-called thin-jet approximation, in which variations along the jet axis are assumed gradual in comparison with variations normal to the axis, allows the calculations of along- and cross-axis structures to be decoupled. The result is a nonlinear equation, with one lesser spatial dimension, governing the meandering of the jet. Here a new such "path equation" is constructed in the context of a one-layer, reduced-gravity model. The formalism retains two distinct physical processes: a vortex-induction mechanism, originating from the jet curvature, that causes meanders to travel downstream (i.e., usually eastward), and the planetary (beta) effect, induced by meridional displacements, that gives the meanders the allure of Rossby waves and generates a westward (i.e., usually upstream) propagation.

After a brief comparison with previous path equations, analytical solutions of the new equation are explored, including solitons and other exact nonlinear wave forms. The presentation concludes with numerical experiments and a brief application to the Gulf Stream.

In Press: Journal of Physical Oceanography.

Supported by: NSF Grant OCE91-15359; ONR Contract N00014-89-J-1182.

WHOI Contribution No. 8021.

TIME-DEPENDENT ISOLATED ANOMALIES IN ZONAL FLOWS

Karl R. Helfrich and Joseph Pedlosky

A theory is developed for time-dependent coherent structures in a marginally stable atmospheric zonal flow. The coherent structures have the form of solitary waves traveling in the zonal direction. Analytical solutions are found for stationary solitary waves but these are shown to be always unstable. The instability manifests itself either as a fission of the structure subsequently emitting two oppositely directed traveling solitary waves or as an implosion in which the structure becomes increasingly more narrow and intense. Which of the two occurs depends sensitively on initial conditions.

These solitary waves are stable in head-on collisions only if their joint zonally integrated amplitude is less than a critical value, otherwise, the implosion instability occurs. General initial conditions can give rise to either solitary waves which split, implode, or break down to form a train of nonlinear wave packets.

A scenario for the birth and decay of isolated disturbances is given utilizing the slow parametric transit of the marginal stability curve of the background zonal flow.

Submitted to: Journal of Fluid Mechanics.

Supported by: NSF Grants ATM 89-03890 and OCE90-22088.

WHOI Contribution No. 8162.

LABORATORY SIMULATION OF EXCHANGE THROUGH FRAM STRAIT

Kenneth Hunkins and J. A. Whitehead

Laboratory experiments and theory were conducted to observe the flow patterns and transport in both buoyancy-driven and wind-driven and rotating fluids. In "lock-exchange" experiments water with one density flows into a second basin after a sliding gate is removed. Water of a second density flows back into the first basin. The size and location of the currents for various values of density difference, rotation rate, and assorted sidewall geometries was recorded. Volume flux of the fluid was also measured and compared with a theory for lock-exchange flow of a rotating fluid. In a separate group of experiments with a passive upper layer, easterly winds (like those in the Arctic Ocean) drive the upper level water into the Arctic Ocean and therefore oppose the buoyant exchange. Westerly winds would drive the water out of the Arctic Ocean. This indicates that the exchange between the Arctic Ocean and the Greenland-Norwegian Sea is likely to be driven by buoyancy rather than by driven by wind. Crude estimates of the volumetric and fresh water exchange rate from the lock-exchange formulas are compared with observed ocean fluxes, and approximate agreement is found.

Published in: Journal of Geophysical Research, 97(C2):11,299-11,321, 1992.

Supported by: ONR Contract N00014-87-K-0204. WHOI Contribution No. 7985.

THE REFLECTION OF UNSTABLE BAROCLINIC WAVES AND THE PRODUCTION OF MEAN COASTAL CURRENTS

Joseph Pedlosky

The problem of the reflection of unstable baroclinic waves from straight boundaries inclined with respect to latitude circles is studied. The basic flow in which the incident unstable wave is embedded is a flow with only vertical shear flowing parallel to the boundary. The analysis is done for a two-layer model on the β -plane.

For a wave packet centered on the most unstable wave, the reflection process produces two reflected modes each trapped to the boundary. The trapping scale is of the order of the Rossby radius of deformation. This trapping occurs whenever the current is inclined with respect to a latitude circle, in which case all shears, no matter how small, will support unstable waves.

It is argued that the trapped character of the reflected disturbance will produce a rectified current along the boundary with a net barotropic component.

Submitted to: Journal of Atmospheric Sciences.

Supported by: NSF Grant ATM 89-03890.

WHOI Contribution No. 8175.

LINEAR AND FINITE-AMPLITUDE LOCALIZED BAROCLINIC INSTABILITY

Joseph Pedlosky, Roger Samelson and Siang Peng Oh

The linear and finite-amplitude dissipative dynamics of unstable, zonally localized baroclinic disturbances is investigated in cases where the supercriticality varies in the zonal direction. The zonal confinement occurs due to 0(1) variations of the frictional influence on the current's instability. A two-layer f-plane model is used. No meridional shear is present in the basic shear flow.

When the basic current is equal and opposite in the two layers, two zonally localized modes with the same growth rate and opposite symmetries exist for all unstable parameter values. Thus an infinite family of unstable modes formed from an arbitrary linear combination of these two modes exists. This degeneracy persists in finite amplitude. Hence the phase of individual crests in the disturbance is a function of initial conditions even for dissipative localized instabilities.

The presence of a mean barotropic flow reduces the growth rates of the localized

disturbances and expunges the symmetry properties of the mode and the resulting degeneracy. The disturbance becomes time-dependent due to phase translation of crests. Localized modes exist even when the flow in both layers is in the same direction. In finite amplitude there is a weak vacillation in energy level.

A discussion of the appropriate boundary condition for the localized modes suggests that the total geostrophic perturbation streamfunction should vanish on the flow boundaries.

Submitted to: Journal of Atmospheric Sciences.

Supported by: NSF Grant OCE91-01461; ONR Contract N00014-91-J-1570.

WHOI Contribution No. 8163.

LINEAR INSTABILITY OF A MIXED-LAYER FRONT

R. M. Samelson

The linear instabilities of a geostrophically-balanced frontal jet are computed numerically in an effort to understand the origin of intense small-scale cold-core features observed in the North Atlantic Subtropical Convergence Zones (STCZ) during the Frontal Air-Sea Interaction Experiment (FASINEX). A simple analytic continuously-stratified basic state is used to represent the observed frontal structure. The most unstable linear modes have e-folding timescales near 15 days, alongfront wavelengths near 60 km, and significant asymmetry across the front. The results provide indirect evidence that baroclinic instabilities of the frontal jet are the source of the cold-core features observed during FASINEX.

Submitted to: Journal of Geophysical Research.

Supported by: NSF Grant OCE91-01461.

WHOI Contribution No. 8189.

A LABORATORY MODEL OF COOLING OVER THE CONTINENTAL SHELF

J. A. Whitchead

A laboratory experiment is conducted where water is cooled by exposure to air in an annular rotating tank with a flat shallow outer "continental shelf" region next to a deeper center region with a sloping conical "continental slope" bottom and a flat deep "ocean" center. Cooling rate is estimated and compared with the temperature difference between "continental shelf" and "deep ocean". It is taken to be a model of wintertime cooling over a continental shelf. Temperature difference as a function of cooling rate is compared with scaling

arguments to produce an empirical best fit formula that agrees with the experiment remarkably well. If this formula is valid for the ocean, water over continental shelves will be much colder due to constraints imposed by rotation of the earth than would be the case if the fluid were not rotating.

Submitted to: Journal of Physical Oceanography.

Supported by: ONR Contract N00014-89-J-1037.

WHOI Contribution No. 8059.

FLOWS DUE TO SURFACE COOLING IN A ROTATING FLUID

J. A. Whitehead, R. E. Frazel and Brian Racine

Three laboratory studies will be described that focus upon the sinking of rotating water from surface cooling. In the first, water cooled in a shallow bay can be removed by density currents of cold water than lean on the bay sidewalls. In the second, water cooled over a shallow but infinitely long continental shelf either adopts a lock-exchange density driven flow or breaks up into heton like eddies. In the third, dense water is formed in deep ocean regions where surface density is highest to begin with, and gyres with closed streamlines allow cooling to have a large cumulative effect. Two instability scales coexistgiant Rayleigh Benard cells transport the cold water downward for periods of days and baroclinic eddies mix from the sides. Photographs of the currents are shown along with laboratory measurements of the rates of the flushing that the dense water encounters for the various geometries.

Submitted to: Dynamics of Atmosphere and Oceans or Laboratory Experiments.

Supported by: ONR Contract N00014-89-J-1037; NSF Grant OCE89-15408; the Summer Student Fellowship from the Education Program at the Woods Hole Oceanographic Institution.

WHOI Contribution No. 8121.

STIRRING A STRATIFIED FLUID-ENERGETICS AND MICROSTRUCTURE GENERATION

J. A. Whitehead, Young Gyu Park and Anand Gnanadesikan

Oceanic mixing operates under the constraint that the potential energy in the stratification is much larger than the kinetic energy of the fluid. This means that the mixing eddy scale will not be as large as the entire water column. We argue that energetic considerations alone indicate that layered structures may be a signal of such mixing and

present results of a laboratory experiment to test this idea. Layers were formed in a salt-stratified fluid by stirring it with a rod at large Richardson and Reynolds numbers. The layers evolved over time, with small layers forming first, and larger layers appearing at later times. The change in potential energy of the density field is compared with estimates of work done by the mixer for the assorted cases. Mixing efficiencies ranged from 0.18 down to less than 0.02, the lower values being for longer times after layers had matured. Layers are formed when the effective eddy diffusivity of the fluid (defined as the area-averaged potential energy change over the square of the buoyancy frequency) is less than 0.2 cm² s⁻¹. A scaling of the flux Richardson number to various parameters shows that the formation of layers is consistent with the theories of Phillips and Posmentier. Energetics show that the early change in potential energy goes into producing steps. In the later stages density flows straight from bottom to top through steps. We suggest that the average ocean region is usually in the early stage.

Submitted to: Journal of Fluid Mechanics.

Supported by: NSF Grant OCE89-15408.

WHOI Contribution No. 8130.

COASTAL CIRCULATION & DYNAMICS

A NUMERICAL STUDY OF STRATIFIED TIDAL RECTIFICATION OVER A FINITE-AMPLITUDE SYMMETRIC BANK

Changsheng Chen and Robert C. Beardsley

Homogeneous and stratified tidal rectification over a two-dimensional finite-amplitude symmetrical bank is studied using the Blumberg and Mellor primitive-equation numerical coastal ocean circulation model with turbulent closure. In the homogeneous case, the tidal currents are characterized by the linear inertial-gravity wave equation modified by horizontal advection. The nonlinear interaction of these tidal currents with the variable bottom topography generates a clockwise jet-like residual circulation around the bank, which tends to increase as either the slope or height of the bank is increased. When initial stratification is included, tidal currents become modified by nonlinear advection, the baroclinic pressure gradient, and vertical friction. Internal waves at tidal and higher frequencies are generated over the sloping sides of the bank, and tidal mixing occurs in the bottom boundary layer which leads to horizontal tidal mixing fronts. The resulting

stratified tidal rectification associated with the tidal mixed front, the generation of internal tides. and the modification of internal friction due to stratification leads to a subsurface intensification of the along-isobath residual current at the front and at the top of the bottom mixed layer over the slope, and a cross-bank double cell circulation pattern centered at the front near the shelf break. The predicted residual currents agree well with previous analytical and numerical work in the homogeneous case, and are consistent with theories of stratified tidal rectification. Model results for tidal mixing are in reasonable agreement with a simple energy argument in which the thickness of the tidal mixed layer is proportional directly to the magnitude of the tidal current and inversely to stratification.

Submitted to: Journal of Physical Oceanography.

Supported by: NSF Grants OCE87-13988 and OCE91-01034; NCAR Grants 35781029 and 35781035.

WHOI Contribution No. 8214.

A NUMERICAL STUDY OF STRATIFIED TIDAL RECTIFICATION OVER GEORGES BANK

Changsheng Chen, Robert C. Beardsley and Richard Limeburner

Homogeneous and stratified tidal rectification over Georges Bank is studied using a two-dimensional version of the Blumberg and Mellor primitive-equation, numerical coastal-ocean circulation model. In the homogeneous case, the model predicts a topographically controlled clockwise residual circulation around Georges Bank, flowing northeastward as a strong jet with a maximum speed of about 16 cm/s along the northern flank and southwestward as a relatively weak and broad flow with a maximum speed of about 3 cm/s from the top of the bank to the southern flank. As stratification is added, internal tidal rectification and tidal mixing intensify the along- and cross-isobath residual currents, and create tidal fronts which modify the vertical structure of the residual flow. During summer, the tidal fronts are located at the 40-m isobath on the northern flank and at the 50-60-m isobath on the southern flank, and the maximum of the along-bank current is increased to about 32 cm/s on the northern flank and 8 cm/s on the southern flank. During winter, the position of the tidal front remains fixed on the northern flank, however, it moves to the shelf break on the southern flank. The winter maximum of clockwise along-bank residual flow is about 26 cm/s on the northern flank and about 6 cm/s at the shelf break on the

southern flank. The model results are consistent with theories for stratified tidally driven flow, and in good agreement with observations on the northern flank. The summertime intensification of the residual flow is mainly due to nonlinear interaction between the stratified tidal currents over the northern flank where the bottom topography is relatively steep and to the baroclinic density gradient created in part by tidal mixing over the southern flank where the bottom slope is relatively small.

Submitted to: Journal of Physical Oceanography.

Supported by: NSF Grants OCE87-13988 and OCE91-01034; NCAR Grants 35781029 and 35781035.

WHOI Contribution No. 8215.

ON THE ESTABLISHMENT OF THE SEASONAL PYCNOCLINE IN THE MIDDLE ATLANTIC BIGHT

David C. Chapman and Glen Gawarkiewicz

Each year the hydrography of the Middle Atlantic Bight changes dramatically from winter conditions with strong horizontal gradients of temperature, salinity and density at the shelfbreak separating shelf and slope waters to the summer stratification with a sharp pycnocline at about 20 m depth across both the shelf and slope. We use a simple one-dimensional diffusion model to demonstrate that this change could result from a uniform surface heating provided that the nonlinearity of the equation of state is taken into account.

Submitted to: Journal of Physical Oceanography.

Supported by: NSF Grants OCE88-16015 and OCE90-16893.

WHOI Contribution No. 8208.

TRAPPING OF A COASTAL DENSITY FRONT BY THE BOTTOM BOUNDARY LAYER

David C. Chapman and Steven J. Lentz

The fate of a surface-to-bottom freshwater inflow onto a uniformly sloping continental shelf is examined using a three-dimensional, primitive-equation, numerical model. The model is linearized except that it allows the advection of density and its feedback to the velocity field. The freshwater inflow turns anti-cyclonically and moves along the coast, generating offshore transport in the bottom boundary layer which advects fresh water offshore and creates a sharp

surface-to-bottom density front with a strong surface-intensified alongshelf jet centered over the front. The offshore buoyancy flux in the bottom boundary layer moves the front offshore until it reaches a depth where the vertical shear within the front causes a reversal in the alongshelf velocity across the entire base of the front. At this point the offshore buoyancy flux in the bottom boundary layer vanishes and the front is 'trapped' to this isobath, i.e. it remains parallel to this isobath and does not move farther offshore. The final offshore location of the front exhibits fairly weak dependence on the inflow density and velocity, and is consistent with a simple thermal-wind relation. The results suggest that the advection of density in the bottom boundary layer, which dominates the dynamics of the robust circulation pattern studied here, may have an important influence on shelf dynamics.

Submitted to: Journal of Physical Oceanography.

Supported by: NSF Grants OCE88-16015 and OCE91-15713.

WHOI Contribution No. 8195.

SEDIMENT RESUSPENSION OVER THE CONTINENTAL SHELF EAST OF THE DELMARVA PENINSULA

James H. Churchill, Creighton D. Wirick, Charles N. Flagg and Leonard J. Pietrafesa

Resuspension of sediment over the continental shelf east of the Delmarva Peninsula has been examined using records of light-beam attenuation, near-bottom current speed and surface-wave height spectra collected during 1988 and 1989. These data give evidence of a factor of three variation in the bottom stress threshold required for sediment resuspension at the outer shelf. This appears to be related to resuspension history as the largest thresholds are observed after lengthy periods without resuspension. Episodes of shelf-wide sediment resuspension are evidenced on only during very intense atmospheric storms. A 7-month-long set of records from the 90 m isobath show storm-induced sediment resuspension on only three occasions. The failure of storms of modest intensity to effect resuspension at the outer shelf is largely due to the decline of surface-wave currents with depth. High-frequency currents, presumably due to internal waves, are shown to be an important agent in initiating sediment motion at the shelf edge. On a number of occasions, supertidal currents pushed the near-bottom current speed measured near the seafloor at the 131 m isobath above the estimated level required for sediment resuspension. Numerous clouds of turbid water detected by the light-beam attenuation

records could not be attributed to local sediment resuspension. A probability analysis indicates that some, but not all, of these could have resulted from sediment resuspension by bottom fishing.

Submitted to: Continental Shelf Research.

Supported by: Department of Energy 11068101.

WHOI Contribution No. 7953.

STEADY WIND FORCING AND RELAXATION OF A DENSITY FRONT OVER A CIRCULAR BANK

Glen Gawarkiewicz

The response of a density front along the edge of a circular bank to wind forcing is examined using a primitive equation numerical model. The density front is allowed to geostrophically and frictionally adjust for ten days from an initial configuration in which light vertically homogeneous water is present in the center of the bank and the density increases linearly with radial distance to the edge of the bank. The adjusted flow is anti-cyclonic over most of the water column and is a maximum at the surface. A weak cyclonic flow is also present near the bottom. This flow is then forced by a spatially uniform, steady wind stress. The surface velocity field of the bank is asymmetrical, with a relative maximum on the downwind side of the bank to the left of the wind direction and a relative minimum on the upwind side of the bank to the right of the wind direction. For the case of small Ekman number considered here, the density-driven flow persists beneath the surface Ekman layer. Light fluid is advected off the bank near the surface in the direction of Ekmar. transport, weakening the surface density gradients. On the opposite side of the bank, the vertical structure of the density field is weakened and the surface density gradients remain relatively constant. After the wind is relaxed, the anti-cyclonic surface velocity is restored in one inertial period, and light fluid remains off the bank. Neutrally buoyant near-surface particles are primarily lost from the downwind region of the bank and the region to the right of the wind direction. The presence of the density front slightly increases the number of particles lost from the bank. A simple formula for the particle loss is presented.

Submitted to: Journal of Marine Research.

Supported by: NSF Grant OCE88-16015.

WHOI Contribution No. 8141.

THE RESPONSE OF THE SHALLOW POLAR SHELF WATER TO NEGATIVE BOUYANCY FORCING: A NEGATIVE STUDY

Hsiao-ming Hsu

The Arctic and Antarctic shelves are both primary source regions producing dense water due to wintertime ice formation. The relatively cold and saline shelf water from atmospheric cooling and brine rejection descends along the continental shelf and slope to the deeper ocean and possibly to the bottom of the ocean. This water makes a significant contribution to the deep thermohaline circulation, and has a strong impact on global climate.

To study the evolution of the dense water and the density current on the shallow shelf and their dynamic structures, a three-dimensional, primitive-equation, ocean circulation numerical model has been coupled with a second-order. turbulent-closure model for this purpose. The model ocean is forced by a constant negative buoyancy flux over a limited open-ocean surface bounded by the coast and sea ice, the coastal polynya. It is assumed that the polynya is maintained by the ice divergence at and near the coast, and that ice forms within the polynya is continuously removed toward the ice edge by an offshore surface current. In order to focus the essential dynamical processes, only vertical cross-shelf variability will be studied with the assumption of no along-shelf variation.

Numerical results indicate a density current can be formed by the downslope pressure gradient force and gravity of the shelf without rotation. With rotation, a density front, which separates the dense water pool from the rest of the shelf water, is maintained under the geostrophic adjustment process. With the addition of an along-shelf geostrophic current, the bottom Ekman transport makes a descending density current in the bottom boundary layer. Wind stress is not only directly responsible for inducing the surface current which removes newly formed ice, but also dynamically produces its own shelf circulation. Within the dense water pool, the along-shelf wind stress can generate coastal upwelling with downwelling at the density front. A density current can be generated from the dense water pool by the offshore branch of the near-bottom downwelling divergence and be further enhanced by the occurrence of the bottom boundary-layer transport due to the along-shelf geostrophic current. These near-bottom density currents can be widespread on a shelf and slope without any topographic features because these processes are shelf-wide and non-local.

Submitted to: Journal of Physical Oceanography.

Supported by: Coastal Science Program; ONR Contract N00014-91-J-1473.

WHOI Contribution No. 8190.

INSTRUMENTATION & EXPERIMENTAL NUMERICAL METHODOLOGY

A VERTICAL COORDINATE MAPPING TECHNIQUE FOR SEMI-SPECTRAL PRIMITIVE EQUATION MODELS OF OCEANIC CIRCULATION

Albert J. Hermann and Hsiao-ming Hsu

A stretched coordinate technique for semi-spectral hydrodynamic models is described, which allows for greater flexibility in the placement of model gridpoints. Stretching is implemented here for the vertical coordinate of an oceanic model which employs Chebyshev polynomials to represent the vertical structure. A three-dimensional test demonstrates how the technique permits greater accuracy in the simulation of internal Kelvin waves, by allowing the placement of gridpoints closer to the regions of maximum curvature in the represented velocity fields. A one-dimensional test demonstrates enhanced accuracy in the simulation of mixed layer dynamics for a Richardson number-based mixing scheme, by allowing the placement of more of the available gridpoints near the ocean surface. These improvements in accuracy are achieved with negligible computational overhead. While the method cannot yield improved accuracy for all situations, for appropriate cases it permits fewer gridpoints, and hence reduced computation, for an accurate result.

In Press: Journal of Atmospheric and Oceanic Technology.

Supported by: ONR Contract N00014-86-K-0751.

WHOI Contribution No. 7974.

A NOTE ON THE ACCURACY OF TIDE GAUGE MEASUREMENTS AT SUBTIDAL FREQUENCIES

Steven J. Lentz

The accuracy of subinertial sea level data is investigated using measurements tide gauge in the Southern California Bight. Sea level differences formed from tide gauges separated by less than 50 km are examined. The observed differences give an upper bound on errors in the sea level data, provided errors at each station are uncorrelated

with each other and with the true sea level signal. Sea level measurements at the San Diego and La Jolla tide gauges are also compared with simultaneous bottom pressure measurements made on the shelf 25 km north of San Diego. Both comparisons suggest that rms errors in tide gauge measurements of sea level are of order 1.5 cm. Approximately half of the observed error variance has a time scale of 1 month and is due, in part, to inaccuracies in determining reference levels.

Submitted to: Journal of Atmospheric and Oceanic Technology.

Supported by: NSF Grant OCE84-10546.

WHOI Contribution No. 8047.

A COMPARISON OF TECHNIQUES FOR REFERENCING GEOSTROPHIC VELOCITIES

Robert S. Pickart and Scott S. Lindstrom

A geostrophic velocity section across the Gulf Stream and Deep Western Boundary Current (DWBC) near 35° N is referenced four different ways: using POGO floats, shipboard Acoustic Doppler Current Profiler, bottom current meters, and by assuming an isotherm level of no motion. The comparison between the first two techniques is emphasized because they are most easily applied. In general, reference velocities calculated using the float data agree well with those obtained from the ADCP data. However, there is disagreement at locations where the ADCP velocity is not in thermal wind balance, in which case the POGO value is deemed more accurate because the float samples deeper into the subsurface geostrophic flow. Disagreement is also caused by insufficient cross-stream POGO spacing (although this could be avoided). The isotherm- and current meter-referenced sections, while similar to each other, both show unrealistic features. It is argued that the POGO method is preferable for a deep water hydrographic experiment.

Submitted to: Journal of Atmospheric and Oceanic Technology.

Supported by: NSF Grant OCE90-09464.

WHOI Contribution No. 8236.

OTHER

BATHYMETRY AT THE VEMA SILL

Walter Zenk, Kevin G. Speer and Nelson G. Hogg

The Vema channel represents a prominent location for the northward flow of bottom water in

the subtropical western South Atlantic. The history of its detection and its terminology are reviewed. A multibeam echo-sounding survey of the Vema Sill on board FS METEOR revealed significant details of the seafloor. Results are presented as a 3-D surface plot and as a bathymetric map (1:250 000). Due to remarkably asymmetric shape of the sill region we raise the question of the interaction between the bottom flow and the shape of the channel.

In Press: Deep-Sea Research.

Supported by: Deutsche Forschungsgemeinschaft (Si 111/38-1) and the Fundesminister für Forschung and Technologie (3FO535A); NSF Grant OCE90-04396.

WHOI Contribution No. 8027.

MARINE POLICY CENTER James M. Broadus III, Director

NORTH SEA HERRING FLUCTUATIONS

Roger S. Bailey and John H. Steele

In historical terms, the North Sea herring is one of the most important marine fish resources in the world; yet in 1977 the directed fisheries were closed following a collapse of the stocks to a small fraction of their earlier levels. A voluminous literature documents the sequence of activities that led up to the closure, but only in hindsight can a reasonably convincing account of the causes be assembled and, even now, there are aspects of the problem that defy explanation. In this contribution, the history of the collapse and subsequent recovery is briefly summarized. In particular, the question addressed is the relevance of environmental changes and whether action could have been taken to prevent or mitigate stock collapse. The impact of the collapse on the fishing industry is discussed and an evaluation is given of what might be required to avoid the consequences of stock collapse in similar instances in the future.

Published in: Climate Variability, Climate Change and Fisheries, Michael H. Glantz, ed. Cambridge University Press, :213-230, 1992.

Supported by: The International Council for Exploration of the Sea, and National Science Foundation grant no. OCE-90-10847.

BIODIVERSITY, RIODIVERSITY

James M. Broadus

This is a report on the outcome of the "Earth Summit" (more properly, the United Nations Conference on Environment and Development, or UNCED) convened in Rio de Janeiro in the summer of 1992. The official conference issued five major products, and all of them touch on ocean affairs in one way or another. The Biological Diversity Convention intends to assure that national actions are taken to curb the destruction of biological species, habitats, and ecosystems. It is important to note that biological diversity is not a very precise object of conservation. Like "sustainability," it seems easier to advocate than to define. The Rio Convention takes it to encompass all the earth's plant, animal, and microorganism species, and the ecosystems of which they are a part. That, of course, pretty well covers everything. It hardly defines a "diversity" resource that can be conserved in the face of competing demands on scarce conservation resources.

Published in: Oceanus, 35(3):6-9,1992.

Supported by: The Marine Policy Center.

CREATURE FEATURE TOO: PRINCIPIUM PRECAUTIONARIUM

James M. Broadus

This is a commentary on a newly emerging doctrine in international law called the "precautionary principle". The problem with the precautionary principle is that it is not a principle at all, but a range of more-or-less rhetorical prescriptions for choice in the face of uncertainty. At its best-in permitting controls even where scientific proof of harm is lacking-the precautionary principle tells us nothing new about how to make prudent decisions. At its worst-in effect requiring proof of no harm before permitting any activity- the precautionary principle is a prescription for absurd and self-defeating choices that completely ignore any reasonable balancing of benefits and costs. If the precautionary principle is to become an integral part of our environmental policies, as now seems probable, a "rule-of-reason" version is needed.

Published in: Oceanus, 35(1):6-7,1992.

Supported by: The John D. and Catherine T.

MacArthur Foundation, the U. S. Environmental
Protection Agency, The Marine Policy Center,
and Oceanus.

WHOI Contribution No. 8057.

JOINT DEVELOPMENT OF NONFUEL MARINE MINERALS IN ASIAN SEAS

James M. Broadus and Porter Hoagland

This paper examines the prospects for joint development of nonfuel marine minerals in east Asian marginal seas. The continuation of existing disputes and the possibilities of heightened conflict resulting from false claims of the economic significance of nonfuel resources in the China Seas are real. We note the relationship between potential resource locations and jurisdictional disputes, on the presumption that joint development may be one device for overcoming some of the disadvantages arising from those disputes. Several modes of joint development are identified, mostly drawn from practices in offshore hydrocarbons, and the cases of joint research associations and deep seabed mining consortia are singled out for special attention. We conclude that joint development projects should be adaptive, uniform, and flexible. Partners in joint development should diversify and avoid committing to a single contingent outcome, reserve action and "wait-and-see", and invest in learning. Joint development relationships are very likely to enable Asian countries to build confidence in each

other as partners, to gain additional experience in planning and managing large-scale international industrial R&D projects, and to hedge against the risk of shortfalls in the supply of certain minerals in the long run. Careful, ongoing investigations of the economic potential and expected net benefits from resource development should be an important element of all joint exploration and development projects organized by the countries of the Asian seas.

In Press: Proceedings of International Conference on East Asian Seas, M. Valencia and S. Hugh, eds.

Supported by: Sea Grant, the East-West
Center-United Nations University, the Korea
Ocean Research and Development Institute
(KORDI) and The Marine Policy Center.

WHOI Contribution No. 8278.

PROTECTING BIODIVERSITY

James M. Broadus

This note comments on Reid's (1992) call for a National Commission on Biodiversity. The idea is apt and timely. There is growing recognition of biological diversity as an important natural resource in its own right. A commission should recognize the importance of marine biological diversity and break the fixation on land management and forests. Another issue is the confusion about the objectives of biodiversity conservation and when they might differ from more traditional "biological resource management" (which often reduces diversity).

Published in: Issues in Science and Technology, IX(1):12-13, 1992.

Supported by: The Pew Charitable Trusts and The Marine Policy Center.

REGARD D'OUTRE-ATLANTIQUE (ON EUROPEAN OCEAN POLICY AND SECURITY)

James M. Broadus

Like European security policy, Europe's ocean policy is unsettled, in a condition of great flux, because of rapidly changing circumstances. Europe is groping toward formal economic and political integration, as the whole world becomes, ad hoc, more economically integrated and politically interdependent than ever before. The Cold War has ended, and the future of the Atlantic Alliance is at issue. The former Soviet Union has disintegrated into institutional chaos, adding a new dimension to traditional North-South tensions that

often seem to revolve around ethnic and religious differences (e.g., Christendom vs. Islam) as much as economic inequalities. At the same time, there is a renewed awareness that security cannot be limited to defense arrangements, but must also involve economic and environmental affairs. Two proposals for European ocean policy: (1) The European community should work to achieve a stable and universally respected international Law of the Sea. (2) A second, longer-term centerpiece for a new European ocean policy would be the creation of a unified European Maritime Space.

Published in: Saviors/Le Monde diplomatique, :88-90, 1992.

Supported by: The John D. and Catherine T.

MacArthur Foundation, the U. S. Environmental
Protection Agency, and The Marine Policy
Center.

WHOI Contribution No. 8056.

REGULATORY/ECONOMIC INSTRUMENTS FOR AGRICULTURAL POLLUTION: ACCOUNTING FOR INPUT SUBSTITUTION

Mark E. Eiswerth

This article explores conceptual approaches to the problem of simultaneously managing multiple categories of agricultural water pollution. A key complication in the control of agricultural pollution is that a policy applied to one type of pollutant or agricultural input (say, a tax on the use of persistent pesticides) can alter farm management practices and lead to an increase in the release of other pollutants (e.g., the runoff of nutrients such as phosphorus). This suggests a possible tension between reducing surface water and groundwater pollution. This article first shows how the "least-cost" spatial pattern of the reduction of a given pollutant may change if a link between that pollutant and other pollutants is considered. Second, a dynamic optimization model is presented that accounts for possible long-term damages that may result when agricultural pollutants (e.g., pesticides) leach into groundwater. Such a model illustrates the way in which site-specific characteristics influence the desired balance between surface water and groundwater pollution abatement.

In Press: Theory, Modeling and Experience in the Management of Nonpoint-Source Pollution, Clifford S. Russell and Jason F. Shogren eds. Kluwer Academic Publishers.

Supported by: The John D. and Catherine T.

MacArthur Foundation, The Pew Charitable
Trusts, and The Marine Policy Center.

WHOI Contribution No. 7994.

UNIVERSITIES, RESEARCH INSTITUTIONS, AND PATENT ASSIGNMENTS

R. Scott Farrow and Porter Hoagland

Many universities and research organizations require that employees assign a share of all patent earnings to the organization. A few patents can earn substantial royalties for both the inventor and the organization, but many patents do not, and many more ideas are never patented. Another component of the invention and innovation system is that concentrations of development and innovation occur close to major research organizations (such as along Route 128 in Massachusetts and Silicon Valley in California) and often are based on technologies developed by former employees of the research centers. This note describes the current practice of many research organizations and presents a model of the effect of patent assignments on the actions of individual researchers and on the objectives of the research organization.

Submitted to: Research Policy.

Supported by: NOAA, through grant no.
NA26AD0156 to The Massachusetts Center for
Excellence in Marine and Polymer Sciences; and
The Marine Policy Center.

WHOI Contribution No. 8286.

THE WOODS HOLE OCEANOGRAPHIC INSTITUTION, MASSACHUSETTS

Arthur G. Gaines

The Woods Hole Oceanographic Institution was founded in 1930 to invigorate the ocean sciences in America. It was to be the third and largest in a community of marine institutes at Woods Hole, MA, beginning with the founding of the U.S. Fisheries Commission and the Marine Biological Laboratory in the late 19th century. These institutions have specialized but partially overlapping functions, which together address the broad topics of ocean science, management and policy, and the special window into the biological sciences from the marine perspective. Education programs ranging from grade school through postdoctoral remain an integral part of the community and its service to society. This essay provides a short history of the ocean sciences community at Woods Hole and some of the principal figures responsible for its development, including scholars, businessmen, and philanthropic organizations.

Published in: Ocean Frontiers, Explorations by Oceanographers on Five Continents, E. Mann Borgese, ed. Harry N. Abrams Publishers, Inc., New York, :54-93, 1992.

Supported by: The publisher.

MEASURING VOTING POWER ON THE COUNCIL OF THE INTERNATIONAL SEABED AUTHORITY

Porter Hoagland

Kim (1989) has proposed a weighted voting scheme for the Council of the International Seabed Authority, a decisionmaking organ to be established under the provisions of the United Nations Convention on the Law of the Sea. Such a voting scheme might encourage some of the nations that have not yet signed the Convention to move toward signature and to participate more fully in preparatory discussions. In this article, we employ two measures from cooperative game theory, the Shapley value and the Banzhaf value, to calculate the voting power of nations on the Council and on one of its subsidiary organs, the Legal and Technical Commission. Under certain reasonable assumptions, we show first that, even with an unweighted voting scheme, nations on the Legal and Technical Commission can be as much as eight times as powerful as nations that are on the Council but not on the Commission. The extent of voting power depends upon the decision rule in effect and the number of nations present for a vote. Second, we analyze Kim's proposed weighted voting scheme. We show that for a majority decision rule under both voting power measures the nation that is given the largest voting weight is actually more powerful than its assigned voting weight suggests (and vice versa for nations with lower voting weight assignments). As the decision rule is strengthened, significant differences appear in voting power as calculated by the two voting power measures. These differences are attributable to assumptions about the extent to which nations make decisions independently when casting their votes for any particular issue. As a result, strategic advantages may exist for those nations which select a measure of voting power most appropriate for any specific voting situation.

In Press: Ocean Research.

Supported by: The Marine Policy Center.

WHOI Contribution No. 8124.

TECHNOLOGY TRANSFER IN OCEANOGRAPHY

Porter Hoagland and Hauke Kite-Powell

How can scientific research results be disseminated and applied in a way that fosters the achievement of national goals such as economic competitiveness, public health, national security, and environmental protection? This "technology transfer" question is central to the emerging debate in the field of science policy concerning the "relevance" of scientific research. During the last decade, much discussion has been generated about the concept of technology transfer, yet it is remarkable that few have attempted to think carefully and clearly about the meaning of the term. In this article, we begin to probe its meaning. Technology transfer is linked to the process of new knowledge creation, and it involves many issues that are fundamentally economic. We therefore adopt an economic approach, examining the issue from the incompletely aligned perspectives of society and the research laboratory. We conclude that substantial technology transfer takes place in oceanography, primarily through the published scientific literature. It is unclear whether or not additional benefits either for society or individual research laboratories can obtain through "forced" technology licensing of patents and other intellectual property rights. Nevertheless, it is sensible, if not necessarily economically efficient, for federal policies to facilitate technology transfer in any form and to permit research institutions the flexibility to choose the most appropriate form for their technology transfers.

Submitted to: Oceanography.

Supported by: ONR grant no. N00014-93-I-0028; and NOAA, through grant no. NA26AD0156 to The Massachusetts Center for Excellence in Marine and Polymer Sciences.

WHOI Contribution No. 8230.

CHINA SEA COASTAL AND MARINE NONFUEL MINERALS: INVESTIGATION AND DEVELOPMENT

Porter Hoagland, J. Yang, James M. Broadus, and David K. Y. Chu

In this chapter, we survey the economic potential of coastal and marine nonfuel minerals in the East and South China Seas. We describe briefly the mineral economies for eight China Sea countries and review historic and current efforts in exploration, development, and production of coastal and marine nonfuel minerals. The benefits of CCOP, an international joint prospecting

organization, are described. Using 1984 data based upon production of marine sand and gravel in Kyushu, Japan, marine tin production in Indonesia, and marine salt production in China, the countries surrounding the two China Seas produce about one-third of a billion dollars' worth of marine nonfuel minerals annually. This figure is small in comparison, for example, with offshore crude oil production, estimated at \$11 billion in that year. From a global perspective, output of marine nonfuel minerals from the East and South China Seas is proportionately much more important to world marine nonfuel production than the output of marine hydrocarbons from the same region is to world marine hydrocarbon production. Taking only sand and gravel and tin production, the marine mines in these two seas produce almost one-quarter of Broadus' (1987) estimated \$600 million annual revenues from all seabed nonfuel materials worldwide. Nearshore minerals have the best prospects, and the prospects for deepsea minerals, although they occur in the region, are remote and should not influence maritime boundary settlements.

Published in: Resources and Environment in Asia's Marine Sector, J. B. Marsh, ed. Taylor & Francis, Washington, DC, :219-275, 1992.

Supported by: Sea Grant, The East-West Center, and The Marine Policy Center.

SUPPLY AND DEMAND OF NEW OIL TANKERS

Di Jin

This paper examines the worldwide supply and demand of new oil tankers. A simultaneous supply and demand model is developed and estimated using two-stage least squares techniques and empirical data from 1972 to 1983. The relationships among tanker newbuilding orders and prices and other relevant market factors are analyzed. Major factors affecting the tanker newbuilding market are identified. The results indicate that: oil price and second-hand tanker price are predominant factors influencing future newbuilding demand; a moderate decrease in laid-up tonnage would not induce a significant increase in newbuilding orders; shipbuilding capacity is a more influential factor for the short-run supply of new tankers than shipbuilding cost. Technological change has also played an important role in the market.

In Press: Maritime Policy & Management.

Supported by: The Marine Policy Center.

WHOI Contribution No. 8187.

ENVIRONMENTAL COMPLIANCE AND ENERGY EXPLORATION AND PRODUCTION: APPLICATION TO OFFSHORE OIL AND GAS

Di Jin and Thomas A. Grigalunas

An integrated investment-production-regulatory model is developed to examine the economic consequences of proposed environmental regulations on firms in the offshore oil and gas industry. This paper discussed OCS-related environmental regulatory issues, the general modeling approach, and selected simulation results. The results show that the impacts of these regulations on OCS firms can be significant, in terms of the reduction in ATNPV, the distribution of economic rent, and minimum field size. The results also indicate that at the firm level, the influences of different sets of regulator proposals vary significantly with more stringent regulations having bigger effects.

Published in: Land Economics, 69(1):82-97, 1992.

Supported by: The Marine Policy Center and The Rhode Island Agricultural Experiment Station.

WHOI Contribution No. 8143.

ENVIRONMENTAL COMPLIANCE AND OFFSHORE OIL AND GAS EXPLORATION AND PRODUCTION

Di Jin and Thomas A. Grigalunas

The economic impacts of multiple environmental regulations on offshore oil and gas exploration and production are examined using an integrated, investment-production-regulatory model developed by the authors. Simulation results indicate that at the firm level, strict environmental regulations can significantly (1) reduce firms' after-tax-net present value and payments to government and (2) increase minimum field size. At the aggregate regional level, compliance with strict regulations can reduce the supply of oil and gas from marginal fields. The paper examines the cost of compliance only; consideration of benefits from regulations is outside the scope of the paper.

In Press: Coastal Zone '93, Proceedings of the Eighth Symposium on Coastal and Ocean Management.

Supported by: The Marine Policy Center and The Rhode Island Agricultural Experiment Station.

WHOI Contribution No. 8257.

ANTARCTICA AND THE LAW OF THE SEA

Christopher C. Joyner

Antarctica and the Southern Ocean cover one-tenth of the earth's surface. Antarctica is the freshest and most pristine of regions, governed by a legal regime that offers the continent and its circumpolar waters the unique possibility of becoming the world's first global wilderness preserve. But in today's age of resource scarcity, Antarctica still provokes much political, global, and legal debate. Over the past decade, interantional attention has increasingly focused on the legal status of the continent, the potential for hydrocarbon exploitation offshore, and opportunities for harvesting circumpolar living marine resources. This book represents the first serious examination of the intimate relationship between Antarctica and the law of the sea. Using Antarctica as a case study, the author probes larger conceptual issues of ocean law and politics. He uses the intricate details of oceanography and law to unravel the dynamics of the Antarctic Treaty System, and in so doing examines how the changing importance of Antarctic issues has affected the development of the law of the sea for the region, the ways in which states define their national interests, and the accommodation through various negotiations that have contributed to the development of law for governing the Southern Ocean. In addition, the book critically analyzes the region's biogeography, the condition of sovreignty on the continent, the lawfulness of asserting jurisdictional zones offshore, and various legal implications for Antarctica's continental shelf, local island groups, circumpolar deep seabed, and the Southern Ocean's high seas. Moreover, the special legal efforts by the international community to protect the Antarctic seas from marine pollution and to conserve its living marine resources are comprehensively appraised.

Published in: Antarctica and the Law of the Sea. By Christopher C. Joyner. Martinus Nijhoff, Dordrecht, 302 pp., 1992.

Supported by: The George Washington University and The Marine Policy Center.

THE 1991 MADRID ENVIRONMENTAL PROTOCOL: RETHINKING THE WORLD PARK STATUS FOR ANTARCTICA

Christopher C. Joyner

The 1991 Environmental Protocol to the Antarctic Treaty and its five annexes supplies vital environmental protection regulations for conservation of the Antarctic. While the Protocol neither formally nor legally establishes Antarctica as a World Park, successful fulfillment of the protective measures that it embodies will create a de facto world park situation for the circumpolar south that benefits future generations.

Published in: Review of European Community and International Environmental Law, 1(3):328-339, 1992.

Supported by: The George Washington University. WHOI Contribution No. 8170.

C'AILE'S "PRESENTIAL SEA" PROPOSAL: IMPLICATIONS FOR STRADDLING STOCKS AND THE INTERNATIONAL LAW OF FISHERIES

Christopher C. Joyner and Peter N. DeCola

Despite rapid evolution in international fisheries law and establishment of the exclusive economic zone, straddling stocks still remain susceptible to heavy harvesting in high seas areas by distant-water fishing states. The notion of mar presencial ("presential sea") has recently been proposed by Chile as a solution for the problem of straddling stocks. The presential sea concept was nationally designed and promoted to curtail such foreign fishing in areas adjacent to Chile's EEZ. This article examines the presential sea as a geostrategic concept, its justification for being, and the question of its permissibility under contemporary international fisheries law. Attention is also given to recent international developments that challenge the legal viability of the presential sea concept. The authors conclude that if this concept were to be widely adopted by coastal states, the traditional freedom to fish on the high seas might be severely compromised. The preferable legal solution is to work within the perimeters set out by the 1982 LOS Convention, more particularly through serious bilateral negotiations between coastal states and fishing states, as well as regional fishery commissions that could set law for and monitor activities in the region.

In Press: Ocean Development and International Law.

Supported by: The George Washington University. WHOI Contribution No. 8188.

COMMERICAL ACTIVITIES AND THE MOVEMENT TOWARD STANDARDS IN ELECTRONIC CHART DISPLAY AND INFORMATION SYSTEMS

Hauke Kite-Powell

Ongoing efforts by the International Maritime Organization (IMO), the International Hydrographic Organization (IHO), and associated national and international member organizations and advisory bodies represent an international regulatory process for creating performance standards for electronic chart display systems (ECDIS) and electronic chart databases. In parallel with these efforts, commercial activities are resulting in standards of their own through the mechanisms of the marketplace. These privately financed and profit-motivated activities include the development of hardware and software for ECDIS products as well as the construction of electronic navigational chart databases, and the sale of these products in the world market. This paper describes the history and present state of commerical activities in the ECDIS field and discusses the relevance of these activities to the development of regulatory standards, the role of national hydrographic offices, and the future of ECDIS technology.

In Press: Proceedings of the U.S. ECDIS Conference '92, February 25-28, 1992, Baltimore, MD.

Supported by: U.S Coast Guard, through ONR grant no. N00014-90-J-4040; Exxon Shipping Co.; American Petroleum Institute; and NOAA, through grant no. NA26AD0156 to The Massachusetts Center for Excellence in Marine and Polymer Sciences.

WHOI Contribution No. 8279.

PATCH DYNAMICS

Simon A. Levin, Thomas A. Powell, and John H. Steele, eds.

In all environments, it is recognized that spatial and temporal variability-patches and population outbursts-are not merely noise but essential features of the food web dynamics ensuring adequate feeding rates and reproduction. However, methods of observation and analysis differ significantly between environments. In the sea, where the primary focus is on physical forcing, continuous spatial records are obtained from ships, and spectral analysis is used to define the

biological patterns and compare them with physical observations. Satellite data now extend the scales and display the complex interactions of physical and biological dynamics. For obvious logistical reasons, different methods of analysis and description are required for interactions on land. where the ecological interactions are considered most important. Freshwater and benthic communities provide significant examples with alternative and sometimes conflicting explanations. Aggregations of organisms imply that, locally, the system is far from a general equilibrium state. The behavioral mechanisms by which aggregations are formed and the consequences for the dynamics of the populations are important phenomena that are currently studied independently for terrestrial and marine systems. This book ventures some comparisons of terrestrial and marine studies with respect to methods and descriptions, concepts and models, and ecological and evolutionary consequences of patchiness.

In Press: Patch Dynamics. Simon A. Levin, Thomas M. Powell, and John H. Steele, eds. Springer-Verlag, Heidelberg, 500 pp.

Supported by: The National Science Foundation, the Department of Energy, and the National Aeronautics and Space Administration, through NSF grant OCE-9024396; and the Ecosystems Research Center, Cornell University.

WHOI Contribution No. 8285.

GOVERNMENT SUPPORT OF MARINE SCIENCE AND TECHNOLOGY IN JAPAN: THE CASE OF MARINE ELECTRONIC INSTRUMENTATION

Matthew J. LaMourie and Porter Hoagland

Two general factors (minimal basic research and closed domestic markets) are thought to favor the relative competitive position of Japanese firms with respect to the firms of other countries. However, it is likely that the scope and degree of these effects depend upon the specific characteristics of individual markets. Thus a close examination of the structure of individual markets and the behavior of firms and government agencies in those markets is needed. In this article, we examine the industrial organization of markets for marine electronic instrumentation (MEI) in Japan and the scope of government policies in support of the development of these advanced marine technologies. We estimate the total value of Japanese MEI production (total export and domestic sales) at between \$992 million and \$1.04 billion. Of this, only 16-18 percent is sold directly to export markets, particularly to U.S. and European civilian end users. The size of the

Japanese domestic market (\$906-954) million-almost equivalent to the European domestic market and one-third the size of the U.S. domestic market) is remarkable considering the relatively small defense end-use sector and the lack of an offshore oil and gas sector. The commercial shipbuilding and commercial fisheries end-use sectors are important, particularly their export market components. We believe that the absence of foreign competitors in the Japanese domestic market is more a function of the size and scope of the market than of specific government policies to restrict the entry of foreign firms. Government R&D programs do not appear to give preference to the products of Japanese firms except on a cost basis. Government financial support for "headline" technologies (e.g., deep diving submersibles and ROVs) has not necessarily contributed to a competitive advantage for Japanese firms. More important to the success of a few Japanese MEI firms in international markets has been (1) the establishment of strategic alliances with U.S. firms in the 1960s and 1970s involving technology transfer in combination with the use of existing distribution networks, and (2) marketing strategies that have focused on after-the-sale servicing and repair.

Submitted to: Marine Policy.

Supported by: The Marine Policy Center and the National Ocean Service/NOAA, through grant no. NA87-AA-D-M00037 to The Massachusetts Centers for Excellence Corporation.

WHOI Contribution No. 8280.

SEARCHING FOR UNCERTAIN BENEFITS AND THE CONSERVATION OF BIOLOGICAL DIVERSITY

Stephen Polasky, Andrew R. Solow, and James M. Broadus

A common argument for protecting plant and animal species from extinction is that one or more of the preserved species may provide a benefit in the future (e.g., a cure for a disease). In this paper, the authors develop a simple search model that incorporates substitutability between species. Under this model, the value of a set of species depends not only on its cardinality but also on its diversity. This provides a utilitarian basis for the conservation of biological diversity.

In Press: Environmental and Resource Economics.

Supported by: The Marine Policy Center.

WHOI Contribution No. 8281.

FISHERIES EXPLOITATION AS A THREAT TO ENVIRONMENTAL SECURITY: THE NORTH PACIFIC OCEAN

Natalia S. Mirovitskaya and Christopher J. Haney

As regional maritime powers and bordering coastal States, both Russia and the US should lead in the process of creating an international regime of environmental security for ecosystems in the North Pacific/Bering Sea region. Fisheries depletion, interception of anadromous species on the high seas, and drift-netting have each contributed to conflicts among "victim" and "culprit" States. Depletion of walleye pollock and protection of salmon, marine mammals, and seabirds in North Pacific/Bering Sea ecosystems are interconnected problems of international environmental security. In the analysis presented here, the authors emphasize temporal evolution of environmental protection and security issues, displacement of identical protection issues from international to domestic levels, and geographic displacement of management problems arising from changing jurisdictional regimes. They also contrast a large disparity between boundary/management lines and "ecosystem limits:" even if management units can be brought into conformity with ecological interdependencies, they are unlikely to reflect current political realities. A new and truly comprehensive regime for environmental security will require multilateral cooperation on fishery conservation, protection of endangered species, and joint monitoring of associated ecosystems in this subarctic region.

Published in: Marine Policy, 16(4):243-258.

Supported by: The John D. and Catherine T. MacArthur Foundation.

WHOI Contribution No. 8101.

DEVELOPMENT OF THE UNITED STATES ELECTRONIC CHART DISPLAY AND INFORMATION (ECDIS) TEST BED PROJECT

David J. Scott and Arthur G. Gaines

Integrated electronic chart technology applied to ship handling promises to improve maritime transportation safety and marine environmental protection in a practical and economical manner. The U.S. ECDIS Test Bed Project is working in support of the international process to set performance standards for this technology. At the center of this effort, the project is assembling and evaluating an experim .. al ECDIS that meets draft standards of both the International Maritime

Organization (for performance) and the International Hydrographic Organization (for chart databases). The project involves many organizations that contribute the specialized skills and knowledge needed to assess this integrative technology. This article provides an update on progress on the project.

In Press: Proceedings of the U.S. Hydrographic Conference '92, Baltimore, MD.

Supported by: The U.S. ECDIS Test Bed Project. WHOI Contribution No. 8284.

EMERGING MARINE ENVIRONMENTAL PROTECTION STRATEGIES FOR THE ARCTIC

Alexei Yu. Roginko and Matthew J. Lc Mourie

Although the open seas of the Arctic Ocean remain among the least polluted of the world's oceans, escalating human pressures on marine ecosystems are causing a gradual deterioration of environmental quality in the Arctic, especially in the coastal zones of Russian Arctic seas. A wide spectrum of legal, technical, and management environment protection measures, adapted from international and regional frameworks, are available to the Arctic rim States. Prospects for marine environmental cooperation can be viewed as favorable, especially with regional policy priorities in many Arctic rim States shifting from military toward environmental and socioeconomic concerns.

Published in: Marine Policy 16(4):259-276.

Supported by: The John D. and Catherine T. MacArthur Foundation.

WHOI Contribution No. 8099.

DETECTING EXFINCTION IN A DECLINING POPULATION

Andrew R. Solow

This note describes a test for extinction in a declining population based on a record of sightings. The test assumes that, prior to extinction, the sightings follow a Poisson process with decreasing rate function. An application to a sighting record of the black footed ferret is presented.

In Press: Journal of Mathematical Biology.

Supported by: The Marine Policy Center.

WHOI Contribution No. 8184.

ESTIMATING RECORD INCLUSION PROBABILITIES

Andrew R. Solow

Historical records of the occurrences of events like earthquakes, volcanic eruptions, and storms are often incomplete, in the sense that the probability that an event is included in the record is less than one. In some cases, it is reasonable to assume that this inclusion probability increases monotonically through time. This paper describes two methods for estimating inclusion probability under this assumption. The first method fits a parametric model to the data, while the second method is based on monotone smoothing. An example involving a record of tropical storm counts is presented.

In Press: American Statistician.

Supported by: The Marine Policy Center.

WHOI Contribution No. 8031.

INFERRING EXTINCTION FROM SIGHTING DATA

Andrew R. Solow

This note describes two simple methods for statistical inference about the extinction of a species using a record of sightings. One method is based on classical hypothesis-testing, while the other method is Bayesian. The methods are illustrated using a record of sightings of the Caribbean monk seal.

In Press: Ecology.

Supported by: The Marine Policy Center.

WHOI Contribution No. 8098.

ON THE EFFICIENCY OF THE INDICATOR APPROACH IN GEOSTATISTICS

Andrew R. Solow

A common problem in geostatistics is to determine whether or not the value of a random field at an unsampled location exceeds a specified threshold using observed values of the random field at sampled locations. Under the indicator approach, the only information used to classify the unobserved value is whether or not the observed values exceed the threshold. This note shows that the loss of information from applying the indicator approach may be modest in the case where the underlying random field is Gaussian.

In Press: Journal of the International Association for Mathematical Geology.

Supported by: The Marine Policy Center.

WHOI Contribution No. 8109.

THE RESPONSE OF SEA LEVEL TO GLOBAL WARMING

Andrew R. Solow

One potential effect of global warming is a change in sea level. This paper outlines the current state of scientific knowledge concerning the response of sea level to global warming.

In Press: Proceedings of the American Physical Society.

Supported by: The Marine Policy Center.

WHOI Contribution No. 8032.

A SIMPLE TEST FOR CHANGE IN COMMUNITY STRUCTURE

Andrew R. Solow

The effect of disturbance on a biological community is commonly measured by a change in an index of community structure. When such an index is calculated from a sample from the community, it is important to assess the statistical significance of an observed change.

In Press: Journal of Animal Ecology.

Supported by: The Marine Policy Center.

WHOI Contribution No. 8145.

STATISTICAL METHODS IN ATMOSPHERIC SCIENCE

Andrew R. Solow

This chapter describes some statistical methods that have been applied in atmospheric science. Three areas of application are considered—acid rain, ozone depletion, and global warming—and within each area two papers are reviewed. The objectives of these papers fall into three broad categories: estimating a trend in multiple time series, spatial interpolation, and estimating a physical parameter.

In Press: Environmental Statistics, G. P. Patil et al., eds. North Holland, Amsterdam.

Supported by: National Institute for Global Environmental Change of the Department of Energy, under subcontract no. 901214-HAR to Harvard University.

WHOI Contribution No. 8248.

AN EMPIRICAL BAYES APPROACH TO MONITORING WATER QUALITY

Andrew R. Solow and Arthur G. Gaines

The level of fecal coliform bacteria in a water body is commonly monitored by multiple tube fermentation experiments. In many cases, interest centers on detecting the exceedance of a standard. This paper describes an empirical Bayes approach to estimating standard exceedance probability from multiple tube fermentation experiments. An example is given.

In Press: Environmetrics.

Supported by: The Edgartown Harbor Association, Inc., and The Marine Policy Center.

WHOI Contribution No. 8282.

MAPPING WATER QUALITY BY LOCAL SCORING

Andrew R. Solow and Arthur G. Gaines

The mean density of bacteria in a water body is commonly monitored using quantal assay. This paper describes the use of local scoring in estimating the spatial distribution of mean density from quantal assay results at a set of point locations. An application to estimating the mean density of fecal coliform bacteria in a coastal pond is presented. Model diagnostics based on a parametric bootstrap are also presented.

In Press: Canadian Journal of Statistics.

Supported by: Friends of Sengekotacket, Inc., and The Marine Policy Center.

WHOI Contribution No. 8283.

ON THE CONSISTENCY OF THE HISTORIC TEMPERATURE RECORD WITH GREENHOUSE WARMING

Andrew R. Solow and Anand Patwardhan

The purpose of this paper is to assess the consistency of the historic record of mean global temperature with a climate model of historic greenhouse warming. Because there is no natural parametric alternative to the climate model, goodness-of-fit is assessed via nonparametric regression. While the historic record is not consistent with the model with high temperature sensitivity, it is not inconsistent with the model using the best-fitting temperature sensitivity.

In Press: Environmetrics.

Supported by: National Institute for Global
Environmental Change Program of the
Department of Energy, under subcontract no.
901214-HAR to Harvard University.

WHOI Contribution No. 8125.

STATISTICAL ANALYSIS WITH AN ORDERED CATEGORICAL REGRESSOR: THE EFFECT OF RAINFALL ON ATTENDANCE

Andrew R. Solow and Victoria E. Starczak

This note describes an approach to the statistical analysis of a linear model in which one regressor is an ordered categorical variable. The approach is based on fitting a model in which the ordered categorical variable is replaced by estimates of the means in each category. Significance is assessed using a randomization test. An application to estimating and testing the effect of rainfall at the Sydney Easter Show is presented.

In Press: Water Resources Research.

Supported by: The Marine Policy Center.

WHOI Contribution No. 8247.

A SIMPLE MODEL FOR PLANKTON PATCHINESS

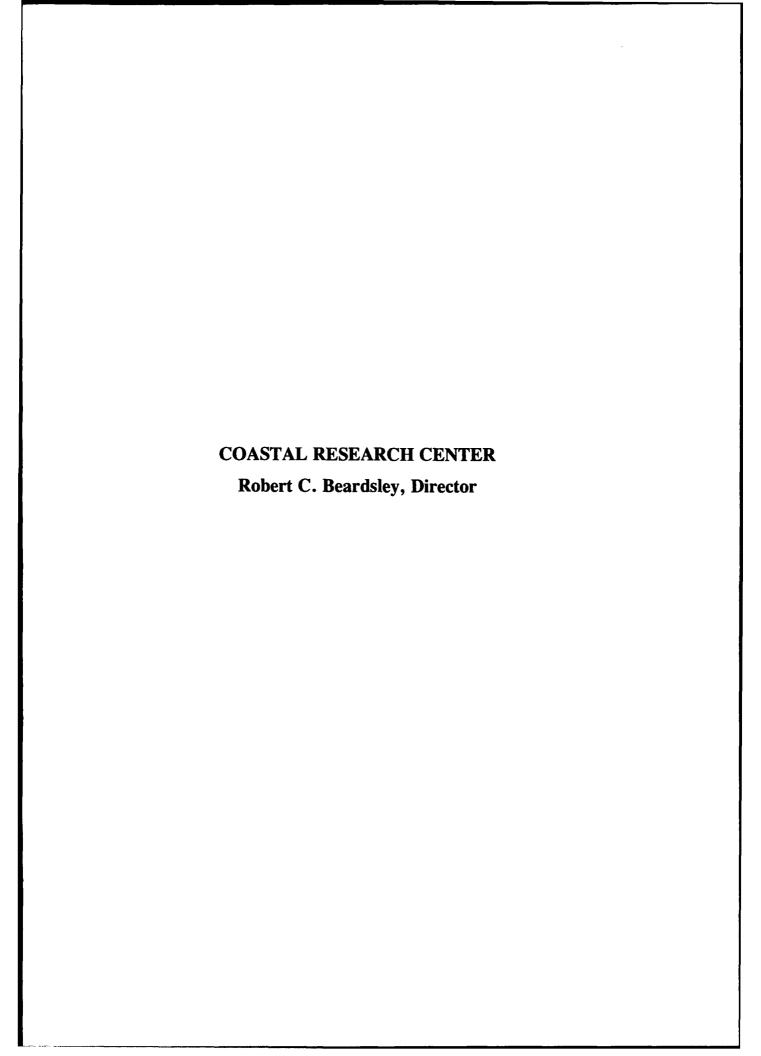
John H. Steele and Eric W. Henderson

Recent work on zooplankton spatial variability shows that the power spectrum of the wave-number variance is flatter than for chlorophyll, as a consequence of greater fine structure in the herbivores. The relative slopes of the power spectra can result from white noise forcing of simple coupled phytoplankton-herbivore models with diffusion.

Published in: Journal of Plankton Research, 14(10):1397-1403, 1992.

Supported by: NSF grant no. OCE-9024396.

WHOI Contribution No. 8038.



TECHNICAL REPORTS

HYDROBLACK 91, REPORT OF THE CTD INTERCALIBRATION WORKSHOP

D. G. Aubrey, T. Oguz, E. Demirev, V. Ivanov, T. McSherry, V. Diaconu, and E. Nikolaenko

An Intercalibration Workshop was held at the Woods Hole Oceanographic Institution (W.H.O.I.) from I-10 December, 1991, for the CTD data acquired during HYDROBLACK '91. This intercalibration exercise was a prelude to an interdisciplinary HYDROBLACK '91 intercalibration to be held in Crimea, Ukraine, in February, 1992, incorporating the full suite of physical, biological, and chemical measurements acquired during the cruise.

HYDROBLACK '91 acquired for the first time a complete hydrographic, biological, and chemical data set for the entire Black Sea, to 2000 m water depth, with the participation of all Black Sea riparian countries as well as the U.S. Nearly 300 hydrographic stations were occupied to full water depth; biological and chemical measurements were made at 100 of these stations. This quasi-synoptic survey was accomplished using five ships during an interval of approximately three weeks.

Results show some disparities between CTD's from the different regions, but the intercalibrated results show a consistent and high resolution detail of the dynamic topography and other physical characteristics of the entire Black Sea basin. The intercalibrated data set is now available within each country and from W.H.O.I., and will form the basis for studies on ocean physics as well as interdisciplinary issues such as oxygen depletion within the basin and hydrogen sulfide distribution. This effort provides an intercalibrated, spatially-dense baseline against which all future and past measurements can be compared.

In spite of significant economic pressures arising from the changes in the eastern European countries, and the inadequate scientific exchange with the west during the past two decades, HYDROBLACK '91 is considered a success and a model for future international scientific and monitoring efforts throughout the Black Sea. Similar efforts are anticipated twice-yearly in the framework of the new Cooperative Marine Science Program for the Black Sea.

Supported by: National Science Foundation through Grant No. OCE-9121788; the Vetlesen Foundation; the Andrew W. Mellon Foundation; the Mobil Foundation, Inc. and the Regional Environmental Center for Central & Eastern Europe (Budapest).

WHOI Technical Report 92-10.

THE BLACK SEA GENERAL CIRCULATION AND CLIMATIC TEMPERATURE AND SALINITY FIELDS

Dimitur Ivanov Trukhchev and Yurii Leonidovich Demin

The Black Sea is a nearly enclosed ocean basin, exhibiting many features common with larger ocean basins. Lacking an open boundary and having a limited exchange with sources of fresh and salt water, this basin is an ideal laboratory for developing and evaluating numerical circulation models. The present report describes one numerical model of the Black Sea, developed by Bulgarian and Russian scientists. The new approach has the advantages of both diagnostic models (incorporation of experimental data) and prognostic models (producing hydrodynamical adjustment and filtered fields). Successive application of diagnostic and prognostic models is used. The temperature and salinity fields obtained from observations, and currents obtained from diagnostic models, are used as the initial approximation to the prognostic model. Judicious selection of an integration time prevents over-smoothing of the results while preserving the stability of the solution.

Using this model, calculations have been made at 25 levels over a grid interval of 0.25° (latitude) by 0.5°. Input data consist of nearly 50,000 observations taken over nearly 100 years, averaged over 0.5° by 0.5° cells. Seasonal fields of temperature, salinity, and velocity form the output of these experiments. The results provide the basis for various hypotheses that must be tested using future field observations and more sophisticated models.

Supported by: Intergovernmental Program "Sections" and WHOI CRC.

WHOI Technical Report 92-34.

GRADUATE STUDENTS

Abstracts of papers of theses submitted in 1992 by graduate students of the Woods Hole Oceanographic Institution Doctoral Degree Program and the Woods Hole Oceanographic Institution/Massachusetts Institute of Technology Joint Program in Oceanography/Oceanographic Engineering. Other papers authored or coauthored by graduate students are included in the departmental sections.

ELECTRONIC AUTOMATION OF A REMOTELY DEPLOYABLE SEAWATER SAMPLING DEVICE

Jonathan N. Betts

A microcomputer-based controller for an oceanographic instrument was designed, prototyped and converted to mass-producible form. The instrument is intended to be tethered at sea, submerged, for periods of up to one year. At a predetermined time during its deployment, it opens a trace-metal clean sample vessel, allowing the vessel to fill with seawater. The instrument then seals the vessel, and waits to be picked up by a ship. Multiple units, programmed to open in succession, can be tethered at one site.

The controller consists of a microprocessor, a real-time clock I.C., motor driving circuitry, motor movement feedback circuitry, micropower management and a wireless serial communications interface, all mounted on two custom printed circuit boards.

The device is designed to withstand the pressure at 100 meters depth, and includes provisions for increasing this, in the future, to 5000 meters.

Initial tests in a laboratory tank were successful. A long-term open-ocean deployment is planned for the near future.

VARIABILITY OF CURRENTS IN GREAT SOUTH CHANNEL AND OVER GEORGES BANK: OBSERVATION AND MODELING

Changsheng Chen

This thesis consists of two parts: (1) variability of currents and water properties in late spring in the northern Great South Channel and (2) numerical study of stratified tidal rectification over Georges Bank.

Part 1. Variability of Currents and Water Properties in Late Spring in the Northern Great South Channel

The South Channel Ocean Productivity
Experiment (SCOPEX) was conducted to
investigate springtime aggregations of right whales
in the northern Great South Channel (GSC) region
and the relationship between physical and
biological variability. As part of SCOPEX, three
regional CTD/ADCP surveys were made in the
northern GSC during April 26-29, 1988, May
18-21, and June 6-11, 1989 to study water
property distribution, structure of the low-salinity
surface plume, tidal mixing boundaries, and the
subtidal circulation. Satellite-tracked drifters
drogued at 5 and 50 m were deployed during each

survey. Several 24-hour CTD/ADCP anchor stations and separate CTD tow-yo transects were made at selected locations in 1989 in support of zooplankton vertical migration and spatial distribution studies.

The surface salinity patterns observed in late April, 1988 and June, 1989 differ significantly in the extent of the freshwater plume which occurs east of Cape Cod in spring. In April, 1988, the surface plume was just beginning to form along the outer coast of Cape Cod while six weeks later in 1989, the minimum salinity was about 1.5°/coless, and a large pool of water fresher than 31.6°/m had pushed east over much of the northern GSC region. The difference in the amount of freshening observed between the two surveys is due primarily to the six-week difference in the seasonal cycle and increased river discharge in 1989. A significant difference is also found at mid-depth in the Maine Intermediate Water (MIW) for the two surveys. In April, 1988, the seasonal thermocline was just beginning to form, and the spatial structure of MIW was relatively uniform. In June 1989, a narrow core of temperature minimum water (with T_{min} in a range of 3.2° to 4.4°C) was found along the western flank of the northern GSC between 40 m and 120 m. This colder and fresher water spread to mix with the MIW as the core flowed southward into the central GSC. Hydrographic data plus satellite Sea Surface Temperature (SST) images showed a continuous tidal mixing boundary along the 80 m isobath in the GSC with a 10 km crossisobath variation during late spring 1988 and 1989, which agreed well with the contour of $log_{10}h/D = 2.1$ based on energy arguments.

An empirical least-squares fit method has been used to separate the SCOPEX ADCP data into tidal and residual current components for each survey and the anchor stations. The resulting field of vertically averaged residual flow shows a cyclonic circulation pattern in the northern GSC, with strong currents in excess of 10 cm/s flowing southward and southeastward along the western flank of the northern GSC, and turning northeastward to flow along the northern flank of Georges Bank. This cyclonic circulation was found at all levels throughout at least the upper 120 m (the maximum sampling depth of the ADCP), with maximum inflow and outflow occurring at the western and eastern ends of the cross-channel transects, respectively. There were two velocity maxima in the vertical; one was at the surface to drive the surface water, the other was at mid-depth to carry MIW into the northern GSC region. The residual ADCP current pattern is consistent with the vertical distributions of water masses and agrees well with trajectories of drifters deployed at 5 and 50 m in the GSC. A relatively strong, deep, jet-like flow was observed in June, 1989, corresponding to the narrow core of

maximum temperature at a depth of 50 m along the western flank of the northern GSC. The vertical shears of geostrophic and ADCP residual flows were consistent within fitting errors in the deeper part of the northern GSC where the tidal current is weak, implying that buoyancy-driven flow was dominant in the central region of the GSC and tidal rectification over the shallower sides of the GSC in late spring.

Part 2. Numerical Study of Stratified Tidal Rectification over Georges Bank

Stratified tidal rectification over Georges Bank has been studied numerically using a two-dimensional primitive equation model with turbulent closure developed by Blumberg and Mellow (1987). A sequence of initial value experiments was first conducted for the homobump, and then the model was applied to the real asymmetrical bottom topography over Georges Bank. In the unstratified case, the model predicts a topographically controlled clockwise residual circulation around Georges Bank, flowing northeastward as a strong jet with a maximum speed of about 16 cm/s along the northern flank and southwestward as a relatively weak and broader flow with a maximum speed of about 5 cm/s from the top of the Bank to the southern flank. As stratification is added, internal tidal rectification and tidal mixing intensify the along-bank and cross-isobath residual currents, and create tidal fronts which modify the vertical structure of the residual flow. During summer, the tidal front is located at the 40-m isobath on the northern flank and at the 50-60-m isobath on the southern flank, and the maximum of the along-bank current is increased up to about 32 cm/s on the northern flank and to 8 cm/s on the southern flank. During winter, the position of the tidal mixing front remains fixed on the northern flank, however, it moves to the shelf break on the southern flank. The winter maximum of clockwise along-bank residual flow is about 26 cm/s on the northern flank and about 6 cm/s at the shelf break on the southern flank. The model results are consistent with theories for stratified tidally driven flow, and in good agreement with observations on the northern flank. The predicted along-bank residual current is relatively weaker than observed on the southern flank, suggesting that buoyancy driving associated with the cross-bank density field and shelf break front is also important in generating residual flow on the southern flank.

Supported by: National Science Foundation through Grants No. OCE87-13988, OCE91-01034 and the National Center for Atmospheric Research through computer time Grants No. 35781029 and 35781035.

KINEMATIC EVALUATION OF END EFFECTOR DESIGN

Gary Wayne Edwards

The complex, many degree-of-freedom end effectors at the leading edge of technology would be unusable in the sea bottom research environment. Simpler designs are required to provide adequate reliability for subsea use. This work examines selection of end effector designs to achieve optimum grasping ability with minimal mechanical complexity. A new method of calculating grasp stability is developed, incorporating elements of previous works in the field. Programs are developed which evaluate the ability of different end effector configurations to grasp representative objects (a cube, sphere and infinite cylinder). End effector designs considered had circular palms with fingers located at the periphery, oriented so that each pointed to the center of the palm. The program tested configurations of from 1 to 4 fingers and from 1 to 3 links per finger. Three sets of finger proportions were considered: equal length links, half length links, and anthropomorphic proportions. The 2 finger, 2 link per finger configuration was determined to be the optimum design, and the half length proportions were selected as the best set of proportions.

Supported by: United States Navy.

APPLICATIONS OF FLUORESCENCE SPECTROSCOPY TO ENVIRONMENTAL CHEMISTRY

Sarah Anita Green

The work presented in this thesis consists of three parts. The first is a photophysical study of the mechanism of fluorescence quenching by stable nitroxyl radicals, which are becoming an important analytical tool for the study of reactive transients in surface waters (1,2). In part two, quenching of dissolved organic matter (DOM) fluorescence by nitroxides is employed to investigate the electrostatic properties of DOM in aqueous solution, with the goal of elucidating the apparent ionic strength and pH dependence of metal-fulvic acid binding constants. In part three, the intrinsic optical properties (absorbance, fluorescence, and fluorescence efficiency) of DOM are examined in a coastal region to understand how these properties vary with source, age and sunlight exposure time.

Nitroxide-fluorophore adducts were employed to investigate the mechanism by which nitroxyl radicals quench fluorescence (3). Fluorescene quantum yields and lifetimes were measured for a series of adducts, and quenching rates were shown

Contract No. N00014-89-J-1260.

to be quite high $(k_q \approx 10^8 - 10^{10} \text{ s}^{-1})$, even at distances of ≈ 12 A. Forster or Dexter energy transfer mechanisms are unable to account for the observed rates and lack of solvent dependence in quenching. An excellent correlation is observed between K_q and the non-radiative relaxation rate. These results confirm that nit oxyl radicals are very non-selective in their quenching abilities, and suggest that the best analytical probe adducts will include a fluorophore with an appreciable non-radiative relaxation rate.

Diffusional quenching by charged and neutral nitroxides was employed to explore the electrostatic properties of fulvic (FA) and humic (HA) acids. Cationic nitroxides were found to be up to 16 times more effective than neutral analogues in quenching the fluorescence of humic materials. This result is attributed to the enhanced coulombic attraction of cations to the anionic FA or HA surface, and is interpreted as an estimate of surface electrostatic potential. Reduction of molecular charge at low pH and shielding of charge at high ionic strength (I) produced diminished enhancements, consistent with this interpretation. The potential was found to be particulary sensitive to ionic strength, suggesting that this electrostatic effect should be of particular importance in transition zones, such as estuaries, where I increases from <5 mM to 0.7 M as river water and seawater mix. High molecular weight fractions of HA have a higher apparent surface potential than lower molecular weight fractions, indicating that larger humic molecules may have an enhanced ability to bind metal ions.

Optical properties of colored DOM may vary with source and age of the material. Absorption spectra can be characterized by their log-linearized slopes (S) as well as by their absolute intensities. The slope, S, is found to be much greater (steeper decrease in absorbance with increasing wavelength) for blue-water samples than for riverine and coastal samples, indicating that the visible-light absorbing fraction of DOM may be similar for a wide variety of samples, but do show some minor differences; changes in quantum yield with excitation wavelength within a single sample are an indication of the heterogeneity of the chromophore mixture present in these materials. To better compare fluorescence data, complete excitation/emission matrix spectra were collected. When normalized to their respective absorbance spectra, these provide a full 'map' of fluorescence quantum efficiency over the entire uv-visible range. This technique is showing promise as a way to identify important spectral regions in these complex chromophore mixtures. DOM isolated on C-18 columns had somewhat different optical characteristics than whole water samples, suggesting selective isolation of absorbing material. Supported by: Office of Naval Research under

EXPERIMENTAL INVESTIGATION OF SCATTERING FROM RANDOMLY ROUGH ELASTIC CYLINDERS

John Van Gurley

Acoustical backscattering from randomly rough infinitely long elastic cylinders surrounded by a fluid medium is examined. The cylinder radius is allowed to vary along its lengthwise axis creating one-dimensional rotationally symmetric roughness. Using recently published rough cylinder formulations [T.K. Stanton, J. Acoust. Soc. Am., 92, 1641-1664 (1992) and T.K. Stanton and D. Chu, J. Acoust. Soc. Am., 92, 1665-1678 (1992)], explicit expressions are derived for the backscattered field for a laboratory pulse-echo environment: spherically spreading directional source and receiver with arbitrary beam patterns. Efficient numerical integration algorithms are developed to solve for the backscattered field from a specified surface profile. Experimental measurements from dense elastic (stainless steel) cylinders immersed in water are presented to quantitatively illustrate the effects of small scale surface roughness $(\sigma_s/a = 0.0131)$ where σ_s is the surface rms roughness and a is the mean cylinder radius) for 4.5 < ka < 70 where k is the acoustic wavenumber. The actual target surface profile is well described and used as an input in the numerical simulations. Agreement is found between measurements and simulation predictions both in the mean field levels and the field fluctuations over a wide range of frequencies.

Supported by: United States Navy.

EDDY GENERATION AT A CONVEX CORNER BY A COASTAL CURRENT IN A ROTATING SYSTEM

Barry A. Klinger

Rotating baroclinic and barotropic boundary currents flowing around a corner in the laboratory were studied in order to discover the circumstances under which eddies were produced at the corner. Such flows are reminiscent of oceanic coastal flows around capes. When the baroclinic currents, which consisted of surface flows bounded by a density front, encountered a sharp corner, immediately downstream of the corner an anticyclone grew in the surface layer for an angle of greater than 40 degrees. Varying the initial condition of the flow or the depth of the lower layer did not noticeably affect the gyre's properties except for its growth speed, which was greater when the lower layer was

shallower. The barotropic currents were pumped along a sloping bottom, and also formed anticyclonic gyres which quickly attained an approximately steady state. For a given topography, the size of the gyre was proportional to the inertial radius u/f. Volume flux calculations based on the surface velocity revealed vertical shear which increased with gyre size. Hydraulic models were also applied to flow around gently curving topography to determine the critical separation curvature as a function of upstream parameters.

Supported by: National Science Foundation under Grant OCE89-15408.

TIME-DEPENDENT VENTILATED THERMOCLINE

Zhengyu Liu

In this thesis, I study the time-varying behavior of a ventilated thermocline with basin scales at annual and decadal time scales. The variability is forced by three external forcings: the wind stress (chapter 3), the surface heat flux (chapter 4) and the upwelling along the eastern boundary (chapter 5). It is found that the thermocline variability is forced mainly by wind in a shadow zone while mainly by surface buoyancy flux in a ventilated zone.

A two-layer planetary geostrophic model is developed (chapter 2) to simulate a thermocline. The model includes some novel physical mechanisms. Most importantly, it captures the essential feature of subduction; it also is able to account for a time-varying surface temperature. The equation for the interface is a quasi-linear equation, which can be solved analytically by the method of characteristics.

The effect of a varying Ekman pumping is investigated. In a shadow zone, it is found that the driving due to the Ekman pumping is mainly balanced by the propagation of planetary waves. However, in a ventilated zone, the cold advection of subducted water plays the essential role in opposing the Ekman pumping. The different dynamics also results in different thermocline variability between the two zones. After a change of Ekman pumping, in the shadow zone, since the baroclinic Rossby wave responds to a changing Ekman pumping, which then excites thermocline variability. However, in the ventilated zone, both the advection and the Ekman pumping vary rapidly after a barotropic process (about one week) to reach a new steady balance, leaving little thermocline variability. In addition, the evolution of the thermocline and circulation are also discussed.

Furthermore, with a periodic Ekman pumping, it is found that linear solutions are approximate the fully nonlinear solution well, particularly for annual forcings. However, the linear disturbance is stronly affected by the basic thermocline structure and circulation. The divergent group velocity field, which is mainly caused by the divergent Sverdrup flow field, produces a decay effect on disturbances. The mean thermocline structure also strongly affects the relative importance of the local Ekman pumping and remote Rossby waves. As a result, in a shadow zone, local response dominates for a shallow interface while the remote Rossby wave dominates for a deep interface. With a strong decadal forcing, the nonlinearity becomes important in the shadow zone, particularly in the western part. The time-mean thermocline which results, becomes shallower than the steady thermocline under the mean Ekman pumping.

Then, we investigate the effect on the permanent thermocline by a moving outcrop line, which simulates the effect of a varying surface heat flux. The two layer model is modified by adding an (essentially passive) mixed layer atop. The outcrop line and the mixed layer depth are specified. It is found that, opposite to a surface wind stress, a surface buoyancy flux causes strong variability in the ventilated zone through subducted water while it affects the shadow zone very little. Furthermore, two regimes of buoyancy-forced solution are found. When the outcrop line moves slowly, the solutions are non-entrainment solutions. For these solutions, the surface heat flux is mainly balanced by the horizontal advection. The mixed layer is never entrained. The time-mean thermocline is close to the steady thermocline with the time-mean outcrop line. When the outcrop line moves southward rapidly during the cooling season, the solutions become entrainment solutions. Now, deep vertical convection must occur, because the horizontal advection in the permanent thermocline is no longer strong enough to balance the surface cooling. The mixed layer penetrates rapidly such that water mass is entrained into the mixed layer through the bottom. The time-mean thermocline resembles the steady thermocline with the early spring mixed layer, as suggested by Stommel (1979). The local variability in the permanent thermocline is most efficiently produced by decadal forcings.

Finally, two issues about the waves radiating from the eastern boundary are discussed. The first is the penetration of planetary waves across the southern boundary of a subtropical gyre. We find that the wave penetration across the southern boundary is substantially changed by the zonal variation of the thermocline structure. The zonal variation alters both the effective β and the wave front orientation. As a result, the wave penetration differs for interfaces at different depths. For an

interface near the surface, part of the waves penetrate into the equatorial region. For middle depths, most waves will be trapped within the subtropical gyre. In contrast, for deep depths, all waves penetrate southward.

The second issue of the eastern boundary waves mainly concerns with the breaking of planetary waves in the presence of an Ekman pumping and the associated two-dimensional mean flow. It is found that the breaking is affected significantly by an Ekman pumping and the associated mean flow. With an Ekman pumping, downwelling breaking is suppressed and the breaking time is delayed; upwelling breaking is enhanced and their times are shortened. The breaking times and positions are mainly determined by the maximum vertical perturbation speed while the intensity of the breaking front mainly depends on the amplitude of the perturbation. The intensity of a breaking front increases with the amplitude of the forcing, but decreases with the distance from the eastern boundary. The orientation of a breaking front is overall in northeast-southwest $(x \sim -1/f^2)$.

Supported by: National Science Foundation under Grant No. ATM-8903890.

LABORATORY MEASUREMENTS OF THE SOUND GENERATED BY BREAKING WAVES

Mark Richard Loewen

Breaking waves dissipate energy, transfer momentum from the wind to surface currents and breaking enhances the transfer of gas and mass across the air-sea interface. Breaking waves are believed to be the dominant source of sea surface sound at frequencies greater than 500 Hz and the presence of breaking waves on the ocean surface has been shown to enhance the scattering of microwave radiation. Previous studies have shown that breaking waves can be detected by measuring the microwave backscatter and acoustic radiation from breaking waves. However, these techniques have not yet proven effective for studying the dynamics of breaking. The primary motivation for the research presented in this thesis was to determine whether measurements of the sound generated by breaking waves could be used to quantitatively study the dynamics of the breaking

Laboratory measurements of the microwave backscatter and acoustic radiation from two-dimensional breaking waves are described in Chapter 2. The major findings of this Chapter are:

1) the mean square acoustic pressure and backscattered microwave power correlate with the wave slope and dissipation for waves of moderate

slope, 2) the mean square acoustic pressure and backscattered microwave power correlate strongly with each other, and 3) the amount of acoustic energy radiated by an individual breaking event scaled with the amount of mechanical energy dissipated by breaking. The observed correlations with the mean square acoustic pressure are only relevant for frequencies greater than 2200 Hz because lower frequences were below the first acoustic cut-off frequency of the wave channel.

In order to study the lower frequency sound generated by breaking waves another series of two-dimensional breaking experiments was conducted. Sound at frequencies as low as 20 Hz was observed and the mean square acoustic pressure in the frequency band from 20 Hz-1 kHz correlated strongly with the wave slope and dissipation. A characteristic low frequency signal was observed immediately following the impact of the plunging wave crest. The origin of this low frequency signal was found to be the pulsating cylinders of air which are entrained by the plunging waves. The pulsation frequency correlated with both the wave slope and dissipation. Following the characteristic constant frequency signal, approximately 0.25 after the initial impact of the plunging crest, another low frequency signal was typically observed. These signals were generally lower in frequency initially and then increased in frequency as time progressed.

To determine if three-dimensional effects were important in the sound generation process and to measure the sound beneath larger breaking waves a series of experiments was conducted in a large multi-paddle wave basin. Three-dimensional breaking waves were generated and the sound produced by breaking was measured in the frequency range from 10 Hz to 20 kHz. The observed sound spectra showed significant increases in level across the entire bandwidth from 10 Hz to 20 kHz and the spectra sloped at -5 to -6 dB per octave at frequencies greater than 1 kHz. The mean square acoustic pressure in the frequency band from 10 Hz to 150 Hz correlated with the wave amplitude similar to the results obtained in the two-dimensional breaking experiments. Large amplitude low frequency spectral peaks were observed approximately 0.75 after the initial impact of the plunging crests.

It was postulated that the low frequency signals observed some time after the initial impact of the plunging crests for both the two and three-dimensional breakers were caused by the collective oscillation of bubble clouds. Void fraction measurements taken by Eric Lamarre were available for five breaking events and therefore the average sound speed inside the bubble clouds and their radii were known. Using this information the resonant frequencies of a two-dimensional cylindrical bubble cloud of equal radius and sound

speed were calculated. The frequencies of the observed signals matched closely with the calculated resonant frequencies of the first and second mode of the two-dimensional cylindrical bubble cloud. The close agreement supports the hypothesis that the low frequency signals were produced by the collective oscillation of bubble clouds.

In Chapter 4 a model of the sound produced by breaking waves is presented which uses the sound radiated by a single bubble oscillating at its linear resonant frequency and the bubble size distribution to estimate the sound spectrum. The model generates a damped sinusiodal pulse for every bubble formed, as calculated from the bubble size distribution. If the range to the receiver is known then the only unknown parameters are ε , the initial fractional amplitude of the bubble oscillation and L, the dipole moment arm or twice the depth of the bubble radius the model reproduces the shape and magnitude of the observed sound spectrum accurately. The success of the model implies that it may be possible to calculate the bubble size distribution from the sound spectrum. The model was validated using data from experiments where the breaking events were small scale gently spilling waves (Medwin and Daniel, 1990).

Supported by: Massachusetts Institute of Technology.

GLOBAL POSITIONING SYSTEM MEASUREMENT OF CRUSTAL DEFORMATION IN CENTRAL CALIFORNIA

Mark Hunter Murray

In Chapter 2, we develop a conventional terrestrial reference frame-designated SV6-for the analysis of Global Positioning System (GPS) observations. The reference frame adopts the geocentric origin and scale defined by eleven years of satellite laser ranging (SLR) observations. The precise relative locations of 80 sites that primarily realize the SV6 frame are derived from very-long-baseline interferometry (VLBI) observations. The orientation is consistent with the International Earth Rotation Service terrestrial reference system. The coordinates of sixteen sites with well-determined local vector ties between collocated VLBI and SLR reference points are used to make the VLBI coordinate system commensurate with the SLR system; the sites are globally distributed, including nine in North America, three in Europe, and one each in China, Australia, Hawaii, and Kwajalein. A scales of the VLBI and SLR systems differ by 4 ± 1 parts in 10^9 . SV6 includes estimates of the temporal evolution and uncertainties of the coordinates from VLBI

and geophysical observations and we develop a methodology for systematically combining temporally heterogeneous space-geodetic observations with geophysical and geological information, such as global plate tectonic motion models.

In Chapter 3, we present estimates of crustal deformation in central California from thirteen GPS campaigns, conducted primarily by a consortium of four universities from December 1986 to February 1991. Each major campaign occupied a network of seven to twenty sites in California repeatedly for four to five days, with additional fiduciary control provided by sites distributed across North America, and in Hawaii and Europe. The precision of the estimated baseline vectors, based on the day-to-day scatter over each campaign, is 3-5 mm in the horizontal components with 1-3x10⁻⁸ dependence on baseline length for well-designed experiments. The precision in the vertical is 15-25 mm. Precision is most strongly affected by changes to the fiducial network and ionospheric conditions. Systematic constant error sources may be responsible for a slight increase in long-term scatter over short-term scatter.

We then estimate relative motion between twelve sites in California that have observations spanning 1.5-4.2 years, with uncertainties at the 1-1.5 mm/yr level. Confidence in some of the estimated rates is limited by apparent inconsistencies between experiments with poor fiducial control. The estimated relative motions of Owens Valley and Palos Verdes with respect to Vandenberg are consistent with VLBI-derived rates. We estimate north-south convergence across the eastern Santa Barbara channel at 5.2 mm/yr, and our results are consistent with a change to left-lateral shear in the central Santa Barbara channel. The estimated deformation across the Santa Maria fold and thrust belt has less convergence and more right-lateral shear than had been previously estimated from triangulation and trilateration measurements. The relative motion of six sites along the western margin in the vicinity of Vandenberg are consistent with 2-4 mm/yr motion on the Hosgri fault. Relative motion east of the San Andreas suggests that an additional 2-4 mm/yr motion may be accommodated within a shear zone located in Owens Valley and the Mojave Desert.

Supported by: Massachusetts Institute of Technology.

STUDY OF BASIN SCALE ACOUSTIC **TRANSMISSIONS**

John Richard Nystrom

A basin-scale acoustic tomography experiment was conducted in the northeast Pacific from May 1987 to September 1987. In this thesis, the stability of the forward model is analyzed. There are large non-linearities in the changes in travel time between ray paths for the four seasons. I constructed a model in which the change in warming in the upper 100 m of the ocean was due only to changes in surface solar irradiance. The value of the surface solar irradiance anomalies necessary to cause the tomography results for warming (Spiesberger and Metzger, 1991) was computed. This value was larger than the actual value of surface solar irradiance anomaly which was computed using inputs measured by satellite (Chertock, 1989).

Supported by: United States Navy.

ADAPTIVE MATCHED FIELD PROCESSING IN AN UNCERTAIN PROPAGATION ENVIRONMENT

James Calvin Preisig

Adaptive array processing algorithms have achieved widespread use because they are very effective at rejecting unwanted signals (i.e., controlling sidelobe levels) and in general have very good resolution (i.e., have narrow mainlobes). However, many adaptive high-resolution array processing algorithms suffer a significant degradation in performance in the presence of environmental mismatch. This sensitivity to environmental mismatch is of particular concern in problems such as long-range acoustic array processing in the ocean where the array processor's knowledge of the propagation characteristics of the ocean is imperfect. An Adaptive Minmax Matched Field Processor has been developed which combines adaptive matched field processing and minmax approximation techniques to achieve the effective interference rejection characteristic of adaptive processors while limiting the sensitivity of the processor to environmental mismatch.

The derivation of the algorithm is carried out within the framework of minmax signal processing. The optimal array weights are those which minimize the maximum conditional mean squared estimation error at the output of a linear weight-and-sum beamformer. The error is conditioned on the propagation characteristics of the environment and the maximum is evaluated over the range of environmental conditions in

which the processor is expected to operate. The theorems developed using this framework characterize the solutions to the minmax array weight problem, and relate the optimal minmax array weights to the solution to a particular type of Wiener filtering problem. This relationship makes possible the development of an efficient algorithm for calculating the optimal minmax array weights and the associated estimate of the signal power emitted by a source at the array focal point. An important feature of this algorithm is that it is guarenteed to converge to an exact solution for the array weights and estimated signal power in a finite number of iterations.

The Adaptive Minmax Matched Field Processor can also be interpreted as a two stage Minimum Variance Distortionless Response (MVDR) Matched Field Processor. The first stage of this processor generates an estimate of the replica vector of the signal emitted by a source at the array focal point, and the second stage is a traditional MVDR Matched Field Processor implemented using the estimate of the signal

replica vector.

Computer simulations using several environmental models and types of environmental uncertainty have shown that the resolution and interference rejection capability of the Adaptive Minmax Matched Field Processor is close to that of a traditional MVDR Matched Field Processor which has perfect knowledge of the characteristics of the propagation environment and far exceeds that of the Bartlett Matched Field Processor. In addition, the simulations show that the Adaptive Minmax Matched Field Processor is able to maintain it's accuracy, resolution and interference rejection capability when it's knowledge of the environment is only approximate, and is therefore much less sensitive to environmental mismatch than is the traditional MVDR Matched Field Processor.

AN ANALYTICAL TWO-LAYER COUPLED HYDRODYNAMIC AND ICE FLOE MOVEMENT MODEL

Mindy Lynn Roberts

A two-layer, coupled analytical hydrodynamic model has been developed for the short-term prediction of ice motion around the continental shelf. Although this application assumes a constant-depth shelf, the thoory may be applied to cross-shelf depth variations. The model assumes an infinite shelf over which the wind field is assumed uniform. The depth-averaged momentum equations are solved in terms of a Fourier solution for the velocity field, maintaining both Coriolis and quasi-nonlinear bottom friction without

relying on the closed-lid approximation. A thin surface layer is coupled to the integrated water column through the stress transfer at the interface, and an ice layer is coupled to the surface layer through the drag at the ice/water interface. When compared with idealized wind conditions, it is clear that a two-layer model more accurately represents the velocity structure of the water column than does a depth-averaged model. Data from a field experiment conducted in the Alaskan Beaufort Sea provided the information necessary to predict the actual motion of two ice floes. It was found that the analytical model trajectory in the stronger, more constant wind field. The prediction of an ice floe movement in a more variable wind field was not as accurate as the previous numerical models, most likely due to the variations in the water depth along the actual path the floe followed. It is suggested that the model be extended to include variations in water depth.

Supported by: Massachusetts Institute of Technology.

A MODEL OF A MEDITERRANEAN SALT LENS IN EXTERNAL SHEAR

David Walsh

A pair of simple models representing the interaction of a continuously stratified {-plane quasigeostrophic lens with a uniform external shear flow is examined. The study is motivated by the desire to understand the processes that affect Mediterranean Salt Lenses and other mesoscale lenses in the ocean. The first model represents the eddy as a pair of quasigeostrophic 'point potential vortices' in uniform external shear, where the two point vortices are imagined to represent the top and bottom of a baroclinic eddy. While highly idealized, the model succeeds in qualitatively reproducing many aspects of the behavior of more complex models. In the second model the eddy is represented by an isolated three dimensional patch characterized by quasigeostrophic potential vorticity linear in z, in a background flow with constant potential vorticity. The boundary of the lens may be deformed by interactions with a uniform background shear. A family of linearized analytical solutions representing such a vortex is discussed in Chapter 3. These solutions represent lens-like eddies with trapped fluid cores, which may propagate through the surrounding water when there is external vertical shear. The analysis predicts the possible forms of the boundary deformation in a specified external flow. The translation speed of the lens with respect to the surrounding fluid is found to be a simple function of the external vertical shear and the core baroclinicity.

A numerical algorithm which is a generalization of the contour dynamics technique to stratified quasigeostrophic flow is used to extend the linear results into the nonlinear regime. This numerical analysis allows a determination of the range of environmental conditions (e.g. the maximum shear and/or core baroclinicity) in which coherent vortex solutions can be found, and allows the stability of the steadily translating solutions to be examined directly. It is found that the solutions are stable if neither the external shear nor the core baroclinicity is too large, and that the breakdown of the unstable solutions is characterized by the loss of an extrusion of core fluid to the surrounding waters. The translation speeds of the large amplitude numerical solutions are found to have the same functional dependence on the external vertical shear and the core baroclinicity that was found in the linear analysis, and it is demonstrated that the solutions translate at a rate which is equal to the background flow speed at the center of potential vorticity of the lens.

As a test of the model results, new data from a recent SOFAR float experiment are presented and compared with the model predictions. The data show that the cores of two different Mediterranean Salt Lenses are tilted, presumably as a result of interactions with external flows. Both the sense of the tilt and its relation to the translation of the lens are in qualitative agreement with the model solutions.

Supported by: Office of Naval Research through Contract No. N00014-89-J-1182 and the National Science Foundation under Grant Nos. OCE89-16446 and OCE87-00601.

THE SEISMIC ATTENUATION STRUCTURE OF THE EAST PACIFIC RISE

William Sam Douglas Wilcock

Studies of seismic propagation through oceanic crust have contributed enormously to our understanding of the generation and evolution of oceanic crust. However, such work has largely been confined to the seismic velocity structure. In this thesis we present results from a study of seismic attenuation using a data set collected for three-dimensional tomographic imaging of a fast-spreading ridge. The experiment location at 9°30'N on the East Pacific Rise is the site of a strong mid-crustal seismic reflector which has been inferred to be the roof of a small axial magma chamber at about 1.6 km depth.

A spectral method is used to estimate t*, a measure of the integrated attenuation along a wave path. Such a method assumes that the dominant frequency-dependent component of propagation is

intrinsic attenuation. A logarithmic parameterization is then used to invert t* measurements for Q^{-1} structure assuming that the velocity structure is given from earlier studies. To evaluate the method of Q tomography a full-waveform finite-difference technique which does not include attenuation is used to calculate solutions for seismic propagation through a two-dimensional velocity model. The results show a complex pattern of seismic propagation in the vicinity of the axial magma chamber. The first arrival always passes above the magma chamber. However, for paths of significant length that cross the rise axis the amplitude of this arrival is very small, and the first phase with significant amplitude is a diffraction below the magma chamber. High-amplitude Moho turning and PP arrivals may also be important secondary arrivals. Synthetic inversions show the importance of selecting time windows for power spectral estimation which are dominated by a single phase and of using wave paths which closely corresponds to that of the selected phase.

A comparison of the finite difference solutions and the predictions of the a two-dimensional, exact ray-tracing algorithm with record sections obtained during the tomography experiment significantly improves our understanding of seismic propagation across the East Pacific Rise. The results enable an objective choice of the position and length of the time window for t* estimation. Moreover, additional constraints are incorporated into an approximate three-dimensional ray-tracing algorithm used in the inversion so that the wave paths more closely correspond to those of the desired phase. The full data set to be inverted comprises about 3500 t* estimates and includes crustal paths which do not cross the rise axis. diffractions above and below the axial magma chamber, and Moho-turning phases. Wave paths for the Moho-turning phases cross the rise axis at a wide range of lower crustal depths.

The Q^{-1} models resulting from two-dimensional and three-dimensional tomographic inversions show that the attenuation of seismic waves on the East Pacific Rise is dominated by two regions of low Q; one in the upper 1 km of crust, and one at depths greater than about 2 km below the rise axis. While the data do not resolve the details of vertical variations in near-surface Q^{-1} , the results show a substantial variation in shallow attenuation within 0.05 My of the rise axis. On-axis, Q values averaged over the upper 1 km are about 100, while off-axis the average value rapidly decreases to about 30. Measurements of the seismic velocity suggest that that thickness of the surficial high-porosity extrusive layer increases substantially off-axis. If such thickening is entirely responsible for the observed change in near-surface attenuation then

Q within the extrusive layer must be much less than 20. Alternatively, in situ changes in porosity may also contribute to the observed increase in attenutaion. Since significant tectonic activity is apparently restricted to locations well off-axis we suggest that such variations in porosity may result from hydrothermal activity. Regions of hydrothermal downwelling located off-axis will be subject to cooling and thermally-induced cracking while upwelling regions on-axis may be accompanied by rapid infilling of existing pores by hydrothermal deposits.

Estimates of t* for all phases propagating below the magma chamber are markedly higher than those for other phases, resulting in Qmodels which include a region of low Q extending from 2 to 7 km depth below the rise axis. The lowest Q values resolved are about 25-30 both immediately below the magma chamber and within the lower crust. While there is some evidence for a small decrease in attenuation with depth in the lower crust, axial Q values at depths ranging from less than 2.5 to 6 km are relatively constant, always lying below 50. Laboratory measurements at seismic frequencies suggest that Q values of 25-50 require only very small fractions of partial melt. The attenuation observations thus place constraints on the dimensions of the axial magma chamber and stronly suggest that the thickness of the region containing more than a few percent of partial melt is no more than 1 km.

Supported by: Office of Naval Research through Grant No. N00014-89-J-1257 to the Massachuse (18.1). Itute of Technology.

AMBIENT NOISE MEASUREMENT IN THE 200-300 HZ BAND DURING THE GREENLAND SEA TOMOGRAPHY EXPERIMENT

Huiria Wu

A six mooring acoustic tomography array was jointly deployed by Scripps Institution of Oceanography and Woods Hole Oceanographic Institution in 1988, and a year long time series of ambient noise in the 200-300 Hz was collected by those moorings. Large scale meteorological environmental information, particularly wind, was provided during that same year by the British Meteorological Office. Time series of ice type and ice concentration were provided by Special Sensor Microwave Imager and Advanced Very High Resolution Rediometer satellite. Using those data sets, we were able to look at the characteristics of the ambient noise and to correlate the noise against significant environmental variables such as wind, ice concentration, ice edge position, etc.

The largest noise levels are generally seen during the winter months and are associated with periods of moderate to strong wind speed. The lowest noise levels are confined to summer; however, there is also an extremely quiet period in mid-winter, coincident with heavy ice cover.

During the ice-free periods, the ambient noise is higher than the Wenz ambient noise for open water. The regressions between the noise and wind speed show that the noise is wind dependent, with slightly lower slopes than the Wenz curve. Under the heavy pack ice cover conditions, noise levels are much lower than during the ice-free periods, even lower in face than Wenz noise for open water when the wind speeds pass 11 m/s. The ambient noise is almost wind independent during this period. The overall noise levels are highest during the ice edge advance/retreat period; the noise is also wind dependent, with the regression slopes higher than that for ice-free period, but still lower than that of the Wenz curves.

Noise and wind fields correlate well in fall and during the ice edge advance/retreat periods, but are less correlated under the heavy ice cover and during low wind speed periods. The spatial cross correlations of the noise fields show quite high levels, up to 0.9 in fall and during the ice edge advance/retreat period, but there is less correlation during other periods.

The MIZ noise levels are dependent on the distance between the receiver and the ice edge and also the ice concentration. The noise peaks at the ice edge and diminishes faster going under the ice than into the open water. The measured noise levels near the ice edges are about 4-7 dB higher than open water, and about 7 to 10 dB higher than levels far into the ice field. In the MIZ, on-ice-wind results in higher noise than off-ice-wind. Ambient noise increases as on-ice-wind increases, but increases much slower or even decreases as off-ice-wind increases.

INVESTIGATION OF THE DYNAMICS OF LOW-TENSION CABLES

Christopher Todd Howell

Low-tension cable problems are particularly complex as linear solutions are unobtainable in most cases, due to the lack of a meaningful static configuration. By contrast, the dynamics to taut cables are only weakly nonlinear.

First, the three-dimensional nonlinear equations of motion and compatibility relations are formulated for a cable with bending stiffness. Forces in bending are included to provide the necessary physical mechanism for energy transfer across isolated points of zero tension and to ensure a smooth cable configuration.

The mechanisms for low-tension response to excitation are explored by considering the limiting case of a cable with zero initial tension, subject to an impulsive force at one end. The three-dimensional equations show the development of impulsive tension. The intensity of the tension and the velocity components depend exclusively on the initial curvature and are independent of the geometric torsion. In addition, singularities are found to develop at points of curvature discontinuity. Incorporating the cable's bending stiffness removes these singularities by ensuring smooth curvature. However, sustained boundary layers are found to develop, demonstrating the importance of the underlying physical mechanism.

The transition from taut to low-tension behavior is examined through an analysis of the dynamics of a hanging chain, driven by planar harmonic excitation at the top. For moderately large excitation amplitudes, asymptotic results demonstrate the existence of distinct regions of stable two-dimensional and stable three-dimensional response, as a function of frequency, as well as a distinct region in which all steady state solutions are found to be unstable. Numerical solutions of the fully nonlinear equations are in close agreement with the asymptotic results. Numerical results for even larger excitation amplitudes show that large impulse-like tension forces develop which cause the chain to lose tension over a region adjacent to its freely hanging end, and then collapse. The transition from low to high tension regions is clearly demonstrated, with low tension effects being confined to the lower portion of the chain.

Experimental studies were conducted using a chain, 3/8 inches in diameter and 5.8 feet in length, which confirm qualitatively and quantitatively the theoretical and numerical predictions.

Supported by: Massachusetts Institute of Technology and The Office of Naval Research.

DEVELOPMENT AND FUNCTIONS OF SIGNATURE WHISTLES OF FREE-RANGING BOTTLENOSE DOLPHINS, TURSIOPS TRUNCATUS

Laela Suad Sayigh

This thesis presents data on the development and functions of individually distinctive signature whistles of free-ranging bottlenose dolphins, Tursiops truncatus. Research was conducted at a study site near Sarasota, Florida, where a resident community of bottlenose dolphins have been the focus of a long-term, ongoing study. Through observations and censuses, researchers have gained information on home ranges and association patterns among individuals. A temporary capture

and release program has provided opportunities to collect basic information regarding age, sex, genetic relationships, and life history of individuals, as well as record vocalizations of known individuals. During the periods 1975-1976 and 1984-1992, 134 different individuals were recorded during temporary capture. More than half of these were recorded on two or more (up to 10) different occasions. These recordings demonstrate that free-ranging dolphins produce individually distinctive signature whistles, as was previously documented for captive dolphins. Each dolphin produced a distinctive frequency contour, or pattern of frequency changes over time, and this whistle comprised a large portion of all whistles produced. Comparisons of whistles recorded from the same individuals over periods of more than a decade indicate that these signature whistle contours are markedly stable. This extensive database of recordings of signature whistles produced by known individuals formed the basis for much of the work described in this thesis.

Playback experiments conducted during temporary capture-release projects indicated that free-ranging dolphins were able to discriminate among signature whistles of familiar individuals. When these results are taken in the context of what is known about dolphin societies, which are characterized by stable individual associations intermixed with fluid patterns of association among many individuals, it appears highly likely that dolphins use signature whistles to recognize one another as individuals.

Sex differences in whistle production were documented through analysis of whistles recorded during temporary capture. Naive judges rated the similarity of signature whistle contours of 42 Sarasota calves and their mothers, and found that males were more likely than females to produce signature whistle contours highly similar to those of their mothers. Conversely, females were more likely than males to produce contours highly distinct from those of their mothers. In addition, preliminary results indicated that male calves were more likely than female calves to produce whistles other than the signature whistle (called "variant" whistles). It was hypothesized that these sex differences may relate to the different roles males and females play in the social structure of the community.

Comparisons of whistle contours of parents and offspring, both in the wild (Sarasota) and in captivity (Miami Seaquarium), do not indicate that signature whistle structure is strictly inherited. Instead, it appears that learning plays a role in determining whistle structure. This contrasts with other non-human mammalian species, where learning does not appear to be involved in vocal development. Focal observations and acoustic recordings of four free-ranging

Sarasota mother-calf pairs were conducted in order to examine the effects of the early social and auditory environment on signature whistle development. Although there was considerable individual variability among these four calves, this study provided some preliminary insights into factors affecting the time course and outcome of signature whistle development in the wild. Two calves which exhibited relatively rapid whistle development and produced contours that resembled those of their mothers also heard proportionately more of their mothers' signature contours than did the other two calves. The other two calves exhibited more prolonged whistle development and produced contours that did not resemble those of their mothers. Preliminary data indicated that these two mothers may have actively taught their calves to produce a distinctive whistle contour by producing "model" contours while their calves were very young. Strength of the mother-calf association, number of associates other than the mother, overall number of whistles heard, and number of whistles produced by the mother all may affect the time course of whistle development and whether or not a calf develops a contour similar to that of its mother.

Supported by: Ocean Ventures Fund, the National Science Foundation, the Office of Naval Research and the National Institutes of Health under contract Nos. N00014-87-K-0236, 1H1R29NS25290 and BNS-9014545.

GEOCHEMICAL AND FLUID DYNAMIC INVESTIGATIONS INTO THE NATURE OF CHEMICAL HETEROGENEITY IN THE EARTH'S MANTLE

Erik Harold Hauri

Variations in the abundances of elements and radiogenic isotopes in mantle derived peridotites and volcanic rocks are chemical integrals over time, space, and process, which ultimately contain information about the role of convection in the earth's mantle in creating, maintaining, and destroying geochemical heterogeneities. Successful inversion of these integrals requires extensive knowledge of the geochemical behavior of elements. the length scales of chemical variability, the evolution with time of geologic systems, the physical properties of mantle rocks, and the driving forces of phenomena which govern heat and mass transport in a dynamic earth. This dissertation attempts to add to this knowledge by examining the trace element and isotope geochemistry of mantle peridotites and oceanic island basalts, and by studying aspects of the flow of viscous fluids driven by thermal buoyancy.

The trace element and isotopic systematics of peridotites and associated mafic layers from the

Ronda Ultramafic Complex, southern Spain (Chapter 2), provides information bearing on the geochemical behavior of the highly incompatible elements U, Th, and Pb in the mantle, and on the length scales of geochemical variability in a well exposed peridotite massif. Garnet is demonstrated to be a significant host for U in the mantle, and together with clinopyroxene, these two minerals control the abundances and partitioning relationships of U and Th during the melting of anhydrous peridotite. Clinopyroxene, plagioclase, and to a lesser extent garnet are hosts for Pb in mantle peridotite; however, the role of trace sulfide may exert some control over the abundance and partitioning of Pb in some samples. Due to the possibility that Pb is partitioned into sulfide, the U/Pb, Th/Pb, and Ce/Pb ratios measured in clinopyroxene are likely to be higher than the bulk rock. U-Pb age systematics of garnet-clinopyroxene pairs from Ronda peridotites and mafic layers indicate Pb isotopic equilibrium in these samples up to 20-50 Ma ago. The Pb-Pb systematics of garnet- and spinel-facies peridotites and mafic layers indicate a heterogeneity on the order of 3 Ga old. This Pb isotope signature may have been created within the massif 3 Ga ago, or may have been metasomatically imprinted on the massif 1.3 Ga ago by basaltic melts with island arc affinities. The isotopic evolution of Ronda is consistent with an origin as ancient (3 Ga) MORB source mantle which experienced a partial melting event at 1.3 Ga ago, and was subsequently incorporated into the subcontinental lithosphere. The very low U, Th, and Pb concentrations in depleted peridotite indicate that recycled crustal materials, with U-Th-Pb concentrations 10^2 - 10^4 times higher than peridotite, will have a larger influence on the isotopic composition of Pb in the mantle than on the Sr and Nd isotopic composition.

An investigation of the trace element and isotopic compositions of clinopyroxenes in peridotite xenoliths from Savaii, Western Samoa and Tubuai, Austral Islands (Chapter 3) reveals geochemical signatures which are not present in basalts from these islands, due to the inherent averaging of melting processes. The data indicate similarities in the melting and melt segregation processes beneath these isotopically extreme islands. Samples with LREE depleted clinopyroxenes, with positive Zr and negative Ti anomalies, are the result of polybaric fractional melting of peridotite in the garnet- and spinel Iherzolite stability fields, with the Savaii samples having experienced a larger mean degree of melting than the Tubuai samples. The extreme fractionation of HREE in the Savaii samples requires that they have melted to the clinopyroxene-out point (about 20%) while retaining residual garnet; the low concentrations of HREE in these same samples requires a further

10-20% melting in the spinel lherzolite stability field. The extremely high total degrees of melting experienced by the Savaii samples (33-42%), as well as the high degree of melting in the garnet lherzolite stability field, suggests a mantle plume origin for these xenoliths.

A large majority of the xenolith clinopyroxenes from both Savaii and Tubuai are LREE enriched to varying degrees, and many samples display significant intergrain trace element heterogeneity was the result of metasomatism by percolating melts undergoing chromatographic trace element fractionation. The trace element compositions of some LREE enriched clinopyroxenes are consistent with the percolating melt being typical oceanic island basalt. The clinopyroxenes with the highest LREE concentrations from both islands, which also have very low Ti and Zr concentrations and large amounts of grain-boundary hosted Ba, require that the percolating melt in these cases had the trace element signature of carbonatite melt. The isotopic composition of one of these "carbonatitic" samples from Tubuai is similar to basalts from this island. The isotopic composition of clinopyroxene in a "carbonatitic" sample from Savaii records ⁸⁷Sr/⁸⁶Sr and ¹⁴³Nd/¹⁴⁴Nd values of .71284 and .512516 respectively, far in excess of the most extreme Samoa basalt values $(^{87}Sr/^{86}Sr=.70742, ^{143}Nd/^{144}Nd=.51264)$. These "carbonatitic" signatures indicate the presence of volatilerich, isotopically extreme components in the mantle beneath Tubuai and Savaii, which likely have their origins in recycled crustal materials.

The Re-Os isotope systematics of oceanic island basalts from Rarotonga, Savaii, Tahaa, Rurutu, Tubuai, and Mangaia are examined (Chapter 4). Os concentration variations suggest that olivine, or a low Re/Os phase associated with olivine, controls the Os concentration in basaltic magmas. The Savaii and Tahaa samples, with high ⁸⁷Sr/⁸⁶Sr and ²⁰⁷Pb/²⁰⁴Pb ratios (EMII), as well as basalts from Rarotonga, have ¹⁸⁷Os/¹⁸⁶Os ratios of 1.026-1.086, within the range of estimates of bulk silicate earth and depleted upper mantle. The basalts from Rurutu, Tubuai, and Mangaia (Macdonald hotspot), characterized by high Pb isotope ratios (HIMU), have 187Os/186Os ratios of 1.117-1.248, higher than any estimates for bulk silicate earth, and higher than Os isotope ratios of metasomatized peridotites. The high 187Os/186Os ratios indicate the presence of recycled oceanic crust in the mantle sources of Rurutu, Tubuai, and Mangaia. Inversion of the isotopic data for Mangaia (endmember HIMU) indicate that the recycled crustal component has Rb/Sr, Sm/Nd, Lu/Hf, and Th/U ratios which are very similar to fresh MORB glasses, and U/Pb and Th/Pb ratios which are within the range of MORB values, but slightly higher than average N-MORB. These results indicate that the low-temperature

alteration signature of altered oceanic crust may be largely removed during subduction, and that oceanic crust was recycled into the lower mantle source of Macdonald hotspot plume. Furthermore, the high ¹⁸⁷Os/¹⁸⁶Os ratios of the Tubuai and Mangaia basalts indicates that percolation through depleted mantle peridotite

(187Os/186Os=1.00-1.08), observed to occur in the Tubuai xenoliths, had little influence on the

composition of the erupted basalts.

A fluid dynamic model for mantle plumes is developed (Chapter 5) by examining a vertical, axisymmetric boundary layer originating from a point source of heat, and incorporating experimentally constrained rheological and physical properties of the mantle. Comparison of linear (n=1) and non-Newtonian (olivine, n=3) rheologies reveals that non-Newtonian plumes have narrower radii and higher vertical velocities than corresponding Newtonian plumes. The non-Newtonian plumes also exhibit "plug flow" at the conduit axis, providing a mechanism for the transport of deep mantle material, through the full depth of the mantle, in an unmixed state. Plumes are demonstrated to entrain ambient mantle via the horizontal conduction of heat, which increases the buoyancy and lowers the viscosity of mantle at the plume boundary. Streamlines calculated from the fluid dynamic model demonstrate that most of the entrained mantle originates from below 1500 km depth. Parameterization of the entrainment mechanism indicates that the factional amount of entrained mantle is lower in stronger, hotter plumes due to their higher vertical velocities.

Examination of the global isotopic database for oceanic island basalts reveals the presence of a mantle component (FOZO), common to many hotspots worldwide, characterized by depleted 87Sr/86Sr and 143Nd/144Nd, radiogenic 206,207,208 Pb/ 204 Pb, and high 3 He/ 4 He. This component is isotopically distinct from the source of MORB; thus, with the exception of ridge centered hotspots such as Iceland and the Galapagos, upper mantle does not appear to be a component in most hotspots, in agreement with entrainment theory. The combined fluid dynamic and isotopic results indicate that both FOZO and the enriched mantle components (EMI, EMII, and HIMU) are located in the lower mantle. Furthermore, high ³He/⁴He in FOZO preculdes an origin for FOZO-bearing plumes in a thermal boundary layer at 670 km depth in the mantle. Since a 670 km thermal boundary layer would be replenished by the downward motion of the upper mantle, an origin for FOZO at 670 km would require either 1) a high ³He/⁴He signature in the MORB source, or 2) entrainment of MORB mantle into intraplate plumes, neither of which is observed in the OIB isotope data. This indicates that the 670 km discontinuity is not a barrier to mantle

convection. The preservation of isotopically different upper and lower mantles does not require layered convection, but is probably the result of an increasing residence time with depth in the mantle, possibly caused by an increase in the mean viscosity of the mantle with depth.

Supported by: National Science Foundation and a Mellon Interdisciplinary Science Award.

INTERACTION OF AN EDDY WITH A CONTINENTAL SLOPE

Xiaoming Wang

This study concerns the barotopic interactions between a mesoscale eddy and a straight monotonic bottom topography. Through simple to relatively complicated modeling effort, some of the fundamental properties of the interaction are

investigated.

In chapter two, the fundamental aspects of the interaction are examined using a simple contour dynamics model. With the simplest model configuration of an ideal vortex and a step topography, the basic dynamical features of the observed oceanic eddy-topography interaction are qualitatively reproduced. The results consist of eddy-induced cross-topography exchange, formation of topographic eddies, eddy propagation

and generation of topographic waves.

In chapter three, a more complicated primitive equation model is used to investigate a mesoscale eddy interacting with an exponential continental shelf/slope topography on both f and β -planes. The f-plane model recasts the important features of chapter two. The roles of the cddy size and strength and the geometry of topography are studied. It is seen that the multiple anticyclonic eddy-slope interactions strongly affect the total cross-slope volume transport and the evolution of both the original anticyclone and the topographic eddy. Since a cyclone is trapped at the slope and eventually moves on to the slope, it is most effective in causing perturbation on the shelf and slope. The responses on the shelf and slope are mainly wavelink with dispersion relation obeying that of the free shelf-trapped wave models. On the β -plane, the problem of an eddy colliding onto a continental shelf/slope from a distance with straight or oblique incident angles is investigated. It is found that the straight eddy incident is more effective in achieving large onslope eddy penetration distance than the oblique eddy incident. The formation of a dipole-like eddy pair consisting of the original anticyclone and the topographic cyclone acts to suppress the eddy decay due to long Rossby wave radiation. A weak along-slope current near the edge of the slope is found, which is part of a outer slope circulation

cell originated from the Rossby wave wake trailing the propagating eddy.

Model-observation comparisons in chapter four show favorable qualitative agreement of the model results with some of the observed events in the eastern U.S. continental margins and in the Gulf of Mexico. The model results give dynamical interpretations to some observed features of the oceanic eddy-topography interactions and provide enlightening insight into the problem.

Supported by: Massachusetts Institute of Technology.

OBSERVATIONS OF TURBULENCE, INTERNAL WAVES AND BACKGROUND FLOWS: AN INQUIRY INTO THE RELATIONSHIPS BETWEEN SCALES AND MOTION

Kurt Louis Polzin

Oceanic profiles of temperature, salinity, horizontal velocity, rate of dissipation of turbulent kinetic energy (ε) and rate of dissipation of thermal variance (χ) are used to examine the parameterization of turbulent mixing in the ocean due to internal waves. Turbulent mixing is quantified through eddy diffusivity parameterizations of the mass ($K\rho$; Osborn, 1980) and heat fluxes (K_T ; Osborn and Cox, 1972) in turbulent production/dissipation balances. Turbulence in the ocean is generally held to result from the occurance of shear instability in regions where the Richardson number is locally supercritical (i.e. Ri < 1/4), permitting the growth of small-scale waves which break and result in turbulent mixing. The occurrence of shear instability results from the local intensification of the shear in the internal wave field. The energy dissipated in such events is provided by the energy flux to higher wavenumber due to nonlinear wave/wave interactions on scales of 10's to 100's of meters. In turn, the strength of the wave/wave interactions depends generally on the energy content of the internal wave field, which can vary considerably over even large scales due to the presence of topography or background flows. The magnitude of turbulent mixing is linked to internal wave dynamics by equating the turbulent dissipation with the energy flux through the vertical wavenumber spectrum under the priviso that the model spectrum which forms the basis for the analysis is statistically stationary with respect to the nonlinear interactions. Dynamical models (McComas and Muller, 1981; Henyey et al., 1986) indicate that the Garrett and Munk (GM; Munk, 1981) spectrum is stationary.

Observations from the far field of a seamount in a region of negligible large-scale flow were examined to address the issue of the buoyancy

scaling of ϵ . These data exhibited large variations in background stratification with depth, but the internal wave characteristics were not substantially differentiable from the GM prescription. The magnitude of ϵ and its functional dependence upon internal wave energy levels (E) and buoyancy frequency (N) was best described by the dynamical model of Henyey et al. (1986) ($\epsilon \sim E^2 N^2$). The Richardson number scaling model of Kunze et al. (1990) produced consistent estimates. A second dynamical model, McComas and Muller (1981), predicted an appropriate (E,N) scaling, but overestimated the observed dissipation rates by a factor of five. Two kinematical dissipation parameterizations (Gargett and Holloway (1984) and Munk (1981)) predicted buoyancy scalings of N^{3/2} which were inconsistent with the observed scaling.

Data from an upper-ocean front, a warm core ring and a region of steep topography were analyzed in order to examine the parameter dependence of ϵ in internal wave fields which exhibited potentially non-stationary characteristics. Evidence was provided which implied the internal wave field in an upper ocean front was interacting with and modified by the background flow. Inhomogeneity and anistropy of the internal wave field were noted in that data set. The model of Gregg (1989), which in turn was based upon the model Henyey et al., effectively collapsed the observed diffusivity estimates from the front. The warm core ring profiles were noted to be anisotropic, dominated by near-inertial frequencies and to have a peaked vertical wavenumber shear spectrum. The data from a region of steep topography were noted to have a peaked vertical wavenumber spectrum and were characterized by higher than GM frequency motions. For the latter two data sets, application of a frequency based correction to the Henyey et al. model (Henyey, 1991) reduced more than an order of magnitude scatter in the parameterized estimates of ϵ to less than a factor of four. Of the possible non-equilibrium conditions in the internal wave field, the (E,N) scaled dissipation rates were most sensitive to deviations in wave field frequency

On the basis of a number of theoretical Richardson number probability distributions (Ri=N²/S², where S² is the sum of the squared vertical derivatives of horizontal velocity), the nominal dissipation scaling of the Kunze ϵt al. model was determined to be E²N³. This scaling is altered to the observed $\epsilon \sim E^2N^2$ scaling by a statistical dependence between N² and S² which reduces the occurrence of supercritical Ri values. This statistical dependence is hypothesized to be an effect of the turbulent momentum and buoyancy fluxes on the internal wave shear and strain profiles caused by shear instability. The

statistical dependence between N^2 and S^2 exhibited a buoyancy scaling which was interpreted as resulting from the decreasing ratio between the time scale of the shear instability mechanism $[T \sim 2\pi/N]$ and the adiabatic time scale $[T \sim 2\pi/(Nf)^{1/2}]$ of the internal wave field (f is the Coriolis parameter). This phenomenology is interpreted in light of saturated spectral theories which suggest that the magnitude and shape of the vertical wavenumber spectrum is controlled by instability mechanisms at large wavenumber $(\geq 1$ cpm). We argue that saturated spectral theories are valid only in the limit where a separation exists between the two time scales, i.e. for large N, low internal wave frequency content, and small f.

These results have immediate implications for oceanic mixing driven by internal wave motions. First, background diffusivities are small: at GM energy levels, $K\rho \sim .03 \times 10^{-4} \text{ m}^2/\text{s}$ ($K\rho = .25\epsilon/\text{N}^2$). Secondly, since $K\rho$ is independent of N at constant E, some process of collection of processes must be responsible for heightened E values in the abyss if internal waves cause the $O(1-10 \times 10^{-4} \text{ m}^2/\text{s})$ diffusivities generally inferred from deep ocean hydrographic data. We view internal wave reflection and/or internal wave generation associated with topographic features to be likely candidates.

Supported by: Office of Naval Research under Contract Nos. N00014-87-K-0007 and N00014-89-J-1073.

MERIDIONAL CIRCULATION IN THE TROPICAL NORTH ATLANTIC

Marjorie A.M. Friedrichs

A transatlantic CTD/ADCP section nominally located at 11°N was carried out in March 1989. In this paper relative geostrophic velocities are computed from these data via the thermal wind balance, with reference level choices based primarily on water mass distributions. Mass is conserved by requiring the geostrophic transport to balance the sum of the Ekman and shallow western boundary current transports.

A brief overview of the meridional circulation of the upper waters resulting from these analysis techniques is presented, and indicates a North Brazil Current transport of nearly 12 Sv.

Transports of the shallow waters are found to support the results of Schmitz and Richardson (1991) who found nearly half of the Florida Current waters to be derived from the South Atlantic. Schematic circulation patterns of the NADW and AABW are also presented. The deep waters of the western basin are dominated by a cyclonic recirculation gyre, consisting of a southward DWBC transport of 26.5 ± 1.8 Sv, with

nearly half of this flow returning northward along the western flank of the MAR. A particularly notable result of the deep western basin analysis is the negligible net flow of middle NADW. Although the northward flows of upper and lower NADW along the western flank of the MAR are believed to be associated with the local recirculation gyre, the northward flow of middle NADW, which nearly balances the southward flow of this water mass along the western boundary, may be derived from the eastern basin of the South Atlantic. The deep waters of the eastern basin are also dominated by a large cyclonic recirculation gyre, consisting primariliy of lower NADW and supplemented by middle NADW and AABW. Each of these water masses, as well as the upper NADW, have small net northward flows within the eastern basin. The AABW most likely enters the castern basin by means of the Vema Fracture Zone, while the lower NADW enters primarily through the Kane Gap.

Although the components of the horizontal circulation discussed above agree well with results from previous CTD, current meter, and float studies, the meridional overturning cell (5.2 \pm 1.6 Sv) and the net heat flux $(2.3 \pm 1.6 \times 10^{14} \text{ w})$ calculated in this study are considerably lower, and the net freshwater flux (-0.60 \pm 1.5 Sv) is slightly higher than previous estimates. These discrepancies may be attributed to: (1) differences in methodologies, (2) the increased resolution of this section (as compared to earlier IGY sections), and (3) temporal (including decadal, synoptic, and most importantly, seasonal) variability. Annual average meridional overturning (12 Sv), heat flux (11 x 10^{14} W), and freshwater flux (-0.35 Sv), are computed based on annual average Ekman and NBC transports, temperatures, and salinities, and agree well with most previous annual estimates. The large difference between the March and the annual estimates is indicative of the importance of seasonal variability within the tropical North Atlantic.

Supported by: The Office of Naval Research.

ANALYSIS AND APPLICATION OF AN UNDERWATER OPTICAL-RANGING SYSTEM

John Gerald Kusters, Jr.

In order to provide a high-resolution underwater-ranging capability for scientific measurement, a commercially available optical-ranging system is analyzed for performance and feasibility. The system employs a structured-lighting technique using a laser-light plane and single-camera imaging system. The mechanics of determining range with such a system are presented along with predicted range error.

Controlled testing of the system is performed and range error is empirically determined. The system is employed in a deep-sea application, and its performance is evaluated. The measurements obtained are used for a scientific application to determine seafloor roughness for very-high-spatial frequencies (greater than 10 cycles/meter). Use and application recommendations for the system are presented.

Supported by: United States Navy.

MODELING A 300 KHZ BATHYMETRIC SONAR SYSTEM

Kenneth Alan Malmquist

The Deep Submergence Laboratory has developed a family of calibrated high frequency bathymetric sonar system for underwater survey. It is useful to have a detailed mathematical description of these systems to assist in data

processing.

A model of a generalized sonar system is developed first. This model then is made specific to the DSL 300-kHz scanning sonar and is implemented using the MATLAB software package. The model consists of a cascaded series of tilters representing the electrical and mechanical components of the system. The model is adjusted after comparison to the transmited pulse. The results are then inverted to demonstrate how the corrupting effects of the system can be reversed. A technique is developed for applying this reverse model to actual data.

The results showed that a good representation of the system can be implemented using relatively simple descriptions of each component. The most important components are the band-limiting filter and the transducer. It is possible to reverse model these components with good results.

Supported by: United States Navy.

Index	
Agrawal, Y. C	Caswell, HalB-2,3,7,9,16
Altabet, Mark A MCG-1,2,7	Cathles, Larry MCG-6
Amaral, Linda AB-3	Catipovic, Josko AAOPE-8
Anderson, Donald MB-1,5,13,23	Cavanaugh, Colleen MB-3
Aoki, Rika BB-3	Chapman, David CPO-2,6,15
Armstrong, AB-26	Chappell, J. M. A
Aubrey, D. G	Chaulk, Edwin AOPE-3
Austin, Jay APO-4	Chave, Alan D AOPE-15;GG-6,8,12
Austin, TAOPE-16	Chen, Changsheng GS-1;PO-14,15
	Chisholm, S. W
Bacon, Michael PMCG-1,7	Chiu, Ching-Sang AOPE-3,4
Bailey, Roger SMPC-1	Chou, Ru Ling
Bates, S. S	Christeson, G. L
Bauer, James EMCG-2	Chu, David K. Y. MPC-4
Beardsley, Robert CPO-14,15	
Beck, J. Warren MCG-7	Churchill James H. AOPE-9,14,18,21
Bemis, Karen GGG-5	Churchill, James HPO-16
Bender, Michael B-13	Clay, Clarence S
Benner, JB-20	Cochran, J. Kirk
Berner, Robert AMCG-14	Cochran, James R
Berninger, Ulrike-GB-2,21	Cohen, G. J
Berteaux, Henri O	Collins, Michael D AOPE-4
Betts, Jonathan NGS-1	Colosi, J. A
Bhatta, Saurav D	Colwell, R. R MCG-1
Bisack, K. D	Comb, D. G
Bjørnland, TMCG-5	Cornuelle, B. D AOPE-8,11
Bloom, A. L. MCG-7	Craig, A. CB-15
	Curry, Ruth APO-5
Blough, Neil V	Curry, William BGG-16,17
Blusztajn, Jerzy	Cushman-Roisin, Benoit PO-12
Bocconcelli, Alessandro	Dahar Massa Assa
Bock, Erik J	Daher, Mary Ann
Bollens, S. M	Dalziel, John AMCG-13
Bothner, M. H	Davis, Andrew R
Bower, Amy SPO-1	DeCola, Peter N MPC-6
Bradley, Albert M AOPE-6	DeGrandpre, Michael DMCG-15
Brady, David AOPE-8	DeLong, Edward F
Brault, SolangeB-2	Demin, Yurii Leonidovich
Brewer, Peter G MCG-3	Demirev, E
Briggs, William GG-16	Dennett, Mark B-8,13
Broadus, James MMPC-1,2,4,7	Des Marais, D. J
Broda, James EAOPE-18	Detrick, R. S
Brown, Neil LAOPE-2	Deuser, Werner GMCG-10
Brumley, Blair H AOPE-20	Diaconu, V
Brunet, Christian MCG-2	DiChristina Thomas J
Bryan, Wilfred B GG-3	Dick, Henry J. B
Bryden, Harry LPO-1,8,9	Dickson, Robert
Buck, John RAOPE-12	Donahue, D
Buesseler, Ken OMCG-1,4	Donelan, M. AAOPE-10
Buhl, P	Doucette, Gregory J
Burns, Daniel R	Dougherty, Martin EGG-13
Burr, G	Doutt, James AAOPE-14
Butman, BMCG-1	Dragos, D. Miosky B-15
Butman, Cheryl Ann	Drennan, W. MAOPE-10
AOPE-1,3,5,10,12,24,25;B-24,25	Druffel, Ellen R. M MCG-2,5,6,7,13
Canuago Indith McDawell D 15 17	DuBois, David L
Capuzzo, Judith McDowell B-15,17	Duda, Timothy F AOPE-11,13
Carlow, C. K	Dunlap, P. V
Caron, David A	Dunn, ToddGG-2
Caruso, Michael JPO-4	

Eck, Cal. ————————————————————————————————————	F. 1. C. 1	0.100.01.11
Edwards, R. Lawrence MCG-7 Grosenbaugh, Mark A AOPE-8 Egli, Thomas B-12 Grosenbaugh, Mark A AOPE-9 Eglinton, Lorraine Buxton MCG-6 Guiral, J. Escartin GG-4 Guiral, J. GG-6 Guiral, J. Guiral, J. Escartin GG-6 Farrington, John W MCG-1,5 Handdad, Robert I MCG-5 Hahn, Mark E B-10 Haidvogel, Dale B PO-2 Hanvey, Christopher J MPC-8 Hanswell, Dennis A B-8 Hard, Stanley R GG-2,18 GG-6 Hard, Stanley R GG-2,18 GG-7 G		
Egli, Thomas B. 12 Eglinton, Lorraine Buxton MCG-6 Eiswerth, Mark E. MPC-2 Elder, Robert L. AOPE-6 Emery, K. O. G. G. G. Guiral, J. Escartin G. G4 Elder, Robert L. AOPE-6 Emery, K. O. G. G. G. Gurley, John Van AOPE-18, G.S-3 Ertel, John R. MCG-2 Etter, Ron J. B. 3,7 Ertel, John R. MCG-2 Etter, Ron J. B. 3,7 Ertel, John R. MCG-1,5 Erter, Ron J. B. 3,7 Errington, John W. MCG-1,5 Earnington, John W. MCG-1,5 Errington, John W. John		
Eginton, Lorraine Buxton MCG-6 Liswerth, Mark E. MPC-2 Liswerth, Mark E. MPC-2 Lider, Robert L. AOPE-6 Curpery, K. O. GG-3 Ertel, John R. MCG-2 Etter, Ron J. B-3, 7 Etter, Ron J. B-3, 8 Etter, Ron J. B-4, 8 Etter, Ron J. B-4, 8 Eddad, Robert 1. MCG-5 Hahn, Mark E. B-10 Edity, John Van CG-5 E		
Eiswerth, Mark E. MPC-2 Idler, Robert L. AOPE-6 Emery, K. O. G.G-3 Ertel, John R. MCG-2 Etter, Ron J. B-3,7 Farrington, John W. MCG-1,5 Farrington, John W. MCG-1,5 Farrington, John W. MCG-1,5 Farrington, John W. MCG-1,5 Filloux, Jean H. AOPE-15 Flindlay, Robert L. AOPE-15 Flindlay, Robert L. AOPE-15 Flatte, S. M. AOPE-1 Flagg, Charles N. PO-16 Flatte, S. M. AOPE-11 Flagg, Charles N. PO-16 Flotte, S. M. AOPE-11 Flagg, Charles N. PO-16 Flotter, S. M. AOPE-15 Flagg, Charles N. PO-16 Flotter, S. M. AOPE-15 Flagg, Charles N. PO-16 Flagg, Charles N. PO-16 Flagg, Charles N. PO-16 Harding, A. J. G.G-6 Hauri, Drik Harold G.G-2,18GS-11 Flotter, S. M. B-12 G.G-2,18 Flotter, S. M. AOPE-15 Hank, Mark E. B-10 Hardway, E. Marker E. M. AOPE-15 Hardway, A. J. B. Haddad, Robert 1. MCG-5 Hardway, A. J. B. Haddad, Robert 1. MCG-6 Harting, A. J. G.G-6 Hauri, Drik Harold G.G-2,18 Hard, Teten N. AOPE-15 Hardway, A. J. B. Haddad, Robert 1. MCG-6 Hauri, Drik Harold G.G-2,18 Hard, Teten N. AOPE-15 Hardway, A. J. B. Haddad, Robert 1. MCG-6 Hauri, Drik Harold G.G-2,18 Hard, Teten N. AOPE-15 Hardway, A. J. Hardway, B. Hard, Teten N. AOPE-11 Hardway, A. J. Hardway, B. Hard, Teten N. AOPE-11 Hardway, A. J. Hardway, B. Hard, Teten N. AOPE-11 Hardway, A. J. Hardway, B. Hard, Teten N. A. B-24 Hard, Teten N. AOPE-13 Hardway, V. L. Hardway, V. L. Hardway, P. A. AOPE-13 Hardway, V. L. Hardway, V. L. Hardway, P. A. AOPE-13 Hardw		
Elder, Robert L. AOPE-6 Emery, K. O. GG-3 Ertel, John R. MCG-2 Etter, Ron J. B-3,7 Ertel, John R. MCG-3 Erter, Ron J. B-3,7 Ertel, John R. MCG-2 Etter, Ron J. B-3,7 Ertel, John R. MCG-3 Etter, Ron J. B-3,7 Ertel, John Wan AOPE-1 Ertel, John Wan AOPE-1 Ertel, John Wan AOPE-1 Ertel, John Wan ACG-3 Ertel, John Wan AOPE-3 Etter, Ron J. AOPE-1 Ertel, John Wan AOPE-3 Ertel, John Wan AOPE-3 Ertel, John Wan AOPE-3 Ertel, John Wan AOPE-3 Exter, Ron J. AOPE-1 Ertel, John Wan AOPE-3 Exter, Ron John Wan AOPE-3 Exter Ron Jo		
Emery, K. O		
Ertel, John R. MCG-2 Etter, Ron J. B-3.7 Parrington, John W. MCG-1,5 Parrow, R. Scott MPC-3 Filloux, Jean H. AOPE-1,5 Plandy, Robert L. AOPE-1 Plandy, Robert L. AOPE-1 Plandy, Robert L. AOPE-1 Plate, S. M. AOPE-1,1 Poote, Kenneth G. AOPE-1,1,1 Porrani, Daniel J. GG-7,8 Porranes, Steven L. GG-16 Pornari, Daniel J. GG-7,8 Porrester, Ned C. AOPE-2,1,1,2 Prancis, Roger MCG-1,2,7 Prancis, Roger MCG-1,2,7 Prankel, S. L. B-4 Prazel, R. E. PO-14 Predericks, Janet J. AOPE-11 Predericks, Janet J. AOPE-1,1,1,2,2 Prew, Nelson M. AOPE-6 Pristrup, Kurt B-26,27,28 Prye, Daniel E. AOPE-2,1,2,1,2,2 Pryer, G. J. GG-6 Pristrup, Kurt B-26,27,28 Prye, Daniel E. AOPE-2,2,5 Prye, G. J. GG-6 Garand, Elizabeth D. B-19 Gawarkiewicz, Glen D-15,16 Goricke, Ralf B-4, MCG-3,5,18,15 Goldman, David W. MCG-3 Grassle, J. Frederick AOPE-10 Grassle, J. Frederick AOPE-10 Grassle, J. Frederick AOPE-13,51,20 Gorassle, J. Frederick AOPE-10 Grassle, J. Frederick AOPE-13,51,20 Grassle, J. Frederick AOPE-13,51,52 Graber, H. AOPE-2, Grassle, J. Frederick AOPE-13,51,52 Graber, H. AOPE-2, Grassle, J. Frederick AOPE-17, MCG-13 Grassle, J. Frederick AOPE-1, John A. AOPE-13 Johnnessen, O. AOPE-8,22 John A. AOPE-17, MCG-13 Johnnessen, O. AOPE-8,22		
Badada, Hobert McG-3		Gurley, John Van AOPE-18;GS-3
Hahn, Mark E. B-10	Ertel, John RMCG-2	H-11-1 D-1-41 MCC 5
Farrington, John W. MCG-1,5 Farrow, R. Scott MPC-3 Haney, Christopher J. MPC-8 Filloux, Jean H. AOPE-15 Hanewell, Dennis A. B-8 Findlay, Robert L. AOPE-11 Hara, Tetsu. AOPE-9,13 Flagg, Charles N. PO-16 Harding, A. J. GG-6 Flatté, S. M. AOPE-11 Hara, Tetsu. AOPE-9,13 Flotte, S. M. AOPE-11 Hara, Tetsu. AOPE-9,13 Forote, Kenneth G. AOPE-14 Hara, Stanley R. GG-2,18 Forman, Steven L. GG-16 Hauri, Erik Harold GG-2,18 Formari, Daniel J. GG-7,8 Helfrich, Karl R. PO-12 Forester, Ned C. AOPE-15 Hempstead, S. K. B-20 Fougere, Alan AOPE-15 Hempstead, S. K. B-20 Fougere, Alan AOPE-16 Hempstead, S. K. B-20 Frankel, S. L. B-4 Hey R. N. GG-4 Frazel, R. E. PO-14 Hildebrand, J. A. AOPE-11 Fredrick, Janet J. AOPE-11 Hill, R. R. MCG-1 Fredrick, Marotel A. AOPE-1 Hill, R. R. MCG-1 Freidrich, Marjorie A. M. GS-15 Hodgkiss, W. S. Jr. AOPE-11 Fristrup, Kurt B-26,27 28 Hogg, Nelson G PO-1,2,18 Fryer, G. J. GG-6 Howe, B. M. AOPE-1 Fryer, G. J. GG-6 Howe, B. M. AOPE-1 Frigerson, John A. AOPE-2,25 Howe, B. M. AOPE-1 Frigerson, John A. AOPE-1 Howell, Christopher Todd GS-10 Garland, Elizabeth D. B-19 Garland, Elizabeth D. B-19 Garland, Elizabeth D. B-19 Garland, Elizabeth D. B-19 Goerricke, Ralf B-4,MCG-2,5 Goerricke, Ralf B-4,MCG-2,5 Goldman, Joel C. B-8,13 Goldman, Joel C.	Etter, Ron J B-3,7	
Farrow, R. Scott	D ' 4 I I W MOO 15	
Fillolux, Jean H. AOPE-15 Findlay, Robert L. AOPE-11 Flagg, Charles N. PO-16 Flatté, S. M. AOPE-11 Flagg, Charles N. PO-16 Flatté, S. M. AOPE-11 Flagg, Charles N. PO-16 Flatté, S. M. AOPE-14, 18 Forto, Kenneth G. AOPE-14, 18 Formari, Daniel J. GG-7, 8 Formari, Dan		
Findlay, Robert L. AOPE-1 Hara, Tetsu AOPE-9,13 Flagg, Charles N. PO-16 Harding, A. J. G-6-6 Flatté, S. M. AOPE-11 Hare, P. E. MCG-5 Foote, Kenneth G. AOPE-14,18 Hart, Stanley R. G-6-2,18,GS-11 Forman, Steven L. G-6-16 Hauri, Erik Harold G-2,18,GS-11 Forman, Steven L. AOPE-15 Helfrich, Karl R. PO-12 Fortester, Ned C. AOPE-15 Helprich, Karl R. PO-12 Forgere, Alan AOPE-2 Hermann, Albert J. PO-2,17 Frankel, S. L. B-4 Hery, R. N. G-6-4 Frazel, R. E. PO-14 Hill, R. R. MCG-10 Fredericks, Janet J. AOPE-11 Hill, R. R. MCG-10 Freitag, Lee E. AOPE-22 Hippenstiel, Ralph AOPE-3 Friedrichs, Marjorie AM. G-5-15 Hoogkiss, W. S., Jr. AOPE-11 Frisk, George V. AOPE-1,14,20 Hoogkiss, W. S., Jr. AOPE-11 Fryer, G. J. G-6 Hook, Natorie A. AOPE-7 Fryer, G. J. G-6 Hook, Natorie A. AOPE-7 Fryer, G. J. G-6 Hook, Natorie A. AOPE-7 Fuller, Charlotte M. AOPE-3 Hook, Natorie A. AOPE-10 Garand, Elizabeth D. B-19 Garland, Elizabeth D. B-19 Garland, Elizabeth D. B-19 Godricke, Ralf B-4;MCG-2,15 Goldberg, D. G-613 Godrigh, David M. MCG-8 Goldberg, D. G-613 Godrigh, David M. MCG-9 Graber, H. AOPE-12, 25 Goldberg, D. G-613 Godricke, Ralf B-4;MCG-2,15 Goldberg, D. G-613 Godrigh, David M. MCG-9 Godrigh, Glenn A. MCG-9 Godrigh, Glenn A. MCG-9 Godrigh, Glenn A. MCG-9 Godrigh, David M. MCG-9 Godrigh, D. G-678, 15 Godrigh, Glenn A. G-678, 15 G		
Flagg, Charles N. PO-16		
Flatik. S. M.		
Foote, Kenneth G		
Forman, Steven L. GG-16 Hauri, Erik Harold GG-2,18;GS-11 Forrarei, Nael C. AOPE-15 Helrich, Karl R. PO-12 Forrester, Ned C. AOPE-15 Helrich, Karl R. PO-12 Forrester, Ned C. AOPE-15 Helrich, Karl R. PO-12 Francois, Roger MCG-1,2,7 Hermann, Albert J. PO-2,17 Frankel, S. L. B-4 Hery, R. N. GG-4 Frazel, R. E. PO-14 Hildebrand, J. A. AOPE-11 Fredericks, Janet J. AOPE-11 Hill, R. R. MCG-1 Freidericks, Janet J. AOPE-11 Hill, R. R. MCG-1 Freidericks, Janet J. AOPE-11 Hill, R. R. MCG-1 Freidericks, Janet J. AOPE-11 Hill, R. R. MCG-1 Fredericks, Janet J. AOPE-11 Hodgaland, Porter MPC-1,3,4,7 Fredericks, Janet J. AOPE-1 Hodgaland, Porter MPC-1,3,4,7 Fredericks, Janet J. AOPE-1 Hodgaland, Porter MPC-1,3,4,7 Hodgalan		
Fornrair, Daniel J. GG-7,8 Helfrich, Karl R. PO-12 Forrester, Ned C. AOPE-15 Hempstead, S. K. B-20 Pougere, Alan AOPE-2 Henderson, Eric W. MPC-10 Franciois, Roger MCG-1, 2,7 Hermann, Albert J. PO-2, 17 Frankel, S. L. B-4 Hermann, Albert J. PO-2, 17 Frazel, R. E. PO-14 Hildebrand, J. A. AOPE-11 Freidrichs, Marjorie A. AOPE-22 Hilpenstel, Ralph. AOPE-3 Frew, Nelson M. AOPE-6 Hoagland, Porter MCG-1 Frisdrichs, Marjorie A.M. GS-15 Hodgkiss, W.S., Jr. AOPE-11 Frisk, George V. AOPE-1,14,20 Hogg, Nelson G. PO-1,2,18 Frye, Daniel E. AOPE-21,78 Hogg, Nelson G. PO-1,2,18 Frye, Daniel E. AOPE-27,78 Hoop, Susumu GG-19 Freichette, Marcel AOPE-24,7 Hoop, Susumu GG-19 Freichtet, Marcel AOPE-14 Howe, B. M. AOPE-17 Fuller, Charlotte M. AOPE-3,810 Howe, B. M. AO		
Forgere, Alan AOPE-2 Fougere, Alan AOPE-2 Fougere, Alan AOPE-2 Fougere, Alan AOPE-2 Francois, Roger MCG-1,2,7 Frankel, S. L. B-4 Frazel, R. E. PO-14 Fredericks, Janet J. AOPE-11 Fredericks, Janet J. AOPE-11 Fredericks, Janet J. AOPE-11 Fredericks, Janet J. AOPE-12 Freik, Nelson M. AOPE-2 Frew, Nelson M. AOPE-6 Friestricks, Marjorie A.M. GS-15 Frisk, George V. AOPE-1,14,20 Fristrup, Kurt B-26,27,28 Frye, Daniel E. AOPE-2,7 Fryer, G. J. GG-6 Fryer, C. J. GG-6 Frechette, Marcel AOPE-24,25 Fuller, Charlotte M. AOPE-7 Fuller, Charlotte M. AOPE-7 Garland, Elizabeth D. B-19 Garland, MCG-3 Geyer, W. Rockwell AOPE-4,22,25 Geyer, W. Rockwell AOPE-4,22,25 Geyer, W. Rockwell AOPE-4,22,25 Geyer, W. Rockwell AOPE-4,22,25 Goldberg, David M. MCG-8 Glover, David M. MCG-8 Glover, David M. MCG-8 Glover, David M. MCG-8 Goricke, Ralf B-4;MCG-2,15 Goericke, Ralf B-4;MCG-2,15 Goericke, Ralf B-4;MCG-5 Gotelli, Nicholas J. B-9 Goyet, Catherine MCG-3,8,13,16 Goodfriend, Glenn A. MCG-5 Gotelli, Nicholas J. B-9 Graber, II. AOPE-12 Graham, David W. MCG-9 Grassel, J. Frederick AOPE-17,MCG-1 Grassel, J. Frederick AOPE-17,MCG-1 Johannessen, O. AOPE-8, 22 Johannessen, O		
Fougere, Alan AOPE-2 Henderson, Eric W MPC-10 Francois, Roger MCG-1,2,7 Frankel, S. L. B-4 Frazel, R. E. PO-14 Fredericks, Janet J. AOPE-11 Friedricks, Janet J. AOPE-11 Frieitag, Lee E. AOPE-22 Friedricks, Marjorie A.M. AOPE-6 Friedricks, Marjorie A.M. AOPE-6 Friedricks, Marjorie A.M. GS-15 Friedricks, Marjorie A.M. GS-16 Friedricks, Marj		
Franceis, Roger MCG-1,2.7 Hermann, Albert J. PO-2,17 Frankel, S. L. B-4 Hey, R. N. GG-4 Frazel, R. E. PO-14 Hilldebrand, J. A. AOPE-11 Fredericks, Janet J. AOPE-11 Hill, R. R. MCG-1 Freitag, Lee E. AOPE-22 Hill, R. R. MCG-1 Frew, Nelson M. AOPE-1 Hill, R. R. MCG-1 Friedrichs, Marjorie A.M. GS-15 Hodgkiss, W. S., Jr. AOPE-3 Frisk, George V. AOPE-11,420 Hoge, Frank E. MCG-16 Fristrup, Kurt. B-26,27,28 Hogg, Nelson G. PO-1,2,18 Frye, Co. J. GG-6 Honjo, Susumu. GG-19 Frèchette, Marcel. AOPE-24,25 Hoor, Franz S. AOPE-7 Fuller, Charlotte M. AOPE-5 Howe, B. M. AOPE-17 Furgerson, John A. AOPE-7 Howe, B. M. AOPE-17 Gagnon, Alan R. GG-1 GG-1 Howell, Christopher Todd. GS-10 Garlad, Elizabeth D. B-19 Howel, Jonathan C. AOPE-10 <td></td> <td></td>		
Frankel, S. L		
Frazel, R. E.		
Fredericks, Janet J. AOPE-11 Freidag, Lee E. AOPE-22 Hippenstiel, Ralph AOPE-3 Frew, Nelson M. AOPE-6 AOPE-6 Frew, Nelson M. AOPE-6 AOPE-15, A,7 Friedrichs, Marjorie A.M. GS-15 Hodgkiss, W. S., Jr. AOPE-13, 4,7 Friedrichs, Marjorie A.M. GS-15 Hodgkiss, W. S., Jr. AOPE-13, 4,7 Friedrichs, Marjorie A.M. GS-15 Hodgkiss, W. S., Jr. AOPE-13, 4,7 Friedrichs, Marjorie A.M. GS-15 Hodgkiss, W. S., Jr. AOPE-13, 4,7 Friedrichs, Marjorie A.M. GS-15 Hogg, Nelson G. PO-1,2,18 Fryer, Daniel E. AOPE-2,7 Hohn, A. A. B-21 Fryer, G. J. GG-6 Hogg, Nelson G. PO-1,2,18 Fryer, G. J. GG-6 Honjo, Susumu. GG-19 Hover, Franz S. AOPE-7 Howe, B.M. AOPE-17 Howe, B.M. AOPE-17 Howe, B.M. AOPE-17 Howell, Christopher Todd GS-10 Howe, Brian L. B-10,19,26 Howell, Christopher Todd GS-10 Howell, Ghristopher Todd GS-10 Howell, Jonathan C. AOPE-10 Howell, Jona		
Freitag, Lee E		
Frew, Nelson M. AOPE-6 Hoagland, Porter MPC-1,3,4,7 Friedrichs, Marjorie A.M. GS-15 Hodgkiss, W. S., Jr. AOPE-11 Frisk, George V. AOPE-1,14,20 Hoge, Frank E. MCG-16 Fristrup, Kurt B-26,27,28 Hoge, Frank E. MCG-16 Fryer, G. J. GG-6 Hong, Nusumu GG-19 Fréchette, Marcel AOPE-24,25 Howel, Jonathan AOPE-7 Fuller, Charlotte M. AOPE-5 Howel, Franz S. AOPE-7 Fuller, Charlotte M. AOPE-1 Howel, S. M. AOPE-11 Furgerson, John A. AOPE-7 Howel, Christopher Todd GS-10 Gamies, Arthur G. MCG-3,8,10 Howel, Jonathan C. AOPE-10 Garland, Elizabeth D. B-19 Howl, Jonathan C. AOPE-10 Gerber, James S. AOPE-3 Hulburt, Edward M. B-11 Geyer, W. Rockwell AOPE-4,22,25 Hunbins, Kenneth PO-12 Glilis, Kathryn M. MCG-8 Hunkins, Kenneth PO-12 Goeit, Frederick E. B-7 Hoge, Frank E. <	Fredericks, Janet JAOPE-11	Hill, R. R
Friedrichs, Marjorie A.M. GS-15 Hodgkiss, W. S., Jr. AOPE-11 Frisk, George V. AOPE-1,14,20 Hoge, Frank E. MCG-16 Fristrup, Kurt B-26,27,28 Hoge, Nelson G. PO-1,2,18 Frye, Daniel E. AOPE-2,7 Hohn, A. A. B-21 Fryer, G. J. GG-6 Honjo, Susumu GG-19 Fréchette, Marcel AOPE-24,25 Howe, Franz S. AOPE-1 Fuller, Charlotte M. AOPE-7 Howe, B. M. AOPE-11 Furgerson, John A. AOPE-7 Howe, B. M. AOPE-11 Gagnon, Alan R. GG-1 Howe, B. M. AOPE-11 Gaines, Arthur G. MPC-3,8,10 Howe, Brian L. B-10,19,26 Garband, Elizabeth D. B-19 Howel, Jonathan C. AOPE-11 Garband, Elizabeth D. B-19 Huang, Rui Xin. PO-3,4 Huang, Rui Xin. PO-3,4 Huang, Rui Xin. PO-3,4 Humphris, Susan E. MCG-9 Hunkins, Kenneth PO-12 Gillis, Kathryn M. MCG-3 Humphris, Susan E. Hooe, Indient A.	Freitag, Lee E AOPE-22	Hippenstiel, RalphAOPE-3
Frisk, George V AOPE-1,14,20 Hoge, Frank E. MCG-16 Fristrup, Kurt B-26,27,28 Hogg, Nelson G. PO-1,2,18 Frye, Daniel E. AOPE-2,7 Hohn, A. A. B-21 Fryer, G. J. GG-6 Honjo, Susumu GG-19 Fréchette, Marcel AOPE-24,25 Hover, Franz S. AOPE-7 Fuller, Charlotte M. AOPE-1 Howel, Frank E. AOPE-19 Fuller, Charlotte M. AOPE-24,25 Hover, Franz S. AOPE-7 Fuller, Charlotte M. AOPE-1 Howel, Shrian L. B-10,19,26 Gagnon, Alan R. GG-1 Howel, Johristopher Todd GS-10 Howel, Johristopher Todd GS-10 Howel, Johnstan C. AOPE-10,19,26 Galanes, Arthur G. MPC-3,8,10 Howel, Johnstan C. AOPE-10 Garland, Elizabeth D. B-19 Howl, Jonathan C. AOPE-10 Gerber, James S. AOPE-3 Hubl, Hsiao-ming PO-17 Huang, Rui Xin PO-3 Hulburt, Edward M. B-11 Geyer, W. Rockwell AOPE-4,22,25 Hunkins, Kenneth	Frew, Nelson MAOPE-6	Hoagland, Porter MPC-1,3,4,7
Fristrup, Kurt. B-26.27.28 Frye, Daniel E. AOPE-2,7 Fryer, G. J	Friedrichs, Marjorie A.M	Hodgkiss, W. S., JrAOPE-11
Fristrup, Kurt. B-26.27.28 Frye, Daniel E. AOPE-2,7 Fryer, G. J	Frisk, George V	Hoge, Frank EMCG-16
Fryer, G. J. GG-6 Honjo, Susumu GG-19 Fréchette, Marcel AOPE-24,25 Hover, Franz S AOPE-7 Fuller, Charlotte M. AOPE-5 Howe, B.M. AOPE-11 Furgerson, John A. AOPE-7 Howe, B.M. AOPE-10 Gagnon, Alan R. GG-1 Howe, B.M. AOPE-10 Gaines, Arthur G. MPC-3,8,10 Howes, Brian L. B-10,19,26 Garland, Elizabeth D. B-19 Howe, B.M. AOPE-10 Garland, Elizabeth D. B-19 Howe, B.M. AOPE-10 Garland, Elizabeth D. B-19 Howl, Jonathan C. AOPE-10 Garber, James S. AOPE-15,16 Howl, Jonathan C. AOPE-10 Gerber, James S. AOPE-15,16 Hulburt, Edward M. B-11 Humphris, Susan E. MCG-9 Hunkins, Kenneth PO-12 Geyer, W. Rockwell AOPE-4,22,25 Hunkins, Kenneth PO-12 Gillis, Kathryn M. MCG-8 Hunkins, Kenneth PO-12 Goerick, Palf B-4;MCG-2,15 Isaksen, Mai F. B-12	Fristrup, Kurt	Hogg, Nelson G PO-1,2,18
Fryer, G. J. GG-6 Honjo, Susumu GG-19 Fréchette, Marcel AOPE-24,25 Hover, Franz S AOPE-7 Fuller, Charlotte M. AOPE-5 Howe, B.M. AOPE-11 Furgerson, John A. AOPE-7 Howe, B.M. AOPE-10 Gagnon, Alan R. GG-1 Howe, B.M. AOPE-10 Gaines, Arthur G. MPC-3,8,10 Howes, Brian L. B-10,19,26 Garland, Elizabeth D. B-19 Howe, B.M. AOPE-10 Garland, Elizabeth D. B-19 Howe, B.M. AOPE-10 Garland, Elizabeth D. B-19 Howl, Jonathan C. AOPE-10 Garber, James S. AOPE-15,16 Howl, Jonathan C. AOPE-10 Gerber, James S. AOPE-15,16 Hulburt, Edward M. B-11 Humphris, Susan E. MCG-9 Hunkins, Kenneth PO-12 Geyer, W. Rockwell AOPE-4,22,25 Hunkins, Kenneth PO-12 Gillis, Kathryn M. MCG-8 Hunkins, Kenneth PO-12 Goerick, Palf B-4;MCG-2,15 Isaksen, Mai F. B-12	Frye, Daniel E AOPE-2,7	Hohn, A. A
Fréchette, Marcel		Honjo, Susumu
Fuller, Charlotte M. AOPE-5 Furgerson, John A. AOPE-7 Furgerson, John A. AOPE-7 Gagnon, Alan R. GG-1 Gaines, Arthur G. MPC-3,8,10 Garland, Elizabeth D. B-19 Gawarkiewicz, Glen PO-15,16 Gerber, James S. AOPE-3 Geyer, W. Rockwell AOPE-4,22,25 Gillis, Kathryn M. MCG-8 Glover, David M. MCG-3 Gmitrowicz, Ed PO-4 Goericke, Ralf B-4;MCG-2,15 Goetz, Frederick E. B-7 Goff, John A. GG-6,7,8,15 Goldberg, D. GG-13 Goldman, Joel C. B-8,13 Goodfriend, Glenn A. MCG-5 Gotelli, Nicholas J. B-9 Goyet, Catherine MCG-3,8,13,16 Graber, H. AOPE-12 Grassle, J. Frederick AOPE-17;MCG-1 Grassle, J. Frederick AOPE-17;MCG-1 Grassle, J. Judith P. AOPE-3,5;B-25 GOLD M. AOPE-13,20 Howe, B. M. AOPE-10 Howell, Christopher Todd GS-10 Howell, Christopher Todd GS-10 GS-10 Howell, Christopher Todd GS-10 Howell, Plove, B-10,19,26 Houl, John AOPE-10 Hsu, Hsiao-ming PO-17 Huang, Rui Xin Po-17 Huang,		Hover, Franz SAOPE-7
Furgerson, John A. AOPE-7 Howell, Christopher Todd GS-10 Gagnon, Alan R. GG-1 B-10,19,26 Gaines, Arthur G. MPC-3,8,10 Howl, Jonathan C. AOPE-10 Garland, Elizabeth D. B-19 Hsu, Hsiao-ming PO-17 Gerber, James S. AOPE-3 Hulburt, Edward M. B-11 Geyer, W. Rockwell AOPE-42,25 Hulburt, Edward M. B-11 Glover, David M. MCG-8 Humphris, Susan E. MCG-9 Glover, David M. MCG-3 Hwang, P. A. AOPE-10 Gnanadesikan, Anand PO-4 Irish, James D. AOPE-13,20 Gnanadesikan, Anand PO-14 Isaksen, Mai F. B-12 Goetringer, Dale D. B-10 Ittekkot, V. GG-16 Goericke, Ralf B-4;MCG-2,15 Ivanov, V. CRC-1 Godf, John A. GG-6,7,8,15 Jannasch, Holger W. B-3,79,12,20,28,29 Gotelli, Nicholas J. B-9 Jasper, John P. MCG-10 Goyet, Catherine MCG-3,8,13,16 Jenkins, William J. MCG-5		
Howes, Brian L. B-10,19,26		
Gagnon, Alan R. GG-1 Gaines, Arthur G. MPC-3,8,10 Howl, Jonathan C. AOPE-10 Garland, Elizabeth D. B-19 Hsu, Hsiao-ming. PO-17 Gawarkiewicz, Glen. PO-15,16 Huang, Rui Xin. PO-3,4 Gerber, James S. AOPE-3 Hubburt, Edward M. B-11 Geyer, W. Rockwell. AOPE-4,22,25 Hunkins, Kenneth. PO-12 Gillis, Kathryn M. MCG-8 Hwang, P. A. AOPE-10 Glover, David M. MCG-3 Hwang, P. A. AOPE-10 Gmitrowicz, Ed. PO-4 Irish, James D. AOPE-13,20 Goenringer, Dale D. B-10 Ittekkot, V. GG-16 Goericke, Ralf. B-4;MCG-2,15 Ivanov, V. CRC-1 Goetz, Frederick E. B-7 Jack, W. E. B-20 Goldberg, D. GG-13 Jannasch, Holger W. B-3,7,9,12,20,28,29 Jannasch, Holger W. B-3,7,9,12,20,28,29 Jack, W. E. B-20 Gotelli, Nicholas J. B-9 Jech, J. Michael AOPE-3 Gotelli, Nicholas J. B-9		
Garland, Elizabeth D. B-19 Huang, Rui Xin PO-3,4 Gawarkiewicz, Glen. PO-15,16 Huang, Rui Xin PO-3,4 Gerber, James S. AOPE-3 Hulburt, Edward M. B-11 Geyer, W. Rockwell. AOPE-4,22,25 Humphris, Susan E. MCG-9 Gillis, Kathryn M. MCG-3 Humphris, Susan E. MCG-9 Glover, David M. MCG-3 Hunkins, Kenneth PO-12 Gmitrowicz, Ed. PO-4 Hwang, P. A. AOPE-10 Gnanadesikan, Anand PO-14 Isaksen, Mai F. B-12 Goehringer, Dale D. B-10 Ittekkot, V. GG-16 Goericke, Ralf B-4;MCG-2,15 Ivanov, V. CRC-1 Goetz, Frederick E. B-7 Jack, W. E. B-20 Goldberg, D. GG-13 Jasper, John P. MCG-10 Goodfriend, Glenn A. MCG-5 Jeffrey, S. W. MCG-5 Gotelli, Nicholas J. B-9 Jenkins, William J. MCG-9 Graber, H. AOPE-17,MCG-1 Jiang, Min. AOPE-18,22 Grassle,		
Garland, Elizabeth D. B-19 Huang, Rui Xin. PO-3,4 Gawarkiewicz, Glen PO-15,16 Hulburt, Edward M. B-11 Gerber, James S. AOPE-3 Hulburt, Edward M. B-11 Geyer, W. Rockwell. AOPE-4,22,25 Hunkins, Kenneth PO-12 Gillis, Kathryn M. MCG-8 Hunkins, Kenneth PO-12 Glover, David M. MCG-3 Huwang, P. A. AOPE-10 Gmitrowicz, Ed. PO-4 Irish, James D. AOPE-13,20 Gnanadesikan, Anand PO-14 Isaksen, Mai F. B-12 Goetricke, Ralf B-4;MCG-2,15 Ivanov, V. CRC-1 Goetz, Frederick E. B-7 Jack, W. E. B-20 Goldberg, D. GG-13 Jannasch, Holger W. B-3,7,9,12,20,28,29 Goldman, Joel C. B-8,13 Jasper, John P. MCG-10 Govet, Catherine MCG-3,8,13,16 Jech, J. Michael AOPE-3 Graber, H. AOPE-12 Jin, Di MCG-5 Jang, Min AOPE-15,23 Jin, Di MPC-4,5 Johann		Hsu, Hsiao-mingPO-17
Gawarkiewicz, Glen PO-15,16 Gerber, James S. AOPE-3 Geyer, W. Rockwell AOPE-4,22,25 Gillis, Kathryn M. MCG-8 Glover, David M. MCG-3 Gmitrowicz, Ed. PO-4 Gnanadesikan, Anand PO-14 Goehringer, Dale D. B-10 Goericke, Ralf B-4;MCG-2,15 Goetz, Frederick E. B-7 Goff, John A. GG-6,7,8,15 Goldberg, D. GG-13 Goldman, Joel C. B-8,13 Gotelli, Nicholas J. B-9 Gotelli, Nicholas J. B-9 Goyet, Catherine MCG-3,8,13,16 Graber, H. AOPE-17;MCG-1 Grassle, J. Frederick AOPE-17;MCG-1 Grassle, J. Udith P. AOPE-17;MCG-1 Grassle, Judith P. AOPE-3,5;B-25		
Gerber, James S. AOPE-3 Humphris, Susan E. MCG-9 Geyer, W. Rockwell AOPE-4,22,25 Hunkins, Kenneth PO-12 Gillis, Kathryn M. MCG-8 Hunkins, Kenneth PO-12 Glover, David M. MCG-3 Hwang, P. A. AOPE-10 Gmitrowicz, Ed. PO-4 Irish, James D. AOPE-13,20 Gnanadesikan, Anand PO-14 Isaksen, Mai F. B-12 Goehringer, Dale D. B-10 Ittekkot, V. GG-16 Goericke, Ralf B-4;MCG-2,15 Ivanov, V. CRC-1 Goetz, Frederick E. B-7 Jack, W. E. B-20 Goldberg, D. GG-13 Jasper, John P. MCG-10 Goodfriend, Glenn A. MCG-5 Jeffrey, S. W. MCG-10 Gotelli, Nicholas J. B-9 Jeffrey, S. W. MCG-5 Goyet, Catherine MCG-3,8,13,16 Jenkins, William J. MCG-9 Jiang, Min. AOPE-15,23 Jin, Di. MPC-4,5 Grassle, J. Frederick AOPE-17;MCG-1 Johannessen, O. AOPE-18 Gra		
Geyer, W. Rockwell AOPE-4,22,25 Hunkins, Kenneth PO-12 Gillis, Kathryn M. MCG-8 Hwang, P. A. AOPE-10 Glover, David M. MCG-3 Hwang, P. A. AOPE-10 Gmitrowicz, Ed. PO-4 Irish, James D. AOPE-13,20 Gnanadesikan, Anand PO-14 Isaksen, Mai F. B-12 Goehringer, Dale D. B-10 Ittekkot, V. GG-16 Goericke, Ralf B-4;MCG-2,15 Ivanov, V. CRC-1 Goetz, Frederick E. B-7 Jack, W. E. B-20 Goldberg, D. GG-13 Jannasch, Holger W. B-3,7,9,12,20,28,29 Jasper, John P. MCG-10 Jech, J. Michael AOPE-3 Goodfriend, Glenn A. MCG-5 Jeffrey, S. W. MCG-5 Goyet, Catherine MCG-3,8,13,16 Jenkins, William J. MCG-9 Graber, H. AOPE-12 Jin, Di. MPC-4,5 Grassle, J. Frederick AOPE-17;MCG-1 Johannessen, O. AOPE-18,22 Grassle, Judith P. AOPE-3,5;B-25 Johannessen, O. AOPE-8,22	Gerber, James S	
Gillis, Kathryn M. MCG-8 Glover, David M. MCG-3 Gmitrowicz, Ed. PO-4 Gnanadesikan, Anand PO-14 Goehringer, Dale D. B-10 Goericke, Ralf B-4;MCG-2,15 Goetz, Frederick E. B-7 Goff, John A. GG-6,7,8,15 Goldberg, D. GG-13 Goldman, Joel C. B-8,13 Goodfriend, Glenn A. MCG-5 Gotelli, Nicholas J. B-9 Goyet, Catherine MCG-3,8,13,16 Graber, H. AOPE-12 Graham, David W. MCG-9 Grassle, J. Frederick AOPE-17;MCG-1 Grassle, Judith P. AOPE-3,5;B-25 Glower, Catherine MCG-3,5;B-25 Glower, Catherine MCG-3,5;B-25 Graber, H. AOPE-3,5;B-25 Glower, Catherine MCG-3,5;B-25 Glower, Catherine MCG-3,5;B-25 Glower, Catherine MCG-3,5;B-25 Grassle, J. Frederick AOPE-17;MCG-1 Grassle, J. Gra		
Glover, David M. MCG-3 Gmitrowicz, Ed PO-4 Gnanadesikan, Anand PO-14 Goehringer, Dale D B-10 Goericke, Ralf B-4;MCG-2,15 Goetz, Frederick E B-7 Goff, John A GG-6,7,8,15 Goldberg, D GG-13 Goldman, Joel C B-8,13 Goodfriend, Glenn A MCG-5 Gotelli, Nicholas J B-9 Goyet, Catherine MCG-3,8,13,16 Graber, H AOPE-17;MCG-1 Grassle, J. Frederick AOPE-17;MCG-1 Grassle, Judith P AOPE-3,5;B-25		
Gnanadesikan, Anand PO-14 Isaksen, Mai F. B-12 Goehringer, Dale D. B-10 Ittekkot, V. GG-16 Goericke, Ralf B-4;MCG-2,15 Ivanov, V. CRC-1 Goetz, Frederick E. B-7 Jack, W. E. B-20 Goldberg, D. GG-13 Jannasch, Holger W. B-3,7,9,12,20,28,29 Goldman, Joel C. B-8,13 Jasper, John P. MCG-10 Goodfriend, Glenn A. MCG-5 Jech, J. Michael AOPE-3 Govet, Catherine MCG-3,8,13,16 Jenkins, William J. MCG-9 Graber, H. AOPE-22 Jiang, Min AOPE-15,23 Grassle, J. Frederick AOPE-17;MCG-1 Jin, Guoliang AOPE-18 Grassle, Judith P. AOPE-3,5;B-25 Johannessen, O. AOPE-8,22		.
Goehringer, Dale D. B-10 Ittekkot, V. GG-16 Goericke, Ralf. B-4;MCG-2,15 Ivanov, V. CRC-1 Goetz, Frederick E. B-7 Jack, W. E. B-20 Goldberg, D. GG-13 Jannasch, Holger W. B-3,7,9,12,20,28,29 Goldman, Joel C. B-8,13 Jasper, John P. MCG-10 Goodfriend, Glenn A. MCG-5 Jech, J. Michael AOPE-3 Gotelli, Nicholas J. B-9 Jeffrey, S. W. MCG-5 Goyet, Catherine MCG-3,8,13,16 Jenkins, William J. MCG-9 Graber, H. AOPE-22 Jin, Di. MPC-4,5 Grassle, J. Frederick AOPE-17;MCG-1 Jin, Guoliang AOPE-18 Grassle, Judith P. AOPE-3,5;B-25 Johannessen, O. AOPE-8,22		
Goericke, Ralf B-4;MCG-2,15 Ivanov, V CRC-1 Goetz, Frederick E B-7 B-7 B-7 Goff, John A GG-6,7,8,15 Jack, W. E B-20 Goldberg, D GG-13 Jannasch, Holger W B-3,7,9,12,20,28,29 Goldman, Joel C B-8,13 Jasper, John P MCG-10 Goodfriend, Glenn A MCG-5 Jech, J. Michael AOPE-3 Gotelli, Nicholas J B-9 Jeffrey, S. W MCG-5 Goyet, Catherine MCG-3,8,13,16 Jenkins, William J MCG-9 Graber, H AOPE-22 Jin, Di MPC-4,5 Grassle, J. Frederick AOPE-17;MCG-1 Jin, Guoliang AOPE-18 Grassle, Judith P AOPE-3,5;B-25 Johannessen, O AOPE-8,22		
Goetz, Frederick E. B-7 Goff, John A. GG-6,7,8,15 Goldberg, D. GG-13 Goldman, Joel C. B-8,13 Goodfriend, Glenn A. MCG-5 Gotelli, Nicholas J. B-9 Goyet, Catherine MCG-3,8,13,16 Graber, H. AOPE-22 Graham, David W. MCG-9 Grassle, J. Frederick AOPE-17;MCG-1 Grassle, Judith P. AOPE-3,5;B-25 Jack, W. E. B-20 Jannasch, Holger W. B-3,7,9,12,20,28,29 Jasper, John P. MCG-10 Jech, J. Michael AOPE-3 Jerkins, William J. MCG-9 Jin, Di. MPC-4,5 Jin, Guoliang. AOPE-18 Johnnessen, O. AOPE-8,22		
Goff, John A GG-6,7,8,15 Jack, W. E. B-20 Goldberg, D. GG-13 Jannasch, Holger W. B-3,7,9,12,20,28,29 Goldman, Joel C. B-8,13 Jasper, John P. MCG-10 Goodfriend, Glenn A. MCG-5 Jech, J. Michael AOPE-3 Gotelli, Nicholas J. B-9 Jeffrey, S. W. MCG-5 Goyet, Catherine MCG-3,8,13,16 Jenkins, William J. MCG-9 Graber, H. AOPE-22 Jin, Di. MPC-4,5 Graham, David W. MCG-9 Jin, Di. MPC-4,5 Grassle, J. Frederick AOPE-17;MCG-1 Jin, Guoliang AOPE-18 Grassle, Judith P. AOPE-3,5;B-25 Johannessen, O. AOPE-8,22	Goericke, RalfB-4;MCG-2,15	Ivanov, VCRC-1
Goldberg, D. GG-13 Goldman, Joel C. B-8,13 Goodfriend, Glenn A. MCG-5 Gotelli, Nicholas J. B-9 Graber, H. AOPE-22 Graham, David W. MCG-9 Grassle, J. Frederick AOPE-17;MCG-1 Grassle, Judith P. AOPE-3,5;B-25 Goldman, Joel C. B-8,13 Jannasch, Holger W. B-3,7,9,12,20,28,29 Jasper, John P. MCG-10 Jasper, John P. MCG-10 Jech, J. Michael AOPE-3 Jeffrey, S. W. MCG-5 Jenkins, William J. MCG-9 Jiang, Min AOPE-15,23 Jin, Di MPC-4,5 Jin, Guoliang AOPE-18 Johannessen, O. AOPE-8,22		1. J. W D
Goldman, Joel C. Goodfriend, Glenn A. Gotelli, Nicholas J. Graber, H. Graber, H. Grassle, J. Frederick Grassle, J. Udith P. Grassle, Judith P. Godfriend, Glenn A. MCG-5 Jech, J. Michael Jech, J	Goff, John A	
Goodfriend, Glenn A. MCG-5 Gotelli, Nicholas J. B-9 Goyet, Catherine MCG-3,8,13,16 Graber, H. AOPE-22 Graham, David W. MCG-9 Grassle, J. Frederick AOPE-17;MCG-1 Grassle, Judith P. AOPE-3,5;B-25 Goodfriend, Glenn A. MCG-5 Jech, J. Michael AOPE-3 Jeffrey, S. W. MCG-9 Jenkins, William J. MCG-9 Jin, Di. MPC-4,5 Jin, Guoliang AOPE-18 Johannessen, O. AOPE-8,22	Goldberg, D	
Gotelli, Nicholas J. B-9 Goyet, Catherine MCG-3,8,13,16 Graber, H. AOPE-22 Graham, David W. MCG-9 Grassle, J. Frederick AOPE-17;MCG-1 Grassle, Judith P. AOPE-3,5;B-25 Gover, Catherine MCG-3,8,13,16 Jeffrey, S. W. MCG-5 Jenkins, William J. MCG-9 Jin, Di. MPC-4,5 Jin, Guoliang AOPE-18 Johannessen, O. AOPE-8,22	Goldman, Joel CB-8,13	
Goyet, Catherine MCG-3,8,13,16 Graber, H. AOPE-22 Graham, David W. MCG-9 Grassle, J. Frederick AOPE-17;MCG-1 Grassle, Judith P. AOPE-3,5;B-25 Grand MCG-9 Jin, Di MPC-4,5 Jin, Guoliang AOPE-18 Johannessen, O. AOPE-8,22		
Graber, H. AOPE-22 Graham, David W. MCG-9 Grassle, J. Frederick AOPE-17; MCG-1 Grassle, Judith P. AOPE-3,5; B-25 Graber, H. AOPE-22 Jing, Min AOPE-15,23 Jin, Di MPC-4,5 Jin, Guoliang AOPE-18 Johannessen, O. AOPE-8,22	Gotelli, Nicholas JB-9	
Graber, H. AOPE-22 Graham, David W. MCG-9 Grassle, J. Frederick AOPE-17;MCG-1 Grassle, Judith P. AOPE-3,5;B-25 Graber, H. AOPE-12 Jing, Min. AOPE-15,23 Jin, Di MPC-4,5 Jin, Guoliang AOPE-18 Johannessen, O. AOPE-8,22		
Graham, David W. MCG-9 Grassle, J. Frederick AOPE-17;MCG-1 Grassle, Judith P. AOPE-3,5;B-25 Jin, Di. MPC-4,5 Jin, Guoliang AOPE-18 Johannessen, O. AOPE-8,22		
Grassle, J. Frederick		
Grassle, Judith P AOPE-3,5;B-25 Johannessen, O AOPE-8,22		
		Jones, Glenn A

Jorgensen, Bo Barker B-9,12	Lobel, Phillip SB-16
Joyce, Terrence M	Lockhart, W. L
Joyner, Christopher CMPC-5,6	Loewen, Mark Richard
Joyner, Christopher C	
Kaartvedt, SB-13	Luther, D. S
Kahma, K. KAOPE-10	Lynch, James F
Kamgar-Parsi, BehzadAOPE-25	Lynch, James FAOF E-5,4,6,16,20,22
Keafer, Bruce A	Malik, SandipaAOPE-21
Keeley, ChristopherGG-7	Malinverno, Alberto
Keenan, RAOPE-22	Malmquist, Kenneth AlanGS-16
Kelley, Deborah S	Malpas, John GGG-14
Kelly, Kathryn A PO-4	Manganini, Stephen J
Kent, Dennis V	Manghnani, MGG-13
Kent, G. M. Kent	Mantoura, R. F. C MCG-5
Kery, Sean	Marra, Martin AOPE-10,15,23
Kiddon, John B-13	Marrasé, CeliaB-3,16
Kim, Stacy LAOPE-1	Martens, Christopher S MCG-5
King, Geoffrey C. P	Martin, J. H MCG-4
Kitaigorodskii, S. A	Martin, William RMCG-3
Kite-Powell, HaukeMPC-4,6	Martinsen, Robert JAOPE-13
Kleinrock, Martin CGG-4	McCartney, Michael SPO-4,5
Klinger, Barry AGS-3	McClain, Charles RMCG-3
Kloepper-Sams, Pamela JB-14	McCorkle, Daniel C MCG-2,3
Knight, I. T MCG-1	McDonald, David B B-16
Koehler, Richard L AOPE-16	McDougall, Trevor JPO-11
Koelsch, Donald EAOPE-18	McElroy, Marguerite KAOPE-11
Koza, Robert AB-14	McIntosh, Janet S B-26
Kraus, S. DB-20	McNichol, A. P
Kucera, R. B	McSherry, TCRC-1
Kulis, David MB-1	Medford, L. V GG-6
Kuo, AlanB-6	Mello, Gilberto A
Kurz, Mark DMCG-9,10,12	Mercer, J. A AOPE-11
Kusters, John Gerald, JrGS-15	Metner, D. A B-19
Inhania Innant D	Metzger, KurtAOPE-7
Labeyrie, Laurent D MCG-7	Meyer, Peter SGG-18
Lamb, Teresa MB-10	Miller, James H AOPE-3,4
LaMourie, Matthew J	Millero, Frank J MCG-13
Langel, R. A	Mills, Susan W AOPE-5
Langworthy, Thomas AB-12	Mindell, David A AOPE-7
Lanzerotti, L. J	Mirovitskaya, Natalia SMPC-8
Larsen, Einer	Moffett, James W
Lawrence, James R	Molyneaux, Stephen J B-12,29
Leavitt, D. F	Monosson, Emily B-17
LeFaivre, Denis	Moore, R. M MCG-4
Leger, C	Moore, Michael J
Lehman, Scott JGG-16	Moran, S. Bradley MCG-4,13
Lentz, Steven J PO-15,17	Moran, L. S
Lerner, Steve	Morawitz, W
Lessios, H. A	Morey, K. E
Levin, Simon AMPC-6	Mullineaux, Lauren S
Lim, Ee Lin	Munk, WAOPE-8
Limeburner, RichardPO-15	Munkittrick, K. R
Lin, Jian	Murray, Mark Hunter
Lindstrom, Timothy E AOPE-20	Mutter, J. C
Lindstrom, Scott SPO-18	
Ling, Hsin YiGG-17	Nikolanenko, ECRC-1
Liu, Zhengyu GS-4	Notarbartolo di Sciara, Giuseppe B-28
Livingston, Hugh DMCG-1	Nuzzi, RB-1
Llewellyn, C. A MCG-5	Nwankwo, D. O

No. 1 Table Dishard CS 7	Roginko, Alexei YuMPC-8
Nystrom, John Richard GS-7	Rohling, Eelco J
Oguz, T	Rosenblum, Lawrence J
Oh, Siang PengPO-13	Ruttenberg, Kathleen CMCG-14,16
Oien, Andrea LAOPE-14	
Olson, R. J	Samelson, Roger PO-9,13
Oppo, D. W	Sanders, Robert WB-2,3,21
Orchardo, Joe	Sayigh, Laela Suad B-22;GS-10
Orcutt, J. A	Scheltema, Amélie HB-22
Orson, Richard RB-19	Scheltema, Rudolf S B-22
Oschmann, L. A	Schilling, Jean-GuyMCG-9
Ostermann, D. R	Schmitt, Raymond WPO-3,9,10,11
Owens, B AOPE-8	Schmitz, William J., JrPO-8,10
Owens, W. BrechnerPO-2	Schneider, David AGG-4,9
	Schneider, R. J
Palenik, P	Scholin, Christopher AB-23
Palka, D	Schultz, Adam
Park, Young GyuPO-14	Schultz, Mary E
Pascual, Mercedes	Scott, David J MPC-8
Patwardhan, Anand MPC-10	Scott, M. D
Pawlik, Joseph R AOPE-10	Sellers, Cynthia JAOPE-14
Pawlowicz, Richard	Shafer, Deborah KMCG-13
Pedlosky, Joseph	Shaw, Peter R
Peltzer, Edward TMCG-8	Sherwood, Christopher R AOPE-20
Perler, F. B	Sholkovitz, Edward R
Petersen, J. E B-26	Shuchman, R AOPE-8,22
Peterson, S. B	Singer, Robin CAOPE-14
Petitt, Robert A., JrAOPE-15	Singh, Hannuman AOPE-21
Pettigrew, N. R AOPE-13	Slatko, B. E
Pickart, Robert S PO-6,18	Slowey, Niall C
Pietrafesa, Leonard J PO-16	Smethie, William M., JrPO-6
Plant, William J	Smith, Stephen P AOPE-14
Plueddemann, Albert J	Smolowitz, Roxanna M B-10,23
Poisson, Alain MCG-2,13	Snelgrove, Paul V. R
Poland, Alan B-10	Snover, A. KMCG-16
Polasky, Stephen	Sogin, Mitchell L
Polzin, Kurt Louis GS-14 Porter, Karen G B-3	Solomon, Sean C
Potter, Daniel F AOPE-10	Solow, Andrew R MPC-7,8,9,10
Powell, Thomas AMPC-6	Spall, Michael APO-10,11
Pratt, Larry PO-12	Speer, Kevin G
Preisig, James Calvin GS-7	Spiesberger, John L
Preisig, James CAOPE-17	Spindel, R. C
Preisig, James CAOI D-17	Stanton, Timothy K AOPE-3,9,14,18,21
Purcell, M	Starczak, Victoria R AOPE-5,25;B-15;MPC-10
Purser, K. H	Steele, John H
Purser, K. n	Stegeman, John JB-10,14,17,18,19,23,25,29
Qiang, B	Stein, Ross S
Qiu, BoPO-7	Stephen, R. A
	Stephens, Robert A
Racine, BrianPO-14	Stewart, W. Kenneth AOPE-10,15,21,23,25
Rajan, Subramaniam D AOPE-4,14	Stokey, Roger P
Ralph, Elise PO-12	Stoizenbach, Keith D Aof D-12
Rau, G. H MCG-4	Stommel, Henry PO-4,6
Read, A. J	Sutton, P
Reinisch, C. L. B-15	
Reiter, Edmund C	Takada, H
Repeta, D. J MCG-4,5	Takahashi, TMCG-4
Richardson, Philip L. PO-7,8	Takahashi, KozoGG-17
Roberts, Mindy Lynn	Tang, Dajun
Robinson, Paul TGG-14,18	O,

Tarits, Pascal	CC-12
Taylor, F. W	
Taylor, Craig D	D 06
Tool I M	D. 00
Teal, J. M	B-26
Terray, E. A	AOPE-10
Theberge, A. E., Jr	GG-4
Thompson, Geoffrey	MCG-8,9
Thomson, Dennis W	AOPE-19
Toksoz, M. N	
Toole, John	
Toomey, Douglas R	GG-13 14
Trukhchev, Dimitur Ivanov	
Takhenev, Difficul Ivanov	
Trull, T. W	
Tyack, Peter LAOPE	-12,22;B-22,26,27
Valois, Frederica W	D 97
Van Douge C. I	
Van Dover, C. L	B-13
Van Scoy, Kim A	MCG-13
van den Heuvel, M. R	B-19
Vodacek, Anthony	MCG-16
von Alt, Christopher J	AOPE-17
Von Herzen, Richard P	
Von Reden, K. F	
Wadhams, Peter	AOPE-18,22
Walsh, David	GS-8
Wang, Xiaoming	
Wansek, Pierre	AOPE-19
Waterbury, John B	R_4 27
Waters, Robert M	D 1
Watkins, William A	1-1 D-1
Waidman Chairtanh D	B-21,28
Weidman, Christopher R	
Weinberg, James R	B-15
Wells, Randall S	B-21,22
Welschmeyer, N	
West-Johnsrud, L	B-4
Westreich, Eric L	AOPE-3,4
Wheatcroft, Robert A	AOPE-23
Whelan, Jean K	MCG-6
Whitehead, J. A G	
Whitney, Sheri	R_3
Wiebe, Peter H	OPF_91.B_13.98
Wijffels, Susan E	
Wilcock, William Sam Douglas.	
Williams, Albert J., III	
Williams, Peter M	
Wilson, D. Keith	
Wirick, Creighton D	PO-16
Wirsen, Carl O	B-3,12,28,29
Woodin, Bruce R	B-29
Worcester, P. F	AOPE-8.11.22
Wright, S. W	
Wroblewski, J. S	MCG-3
Wu, Huixia	AOPE-22-CS-0
	·
Yang, J	MPC-4
Yeats, Philip A	
Yoerger, Dana R	
You, Yuzhu	
ava, aubiiu	r O-11

Zenk, Walter ZenkPO-Zettler, E. R	-18 3-4

DOCUMENT LIBRARY

February 5, 1993

Distribution List for Technical Report Exchange

University of California, San Diego SIO Library 0175C (TRC) 9500 Gilman Drive La Jolla, CA 92093-0175

Hancock Library of Biology & Oceanography

Alan Hancock Laboratory

University of Southern California

University Park

Los Angeles, CA 90089-0371

Gifts & Exchanges

Library

Bedford Institute of Oceanography

P.O. Box 1006

Dartmouth, NS, B2Y 4A2, CANADA

Office of the International

Ice Patrol

c/c Coast Guard R & D Center

Avery Point

Groton, CT 06340

NOAA/EDIS Miami Library Center 4301 Rickenbacker Causeway

Miami, FL 33149

Library

Skidaway Institute of Oceanography

P.O. Box 13687

Savannah, GA 31416

Institute of Geophysics University of Hawaii Library Room 252 2525 Correa Road Honolulu, HI 96822

Marine Resources Information Center

Building E38-320

MIT

Cambridge, MA 02139

Library

Lamont-Doherty Geological

Observatory Columbia University Palisades, NY 10964

Library

Serials Department
Oregon State University
Corvallis, OR 97331

Pell Marine Science Library University of Rhode Island Narragansett Bay Campus Narragansett, RI 02882

Working Collection Texas A&M University Dept. of Oceanography College Station, TX 77843

Fisheries-Oceanography Library 151 Oceanography Teaching Bldg. University of Washington Seattle, WA 98195

Library R.S.M.A.S.

University of Miami

4600 Rickenbacker Causeway

Miami, FL 33149

Maury Oceanographic Library Naval Oceanographic Office Stennis Space Center NSTL, MS 39522-500!

Marine Sciences Collection Mayaguez Campus Library University of Puerto Rico Mayaguez, Puerto Rico 00708

Library

Institute of Oceanographic Sciences

Deacon Laboratory Wormley, Godalming Surrey GU8 5UB UNITED KINGDOM

The Librarian

CSIRO Marine Laboratories

G.P.O. Box 1538 Hobart, Tasmania AUSTRALIA 7001

Library

Proudman Oceanographic Laboratory

Bidston Observatory

Birkenhead

Merseyside L43 7 RA UNITED KINGDOM

IFREMER

Centre de Brest

Service Documentation - Publications

BP 70 29280 PLOUZANE

FRANCE

50272-101

4. Title and Subtitle	WHOI-93-11	2.	3. Recipient's	Accession No.
	Submitted in 1992 for Publi	ication	5. Report Dat April, 1	
			6.	
. Author(s) Editor: Alora Paul			8. Performing	Organization Rept. No.
			WHOI-	
. Performing Organization Name and	Address		10. Project/Ta	ask/Work Unit No.
Woods Hole Oceanographic Ins			11. Contract(C) or Grant(G) No.
Woods Hole, Massachusetts 02:	543		(C)	
			(G)	
2. Sponsoring Organization Name ar	nd Address		13. Type of R	eport & Period Covered
			Technic	al Report
			14.	W + W + W + W + W + W + W + W + W + W +
5. Supplementary Notes			<u> </u>	
This report should be cited as:	Woods Hole Oceanog. Inst. Tech. R	Rept., WHOI-93-11.		
6. Abstract (Limit: 200 words)				
	bstracts of manuscripts submitted for	nublication during c	alendar vear 1002 hv	the staff and students
The abstracts are listed by t Center, Coastal Research Center	nded to be informative, but not a biblititle in the Table of Contents and are er, or the student category. An author	grouped into one of		
papers.				
•	ora			
abstracts	ors			
abstracts oceanography	OF8			
abstracts oceanography ocean engineering	QF8			
abstracts oceanography	OFB			
abstracts oceanography ocean engineering	ora			
abstracts oceanography ocean engineering b. Identifiers/Open-Ended Terms	ore			
abstracts oceanography ocean engineering b. Identifiers/Open-Ended Terms c. COSATI Field/Group	OF8	10 Committee (1)	the (This Board)	24 No of Pares
abstracts oceanography ocean engineering b. Identifiers/Open-Ended Terms c. COSATI Fleid/Group 8. Availability Statement	n; distribution unlimited.		iss (This Report)	21. No. of Pages 206